Synthesis, Characterisation and Analysis of Structurally Imposing Eight-Membered Ring Heterocyclic Carbenes: Salts, Free Carbenes, Metal Complexes and Catalysis

By

Wei Ye Lu

Submitted in fulfilment of the requirements of degree of

Doctor of Philosophy

School of Chemistry

Cardiff University

Wales, UK

Abstract

The work reported in this thesis is concerned with the preparation, metal coordination and catalytic applications of expanded eight-membered N-heterocyclic carbenes. This is divided into four chapters, which cover the following areas of research.

Chapter One provides the historical and literature overview of synthesis, reactions and catalysis applications for the six- and seven-membered NHCs. Structure and electronic properties of the expanded ring NHC systems are also discussed and compared with their phosphine and five-membered NHC counterparts.

Chapter Two focuses on the synthesis and characterisation of symmetrical, unsymmetrical and backbone functionalised eight-membered NHC halide salts and free carbenes. The precursor salts were all prepared by the amidine route while treatment with KHMDS forms the free NHCs. The 8-NHC ring adopts a boat conformation with the backbone folded over the central NHC carbon. Their N-C_{NHC}-N angles are large, ranging between 129° and 131°, with the attendant C_{NHC}-N-$C_{N\text{-substituent}}$ angles being very small.

Chapter Three describes the synthesis and characterisation of a series of Ag(I), Rh(I), Ir(I) and Ni(I) complexes. Structural analysis of silver-(8-NHC) complexes reveal that these large rings cause the aromatic substituents on the ring nitrogens to bend around and essentially enclose the Ag centre. The percentage buried volume (%V_{bur}) of silver complexes increases considerably as the ring size expands from 5- to 8-membered NHC, reflecting the high steric demand imposed by the larger ring systems. It was also found that the 8-Mes ligand was too large to coordinate to the [Rh/IrCl(COD)]$_2$ dimer, only the less sterically demanding 8-*o*-Tol was able to form stable [Rh/IrCl(8-*o*-Tol)(COD)] complexes. Comparison of CO stretching frequencies for [RhCl(NHC)(CO)$_2$] complexes with 5-, 6-, 7- and 8-membered rings reveal that 8-*o*-Tol is the most basic of all the NHC ligands. A series of paramagnetic (8-NHC) Ni(I) complexes were prepared also, along with their characterization and EPR analysis.

Chapter Four provides the results of catalytic performances for the 8-membered NHC rhodium and iridium complexes in the transfer hydrogenation of ketones. 8-NHC nickel complexes were also tested as catalysts in Suzuki and Kumada cross-coupling reactions.

Acknowledgments

Pursing a Ph.D. project is a both agonizing and enjoyable experience. It reminds me of the first time I climbed Pen y Fan in the Brecon Beacons, step by step, accompanied with bitterness, hardships, frustration, encouragement and with so many people's kind help and support. I realized that it was, in fact, team-work that got me there. Though it is not enough to express my gratitude in words to all those people, I would still like to give my many, many thanks to all these people.

First of all, I would like to express my most sincere gratitude to my supervisor, Prof. Kingsley J. Cavell, who accepted me as a Ph.D. student. I have benefited from your guidance, great kindness and patience and I would to like to give my heartfelt thank-you. I would also like to extend my warmest thanks to Dr Paul Newman, for his kindly and unselfish help and advice.

Special thanks are also given to Dr Emma Carter and Dr Damien Murphy for their help with EPR analyses and Dr Ben Ward for his advice and assistance on fixing/maintaining our various items of laboratory equipment. To the technical staff at Cardiff University; I'd like to give my thanks to Robyn for his help in attaining mass spec data for sensitive complexes, Rob for his service with many analytical techniques and Dr Benson Kariuki for the X-ray structure determinations including his excellent skills with the handling of air sensitive complexes.

My sincere thanks to Jay, Kate, Becky, James W and Steve for their support, understanding and always making me feel positive. My time at Cardiff University would not have been the same without you guys. My thanks also go to Tracey and Abeer for helping me at the start of my Ph.D. In addition, I like to further extend my thanks to James H, Tim and Flo for giving me their kind support.

In addition, I must thank Prof. Gerhard Erker and his group for their generosity and hospitality during my three month visit in Muenster University. I give my sincere thanks to Prof. Mike Whittlesey and Bec at Bath University for their help and guidance on air sensitive catalysis study.

I would like to express my appreciation for the support from all those outside of Cardiff University, of which there are too many to mention.

Last but not least, I would like to convey my most heartfelt thanks to my wonderful mother and father for their endless love and continual support. Their firm and kind-hearted personality has affected me to be steadfast and never bend to difficulty. I would also like to give a huge thank-you to my amazing little brother and sister for always putting a smile on my face, especially during the difficult days of my Ph.D. I owe my every achievement to them.

Abbreviations

acac	Acetylacetonate
Ad	Adamantyl
Anis	Ortho-anisidyl
b	Broad
bimy	benzimidazolin-2-ylidene
BOC	tert-Butyloxycarbonyl
Bu	Butyl
BuLi	Butyllithium
BuOK	Potassium-tert-butoxide
C_{NHC}	Carbene carbene
COD	1,5-Cyclooctadiene
CW	Continuous Wave
Cy	Cyclohexyl
d	Doublet
dd	Double-doublet
DAB	2-Propanamine
DBU	1,8-Diazabicyclo[5.4.0]undec-7-ene
DCM	Dichloromethane
DIPP	Diisopropylphenyl
EPR	Electron Paramagnetic Resonance
ES-MS	Electrospray Mass Spectrometry
FSED	Field-Swept, Echo-Detected
GC-MS	Gas Chromatography Mass Spectrometry
HRMS	High resolution Mass Spectrometry
IMes	1,3-bis(2,4,6-trimethylphenyl)imidazol-2-ylidene
IPr	1,3-bis(2,6-diisopropylphenyl)imidazol-2-ylidene
K	Kelvin
KHMDS	Potassium hexamethyldisilazide
m	multiplet
ma	Maleic anhydride
Mes	Mesityl (1,3-trimethylphenyl)

NHC	N-Heterocyclic carbene
ORTEP	Oak-Ridge thermal ellipsoid plot
o-Tol	*ortho*-Tolyl
Ph	Phenyl
q	Quartet
R	Alkyl or aryl
r.t.	Room temperature
t	Triplet
*t*Bu	tert-Butyl
TEP	Tolman Electronic Parameter
THF	Tetrahydrofuran
THP	Tetrahydropyrimidin-2-ylidene
TMS	Trimethylsilane
TOF	Turnover frequency
TON	Turnover number
$\%V_{bur}$	Percentage Buried Volume
X	Halogen
Xyl	Xylyl

Table of Contents

Chapter One

Introduction

1.1 Denotation of carbene

The term carbene denotes neutral compounds possessing a divalent carbon atom with six electrons in its valence shell (Figure 1.1).[1] The carbene carbon is linked to two adjacent groups by covalent bonds and possesses two unshared electrons, which are either in a singlet or triplet state.

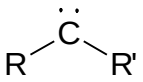

Figure 1.1: Schematic portrayal of a carbene

A free carbene is a highly reactive, electron-deficient species that lacks an octet of electrons. Majority of free carbenes, to some extent, adopt a bent shaped structure. This implies a sp^2-hybridization carbene carbon with two non-bonding orbitals (Figure 1.2).

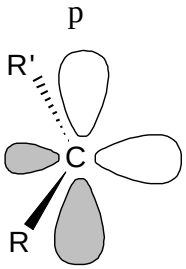

Figure 1.2: Schematic representation of an sp^2-hybridized carbene atom

1.2 Historical background

Carbenes were first recognized over 100 years ago.[2] After 1930, recognition of the existence of free radicals and their involvement in organic chemistry as reaction intermediates were becoming increasingly popular.[3] Carbene moieties, notably methylene carbene were regarded as diradicals. However, it wasn't until the beginning of the 1950s when these compounds were first investigated in organic chemical reactions.[4-6] Doering and Knox in 1953, reported the synthesis of tropolones through the insertion of methylene to substituted benzene (Scheme 1.1).[7]

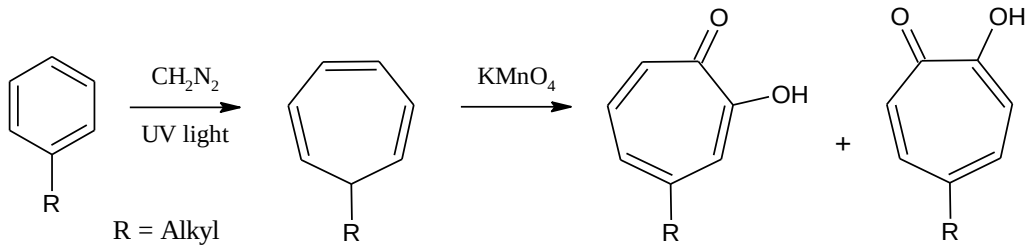

Scheme 1.1. Synthesis of tropolone-derivatives via addition of methylene intermediate to substituted benzene

A subsequent paper published a year later by Doering and colleagues disclosed the existence of a dibromomethylene intermediate via the addition of bromoform to an alkene in a cyclopropanation reaction (Scheme 1.2).[8] As a result, an increasing number of organic syntheses were reported using methylene, which prompted many researchers to undertake detailed examinations of the carbenic intermediate.[9-11]

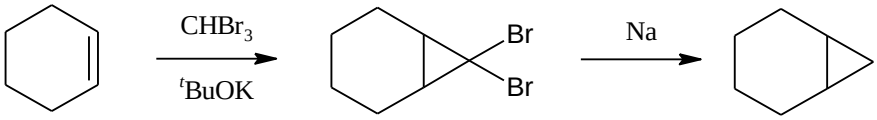

Scheme 1.2. Alkene cyclopropanation *via* a methylene intermediate

A decade later, Wanzlick et al. reported the first N-heterocyclic carbene, 1,3-diphenyldihydroimidazole-2-ylidene, which existed as a dimer.[12] This compound was synthesized by the thermolysis of 1,3-diphenyl-2-(trichloromethyl)imidazolidine with the loss of chloroform (Scheme 1.3). The initial view was that once these free carbenes are prepared, they would result in an unfavourable equilibrium with their corresponding inactive dimers. But when the substituted tetraaminoethylene dimeric species reacted with other functional group derivatives, it gave products that could be formally derived from the dihydroimidazole-2-ylidene compound. Thus arrives the idea of 'Wanzlick equilibrium', that the dimeric species dissociates under the reaction conditions.[13]

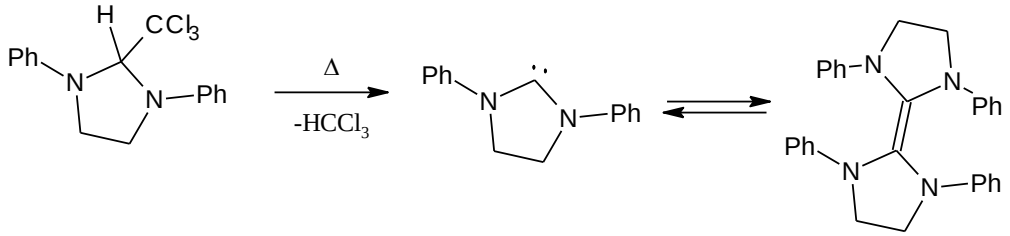

Scheme 1.3. Preparation and Wanzlick equilibrium of 1,3-diphenyldihydroimidazole-2-ylidenes

Wanzlick's concept of carbene-dimer equilibrium was examined by Lemal et al. using "cross-over experiments" (Scheme 1.4a).[14] The reactions were conducted between a pair of tetraaminoethylene derivatives, one bearing tetraphenyl substituents and the other is its *p*-tolyl analog. Upon heating the mixture, no mixed dimer was formed. The author suggested that the reactions of the dimeric carbene species, observed by Wanzlick, were due to the attack on the electron-rich double bond to generate a cationic species followed by cleavage into the free carbene and the resultant salt (Scheme 1.4b). At this point, the free carbene could either re-dimerise or react with another electrophile to form the dihydroimidazolium salt.

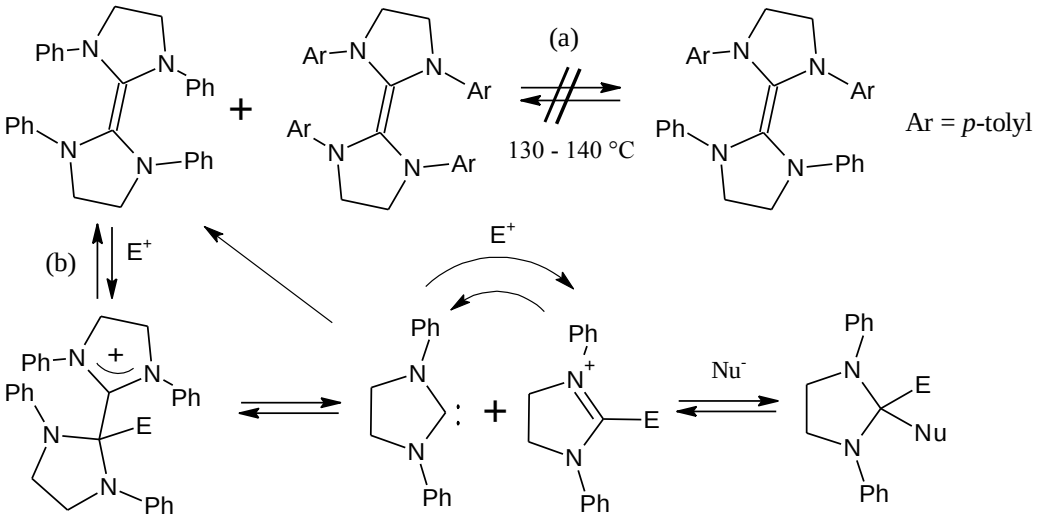

Scheme 1.4. Lemal's dimer "cross-over" experiment

In 1999, Denk et al. re-examined the "cross-over" reactions and reported successful mixed dimers with the tetraaminoethylene analogues.[15] Lemal repeated his previous experiments and confirmed that no cross-over products were visible in the presence of potassium hydride and under the conditions reported by Denk et al.[16] The notion of Wanzlick equilibrium

between a tetraaminoethylene and its corresponding carbene was finally acknowledged and confirmed by others at a later date.[13, 17] In 1965, it was already clear how stable carbenes could be obtained; exclusion of electrophiles from the synthesis and the use of bulky N-substituents to avoid dimerization. Armed with this knowledge, Wanzlick and Schnönherr prepared 1,3-diphenylimidazole-2-ylidene and 1,3,4,5-tetraphenylimidazole-2-ylidene from their corresponding imidazolium salts via in situ deprotonation.[18] In this case, dimerization did not occur and consecutively produced the first metal-NHC complex. In 1991, Arduengo isolated and crystallographically characterised the first stable imidazole-2-ylidene.[19] Arduengo's carbene was prepared by deprotonation of the correspondent imidazolium salt with sodium hydride and a catalytic amount of DMSO (Scheme 1.5).

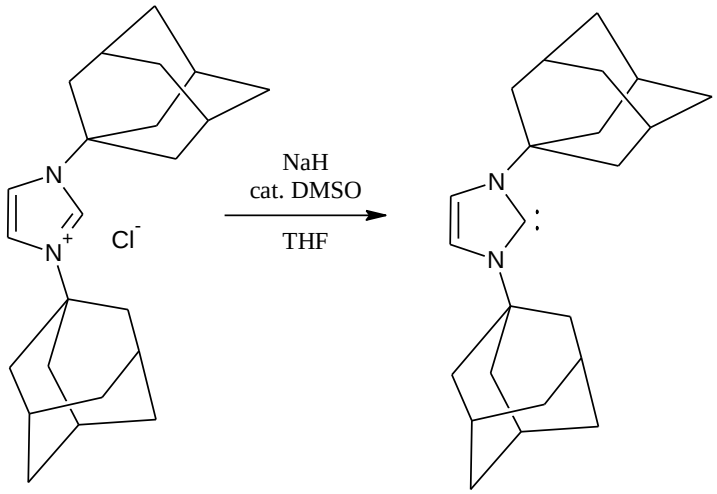

Scheme 1.5. Synthesis of the first crystalline free carbene

1.3 Singlet vs triplet state carbenes

A divalent carbene carbon, bonded to two substituents can adopt either a bent or linear geometry (Figure 1.3). The latter geometry is based on a sp-hybridized carbon atom possessing two non-bonding degenerate orbitals (p_x and p_y), each filled with a single electron with parallel spins. This is otherwise known as the triplet state $^3B_1$. The degeneracy of these orbitals breaks for a sp^2-hydridized carbon atom. The energy of p_y orbital remains constant by going from the sp to the sp^2-hybridized state, while the p_x orbital increases it's s character and thus decreasing in energy; these orbital's are usually known as p_π and σ orbital respectively.[20] The two non-bonding electrons of antiparallel spins occupy the same σ

orbital and therefore known as the singlet state $^1A_1$. The excited singlet state $^1B_1$ consists of two unpaired electrons in two different orbitals.[1]

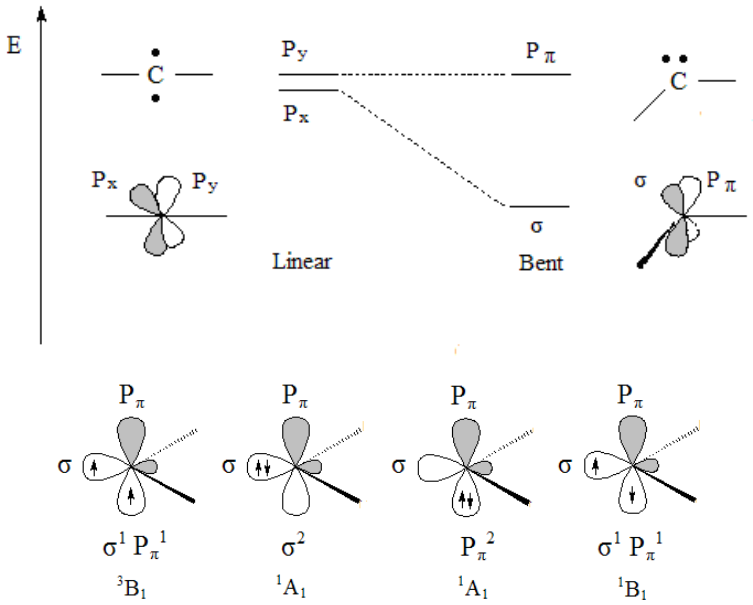

Figure 1.3: Carbene bond angle and its concomitant effect with the nature of the frontier orbitals and its electronic states

The relative energies of σ and p_π orbitals are used to determine whether the carbene is in the singlet or triplet ground state. If the difference between the two states exceeds ~40 kcal mol^{-1} then the singlet ground state is favoured.[21] It is also important to note that the extent of stability and reactivity of carbenes will be affected by the different ground states it possesses.[22] Triplet carbenes can be generated by photolysis from diazo compounds. The methylene centres usually bear two α-phenyl groups, but even with the steric bulk provided by the substituents, these species are very reactive and difficult to isolate.[23, 24] The synthetic reactions are frequently performed at low temperatures (77 K) and can be characterised using EPR. Tomioka et. al. managed to successfully isolate a stable triplet carbene for up to one week in solution at room temperature (Scheme 1.6).[25] It was also revealed that these species could be stabilized with bromo- and trifluoromethyl groups present in its vicinity or within an aromatic network such as an anthryl group which delocalises the unpaired electrons.[25, 26]

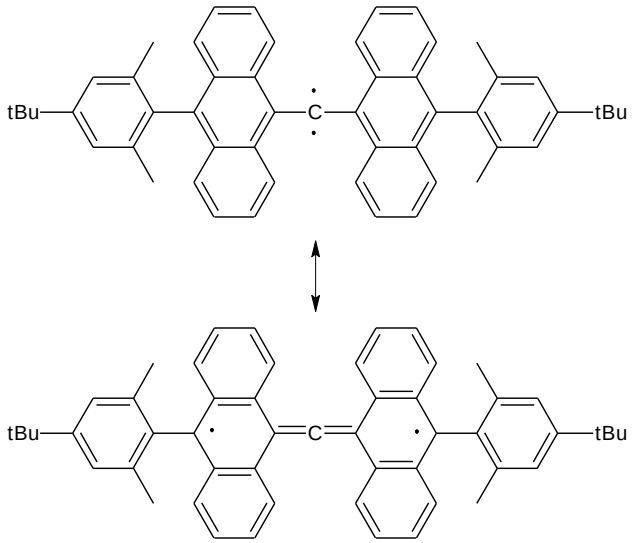

Scheme 1.6. Stable triplet carbene

Ground state multiplicity is determined by the electronegativity of α-substituents (known as the inductive effect), hence σ-electron-withdrawing groups give rise to singlet carbenes.[27] Alternatively, determination of the carbene geometry (linear or bent) is directly related to the electronic delocalization (known as mesomeric effect ±M) between the methylene and its α-substituents.[28] Different combinations of mesomeric effects brought by the stabilization of various α-substituents causes the singlet carbene to be categorized into five sectors: +M/+M, -M/-M, -M/+M, +M/- and aromatic cylcopropylidenes.[1, 29, 30] +M/+M singlet cabenes contain two electron-donating α-substituents including F, Cl, Br, I, OR, SR, SR_3, NR_2, PR_2 and are presumed bent in geometry. Stabilization of these carbenes arises by donation of the substituent's p orbital electrons to the unfilled p orbital of methylene. Dihalocarbenes, dioxacarbenes and oxahalocarbenes exist as intermediate species before they dimerize together.[31-33] Such carbene species can be generated by thermolysis/photolysis from their corresponding diazirines (Scheme 1.7a) or transfer reaction of a oxygen atom from urea and carbonate derivatives to fluorenylidene and methylene carbenes (Scheme 1.7b).[34] Whereas amino-(oxy, thio)carbenes and particularly diaminocarbenes are generally kinetically stable in solution and can be isolated as solids in absence of moisture.

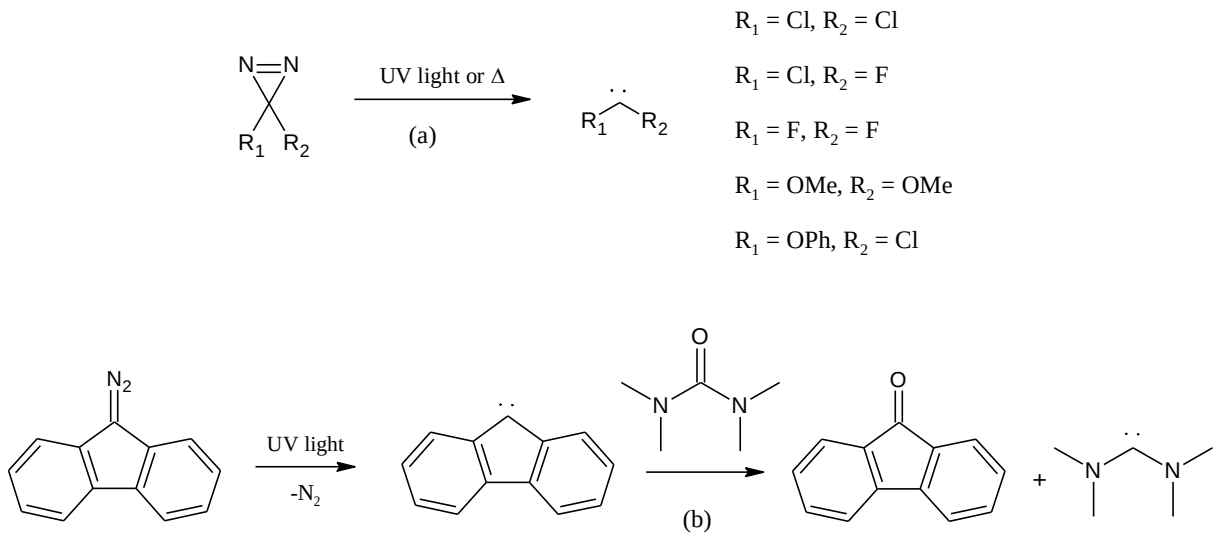

Scheme 1.7. Generation of carbenes (a) from diazarine precursors, (b) *via* oxygen atom transfer

-M/-M singlet carbenes contain α-substituents with electron-withdrawing abilities such as COR, CN, CF_3, BR_2, and SiR_3.[1] The geometry of such compounds are predicted to be linear.[35] Stabilization is achieved by donation of the unpaired electrons from methylene's filled p-orbital to the substituents empty p-orbital. These species have never successfully been isolated. Examples include borinanylideneboranes as masked analogues which exhibit topomeric equilibrium with their corresponding diborylcarbenes (Scheme 1.8),[36, 37] facile topomerization was also found with its acyclic equivalent.[38] The chemical properties of these compounds resemble those of electrophilic carbenes in trapping reactions with germylenes and stannylenes.[39]

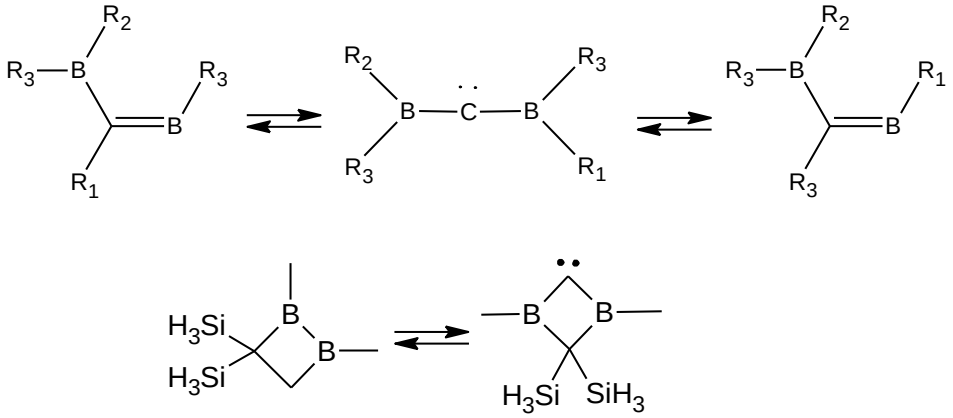

Scheme 1.8. Masked analogues of -M/-M diborylcarbenes

+M/-M singlet carbenes occupy two α-groups with opposite electronic effects with a quasi linear geometry.[27] Stabilization is accompanied by a push-pull effect, where the substituent's p-orbital present a strong donation towards methylene empty p-orbital while at the same time, a weaker donation is emitted from the methylene filled p-orbital to the substituents empty p-orbital. For example, phosphinophosphoniocarbenes are formed by thermolysis of their corresponding diazo compound and such phosphinocarbenes are stabilized by extensive delocalization (Scheme 1.9).[40, 41]

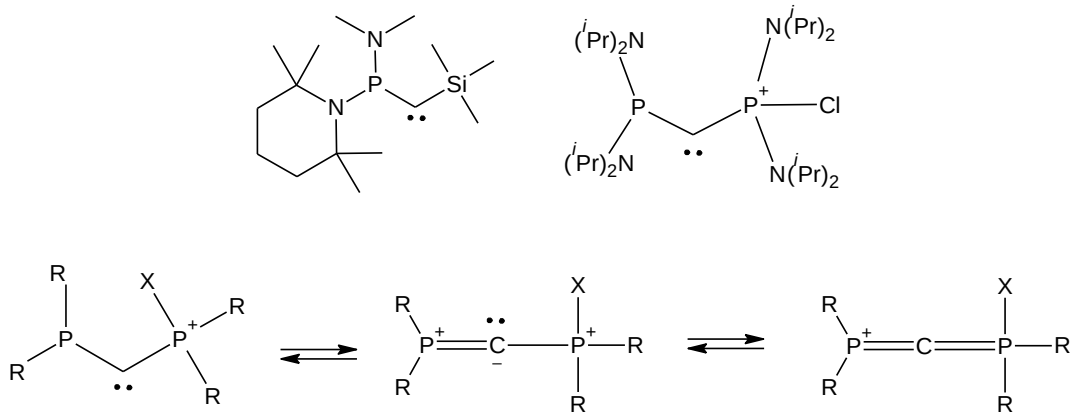

Scheme 1.9. +M/-M phosphinophosphoniocarbenes and the mesomeric stabilization of phosphinocarbenes

+M/- singlet carbenes are those which bear stabilizing α-group such as an amino or phosphino-group, the other generally acts as a spectator ligand. Such examples include stable arylphosphinocarbenes,[42] alkylaminocarbenes,[43] and silylaminocarbenes (Figure 1.4).[44] These species are consider being nucleophilic and are synthesized by deprotonation of the corresponding salt.

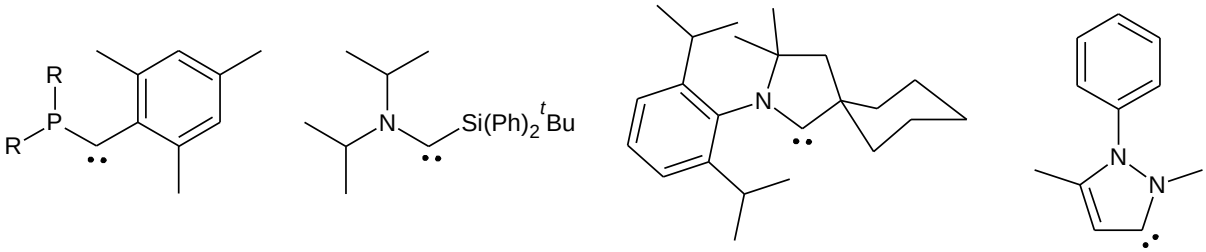

Figure 1.4: +M/- singlet carbenes

Cyclopropenylidenes, more specifically bis(diisopropylamino)cyclopropenylidene have been recently isolated by Bertrand et al. in low yield.[30] This compound bears no stabilizing α-substituents and it is prepared by deprotonation of the corresponding cyclopropenium tetraborate salt (Scheme 1.10).

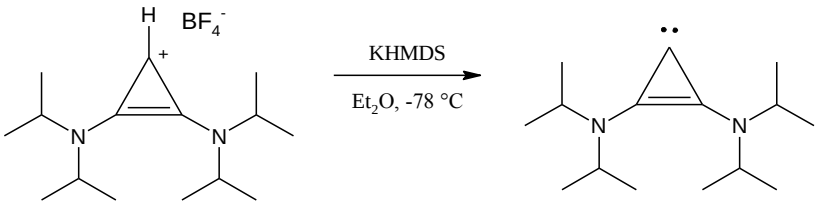

Scheme 1.10. Snthesis of bis(diisopropylamino)cyclopropenylidene

1.4 Fischer, Schrock carbenes

Fischer was the first to reveal complexes with metal-to-carbon double bonds. $[W(CO)_5(C(CH_3)OCH_3)]$ is the initial example of a carbene in coordination chemistry, bearing metal atoms of low oxidation states with 18-electrons.[45] In contrast, Schrock's alkylidene complexes (such as $[TaCl_2H(PR_3)_3(CHCMe_3)]$, prepared by α-hydrogen abstraction from an alkyl group), were found with high oxidation state among early transition metals bearing fewer than 18 electrons.[46] The two types of complexes are referred as Fischer and Schrock carbenes (Figure 1.5).

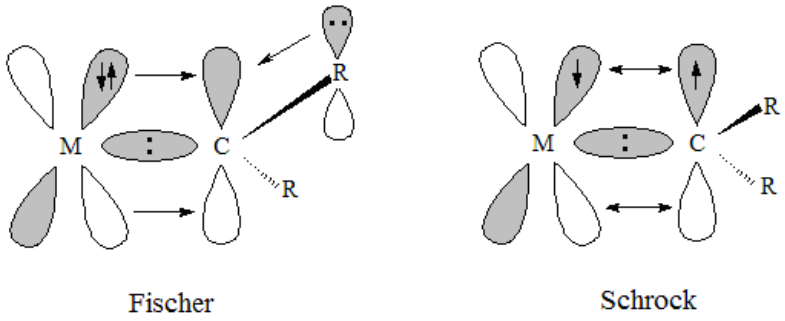

Figure 1.5: Fischer and Schrock carbene

Fischer carbene complexes form a metal-carbene bond that is constituted by synergistic σ donation to the metal and significant π back-bonding contribution from the metal to the empty p orbital of the carbene.[1] The metal possesses π-acidic ligands, this makes back-bonding weak and does not restitute the σ-donation from ligand to metal. Therefore the

methylene carbon is electrophilic and readily undergoes nucleophilic attack. (Scheme 1.11a).[47] They are stabilized singlet carbenes with a significant gap between their singlet and triplet ground states. Schrock carbenes are less stable in comparison, with a smaller gap between the two ground states.[48] The coupling of two triplet fragments forms a covalent metal-carbon bond with equal distribution of the π-electrons between the carbon and the metal. The carbene centre, on which electron density is aggregated through back-bonding, is nucleophilic and are therefore susceptible to react with electrophiles (Scheme 1.11b).[49]

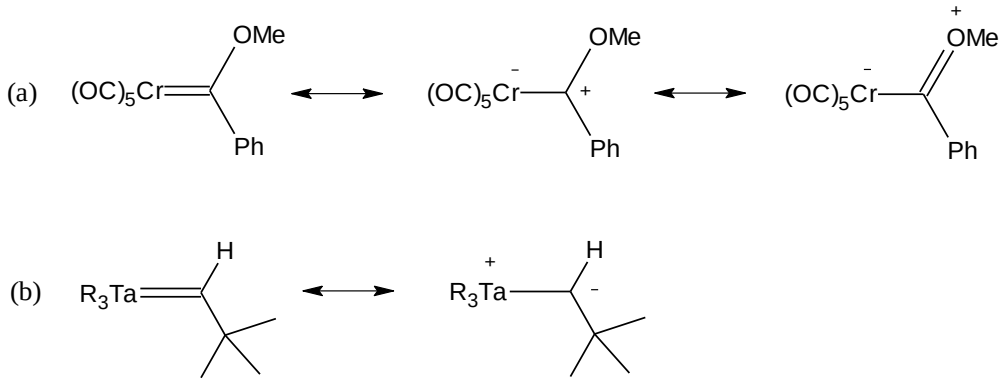

Scheme 1.11. Mesomeric forms of metal-carbene bonding Fischer (a) and Schrock (b) carbene complexes

1.5 N-Heterocyclic carbenes

NHCs otherwise known as diaminocarbenes are the most heavily studied ligand class in carbene chemistry. In many examples, these carbenes are being used as the more favourable ligand than their phosphine counterparts in the field of organometallic chemistry and its related catalysis.[3, 50-53] A famous example bears the application of Grubbs's ruthenium catalysts in olefin metathesis reactions.[54-58] The original Grubbs I catalyst involved competition between the binding of olefin and phosphine ligands at the metal centre (Scheme 1.12a). Hence a phosphine ligand must depart the catalyst before olefin metathesis could successfully take place. However, replacement of the *trans*-ligand with a stronger σ-donating NHC ligand further accelerates ligand dissociation (Scheme 1.12b). This outcome is subjected to the *trans* effect, otherwise known as labilization of ligand *trans* to σ-donating ligands.

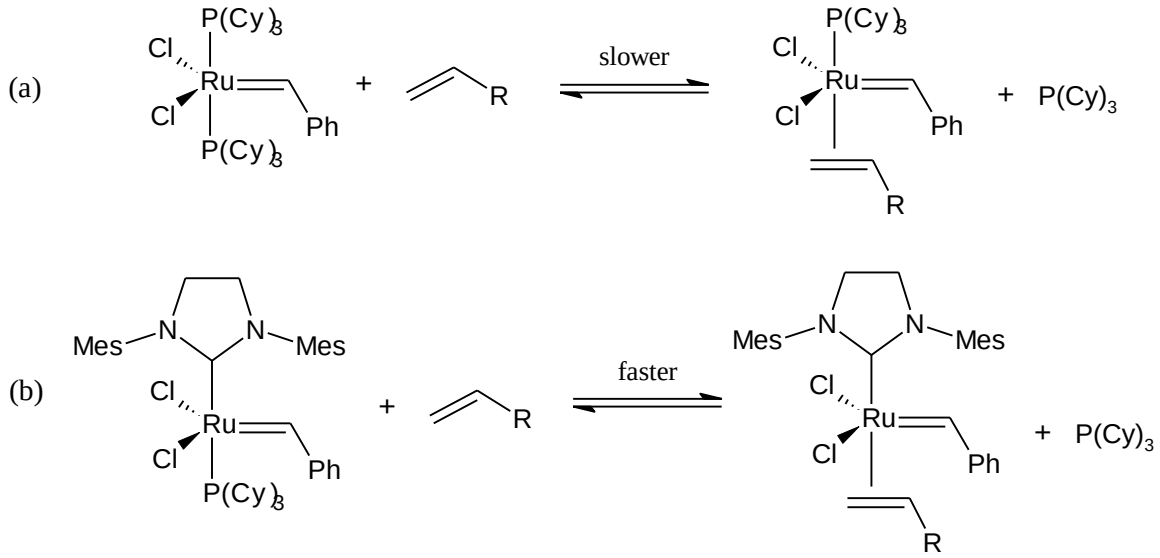

Scheme 1.12. Phosphine dissociation in oliefin metathesis with Grubbs I (a) and Grubbs II (b) complex

Stability of NHCs is mainly determined by the electronic mesomeric interaction of the π-electrons on the nitrogen atoms with the empty p_π-orbital of the sp^2-hybridized carbene carbon (Scheme 1.13). Thus the resonance structures shown below illustrate why NHCs are electron-rich nucleophilic species.

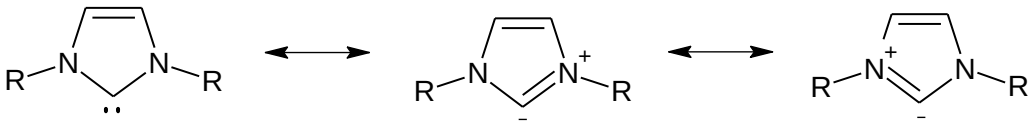

Scheme 1.13. Resonance structures of five-membered NHCs

The two nitrogen atoms donate electron density to the carbene's empty p_π-orbital via mesomeric effect while inductively withdrawing electron density from the σ-nonbonding orbital (push-pull effect). This results in a significant increase between the σ and p_π orbitals, thus induces a singlet ground state multiplicity. Steric impact imposed by the N-substituents also affects the stability of NHCs. Steric protection exerted on the carbene enhances its stability but in addition have an adverse affect upon metal coordination.[59, 60]

NHCs were frequently compared with phosphines (PR_3), an established group of spectator ligands in homogeneous catalysis. Phosphines and phosphites are sp^3-hybridised Lewis bases with lone pairs of electrons, donated to a transition metal to form a complex of the type $(R_3P)_nM–L$.[61] With the accessibility of Tolman's parameters, phosphines were able to

acquire predictable and tunable steric and electronic effects.[62] An early review based on spectroscopic measurements of NHCs confirmed that they had comparable electronic structures with phosphines (good σ-donors, poor π-acceptors).[63] Later studies show that NHCs are stronger donors than most basic phosphines and in several cases NHCs could act as a π-acceptor in complexes.[64-67] When σ-donating abilities was compared amid the two spectator ligands, comparable complexes of NHCs showed higher bond dissociation energies. For example, calculations conducted for the loss of PMe_3 from trans-[$PdCl_2(PMe_3)$(NHC)] requires 38.4 kcal mol^{-1}, whereas the elimination of NHC (N-unsubstituted imidazol-2-ylidene) needs 54.4 kcal mol^{-1}.[68] Another crucial difference between NHCs and phosphines is their orientation of the steric bulk. The orientation of three R-substituents in phosphine ligands, depending on their sizes, are generally pointed back from the apex of a cone at the metal centre (though sometimes this is not the case, take $AuCl(PEt_3)$ for example, the three alkyl groups on the phosphine atom tend to point towards the metal centre as the substituents are set as far away from each other as possible due to sterics), while the two N-substituents of NHCs may flank towards the metal.[62, 69, 70] Also, unlike phosphines, the substituents on the NHCs are not directly connected to the coordinating carbene carbon atom. Therefore this allows for the electronic and steric properties to be tuned separately.

1.6 Synthesis of expanded-ring N-Heterocyclic carbenes

Carbenes derived from five-membered heterocycles have been the most widely studied of the NHCs. Imidazolin-2-ylidenes in particular, constitute the largest group of stable heterocycle carbenes reported in the literature. An array of different methods for the synthesis of these five-membered ring precursors can be found in many NHC reviews.[1, 60, 71, 72] However, this subsection will focus solely on the preparation of expanded ring NHCs. A common feature of expanded-ring NHC preparation is that their construction requires a final systematic cyclization step. Such synthetic protocol can be subdivided into 2 main categories; (i) ring closure by introduction of the precarbenic unit, (ii) ring closure by linkage of the backbone to the pre-assembled precarbenic and amino units.

1.6.1 (i) Ring closure by introduction of precarbenic C_1 unit

This approach is still widely used as the final cyclization step to NHC precursors. The use of commercially available primary diamines as building blocks for NHC precursors is a well established and convenient reaction pathway. Hence cyclization to form NHC precursor salts starts from the diamine core, as illustrated in Scheme 1.14.

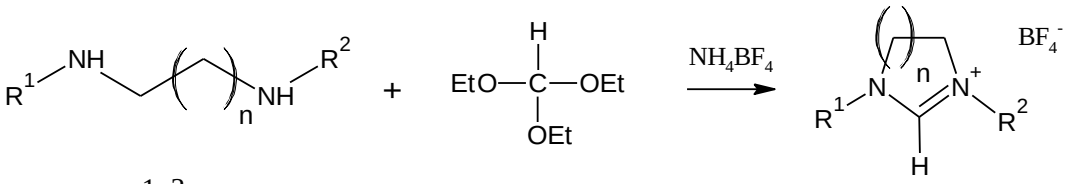

n = 1, 3

R^1, R^2 = alkyl or aryl

Scheme 1.14. Cyclization of formamidine salt by condensation of diamine with ortho ester

Examples of expanded ring formamidiniums with a saturated backbone prepared from this strategic route were recorded by Cavell et. al.; along with camphor-derived chiral NHCs containing fused six- and seven-membered central rings.[73-77] Other early expanded ring NHCs prepared through this method includes Richeson's ligand,[78, 79] derived from N-isopropyl-1,8-diaminonaphthalene intermediate and Stahl and co-workers' 1,3-dialkyldiazepinium ligands, synthesized from either 2,2'-diaminobiphenyl or (R)-2,2'-diaminobinaphthyl.[80, 81] Also novel diaminocarbene[3]ferrocenophane precursors were independently created by Bielawski and Siemeling.[82-85] Examples of the expanded ring NHCs reported above are depicted in Chart 1.1.

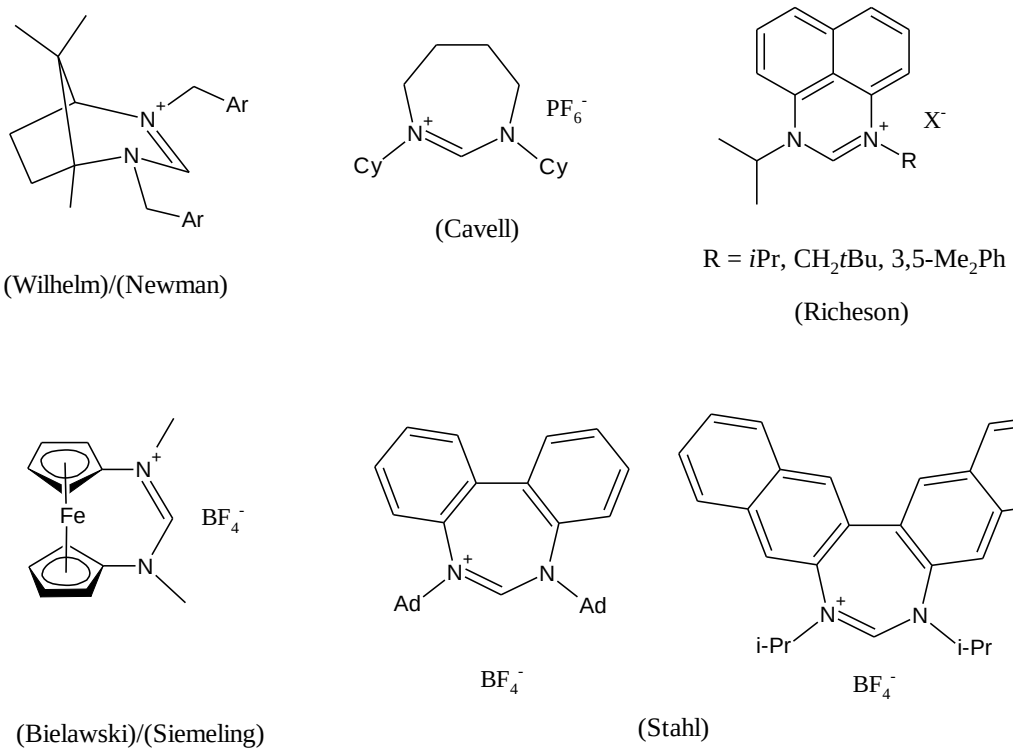

Chart 1.1. Expanded ring NHC precursors derived from diamines

Perillo and co-workers were the first to report the synthesis of expanded six-membered NHC precursors using the paraformaldehyde route via oxidation of a cyclic aminal.[86] Thus formation of 3-substituted 3,4,5,6-tetrahydropyrimidinium salts from cyclization of the corresponding diamines into hexahydropyrimidines and subsequent dehydrogenation with *N*-halosuccinimide. Buchmeiser et. al. used this approach to synthesize symmetrical 1,3-dimesityl- and 1,3-diisopropyl-3,4,5,6-tetrahydropyrimidinium bromides.[87] Hence aqueous paraformaldehyde was used to cyclize *N*,*N*'-disubstituted propane-1,3-diamine to the corresponding 1,3-disubstituted hexahydropyrimidine, followed by dehydrogenation using *N*-bromosuccinimide (Scheme 1.15).

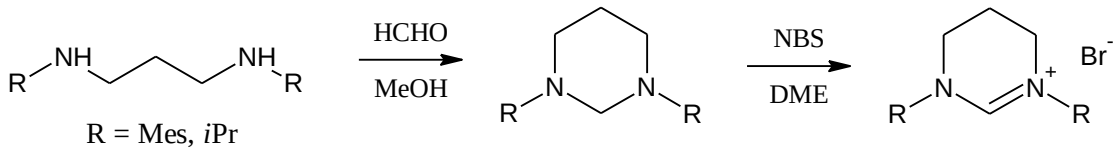

Scheme 1.15. Synthesis of 6-membered 1,3-disubstituted-3,4,5,6-tetrahydropyrimidinium bromides via oxidation of a cyclic aminal

5-Hydroxy-1,3-dimesityl-3,4,5,6-tetrahydropyrimidinium bromide was also prepared using exactly the same approach shown above. The starting precursor 1,3-bis(mesitylamino)-2-hydroxypropane was subjected to O-protection with chlorotrimethylsilane prior to the ring closure stage. Deprotection at the end afforded 5-hydroxy-1,3-dimesityl-3,4,5,6-tetrahydropyridinium bromide, providing a platform for further functionalization to afford a supported catalyst precursor (Scheme 1.16).[88]

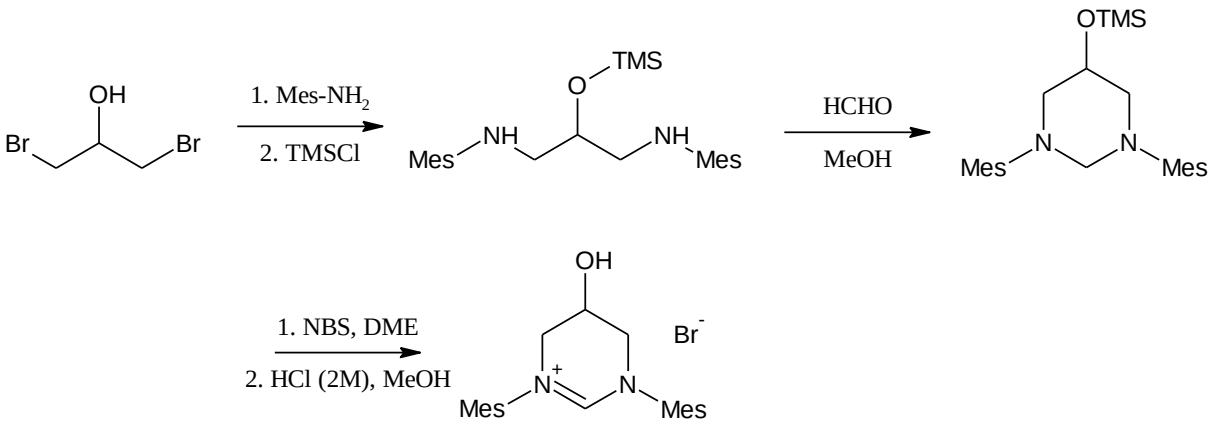

Scheme 1.16. Synthesis of 6-membered 5-hydroxy-1,3-dimesityl-3,4,5,6-tetrahydropyrimidinium bromide via oxidation of a cyclic aminal

Cavell and co-workers furthered this synthetic research by preparing a seven-membered NHC precursor containing a strained 5,6-dioxolane moiety.[76]

Grubbs et. al. reported the formation of a symmetrical six-membered, 1,3-dimesityl-5,5-dimethyltetrahydropyrimidinium salt in good yields through an alternative bisacylation/reduction route (Scheme 1.17).[89]

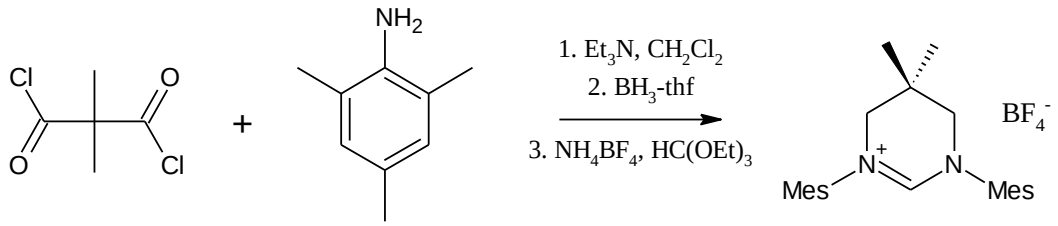

Scheme 1.17. Synthesis of expanded 6-membered NHC salt from mesitylamine and dimethylmalonyl dichloride

1.6.2 (ii) Ring closure by linkage of the backbone to the presembled precarbenic and amino units

Ring closure by linkage of the precarbenic unit with the desired backbone is a fairly new approach to acquire NHC precursors. Nonetheless it is one of the most widely and frequently used reactions due to the many different possible cyclic diaminocarbene precursors it could access. Synthesis of symmetrical and unsymmetrical *N*,*N*'-functionalized formamidine is a well established platform, only the cyclization step differentiates methodologies from one another.

Synthesis of symmetrical *N*,*N*'-diaryl formamidine is simple, through condensation of 1 equivalent of triethyl orthoformate with 2 equivalents of a primary amine in the presence of a catalytic amount of acetic acid. The reaction mixture is stirred for a few hours at 110-120°C until solid precipitates from solution (Scheme 1.18). Filtration of the solids whilst washing with cold hexane yields pure *N*,*N*'-diaryl formamidine.[90] Unsymmetrical *N*,*N*'-diaryl formamidines can be obtained from a slight modification of the method above. Refer to Results and Discussions (Synthesis of unsymmetrical 8-membered NHC Halide Salt) sub-chapter (page 53) for more details on this reaction.

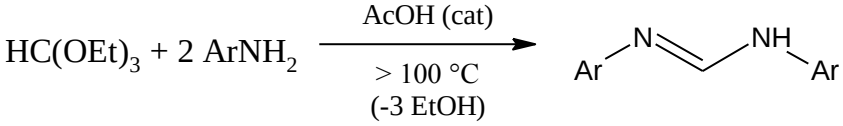

Scheme 1.18. Synthesis of *N*,*N*'-diarylformamidines

Armed with either the symmetrical or unsymmetrical *N*,*N*'-diaryl formamidine, cyclization could now take place with a selected heterocyclic backbone to form the corresponding symmetrical/unsymmetrical NHC precursor. One example is the cyclization via a bisalkylation route, exihibited by Bertrand and colleagues in 2006.[91] Five-, six-, and seven-membered carbene precursors were synthesized in the report (Scheme 1.19). Both expanded 6-, and 7-membered NHC salts were prepared by direct alkylation with lithium formamidine (formed from deprotonation of the corresponding formamidine with *n*-BuLi in THF) with 1,3-dibromopropane and α,α'-dibromo-*o*-xylene respectively. Whereas the 5-membered NHC salt undergoes alkylation with 1,3,2-dioxathiolane-2,2-dioxide instead.

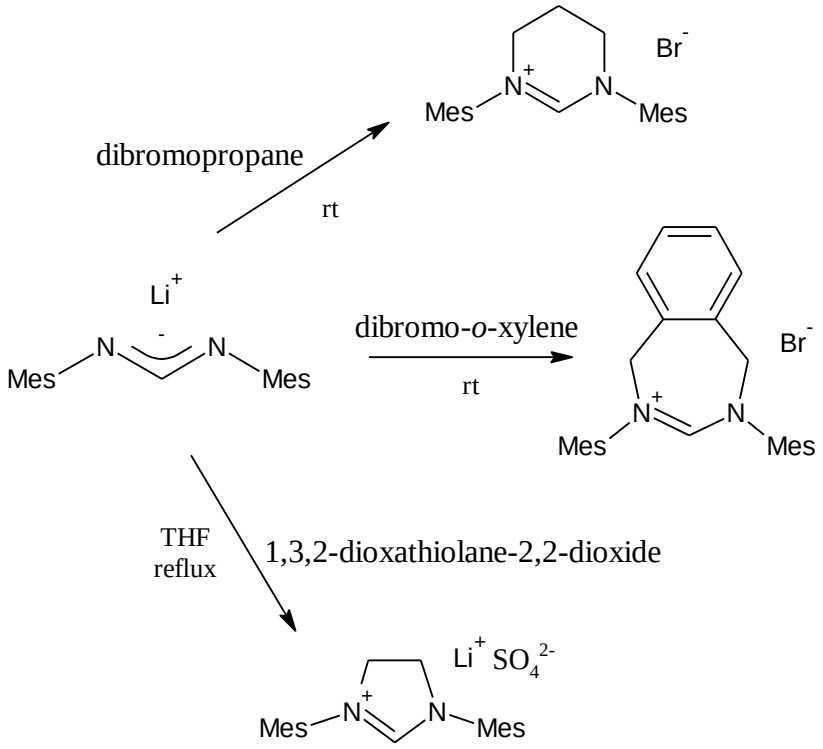

Scheme 1.19. Synthesis of 5-, 6-, and 7-membered NHC salt via bisalkylation of lithium formamidine

Cavell and coworkers later addressed a similar approach by reacting formamidine with biselectrophile alkylating reagents with half an equivalent of potassium carbonate in refluxing acetonitrile. This extended the scope of cyclic carbene precursors available, covering various ring sizes including imidazolinium, tetrahydropyrimidinium and tetrahydrodiazepinium cores.[92]

An alternate cyclization method to obtain NHC precursors is via direct bisacylation of the formamidines, Scheme 1.20 illustrates all the NHC precursors/compounds reported in the literature that were made by this pathway.

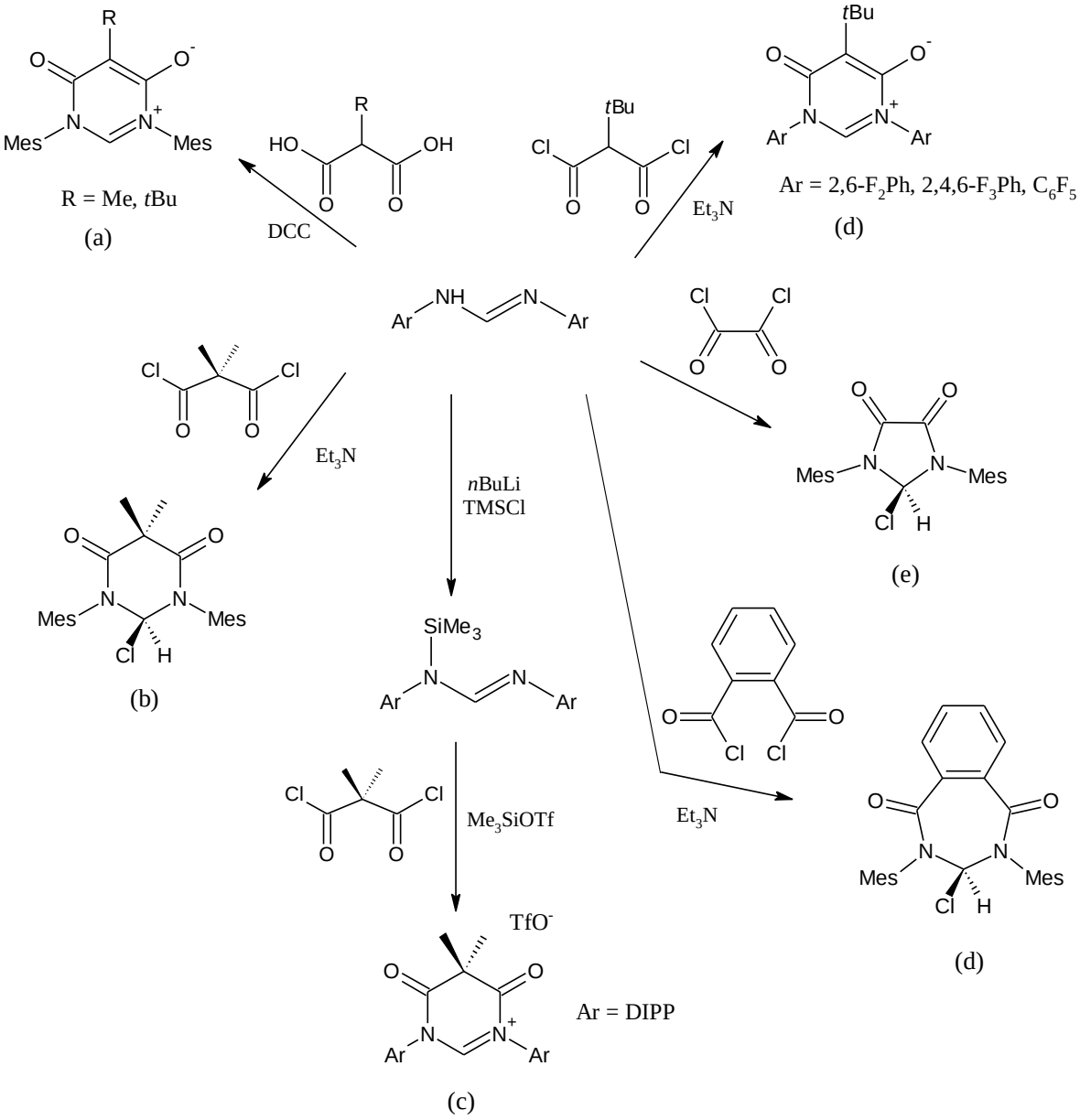

Scheme 1.20. Synthesis of five-, six- and seven-membered heterocyclic compounds via bisacylation of formamidines

A seven-membered, 2-chloro-1,3-diazepin-4,7-dione heterocycle was also formed by condensation of *N*,*N*'-dimesitylformamidine with phthaloyl chloride (Scheme 1.20d).[93]

1.7 Properties of expanded ring NHC systems

Several distinct structural differences were observed and reported in the literature, other than the obvious increase in size of the heterocyclic ring, between five-membered and expanded ring NHCs. One noticeable change is that six- and seven-membered rings become distorted to alleviate constraints on the heterocyclic framework and the spatial disposition of the N-substituents, whereas the five membered rings adopt a planar conformation. This was seen early on with seven-membered NHC amidinium salts bearing N-adamantyl substituents, reported by Stahl et al.[80, 81] The twisted structure exhibits a C_2 axial symmetry arising from the carbenic carbon atom. Cavell and colleagues also revealed, from X-ray crystallography, ring strain in six- and seven-membered saturated NHC amidinium salts.[76, 92] Furthermore, the N-C_{NHC}-N bond angle in expanded NHCs which remained planar showed remarkable increase in size compared to that of the five-NHCs. The N-C_{NHC}-N angles for five- and seven-membered carbenes were recorded in the ranges of 100-110° and 115-125° respectively.[78] It was also noted that such wide angles for the large rings resulted in the projection of the N-substituents into the metal coordination sphere. Such impediments around the metal-carbene bond may affect the availability of the metal and subsequently the system's potential catalytic properties.[94] Recent reports show that six-membered NHCs have higher pK_a values than their saturated five-membered counterparts; pK_a values are in the range 27.8-28.2 and 20.7-21.5 respectively.[95] Such values were determined in water and the increase in pK_as correlates with the greater N-C_{NHC}-N angles. This suggests that the large ring systems are more basic and thus provide better donor ability toward metal centres.

1.8 Synthesis of expanded ring NHC-metal complexes

Many methods are known for the synthesis of metal-NHC complexes. The appropriate route employed for the preparation of specific NHC complexes depends on the electronic and steric nature of the carbene, as well as the substituents in the metal centre.[96] The most generic approach is via free carbenes.[19, 59] A well-known method involves the cleavage of dimeric complexes to generate monomeric NHC-Rh(I), Ir(I) and Pd(II) complexes (Scheme 1.21).[80, 81, 97-100]

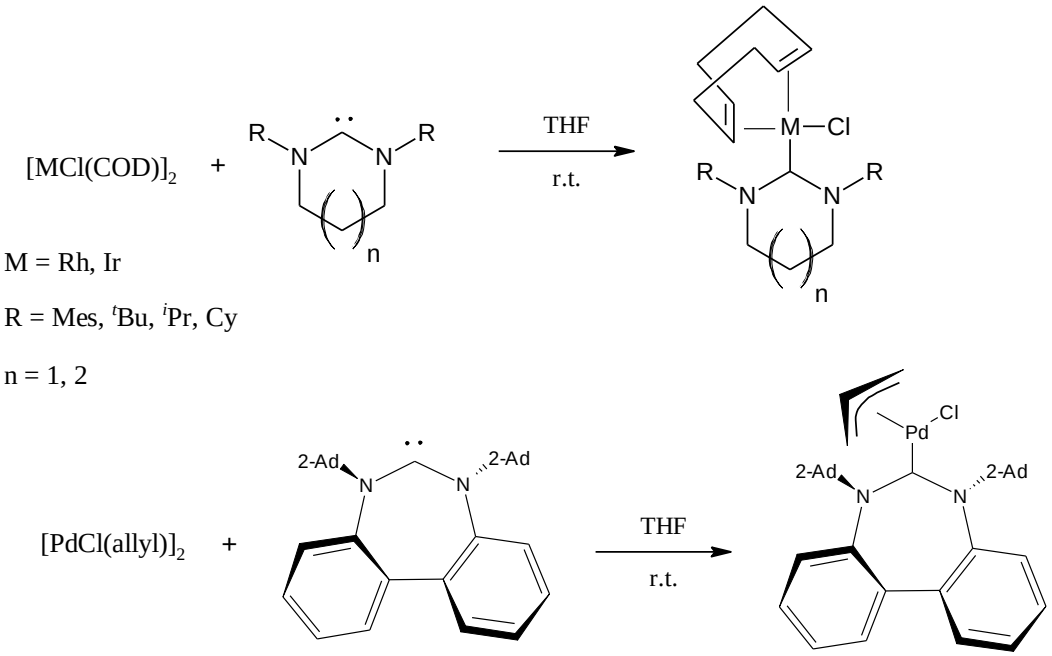

Scheme 1.21. Synthesis of expanded ring NHC-coordinated Rh(I), Ir(I) and Pd(II) complexes via dimeric cleavage from $[Rh/IrCl(COD)]_2$ and $[PdCl(allyl)]_2$ respectively

Furthermore, free carbenes could react with other metal systems to give the desired product. For example, reaction of free expanded ring carbenes with gold(tetrahydrothiophene) chloride in toluene gave an NHC-Au(I) complex;[93] copper(I) chloride in THF yielded the NHC-Cu(I) complex;[101, 102] or reaction with platinum (divinyltetramethyldisiloxane) in toluene afforded NHC-Pt(0) complexes in the form of [Pt(6-NHC)(dvtms)].[103] Newman and Cavell recently reported the formation of a square-planar camphor-derived chiral NHC-Ni(II) complex.[75] This compound was generated via oxidative addition of the azolium salt with a Ni(0) precursor, $[Ni(1,5\text{-}COD)_2]$ in THF followed by dissolving the intermediate in chloroform (Scheme 1.22).

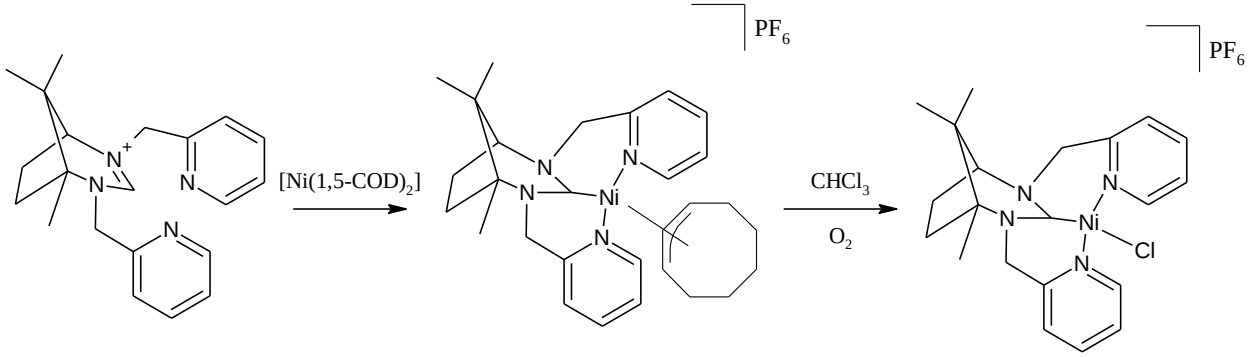

Scheme 1.22. Synthesis of [Ni(camphor-derived chiral NHC)(η^3-C_8H_{13})]PF_6 followed by [Ni(camphor-derived chiral NHC)Cl]PF_6 complex

In an interesting report, Whittlesey et al. reported that reaction of six-membered NHCs with $[Ni(COD)_2]$ facilitates the formation of a C-H activated NHC-Ni(II) complex. However in the presence of $[NiBr_2(PPh_3)_2]$, it yields a novel three-coordinate NHC-Ni(I) species instead (Scheme 1.23).[104]

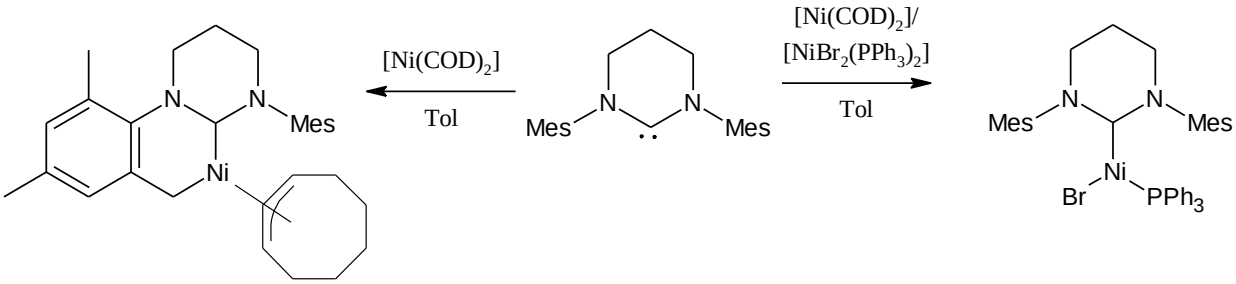

Scheme 1.23. Synthesis of (6-Mes)-Ni(II) and (6-Mes)-Ni(I) complexes

These free carbene procedures are sensitive to both air and moisture hence the reactions have to be performed under inert atmosphere. Free carbenes are susceptible to attack by water which ultimately leads to ring-opening (Scheme 1.24).[105]

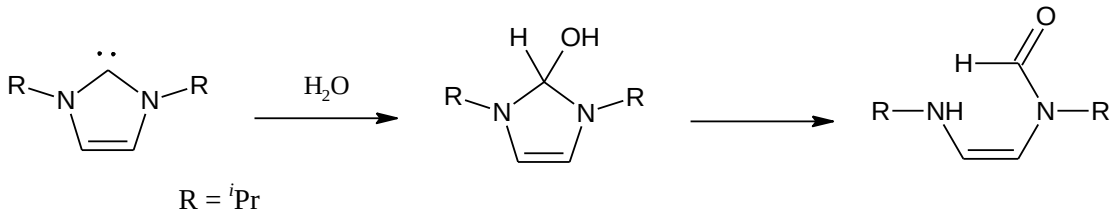

Scheme 1.24. Hydrolysis of NHCs

It is also noteworthy that attempts to react free carbenes, particularly those bearing *N*-mesityl substitutents, with metal complexes at elevated temperatures results in C-H insertion between the carbene centre and the *ortho*-methyl C-H bonds (Scheme 1.25).[106]

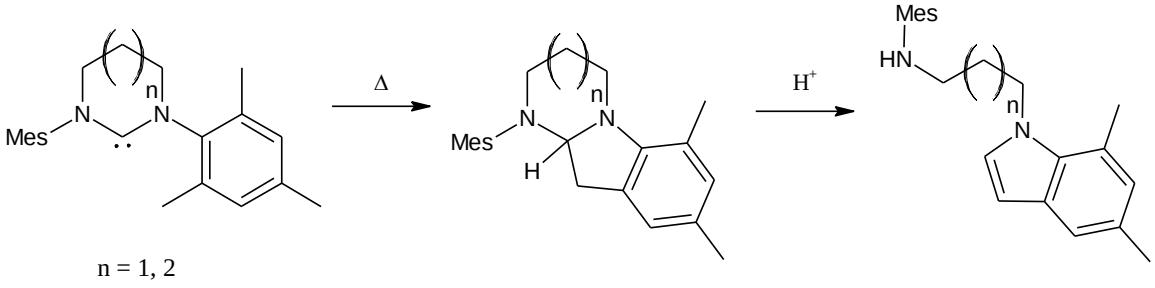

Scheme 1.25. Free carbene undergoing C-H insertion at elevated temperatures

An alternative method employed for the synthesis of NHC complexes involves transferring NHC ligands from one metal complex to another.[107-109] Application of Ag(I) NHC complexes, generated by in-situ deprotonation of the azolium salt with silver oxide or silver carbonate,[110] has evolved into a very useful transmetallation method.[111, 112] This reaction pathway is popular with 5-membered carbenes, however application with expanded ring NHCs are less well defined. A recent example reports the transmetallation of [Ag(I)Br(6-DIPP)] and [Ag(I)Br(7-DIPP)] to give [Cu(I)Br(6-DIPP)] and [Cu(I)Br(7-DIPP)] respectively (Scheme 1.26).[102]

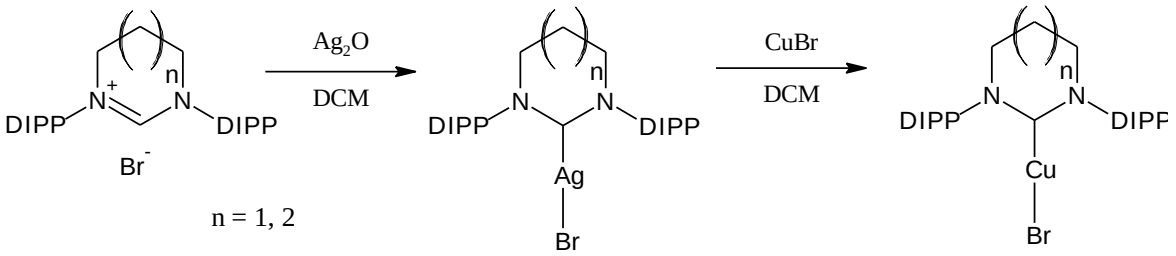

Scheme 1.26. Synthesis of six- and seven-membered Ag(I) complexes followed by transmetallation to Cu(I) complexes

1.9 Structural and electronic effects of NHC-metal complexes

The unique structural and electronic features of NHCs enable them to form strong bonds to late transition metals, to the extent that this class of ligands are slowly replacing phosphine based metal systems due to their (i) stabilizing effect, (ii) high thermal stability and (iii) resistance to dissociation from the metal centre.[113] It was originally thought that the metal-NHC bond was bound only by σ-donation of the carbene. This concept was later replaced by the notion of a synergistic π*-backdonation and π-donation bonding scheme between the metal and the NHC ligand.[114] The strength of this metal-NHC bond depends on the nature of the NHC ligand skeleton, for example saturated NHCs based on the imidazolin-2-ylidene core are considered more basic than those with an aromatic fused ring on the NHC ring, benzimindazol-2-ylidene core, and those of unsaturated NHCs based imidazol-2-ylidene core. This facility coupled with the ability to incorporate different N-substituents allows the electronic and steric properties to be tailored to specific needs. Such modifications provide improved catalytic performances of known organic reactions.[115]

The extent of electron-donation can be measured and quantified using several distinct methods. The latest technique employs the $^{13}C\{^{1}H\}$ chemical shift of the N*C*N carbon in

palladium(II)-benzimidazolylidene complexes as a spectroscopic probe for the donor strength measurement of the NHC ligand trans to it (Figure 1.6).[116] Huynh et. al. applied this method to analyze ten different NHC ligands in the form of hetero-bis(carbene) Pd(II) complexes and found that stronger donating co-ligand lead to a further downfield shift of the $^{13}C\{^{1}H\}$ NMR C_{NHC} carbon atom on the $^{i}Pr_2$-bimy ligand.

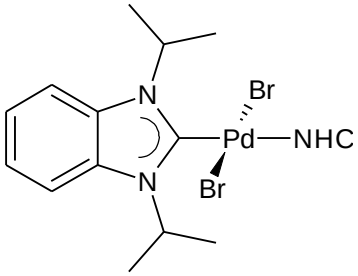

Figure 1.6: [$PdBr_2$($^{i}Pr_2$-bimy)(NHC)] used as a $^{13}C\{^{1}H\}$ spectroscopic probe for NHC donation

One older but more widely known method involves the formation of *cis*-[Rh/IrCl(NHC)$(CO)_2$] complexes and comparison of the IR stretch of the carbonyl monoxide ligands as the NHC is varied. This in effect determines the extent of basicity of the carbene moiety. Such complexes are generally made by passing carbon monoxide gas into an organic solution containing complexes of the type [Rh/IrCl(NHC)(COD)], thus the COD ligand is replaced by two CO units while leaving the metal environment essentially unchanged (Scheme 1.27).[117]

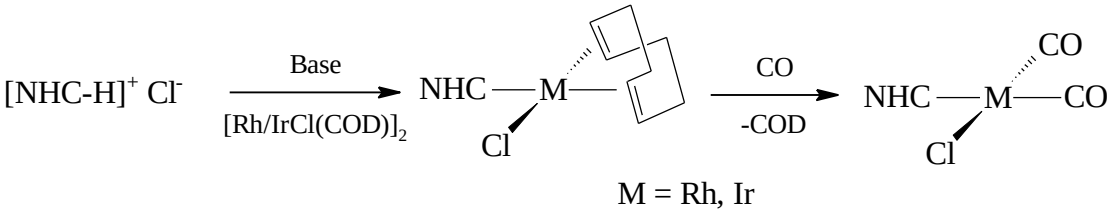

Scheme 1.27. Synthesis of carbene(1,5-cyclooctadiene) and carbene(carbonyl) metal complexes

A low wavenumber (cm^{-1}) will exhibit a very basic NHC ligand with strong σ-donation upon the NHC → metal bond and a slight π-back-donation from the metal to the carbene carbon.[118] Instead, π-electron density will be referred more towards the two π-acidic carbonyl groups. This method for measuring the electronic character is also referred as

'Tolman's electronic parameter' (TEP).[62] It is noteworthy that comparison of these IR data can only be reliable and consistent if the measurements are performed in the same manner, for instance, the same solution (normally with CH_2Cl_2) is used throughout. Otherwise the υ_{CO} values can differ dramatically and direct comparison would be incongruous.[119] In addition, the electronic properties of the NHC ligand are influenced by the nature of its NHC heterocycles, chiefly the position and the type of heteroatoms incorporated. Theoretical calculations of TEP for oxazolylidene, thiazolylidene and triazolylidene were found to be amongst the least electron-rich NHCs.[120] Conversely, it was found that the NHC would become more electron-rich as the ring size increases to six- and seven-membered carbenes.[76, 121]

Structural properties of the NHC ligand also play a big role in determining chemical behaviour between the carbene and metal moieties along with its catalytic performance as a complex. Thus applying the established Tolman cone angle (commonly used for phosphines)[62] to quantify steric properties in NHC ligands will be ill-fitted due to their anisotropic structures and the way different sizes of N-substituents dictate the length and ease of rotation along the metal-NHC bond. Instead, the percent 'buried volume', $\%V_{bur}$ concept was created by Cavallo and co-workers to measure steric demands of NHCs.[122, 123] $\%V_{bur}$ represents the volume of the first coordination sphere around the metal, with a certain radius, that is occupied by the atoms of the ligand under investigation (Figure 1.7).[124] Hence the value of $\%V_{bur}$ increases as the ligand becomes more sterically demanding.

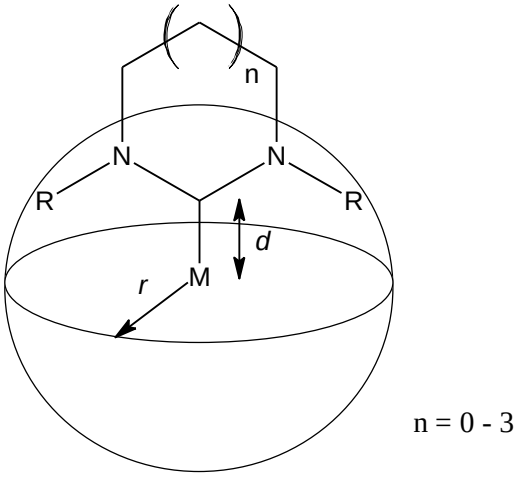

Figure 1.7: Sphere dimension for the $\%V_{bur}$ concept of an NHC ligand

A beneficial feature of using $\%V_{bur}$ to characterize the steric properties of ligands is that it possesses the ability to not only measure NHCs but also tertiary phosphines as well. Unquestionably, it is essential to apply the same set of parameters during the use of this method for various ligand classes in order to keep the comparable results. Common specifications involve a sphere with the radius of 3.5 Å and a distance between the metal and coordinating carbene of 2.0 Å. Calculation for the value of $\%V_{bur}$ can primarily be derived from the ligand structure obtained from crystallographic data.

Clavier and Nolan have carried out an extensive study to determine the buried volume of many NHCs that formed complexes with Group 11 metals.[125] Thus [AgCl(NHC)], [CuCl(NHC)] and [AuCl(NHC)] complexes and their crystal structures were used in this case. These complexes were chosen due to their linear geometry with spectator halide ions that are expected to have little steric influence on the metal centre upon determination and comparison of NHC $\%V_{bur}$. The $\%V_{bur}$ reported for these complexes are represented in Table 1.1.

Table 1.1: $\%V_{bur}$ values of common NHCs in [CuCl(NHC)], [AgCl(NHC)] and [AuCl(NHC)] complexes[a]

NHC	$\%V_{bur}$ (Cu)	$\%V_{bur}$ (Ag)	$\%V_{bur}$ (Au)
Icy[b]	28.8[126]	27.7[127]	27.4[128]
IMes	36.3[129]	36.1[130]	36.5[131]
SIMes	36.9[126]	36.1[127]	36.9[131]
IPr	47.6[132]	46.5[133]	44.5[134]
SIPr	46.4[135]	44.5[133]	47.0[131]

[a]NHC structures extracted from crystal structures (r = 3.5 Å, d = 2.0 Å, Bond radii scaled by 1.17). [b] ICy = dicyclohexylimidazolin-2-ylidene.

A linear correlation between the buried volume of NHCs and the type of N-substituent is observed for these different coinage metal complexes. As the N-substituents become more sterically demanding, $\%V_{bur}$ value for the corresponding NHC increases. However, the case of IPr/SIPr proved exceptional in that the $\%V_{bur}$ of SIPr ligand is bigger compared to IPr in [AuCl(NHC)] complexes, but smaller for the Ag and Cu chloride complexes. There are no clear reasons why this is. Overall, the buried volume for some of the most common NHCs (measured in NHC coinage metal chloride complexes) lies in the region from 36% to 48%. Interestingly, square-planar $[Ir(NHC)(CO)_2Cl]$ complexes with e.g. IMes/SIMes and IPr/SIPr give smaller buried volumes (in a range between 33.5% and 38%) compared to those of the

linear [AuCl(NHC)] complexes.[124] Thus this proves that the extent of steric hinderance induced by different NHCs are changeable and dependent upon the nature of the metal complexes they are coordinated to and the relative orientation of the exocyclic N-substituents. In an extensive report, Frenking and co-workers determined the interactions between NHCs and group 11 metals using DFT calculations at BP86 level via energy decomposition analysis (otherwise known as EDA, the energy difference between the molecule and the broken fragments of NHC ligand and metal complex in frozen geometry of the compounds before interconnection occurs).[136, 137] The total interaction energy of (NHC)-M bond in monomeric (NHC)-MCl systems increases with the order Ag < Cu < Au. The attractive energy between the ligand and the metal consists of electrostatic contribution of 75% or higher and the π contribution to the total orbital energy ranges from 27% to 38%.

The first isolated 14 electron two-coordinate Ni(0) and Pt(0) complexes bearing IMes NHC ligands were reported by Arduengo in 1994.[138] Structural X-ray diffraction analysis of both complexes exhibited abnormally short carbene-metal bond distances, to which the authors deduced that the cause of this effect was a result of M → NHC π*-backdonation. In support of this theory, Jacobsen et al. conducted bond analysis DFT studies upon d^{10} metal systems of [M(NHC)(ethylene)$_2$] and [Ni(NHC)(CO)$_2$], where NHC is imidazol-2-ylidene and M are Ni, Pd, Pt.[67] Both Ni(0) systems afforded reasonably high π contribution, of 24-25%, to the total bond orbital interaction and > 95% of which is due to M → NHC π*-backdonation. Pd(0) and Pt(0) on the other hand, afforded π contribution of < 20% of which 85-90% is due to the M → NHC π*-backdonation.

Efforts to understand the unique properties of carbenes and their influence upon the metal complex have progressed significantly over the pass decade (their structural and electronic features summarized above). This was made possible by the use of X-ray diffraction, NMR spectroscopy, IR spectroscopy and density functional theory. However, paramagnetic NHC complexes with e.g. Cr(I) based metals require the use of electron paramagnetic resonance (EPR) spectroscopy.[139-141] EPR spectroscopy is widely used to analyse species with one or more unpaired electrons such as free radicals and other unstable paramagnetic compounds generated in *situ*. Most importantly, this technique determines the structural and electronic information of these compounds. There are many textbooks which explain in detail the applied physics of this technique and its practicality among different areas of chemistry.[142-144]

1.10 Catalysis with expanded ring-NHC metal complexes

One of the main purposes for the synthesis of metal-NHC complexes is their application in homogeneous catalysis. They provide improved catalytic performance with possibility for topological modification of the already established metal based catalysts.[115, 145, 146] Details of different catalytic reactions using five-membered NHC metal complexes can be found in various reviews.[60, 147-152] Therefore, catalysis with large ring NHC metal complexes will be the main discussion in this section.

Buchmeiser and colleagues examined the catalytic activity of 1,3-dialkyl- and 1,3-diaryl-substituted [Pd(6-NHC)] complexes in Heck-type reactions.[153] The expanded bis-NHC palladium(II) complexes were found to be good catalysts for the coupling of aliphatic and aromatic vinyl compounds with aryl bromides and chlorides. Using 0.00005 mol% catalyst gave TONs of up to 2×10^6. Siemeling et al. studied the catalytic behaviour of *trans*-[$PdCl_2$(**1**-Np)$_2$] in Mizoroki-Heck reactions between *n*-butyl acrylate and aryl bromides (Scheme 1.28).[154] The results were compared to those of the [$PdCl_2$(THP-*i*Pr)$_2$] complex reported by Buchmeiser and co-workers.[153] The reactions were conducted in dimethylacetamide with 0.05 mol% of catalyst and sodium acetate as base. In some cases the two catalysts showed similar results, e.g. cross-coupling of butyl acrylate with bromobenzene gave TONs of 1.6×10^3 and 1.8×10^3 for [$PdCl_2$(**1**-Np)$_2$] and [$PdCl_2$(THP-*i*Pr)$_2$] respectively. But overall, the respective THP-iPr-containing complex was the better catalyst.

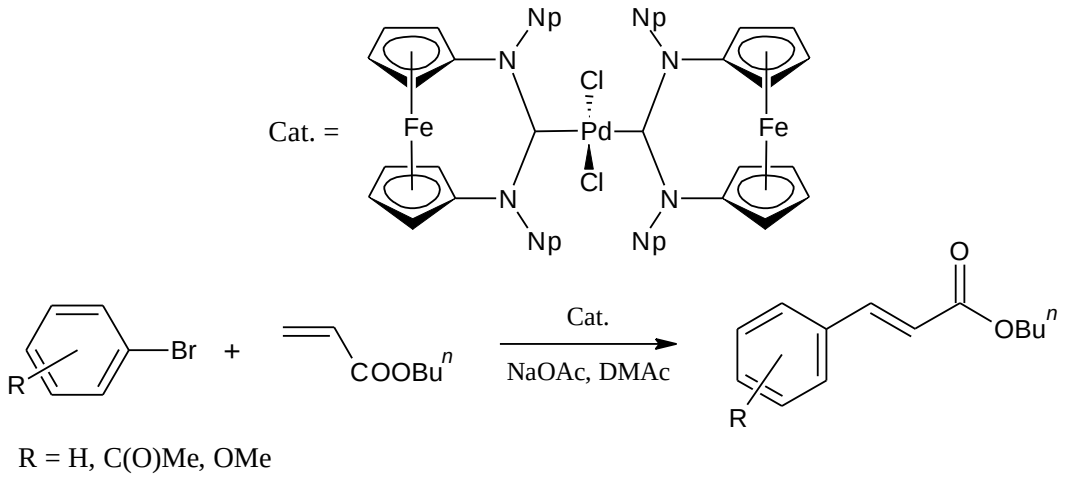

Scheme 1.28. *trans*-[$PdCl_2$(**1**-Np)$_2$] catalyzed Heck cross-coupling of n-butyl acrylate with Br-*p*-C_6H_4-R.

The *cis*-[$PdCl_2$(**1**-Np)(PPh_3)] complex was tested in Suzuki-Miyaura cross-coupling reactions of $PhB(OH)_2$ with *p*-substituted aryl halides. The catalytic activity of this complex was compared to those of *cis*-[$PdCl_2$(THP-*i*Pr)(PPh_3)] reported by Herrmann and co-workers.[155] It was found that both catalysts gave TONs of the order of 10^6 with aryl bromide substrates; whereas for aryl chlorides, the latter complex demonstrated superior performance.

Cavell and co-worker studied a series of 6- and 7-membered NHC-Pd divinyltetramethyldisiloxane (dvtms) complexes in the Mizoroki-Heck coupling of 4-bromoacetophenone and *n*-butyl acrylate.[156] These systems significantly outperformed their 5-membered NHC Pd counterparts with the 7-membered derivatives displaying the greatest catalytic efficiency. Using 0.1 mol% of [Pd(7-NHC)(dvtms)] complex gave 100% conversion after 3 h, whereas the complexes bearing 6- and 5-NHC ligands demonstrated overall percentage conversion of 85% and 14% respectively.

McQuade and colleagues reported a chiral six-membered NHC Cu(I) complex that could catalyze β-borylations with high yield and enantioselectivity.[101] This catalyst proved to be very stable, showing 10^3 TONs at 0.01 mol% of catalyst.

Furthermore, a gold complex bearing a seven-membered N,N'-diamidocarbene was found to facilitate the hydration of phenylacetylene to acetophenone in yields up to 78% after 12 h at 80°C at catalyst loading of 2 mol%.[93]

Cavell et al. also investigated unsymmetrical *N*,*N*'-substituted 6- and 7-membered NHC Rh(I) complexes in hydrogenation of alkenes (Scheme 1.29).[157] The enhanced catalytic activity of these expanded ring NHC complexes was attributed to a linear [RhCl(NHC)] species, stabilized by the presence of weakly coordinated ethanol solvent. Complete conversions were recorded within 24 h for 1 mol% catalyst loading at 3.5 atm H_2.

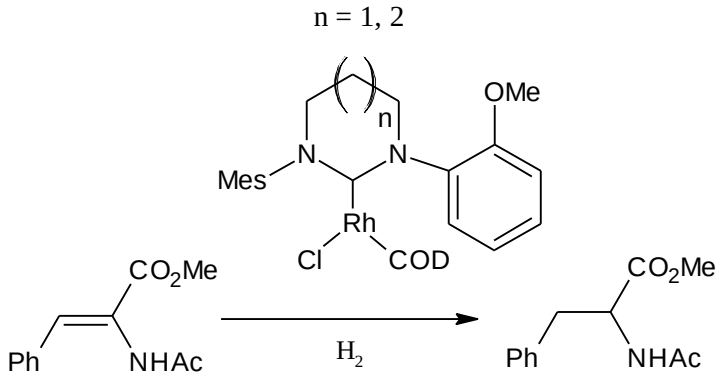

Scheme 1.29. Catalytic hydrogenation of alkene with [RhCl(6-/7-NHC)(COD)]

Ir(I) complexes bearing *o*-methoxyphenyl-functionalised 6- and 7-NHCs showed excellent catalytic activity in transfer hydrogenations of ketones.[158] Full conversions were observed after 20 min, giving an estimated TOF_{50} of 1500 h^{-1} for 1 mol% catalyst concentration in the transfer hydrogenation of 4-bromoacetophenone (Scheme 1.30). Using catalyst loadings of 0.1 and 0.01 mol% also gave near 100% conversion, whereas the Rh complexes bearing the same ligands showed no activity. The strong donor properties coupled with the steric demands of the large ring NHCs, resulting from their large NCN angles, may play an important role in the catalytic performance of the Ir systems.

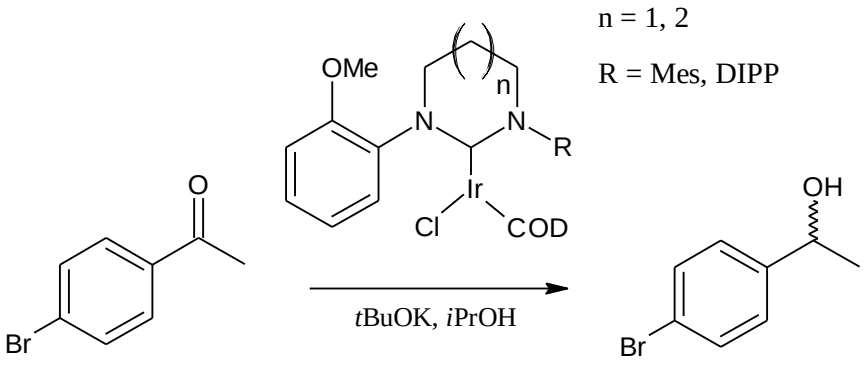

Scheme 1.30. Transfer hydrogenation of 4-bromoacetophenone with Ir complexes of *o*-methoxyphenyl-functionalised NHCs

Rh and Ir complexes containing asymmetric bicyclic NHC bearing secondary pyridyl donors were also used in catalytic transfer hydrogenation reactions of prochiral ketones.[159] These reactions were conducted in *i*PrOH solvent at reflux in the presence of 10% KOH. Complete conversion was achieved only for the acetophenone substrate with NHC-Ir complex at 0.1 mol%. Enantioselectivity was not monitored in the catalysis.

Platinum complexes bearing 6-NHC/dvtms ligands were reported to be good catalysts for hydrosilylation reactions.[103] The choice of silane and catalytic system determines the outcome of the hydrosilylation transformations. For example, hydrosilylation of 1-octyne with 0.005 mol% [Pt(6-NHC)(dvtms)] catalyst affords three possible regioisomers (Scheme 1.31). Using triethylsilane as the substrate, the Pt complexes bearing 6-Mes and 6-*o*-Tol ligands gave decent yields with the β-(E) product as the major isomer and TOF of 12500 and 9090 h^{-1} respectively. But changing the substrate silane to bis(trimethylsiloxy)methylsilane, the percentage yield drops from 82.7 to 75 and 86.5 to 18.7 for 6-Mes and 6-*o*-Tol-Pt

complex respectively. Meanwhile the steric demand of the catalyst systems has little effect on the regioselectivity of the products.

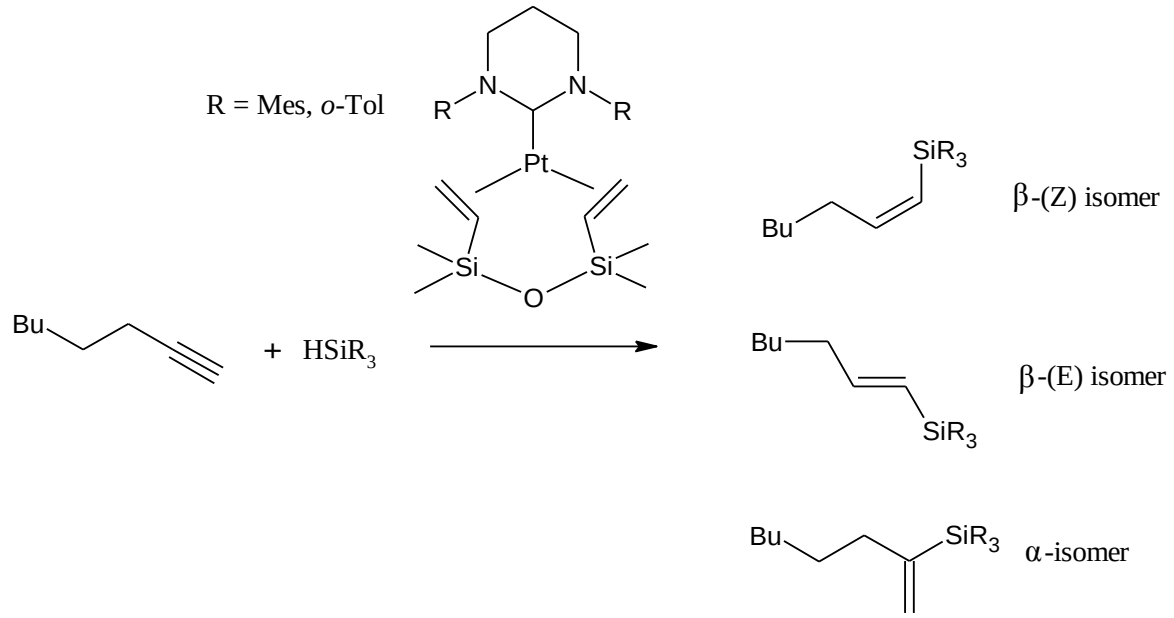

Scheme 1.31. [Pt(6-NHC)(dvtms)] catalyzed hydrosilylation transformations of 1-octyne

Whittlesey et al. reported a rare three coordinate [Ni(I)Br(6-Mes)(PPh_3)] species.[104] This complex was used as a precursor for the hydrodehalogenation of aryl halides; 4.5 mol% of this catalyst gave complete reduction of 1-bromo-4-fluorobenzene to fluorobenzene at room temperature in 30 min. Other substrates were also tested, such as 1-chloro-4-fluorobenzene and fluorobenzene, but they only achieved conversions of 73% in 48 h and 18% in 22 h respectively.

1.11 Thesis overview

The work presented in this thesis focuses on the construction, development and characterisation of novel expanded-(8-membered)-ring NHCs. Their electronic and structural properties will be compared to those of the already known five-, six- and seven-membered carbenes. These ligands will also be coordinated to various metal systems and employed in catalytic reactions to evaluate their effectiveness against the more well known-types. Hopefully, these investigations will help us identify and understand what the limitations are for NHCs and thus narrow the gap between studies of five-membered and the expanded carbenes.

1.12 References

1. Bourissou, D.; Guerret, O.; Gabbai, F. P.; Bertrand, G. *Chem. Rev.* **2000**, 100, 39.
2. Buchner, E.; Curtis, T. *Ber. Dtsch Chem. Ges.* **1885**, 2377.
3. Frémonta, P.; Marionb, N.; Nolan, S. P. *Coordination Chemistry Reviews* **2009**, 253, 862–892.
4. Hine, J. *J. Am. Chem. Soc.* **1950**, 72, 2438.
5. Urry, W. H.; Eizner, J. R. *J. Am. Chem. Soc.* **1951**, 73, 2977.
6. Hennion, G. F.; Maloney, D. E. *J. Am. Chem. Soc.* **1951**, 73, 4735.
7. Doering, W. E.; Knox, L. H. *J. Am. Chem. Soc.* **1953**, 75, 297.
8. Doering, W. E.; Hoffmann, A. K. *J. Am. Chem. Soc.* **1954**, 76, 6162.
9. Parham, W. E.; Reiff, H. E. *J. Am. Chem. Soc.* **1955**, 77, 1177.
10. Parham, W .E.; Twelves, R. R. *J. Org. Chem.* **1957**, 22, 730.
11. Skell, P. S.; Sandler, S. R. *J. Am. Chem. Soc.* **1958**, 80, 2024.
12. Wanzlick, H. W.; *Angew. Chem. Int. Ed.* **1962**, 1, 75.
13. Bohm, V. P. W.; Herrmann, W. A. *Angew. Chem. Int. Ed.* **2000**, 39, 4036 – 4038.
14. Lemal, D. M.; Lovald, R. A.; Kawano, K. I. *J. Am. Chem. Soc.* **1964**, 86, 2518 – 2519.
15. Denk, M. K.; Hatano, K.; Ma, M. *Tetrahedron Lett.* **1999**, 40, 2057 – 2060.
16. Liu, Y.; Lemal, D. M. *Tetrahedron Lett.* **2000**, 41, 599 – 602.
17. Kirmse, W. *Angew. Chem. Int. Ed.* **2010**, 49, 8798 – 8801.
18. Wanzlick, H. W.; Schonherr, H. J. *Angew. Chem. Int. Ed.* **1968**, 7, 141-142.
19. Arduengo, A. J.; Harlow, R. L.; Kline, M. A. *J. Am. Chem. Soc.* **1991**, 113, 361-363.
20. Hoffmann, R.; Gleiter, R. *J. Am. Chem. Soc.* **1968**, 90, 5457.
21. Hoffmann, R.; Zeiss, G. D.; Vandine, G. W. *J. Am. Chem. Soc.* **1968**, 90, 1485.
22. Schuster, G. B. *Adv. Phys. Org. Chem.* **1986**, 22, 311.
23. Tomioka, H.; Hattori, M.; Hirai, K.; Murata, S. *J. Am. Chem. Soc.* **1996**, 118, 8723.
24. Regitz, M. *Angew. Chem., Int. Ed.* **1991**, 30, 674.
25. Iwamoto, E.; Hirai, K.; Tomioka, H. *J. Am. Chem. Soc.* **2003**, 125, 14664.
26. Tomioka, H.; Watanabe, T.; Hattori, M.; Nomura, N.; Hirai, K.; *J. Am. Chem. Soc.* **2002**, 124, 474.
27. Irikura, K. K.; Goddard, W. A.; Beauchamp, J. L. *J. Am. Chem. Soc.* **1992**, 114, 48.
28. Hoffmann, R.; Zeiss, G. D.; Van Dine, G.W. *J. Am. Chem. Soc.* **1968**, 90, 1485.
29. Schmidt, A.; Habeck, T. *Lett. Org. Chem.* **2005**, 2, 37.

30. Lavallo, V.; Canac, Y.; Donnadieu, B.; Schoeller, W. W.; Bertrand, G. *Science* **2006**, 312, 722.
31. Fedorynski, M. *Chem. Rev.* **2003**, 103, 1099.
32. Moss, R. A.; Wlostowski, M.; Shen, S.; Krogh-Jespersen, K.; Matro, A. *J. Am. Chem. Soc.* **1988**, 110, 4443.
33. Liu, X.; Chu, G.; Moss, R. A.; Sauers, R. R.; Warmuth, R. *Angew. Chem., Int. Ed.* **2005**, 44, 1994.
34. Kovacs, D.; Lee, M. S.; Olson, D.; Jacskon, J. E. *J. Am. Chem. Soc.* **1996**, 118, 8144.
35. Pauling, L. *Chem. Commun.* **1980**, 688.
36. Klusik, H.; Berndt, A. *Angew. Chem., Int. Ed.* **1983**, 22, 877.
37. Budzelaar, P. H. M.; Krogh-Jepersen, K.; Clark, T.; Schleyer, P. v. R. *J. Am. Chem. Soc.* **1985**, 107, 2773.
38. Menzel, M.; Winckler, H. J.; Ablelom, T.; Steiner, D.; Fau, S.; Frenking, G.; Massa, W.; Berndt, A. *Angew. Chem., Int. Ed.* **1995**, 34, 1340.
39. Meyer, H.; Baum, G.; Massa, W.; Berndt, A. *Angew. Chem., Int. Ed.* **1987**, 26, 798.
40. Dyer, P.; Baceiredo, A.; Bertrand, G. *Inorg. Chem.* **1996**, 35, 46.
41. Dixon, D. A.; Dobbs, K. D.; Arduengo, A. J.; Bertrand, G. *J. Am. Chem. Soc.* **1991**, 113, 8782.
42. Despagnet, E.; Gornitzka, H.; Rozhenko, A. B.; Schoeller, W. W.; Bourissou, D.; Bertrand, G. *Angew. Chem., Int. Ed.* **2005**, 41, 2835.
43. Lavallo, V.; Canac, Y.; DeHope, A.; Donnadieu, B.; Bertrand, G. *Angew. Chem., Int. Ed.* **2005**, 44, 7236.
44. Canac, Y.; Conejero, S.; Donnadieu, B.; Schoeller, W. W.; Bertrand, G. *J. Am. Chem. Soc.* **2005**, 127, 7312.
45. Fischer, E. O.; Maasbol, A. *Angew. Chem. Int. Ed.* **1964**, 3, 580.
46. Schrock, R. R. *J. Am. Chem. Soc.* **1974**, 96, 6796.
47. Taylor, T. E.; Hall, M. B. *J. Am. Chem. Soc.* **1984**, 106, 1576.
48. Vyboishchikov, S. F.; Frenking, G. *Chem. Eur. J.* **1998**, 4, 1428.
49. Lappert, M. F. *J. Organomet. Chem.* **1988**, 358, 185.
50. Kantchev, E. A. B.; O'Brien, C. J.; Organ, M. G. *Angew. Chem. Int. Ed.* **2007**, 46, 2768.
51. Clavier, H.; Nolan, S. P. *Annu. Rep. Prog. Chem., Sect. B.* **2007**, 103, 193.
52. Gade, L. H.; Bellemin-Laponnaz, S. *Coord. Chem. Rev.* **2007**, 251, 718.
53. Sommer, W. J.; Weck, M. *Coord. Chem. Rev.* **2007**, 251, 860.

54. Schwab, P.; Grubbs, R. H.; Ziller, J. W. *J. Am. Chem. Soc.* **1996**, 118, 100-110.
55. Scholl, M.; Ding, S.; Lee, C. W.; Grubbs, R. H. *Org. Lett.* **1999**, 1, 953.
56. Huang, J.; Stevens, E. D.; Nolan, S. P.; Petersen, J. L. *J. Am. Chem. Soc.* **1999**, 121, 2674–2678.
57. Antonova, N. S.; Carbo, J. J.; Poblet, J. M. *Organometallics* **2009**, 28, 4283–4287.
58. Lund, C. L.; Sgro, M. J.; Cariou, R.; Stephan, D. W. *Organometallics* **2012**, 31, 802-805.
59. Arduengo, A. J.; Dias, H. V. R.; Harlow, R. L.; Kline, M. *J. Am. Chem. Soc.* **1992**, 114, 5530.
60. Hahn, F. E.; Jahnke, M. C. *Angew. Chem., Int. Ed.* **2008**, 47, 3122.
61. Dias, P. B.; Minas de Piedade, M. E.; Martinho Simões, J. A. *Coord. Chem. Rev.* **1994**, 135, 737-807.
62. Tolman, C. A. *Chem. Rev.* **1977**, 77, 313.
63. Green, J. C.; Scur, R. G.; Arnold, P. L.; Cloke, G. N. *Chem. Commun.* **1997**, 1963–1964.
64. Peris, E.; Crabtree, R. H. *Coord. Chem. Rev.* **2004**, 248, 2239.
65. Magill, A. M.; Cavell, K. J.; Yates, B. F. *J. Am. Chem. Soc.* **2004**, 126, 8717-8724.
66. Radius, U.; Bickelhaupt, F. M. *Organometallics* **2008**, 27, 3410.
67. Jacobsen, H.; Correa, A.; Costabile, C.; Cavallo, L. *J. Organomet. Chem.* **2006**, 691, 4350.
68. Schwarz, J.; Bohm, V. P. W.; Gardiner, M. G.; Grosche, M.; Herrmann, W. A.; Hieringer, W.; Raudaschl-Sieber, G. *Chem.-Eur. J.* **2000**, 6, 1773.
69. Hillier, A. C.; Sommer, W. J.; Yong, B. S.; Peterson, J. L.; Cavallo, L.; Nolan, S. *Organometallics* **2003**, 22, 4322-4326.
70. Crabtree, R. H. *J. Organomet. Chem.* **2005**, 690, 5451-5457.
71. Benhamou, L.; Chardon, E.; Lavigne, G.; Laponnaz, S. B.; Cesar, V. *Chem. Rev.* **2011**, 111, 2705–2733.
72. Frémont, P.; Marion, N.; Nolan, S. P. *Coordination Chemistry Reviews* **2009**, 253, 862–892.
73. Iglesias, M.; Beetstra, D. J.; Stasch, A.; Horton, P. N.; Hursthouse, M. B.; Coles, S. J.; Cavell, K. J.; Dervisi, A.; Fallis I. A. *Organometallics* **2007**, 26, 4800.
74. Reddy, P. V. G.; Tabassum, S.; Blanrue, A.; Wilhelm, R. *Chem. Commun.* **2009**, 5910.
75. Newman, P. D.; Cavell, K. J.; Kariuki, B. M. *Organometallis* **2010**, 29, 2724.

76. Iglesias, M.; Beetstra, D. J.; Stasch, A.; Horton, P. N.; Hursthouse, M. B.; Coles, S. J.; Cavell, K. J.; Dervisi, A.; Fallis I. A. Organometallics. **2007**, 26, 4800.
77. Iglesias, M.; Beetstra, D. J.; Knight, J. C.; Ooi, L.; Stasch, A.; Male, L.; Hursthouse, M. B.; Coles, S. J.; Cavell, K. J.; Dervisi, A.; Fallis, I. A. *Organometallics* **2008**, 27, 3279.
78. Bazinet, P.; Yap, G. P. A.; Richeson, D. S. *J. Am. Chem. Soc.* **2003**, 125, 13314.
79. Bazinet, P.; Ong, T. G.; O'Brien, J. S.; Lavoie, N.; Bell, E.; Yap, G. P. A.; Korobkov, I.; Richeson, D. S. *Organometallics* **2007**, 26, 2885.
80. Scarborough, C. C.; Popp, I. A.; Guzei, B. V.; Stahl, S. S. *J. Organomet. Chem.* **2005**, 690, 6143.
81. Scarborough, C. C.; Grady, M. J. W.; Guzei, I. A.; Gandhi, B. A.; Bunel, E. E.; Stahl, S. S. *Angew. Chem. Int. Ed.* **2005**, 44, 5269.
82. Siemeling, U.; Farber, C.; Bruhn, C. *Chem. Commun.* **2009**, 98.
83. Siemeling, U.; Farber, C.; Leibold, M.; Bruhn, C.; Mucke, P.; Winter, R. F.; Sarkar, B.; Hopffgarten, M. V.; Frenking, G. *Eur. J. Inorg. Chem.* **2009**, 4607.
84. Khramov, D. M.; Rosen, E. L.; Lynch, V. M.; Bielawski, C. W. *Angew. Chem. Int. Ed.* **2006**, 47, 2267.
85. Rosen, E. L.; Varnado, C. D.; Tennyson, A. G.; Khramov, D. M.; Kamplain, J. W.; Sung, D. H.; Cresswell, P. T.; Lynch, V. M.; Bielawski, C. W. *Organometallics* **2009**, 28, 6695.
86. Orelli, L. R.; Garcia, M. B.; Perillo, I. A. *Heterocycles* **2000**, 53, 2437.
87. Mayr, M.; Wurst. K.; Onania, K. H.; Buchmeiser, M. R. *Chem. Eur. J.* **2004**, 10, 1256-1266.
88. Mayr, M.; Buchmeiser, M. R. *Macromol. Rapid Commun*. **2004**, 25, 231.
89. Yun, J.; Marinez, E. R.; Grubbs, R. H. *Organometallics* **2004**, 23, 4172.
90. Cotton, F. A.; Haefner, S. C.; Matonic, J. H.; Wang, X.; Murillo, C. A. *Polyhedron* **1997**, 16, 541.
91. Jazzar, R.; Donnadieu, B.; Bertrand, G. *J. Organomet. Chem.* **2006**, 691, 3201.
92. Iglesias, M.; Beestra, D. J.; Knight, J. C.; Ooi, L.; Stasch, A.; Male, L.; Hursthouse, M. B.; Coles, S. J.; Cavell, K. J.; Dervisi, A.; Fallis, I. A. *Organometallics* **2008**, 27, 3279.
93. Hudnall, T. W.; Tennyson, A. G.; Bielawski, C. W. *Organometallics* **2010**, 29, 4569.
94. Lu, W. Y.; Cavell, K. J.; Wixey, J. S.; Kariuki, B. *Organometllics* **2011**, 30, 5649–5655.

95. Higgins, E. M.; Sherwood, J. A.; Lindsay, A. G.; Armstrong, J.; Massey, R. S.; Alder, R. W.; O'Donoghue, A. C. *Chem. Commun.* **2011**, 47, 1559-1561.
96. Weskamp, T.; Böhm, V. P. W.; Herrmann, W. A. *J. Organomet. Chem.* **2000**, 600, 12.
97. Herrmann, W. A.; Kocher, C.; Goossen, L. J.; Artus, G. R. J. *Chem. Eur. J.* **1996**, 2, 1627.
98. Herrmann, W. A.; Elison, M.; Fischer, J.; Kocher, C.; Artus, G. R. *J. Angew. Chem. Int. Ed.* **1995**, 34, 2371.
99. Weskamp, T.; Schattenmann, W. C.; Spiegler, M.; Herrmann, W. A. *Angew. Chem. Int. Ed.* **1998**, 37, 2490.
100. Douthwaite, R. E.; Haussinger, D.; Green, M. L. H.; Silcock, P. J.; Gomes, P. T.; Martins, A. M.; Danopolous, A. A. *Organometallics* **1999**, 18, 4584.
101. Park, J. K.; Lackey, H. H.; Rexford, M. D.; Kovnir, K.; Shatruk, M.; McQuade, D. T. *Org. Lett.* **2010**, 12, 5008-5011.
102. Kolychev, E. L.; Portnyagin, I. A.; Shuntikov, V. V.; Khrustalev, V. N.; Nechaev, M. S. *J. Organomet. Chem.* **2009**, 694, 2454-2462.
103. Dunsford, J. J.; Cavell, K. J.; Kariuki, B. *J. Organomet. Chem.* **2011**, 696, 188-194.
104. Davies, C. J. E.; Page, M. J.; Ellul, C. E.; Mahon, M. F.; Whittlesey, M. K. *Chem. Commun.* **2010**, 46, 5151-5153.
105. Denk, M. K.; Rodezno, J. M.; Gupta, S.; Lough, A. J. *J. Organomet. Chem.* **2001**, 617, 242.
106. Holdroyd, R. S.; Page, M. J.; Warren, M. R.; Whittlesey, M. K. *Tetrahedron Lett.* **2010**, 51, 557-559.
107. Wang H. M. J.; Lin, I. J. B.; *Organometallics* **1998**, 17, 972.
108. Liu, S. T.; Hsieh, T. Y.; Lee, G. H.; Peng, S. M. *Organometallics* **1998**, 17, 993.
109. Ku, R. Z.; Huang, J. C.; Cho, J. Y.; Kiang, F. M.; Reddy, K. R.; Chen, Y. C.; Lee, K. J.; Lee, J. H.; Lee, G. H.; Peng, S. M.; Liu, S. T. *Organometallics* **1999**, 18, 2145.
110. Wang, X.; Liu, S.; Jin, G. X. *Organometallics* **2004**, 23, 6002.
111. McGuinness, D. S.; Cavell, K. J. *Organometallics* **2000**, 19, 741.
112. Magill, A. M.; McGuinness, D. S.; Cavell, K. J.; Britovsek, G. J. P.; Gibson, V. C.; White, A. J. P.; Williams, D. J.; White, A. H.; Skelton, B. W. *J. Organomet. Chem.* **2001**, 617, 546.
113. Herrmann, W. A. *Angew. Chem. Int. Ed.* **2002**, 41, 1291.
114. Jacobsena, H.; Correab, A.; Poaterb, A.; Costabile, C.; Cavallo, L. *Coordination Chemistry* **2009**, 253, 687-703.

115. Bantreil, X.; Broggi, J.; Nolan, S. P. *Annu. Rep. Prog. Chem., Sect. B: Org. Chem.* **2009**, 105, 232–263.
116. Huynh, H. V.; Han, Y.; Jothibasu, R.; Yang, J. A. *Organometallics* **2009**, 28, 5395.
117. Herrmann, W. A.; Schutz, J.; Frey G. D.; Herdtweck, E. *Organometallics* **2006**, 25, 2437-2448.
118. Denk, K.; Sirsch, P.; Herrmann, W. A. *J. Organomet. Chem.* **2002**, 649, 219.
119. Furstner, A.; Alcarazo, M.; Krause, H.; Lehmann, C. W.; *J. Am. Chem. Soc.* **2007**, 129, 12676-12677.
120. Hudnall, T. W.; Moorhead, E. J.; Gusev, D. G.; Bielawski, C. W.; *J. Org. Chem.* **2010**, 75, 2763.
121. Scarborough, C. C.; Guzei, I. A.; Stahl, S.S. *Dalton Trans.* **2009**, 2284.
122. Cavallo, L.; Correa, A.; Costabile, C.; Jacobsen, H. *J. Organomet. Chem.* **2005**, 690, 5407.
123. Poater, A.; Cosenza, B.; Correa, A.; Giudice, S.; Ragone, F.; Scarano, V.; Cavallo, L. *Eur. J. Inorg. Chem.* **2009**, 1759.
124. Droge, T.; Glorius, F. *Angew. Chem. Int. Ed.* **2010**, 49, 6940-6952.
125. Clavier, H.; Nolan, S. P. *Chem. Commun.* **2010**, 841.
126. Diez-Gonzalez, S.; Kaur, H.; Zinn, F. K.; Stevens, E. D.; Nolan, S. P. *J. Org. Chem.* **2005**, 70, 4784.
127. Fremont, P.; Scott, N. M.; Stevens, E. D.; Ramnial, T.; Lightbody, O. C.; Macdonald, C. L. B.; Clyburne, J. A. C.; Abernethy, C. D.; Nolan, S. P. *Organometallics* **2005**, 24, 6301.
128. Frey, G. D.; Lavallo, V.; Donnadieu, B.; Schoeller, W. W.; Bertrand, G. *Science* **2007**, 316, 439.
129. Broggi, J.; Diez-Gonzalez, S.; Petersen, J. L.; Berteina-Rabion, S.; Nolan, S. P.; Agrofoglio L. A. *Synthesis* **2008**, 141.
130. Raminal, T.; Abernethy, C. D.; Spicer, M. D.; McKenzie, I. D.; Gay, I. D.; Clyburne, J. A. C. *Inorg. Chem.* **2003**, 42, 1391.
131. Fremont, P.; Sott, N. M.; Stevens, E. D.; Nolan, S. P. *Organometallics* **2005**, 24, 2411.
132. Kaur, H.; Zinn, F. K.; Stevens, E. D.; Nolan, S. P. *Organometallics* **2004**, 23, 1157.
133. Yu, X. Y.; Patrick, B. O.; James, B. R. *Organometallics* **2006**, 25, 2359.
134. Fructos, M. R.; Belderrain, T. R.; Fremont, P.; Scott, N. M.; Nolan, S. P.; Diaz-Requejo, M. M.; Perez, P. J. *Angew. Chem.* **2005**, 117, 5418.
135. Diez-Gonzalez, S.; Stevens, E. D.; Nolan, S. P. *Chem. Commun.* **2008**, 4747.

136. Nemcsok, D.; Wichmann, K.; Frenking, G. *Organometallics* **2004**, 23, 3640.
137. Bickelhaupt, F. M.; Baerends, E. J. *Rev. Comp. Chem.* **2000**, 15, 1.
138. Arduengo, A. J.; Camper, S. F.; Calabrese, J. C.; Davidson, F. *J. Am. Chem. Soc.* **1994**, 116, 4391-4394.
139. Sakurai, H.; Sugitani, K.; Moriuchi, T.; Hirao, T. *J. Organomet. Chem.* **2005**, 690, 1750.
140. McDyre, L. E.; Hamilton, T.; Murphy, D. M.; Cavell, K. J.; Gabrielli, W. F.; Hanton, M. J.; Smith, D. M. *Dalton Trans.* **2010**, 39, 7792-7799.
141. Lappert, M. F.; McCabe, R. W.; MacQuitty, J. J.; Pye, P. L.; Riley, P. I. *Dalton Trans.* **1980**, 90.
142. Wertz, J. E.; Bolton, A. R. *Electron Spin Resonance: Elementary Theory and Practical Applications* **1972**, McGraw-Hill Inc, New York.
143. Gilbert, B. C.; Davies, M. J.; Murphy, D. M.; Beckert, D. *Electron Paramagnetic Resonance* **2002**, Royal Society of Chemistry.
144. Mabbs, F. E.; Collison, D. *Electron Paramagnetic Resonance of d-transition Metal Compounds* **1992**, Elsevier Science Publisher B. V., Amsterdam.
145. Zinn, F. K.; Viciu, M. S.; Nolan, S. P. *Annu. Rep. Prog. Chem., Sect. B.* **2004**, 100, 231-249.
146. Navarro, O.; Viciu, M. S. *Annu. Rep. Prog. Chem., Sect. B.* **2010**, 106, 243–259.
147. Corberán, R.; Mas-Marzá, E.; Peris, E. *Eur. J. Inorg. Chem.* **2009**, 1700–1716.
148. Praetorius, J. M.; Crudden, C. M. *Dalton Trans.* **2008**, 4079–4094.
149. Diez-Gonzalez, S.; Marion, N.; Nolan, S. P. *Chem. Rev.* **2009**, 109, 3612–3676.
150. Poyatos, M.; Mata, J. A.; Peris, E. *Chem. Rev.* **2009**, 109, 3677–3707.
151. Fortman, G. C.; Nolan, S. P. *Chem. Soc. Rev.* **2011**, 40, 5151-5169.
152. Gil, W.; Trzeciak, A. M. *Coord. Chem. Rev.* **2011**, 255, 473-483.
153. Mayr, M.; Wurst, K.; Onania, K. H.; Buchmeiser, M. R. *Chem. Eur. J.* **2004**, 10, 1256-1266.
154. Siemeling, U.; Faber, C.; Bruhn, C.; Furmeier, S.; Schulz, T.; Kurlemann, M.; Tripp, S. *Eur. J. Inorg. Chem.* **2012**, 1413-1422.
155. Schneider, S. K.; Herrmann, W. A.; Herdtweck, E. *J. Mol. Catal. A.* **2006**, 245, 248-254.
156. Dunsford, J. J.; Cavell, K. J. *Dalton Trans.* **2011**, 40, 9131-9135.
157. Binobaid, A.; Iglesias, M.; Beetstra, D. J.; Kariuki, B.; Dervisi, A.; Fallis, I. A.; Cavell, K. J. *Dalton Trans.* **2009**, 7099-7112.

158. Binobaid, A.; Iglesias, M.; Beetstra, D.; Dervisi, A.; Fallis, I.; Cavell, K. J. *Eur. J. Inorg. Chem.* **2010**, 5426–5431.

159. Newman, P. D.; Cavell, K. J.; Hallet, A. J.; Kariuki, B. M. *Dalton Trans.* **2011**, 40, 8807-8813.

Chapter Two

Synthesis and characterisation of novel eight-membered N-Heterocyclic carbenes: salts and free carbenes

2.1. Introduction

One of the most challenging aspects of N-heterocyclic carbene chemistry is the architectural design of the ligand itself. Over the past decades there has been an assorted array of different synthetic developments for the construction of NHC precursors, in which all undergo a final systematically critical cyclization step. The expanded-NHCs have received less attention compared to their 5-membered counterparts. The earliest examples of expanded six- and seven-membered NHC salts were reported by Saba et. al. in 1991.[1] The synthesis of the precursor salts follows the one proposed for imidazolium salts; hence *N*,*N*'-disubstituted-1,3-propanediamine or 1,4-butanediamine are condensed with triethyl orthoformate under acidic conditions (in the presence of ammonium halide in this case). The first 1,3-isopropylperimidinium-2-ylidenes were synthesized in 2003 via deprotonation of N,N'-perimidinium salts with lithium bis(trimethylsilyl)amide (Scheme 2.1).[2]

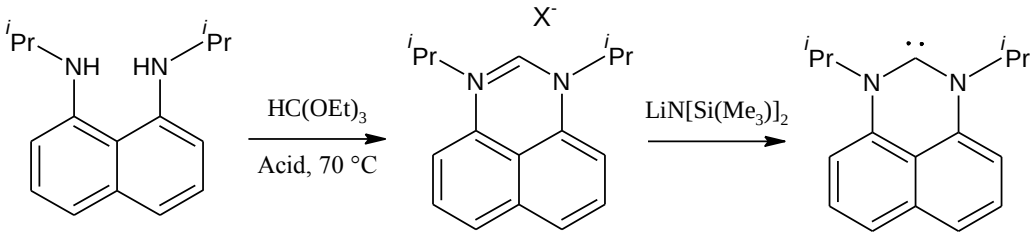

Scheme 2.1. Synthesis of 1,3-isopropylperimidinium salt under acidic conditions followed by deprotonation to *N*,*N*'-perimidinium-2-ylidenes

Many other expanded ring NHC variants have been developed afterwards.[3-6] Cavell and co-workers later established six- and seven-membered N-heterocyclic amidinium salts and their corresponding free carbenes.[7, 8] Their electronic and structural properties were compared with those of the five-membered NHCs. Several differences were noticeable, especially the distortion of the heterocyclic ring from a planar conformation. It was observed that as the ring size increases, the ring twists to alleviate the internal ring strain. While torsional strain occurs in the backbone, the N-C_{NHC}-N link remains planar for every carbene. However, this bond angle becomes more obtuse as the ring increases in size. It is in the range of 100-110° in five-

membered carbenes, whereas in seven-membered carbenes, the range increases to between 115-125°.[9-13] O'Donoghue and colleagues recently reported the pK_a's for the conjugate acid azolium ions of imidazolyl, imidazolinyl, tetrahydropyrimidinyl and bis-imidazolyl systems in aqueous solution.[14] It was found that the pK_a values for tetrahydropyrimidinium salts were 8.4 units higher than the five-membered diaminocarbenes, with pK_a's ranging between 27.8-28.2 and 19.8-25.4 respectively. The increased pK_a's correlate to the one-carbon increase in ring size with greater N-C_{NHC}-N angles in the expanded ring systems compared to the five-membered ring series. In short, this suggests that the expanded ring NHCs are more basic than the saturated and unsaturated five-membered NHCs.

There are many different ways to generate the free NHC (Scheme 2.2),[15] but by far the most widely used method is the deprotonation of an azolium salt precursor with a base. The stabililty of these azolium salts, coupled with their rather mild deprotonation reaction conditions (at room temperature) makes it a popular route. Nevertheless, separation of the free NHC from the protonated base can sometimes be tricky and, consequently, impurities often remain in the reaction mixture.

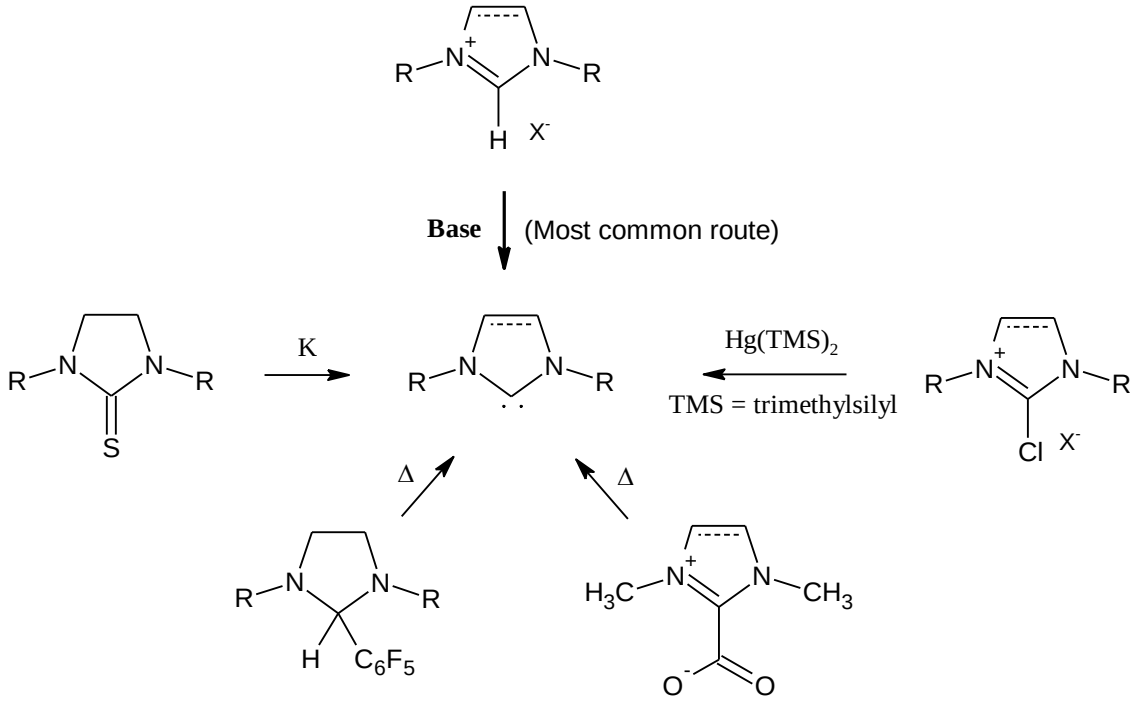

Scheme 2.2. Generation of free NHCs

The stability of the free NHCs is partly due to their shielding by sterically demanding exo-substituents. But, it is the electronic stabilization effect via mesomeric interaction of the lone pairs on the nitrogen atoms and the sp^2 hybridised C_1 carbene which plays a bigger role (Scheme 2.3).

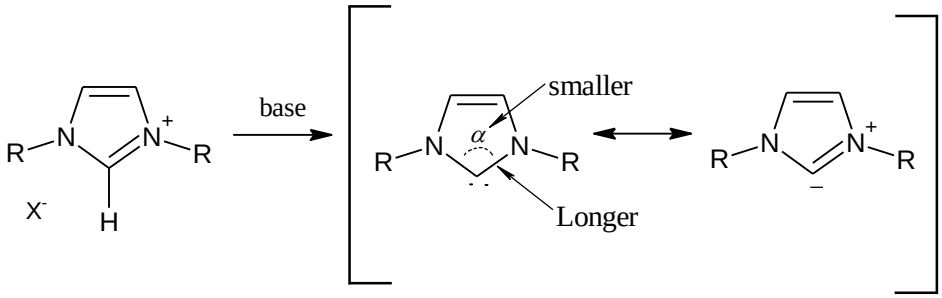

Scheme 2.3. Electronic stabilization through mesomeric effect of NHCs

Structural comparison between the imidazolin-2-ylidene and its corresponding imidazolium salt indicated that the C_{NHC}-N is longer and the N-C_{NHC}-N becomes smaller in the free carbene than in the NHC salt precursor.[16]

This chapter reports the synthesis of various types of eight-membered NHCs. Their structural and electronic characteristics are examined in contrast with its five-, six- and seven-membered NHC counterparts. Unexpected results and failed attempts to yield the desired products are also recorded.

2.2. Results and Discussion

2.2.1. Synthesis of Symmetrical 8-membered NHC Halide Salts

Bromide salts of the eight-membered 1,3-diazocane ring were prepared the same way as the six- and seven-membered expanded N-heterocyclic carbenes,[17, 18] using a modification of Bertrand's methodology.[19] It involves the addition of di-substituted aromatic formamidines to 1,5-dibromopentane in a polar solvent with the presence of a mild base, potassium carbonate in this case, at 90°C. The reaction time varies with the size of the aromatic groups on the nitrogen atoms; varying from 10 to 14 days as the bulkiness of the nitrogen substituents increases (Scheme 2.4). The reaction is slow (due to steric hindrance) but the yield is generally good (≥75%), with the exception of 8-DIPP NHC. Furthermore, a high dilution of solvent is required in this reaction in order to yield the desired ring-closed product. If this precaution is not taken into consideration, then there is the possibility that the formamidine could form an undesired dimeric species with the dihalides. The diazocanylium salts of the eight-membered expanded ring carbenes are air and moisture stable.

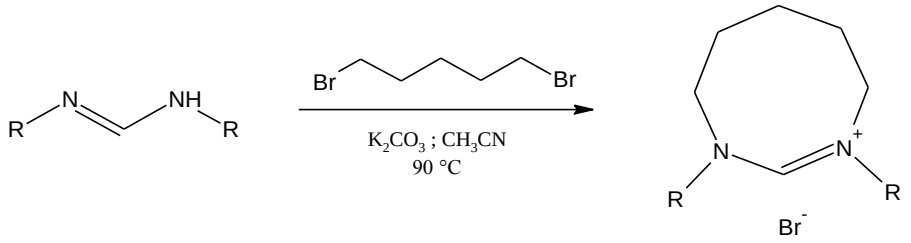

R = Mesityl (Mes); Xylyl (Xyl); di-Isopropylphenyl (DIPP); *o*-Tolyl (^{o}Tol)

	Yield
8-Mes·HBr	75%
8-Xyl·HBr	79%
8-DIPP·HBr	44%
8-*o*-Tol·HBr	77%

Scheme 2.4. Preparation of 8-membered saturated NHC ligands

The solution was filtered and the volatiles removed under reduced pressure before addition of dichloromethane and layering with diethyl ether to afford light yellow solids. Such salts were characterised by ^{1}H and $^{13}C\{^{1}H\}$ NMR spectroscopy, mass spectrometry and micro-analysis. Corresponding compounds show characteristic chemical shifts ($CDCl_3$) of the C_{NHC}-*H* protons which range between 7.31-7.61 ppm in the ^{1}H NMR spectra, while in $^{13}C\{^{1}H\}$ NMR spectra the C_{NHC} shifts were collected in the area of 156.8-158.0 ppm.

2.2.1.1. Solution NMR studies of 8-NHC halide salts

The halide counterions could be exchanged for BF_4^- by simple salt metathesis. Upon changing the counter ion from bromide to the tetrafluoroborate salt, there was a slight shift of the C_{NHC}-*H* proton and C_{NHC} carbon in the ^{1}H and $^{13}C\{^{1}H\}$ NMR spectra respectively. However in a comparison of the amidinium HBF_4 salts between different ring sizes, the C_{NHC}-*H* proton for the 8-membered rings shows increased upfield shifts from 5- and 6-membered rings in the ^{1}H NMR spectra ($CDCl_3$). The same cannot be said for the 7-membered rings as they possess the highest C_{NHC}-*H* proton chemical shifts (Table 2.1). This indicates a reduction of acidity for the carbenic proton in 8-NHC·HBF_4 salts compared to 5- and 6-NHC·HBF_4 salts and conversely an increased basicity of the conjugate base - the free carbene. Whereas $^{13}C\{^{1}H\}$ NMR spectra for the amidinium carbon shows no sign of this trend, as 5-, 7- and 8-membered rings display downfield shifts in contrast to the 6-NHC ring.

Table 2.1: ^{1}H and $^{13}C\{^{1}H\}$ NMR spectral shifts (ppm) in $CDCl_3$ for C_{NHC}-*H* (C_{NHC})

R / Ring size	*o*-Tol	Mes	Xyl	DIPP
8-R·HBr	7.55 (156.8)	7.33 (158.0)	7.37 (157.8)	7.44 (157.0)
7-R·HI[17]	7.41 (156.3)	7.22 (157.8)	7.28 (157.6)	7.27 (157.0)
6-R·HBr[17]	7.72 (153.7)	7.57 (153.5)	7.68 (153.3)	7.55 (152.8)
5-R·HBr[17]	-	8.92 (159.0)	9.20 (159.0)	8.10 (158.0)
8-R·HBF_4	7.61 (157.4)	7.31 (158.0)	7.37 (158.0)	7.42 (156.9)
7-R·HBF_4[17]	7.36 (156.5)	7.21 (158.2)	7.28 (158.0)	7.29 (157.3)
6-R·HBF_4[17]	7.55 (153.3)	7.52 (154.0)	7.83 (154.3)	7.57 (153.1)
5-R·HBF_4[17]	-	7.96 (158.9)	8.16 (160.1)[a]	7.66 (160.0)[a]

[a]NMR data recorded in DMSO

2.2.1.2. Isolation of free carbenes

Free carbenes were isolated after being generated from the bromide salts containing Mes, Xyl, *o*-Tol and DIPP substituents. These salt precursors were reacted with a slight excess of KHMDS in THF affording modest yields (Scheme 2.5); these reactions were characterised by the disappearance of the azolium C_{NHC}-*H* proton signal in the ^{1}H NMR spectrum, and the appearance of the C_{NHC} carbon signal in the $^{13}C\{^{1}H\}$ NMR spectrum. The free NHCs show significant downfield shifts for the C_{NHC} peak in $^{13}C\{^{1}H\}$ NMR spectrum, appearing in the region between 250 to 260 ppm.[20] Although separation of free NHC from the protonated base is not trivial, 8-Xyl was obtained as colourless crystals suitable for X-ray structure analysis, from a concentrated solution of the compound in pentane at -30°C under inert atmosphere.

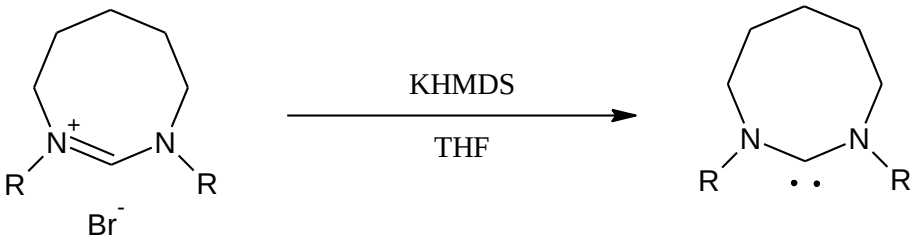

R = Mes, Xyl, *o*-Tol, DIPP

	Yield
8-Mes	51%
8-Xyl	51%
8-oTol	60%
8-DIPP	31%

Scheme 2.5. Deprotonation of azolium salts under mild conditions

2.2.1.3. Solution NMR studies of free 8-NHCs

The existence of free-NHCs are usually identified by the presence of a C_{NHC} $^{13}C\{^1H\}$ NMR spectral signal at >200 ppm. Compared with other large ring structures, [17] the 8-membered C_{NHC} carbon typically shows a significant shift of between 240-250 ppm in the $^{13}C\{^1H\}$ NMR spectrum (Table 2.2).

Table 2.2: Free N-C_{NHC}-N carbon $^{13}C\{^1H\}$ NMR spectral shift (ppm) in [D_6] benzene

R / Ring size	*o*-Tol	Mes	Xyl	DIPP
8	244.05	245.4	251.1	253.2
7[17]	-	257.3	258.8	260.2
6[17]	-	244.9	244.5	245.1
5[17]	-	241.2	242.0	244.0

Such low-field shifts for the carbene carbon also appear in acylic NE-aminocarbenes (E = N, O, S), in the region 235–300 ppm.[21-23] Nonnenmacher et al. noticed a trend between the chemical shift of the C_{NHC} $^{13}C\{^1H\}$ NMR spectroscopic signal and the N-C_{NHC}-N angles when comparing various N-substituted imidazoline derived NHCs: the larger the chemical shift, the larger the N-C_{NHC}-N angle.[24] This trend can also be seen going from 5- to 6- to 8-membered NHC rings, with 7-NHC being the exception. In the $^{13}C\{^1H\}$ NMR spectra of the 5-, 6- and 8-NHCs (Table 2.2) the C_{NHC} carbon signal shifts downfield with increasing ring size. This implies that for larger NHC ring systems, the vacant p_π orbital of the C_{NHC} carbon centre experience weaker interaction with the neighbouring nitrogen p-orbital lone pairs of electrons. The chemical shift of the $^{13}C\{^1H\}$ NMR C_{NHC} carbon signal for the 7-membered NHC rings, however, are found at a lower field (at around 257 – 260 ppm) than those of the 5-, 6-, and 8-membered NHCs. Such low-field shifts can be attributed to poor interaction between the nitrogen (p) orbitals and the C_{NHC} (p_π) orbital and the consequential reduced donation of electron density from the nitrogen into the carbene p_π orbital.

2.2.1.4. Structural properties of expanded 8-membered NHC salts and free carbene

Crystals of 8-Mes·HBF_4, 8-Xyl·HBF_4 and 8-DIPP·HBF_4 suitable for X-ray diffraction were grown via vapour diffusion of diethyl ether into a solution of dichloromethane containing the NHC salt at 0°C. Ortep plots for these structures are shown in Figures 2.1. Selected bond lengths (Å) and angles (°) are also displayed in tables 2.3 and 2.4 respectively.

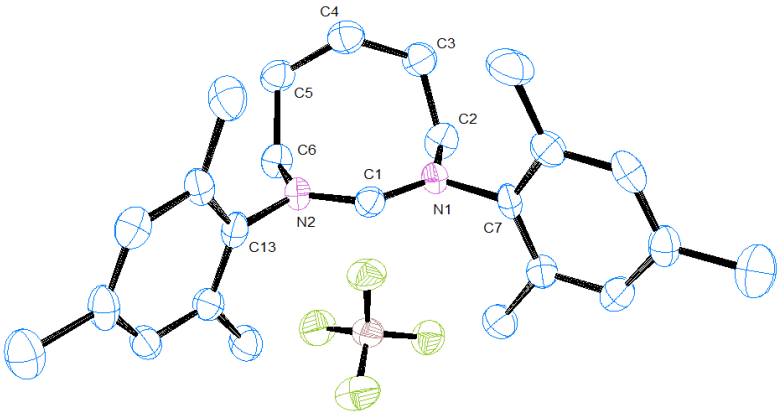

8-Mes·HBF$_4$

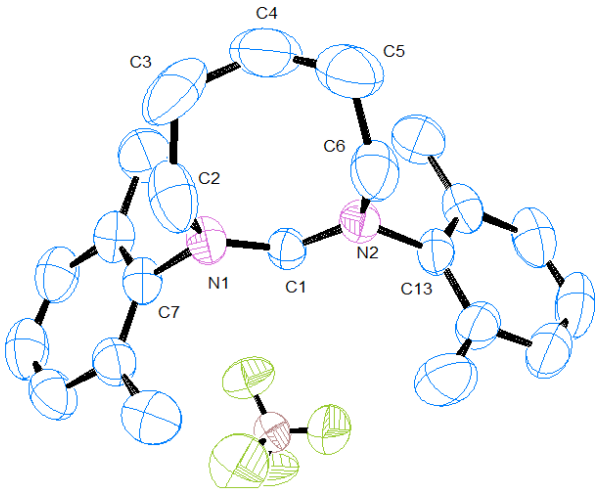

8-Xyl·HBF$_4$

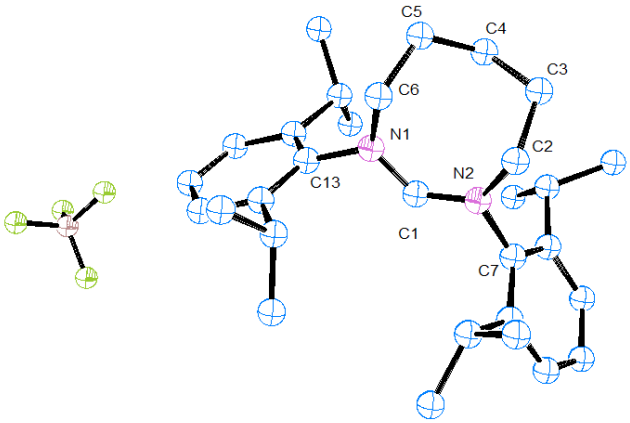

8-DIPP·HBF$_4$

Figure 2.1: Ortep ellipsoid plots at 50% probability of the molecular structure of symmetrical 8-membered salts. Hydrogen atoms are omitted for clarity

Table 2.3: Selected bond lengths (Å) for the symmetrical 8-membered salts

Lengths (Å)	8-Mes·HBF_4	8-Xyl·HBF_4	8-DIPP·HBF_4
C(1)-N(1)	1.308(6)	1.322(4)	1.317(3)
C(1)-N(2)	1.320(6)	1.305(4)	1.318(3)
C(2)-N(1)	1.489(5)	1.482(4)	1.508(5)
C(2)-C(3)	1.537(7)	1.534(7)	1.562(6)
C(3)-C(4)	1.525(7)	1.576(8)	1.565(6)
C(4)-C(5)	1.509(7)	1.430(7)	1.505(7)
C(5)-C(6)	1.533(7)	1.498(6)	1.534(7)
C(6)-N(2)	1.488(5)	1.503(4)	1.522(5)
C(7)-N(1)	1.475(6)	1.466(4)	1.461(3)
C(13)-N(2)	1.451(6)	1.455(4)	1.465(3)

Table 2.4: Selected bond angles (°) for the symmetrical 8-membered salts

Angles (°)	8-Mes·HBF_4	8-Xyl·HBF_4	8-DIPP·HBF_4
N(1)-C(1)-N(2)	131.3(4)	130.0(3)	130.6(2)
C(1)-N(1)-C(2)	126.8(4)	126.8(3)	127.5(3)
C(1)-N(1)-C(7)	116.6(4)	117.0(2)	116.4(18)
C(7)-N(1)-C(2)	116.2(4)	116.1(2)	115.0(3)
C(1)-N(2)-C(6)	126.0(4)	126.6(2)	122.0(3)
C(1)-N(2)-C(13)	115.8(3)	116.6(2)	116.2(19)
C(13)-N(2)-C(6)	117.9(4)	116.0(2)	118.8(3)
N(1)-C(2)-C(3)	114.0(4)	115.9(4)	111.2(4)
C(4)-C(3)-C(2)	116.3(4)	114.4(4)	114.8(4)
C(5)-C(4)-C(3)	117.6(5)	117.7(5)	115.8(4)
C(4)-C(5)-C(6)	116.1(4)	116.8(4)	117.2(4)
N(2)-C(6)-C(5)	113.3(4)	115.4(4)	111.1(5)

The molecular structures reveal the backbone of each 8-NHC ring is neatly folded back towards the C_{NHC} atom. This feature is absent in other NHC rings and provides an opportunity to functionalise the backbone with a tether, anchoring near the metal centre to administer an extra coordination site. Another distinct feature posed by these ligands is their large $NC_{NHC}N$ angles (131° – 130°). Widening of this angle consequently leads to the compression of the C_{NHC}-N-$C_{N\text{-substituent}}$ angles; for example, in the N-Xylyl (8-Xyl·HBF_4) salt the angles are 117.0(2)° and 116.6(2)° respectively. As the large ring size causes enlargement of the N-C_{NHC}-N angle, it maybe useful to note that the ligands as a whole show little to no ring strain. This is defined by the torsional angle (β), a function that alleviate steric tension through the motion of C_{ring}-N···N-C_{ring} atoms caused by the expansion of the ring (Figure 2.2).[17] Due to the conformation of 8-membered rings, the planes between the C_{ring}-N···N-C_{ring} atoms deviate from planarity by only a fraction of 0.99°, 0.21° and 3.10° for 8-Mes·HBF_4, 8-Xyl·HBF_4 and 8-DIPP·HBF_4 respectively.

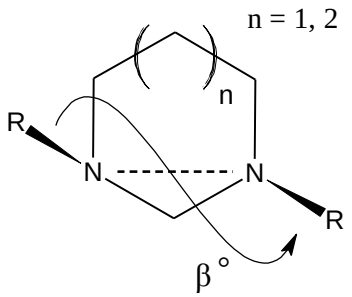

Figure 2.2: Torsional angle (β)

Crystals of 8-Xyl free carbene suitable for single-crystal X-ray diffraction were grown from a THF/pentane solution and the Ortep plot is shown below in Figure 2.3. A comparison of its selected bond lengths (Å) and angles (°) with free 7-Mes-NHC are displayed in Table 2.5.

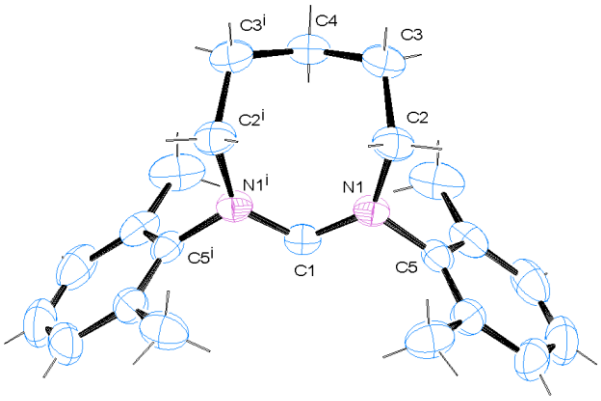

Figure 2.3: Ortep ellipsoid plots at 50% probability of the molecular structure free 8-Xyl-NHC

Table 2.5: Selected bond lengths (Å) and angles (°) for the free NHCs: 7-Mes and 8-Xyl

Lengths (Å)		Angles (°)	
7-Mes [17]			
C(1) –N(2)	1.346(5)	N(1)–C(1)–N(2)	116.6(4)
C(2)–N(1)	1.483(5)	C(1)–N(1)–C(6)	115.5(3)
C(5)–N(2)	1.502(6)	C(1)–N(2)–C(15)	115.0(4)
8-Xyl			
C(1) –N(1/1')	1.3475(16)	N(1)–C(1)–N(1')	120.11(18)
C(2/2')–N(1/1')	1.4982(19)	C(1)–N(1/1')–C(5/5')	113.75(12)
C(5/5')–N(1/1')	1.443(2)		

The crystal structure of the free 8-Xyl-NHC shows similar structural features to the salts. The shape of the 8-membered ring adopts a boat conformation with the backbone folded over the central NHC carbon. The N-C_{NHC}-N angle [120.11(18)°] is large, wider than its 7-Mes counterpart. The expansion of this angle from 7- to 8-membered NHC is a direct result of the increase size of the ring. This in effect pushes the xylyl substituents ever closer towards the C_{NHC} (and the metal centre on coordination). The structure of the free NHC is completely symmetrical with both halves of the molecule having equivalent bond lengths and angles. The molecule shows minimal ring strain in contrast to the 7-Mes, where the torsion angle (β) increases to 25.4°.[17]

2.2.2. Synthesis and characterisation of Unsymmetrical 8-membered NHC Halide Salts

As the symmetrically substituted rings are obtained via ring closure of the corresponding di-substituted formamide with hydrocarbyldihalide; the asymmetric salts are formed through a step-wise reaction scheme via the synthesis of unsymmetrical formamidines. Adopting the same synthetic approach as Cavell et al., the unsymmetrical formamidine was produced in a two step synthesis.[25] The first step involves reacting *o*-anisidine with two drops of hydrochloric acid and an excess amount of triethylorthoformate to produce o-anisidylformimidate (Scheme 2.6a). The product was then stirred with one equivalent of *o*-toluidine at 60°C overnight, resulting in the formation of 2-methoxyphenyl-2-methylphenyl imidoformamide (Scheme 2.6b). It is important that this step is carried out in an acid-free environment otherwise traces of acid will lead to disproportionation to the appropriate symmetrical formamidine. Finally, ring closure is achieved by reacting unsymmetrical formamidine with dibromopentane using the same preparation as described for the synthesis of symmetrical NHC salts (Scheme 2.6c). The reaction took 18 days at reflux and the product was isolated in 47% yield. The 8-*o*-Tol/Anis·HBr salt was obtained as a yellow hygroscopic solid. Crystals suitable for X-ray analysis were obtained from dichloromethane/diethyl ether. A characteristic signal for the C_{NHC}-*H* proton was observed at 7.77 ppm in ^{1}H NMR spectrum and the C_{NHC} carbon at 157.9 ppm in $^{13}C\{^{1}H\}$ NMR spectrum, thus providing analytical proof that the desired product was formed.

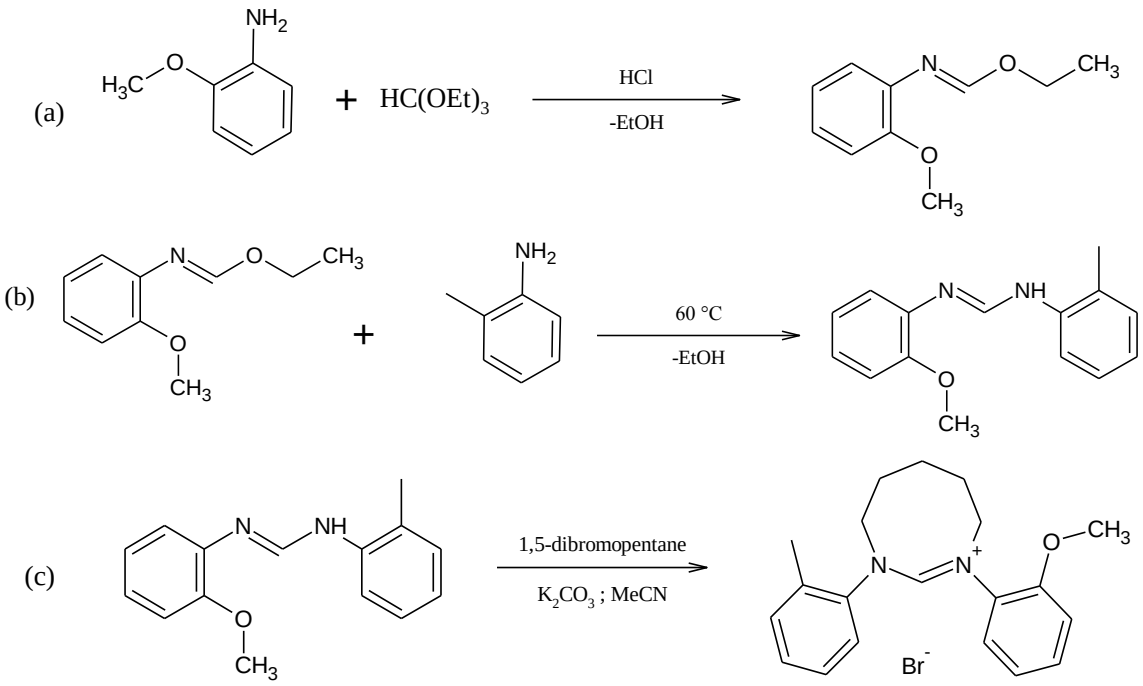

Scheme 2.6. Step-wise synthesis to unsymmetric 8-membered NHC salt; (a) synthesis of o-anisidylformimidate, (b) formation of unsymmetric 2-methoxyphenyl-2-methylphenyl imidoformate, (c) Preparation of unsymmetric 8-*o*-Tol/Anis·HBr saturated NHC ligand

Single-crystal X-ray diffraction data was collected for the unsymmetrical 8-*o*-Tol/Anis·HBr salt; the Ortep plot is shown in Figure 2.4 along with its selected bond lengths (Å) and angles (°) in Table 2.6.

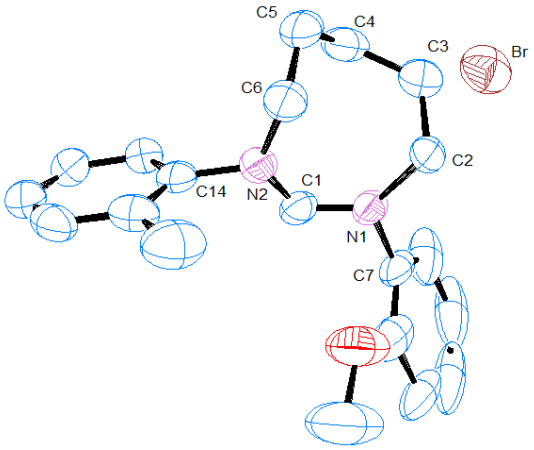

Figure 2.4: Ortep ellipsoid plots at 50% probability of the molecular structure of unsymmetrical 8-*o*-Tol/Anis·HBr salt. Hydrogen atoms are omitted for clarity

Table 2.6: Selected bond lengths (Å) and angles (°) for 8-o-Tol/Anis·HBr salt

Lengths (Å)		Angles (°)	
C(1)-N(1)	1.321(7)	N(1)-C(1)-N(2)	129.2(5)
C(1)-N(2)	1.298(7)	C(1)-N(1)-C(2)	128.0(4)
C(2)-N(1)	1.493(6)	C(1)-N(1)-C(7)	116.2(4)
C(2)-C(3)	1.510(7)	C(7)-N(1)-C(2)	128.0(4)
C(3)-C(4)	1.520(8)	C(1)-N(2)-C(6)	127.1(4)
C(4)-C(5)	1.525(9)	C(1)-N(2)-C(14)	116.0(4)
C(5)-C(6)	1.517(8)	C(14)-N(2)-C(6)	116.9(4)
C(6)-N(2)	1.485(6)	N(1)-C(2)-C(3)	114.7(4)
C(7)-N(1)	1.447(7)	C(4)-C(3)-C(2)	117.8(5)
C(14)-N(2)	1.459(7)	C(5)-C(4)-C(3)	116.1(5)
		C(4)-C(5)-C(6)	115.4(5)
		N(2)-C(6)-C(5)	112.8(5)

The solid state structure of the unsymmetrical 8-membered ring again shows a large N-C_{NHC}-N angle, 129.2(5)°, slightly smaller than those of the symmetrical 8-NHC ligands. This ring also posseses a slightly larger torsional angle (β) (deviating 4.96° from planarity) than the

symmetrical-NHCs. Both *ortho*-aromatic substituents are pointing away from the ring backbone. This noticeable feature may play an important role in complex coordination.

2.2.3. Synthesis and characterisation of 8-membered NHC halide salts with functionalised backbone

Due to the unique structure of 8-membered rings (folded backbone) it was of interest to synthesise 8-membered rings with a functionalised backbone. The notion was that this would act as a 'scorpion tail', thus providing an extra coordination site for the metal centre upon complexation, or acting as a linker to anchor to supports, affording a combined homogeneous and heterogeneous catalyst.[26]

Commercially available bis(2-chloroethyl)amine was chosen for this as the starting material to attain an 8-membered NHC ring with a nitrogen atom upon its backbone. Thus the idea was that the secondary amine centre would provide the foundation for a 'scorpion tail', through S_N2 reaction with tethered substituents. The amide was first protected with a BOC group, using BOC_2O and NaOH in water at 0°C, rendering it inert in order to prevent side reactions to occur during the ring closure. Attempts were then made to ring close the protected, tert-butyl bis(2-choroethyl)carbamate with the corresponding formamidine via the conventional method, using K_2CO_3 in acetonitrile under reflux for 20 days. The ^{1}H NMR spectrum showed no sign of the characteristic C_{NHC}-*H* proton peak in the region expected for expanded ring NHCs (7.31-7.77 ppm). A singlet at 8.71 ppm is present instead; such low field shift is comparable with those of the 5-membered NHCs.[27] In order to identify the product, the oily white chloride salt was exchanged with the BF_4^- counterion. Colourless crystals appropriate for X-ray determination were then obtained by diffusion of hexane into a dichloromethane solution of the salt. The result showed that the reaction did not undergo ring closure as expected, but instead shows the formation of an unsymmetrical imidoforamidine salt (Figure 2.5). This product may have derived from an unsymmetric aziridation type reaction between the formamidine and the carbamate moiety (Scheme 2.7).[28]

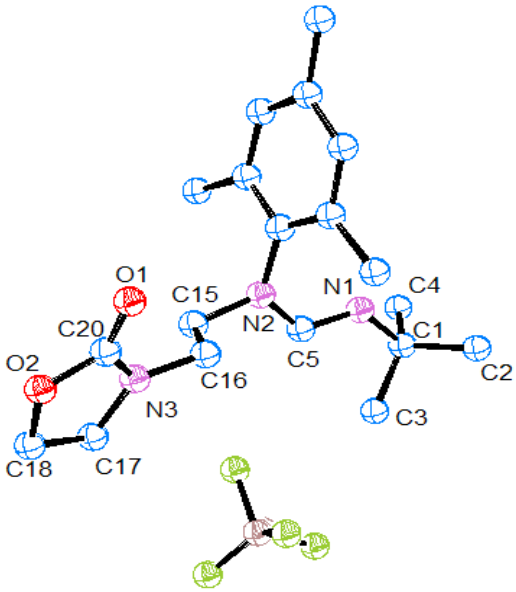

Figure 2.5: Ortep ellipsoid plots at 50% probability of the asymmetric aziridation product. Hydrogen atoms are omitted for clarity

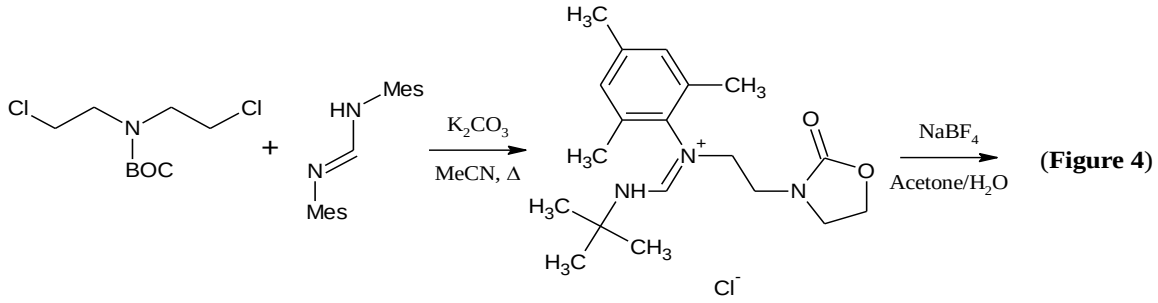

(Figure 4)

Scheme 2.7. Unexpected synthesis of 2,4,6-trimethyl-N-[(tert-butylamino)methylidene]-N-[(2-oxo-1,3-oxazolidin-3-yl)methyl]anilinium salt

In an attempt to prevent the undesired aziridation type product, diethylenetriamine was later employed as an alternate starting material in the synthesis of nitrogen functionalized 8-membered NHC. The primary amines were first functionalized with mesityl groups; this was accomplished by reacting diethylenetriamine with two equivalents of bromomesityl upon a Pd-catalyzed arylamination reaction using Buchwarld's $Pd_2(dba)_3$/BINAP catalyst in toluene under N_2 atmosphere (Scheme 2.8a).[29] Treatment of this product with chloromethylsilane in the presence of DBU in ether under inert atmosphere provided a selective route for the silylation of the central amine to afford $(MesNHCH_2CH_2)_2NSiMe_3$ (Scheme 2.8b).[30, 31]

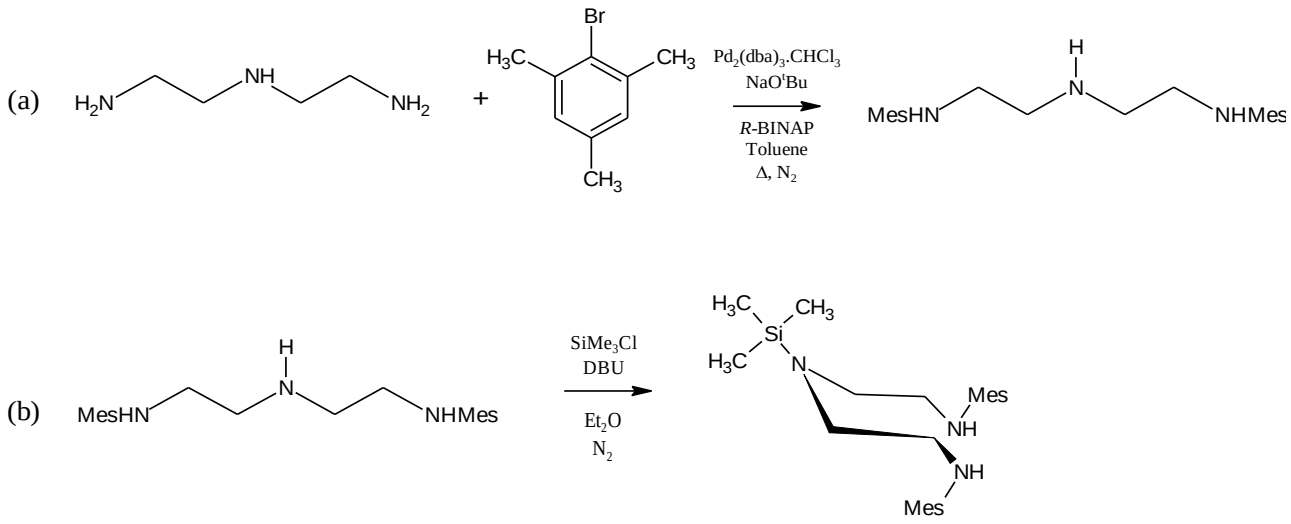

Scheme 2.8. (a) Arylamination of diethylenetriamine with 2 equiv. of bromomesityl with $Pd_2(dba)_3$/BINAP Buchwald's catalyst, (b) silylation of central amine using $SiMe_3Cl$ in the presence of DBU

Buchmeiser et al. reported ring cyclization of 1,3-dimesitylaminopropane with aqueous formaldehyde in methanol and subsequently with N-bromosuccinimide to afford expanded 6-membered NHC.[32] Similar methodology was adopted for ring closure of the $(MesNHCH_2CH_2)_2NSiMe_3$ product, however aqueous formaldehyde was not used on this occasion for fear that the water would react with the trimethylsilyl protecting group leading to elimination. Triethylorthoformate was used instead in the presence of NH_4BF_4 and the reaction was refluxed in acetonitrile for 20 days (Scheme 2.9). Work-up of the reaction yielded an oily brown solid. ^{1}H NMR spectrum of the product showed a singlet peak at 8.17 ppm resembling the C_{NHC}-*H* proton, this signal has shifted downfield in contrast to the previous expanded 8-membered rings, which lie in the region between 7.31-7.61 ppm. $^{13}C\{^1H\}$ NMR spectrum for the C_{NHC} carbon also showed an upfield shift to 163 ppm from the usual range of 156-158 ppm. Data obtained from HRMS in the electrospray mode indicated the parent ion at *m/z* = 350, this accords to the ring closed product but with the lost of the trimethylsilyl protecting group. Such findings suggest that the ring cyclization did not occur between the terminal nitrogens, but instead with the central amine. This was confirmed via X-ray diffraction (Figure 2.6); crystals were grown by diffusion of hexane into a dichloromethane solution of the product below 0°C.

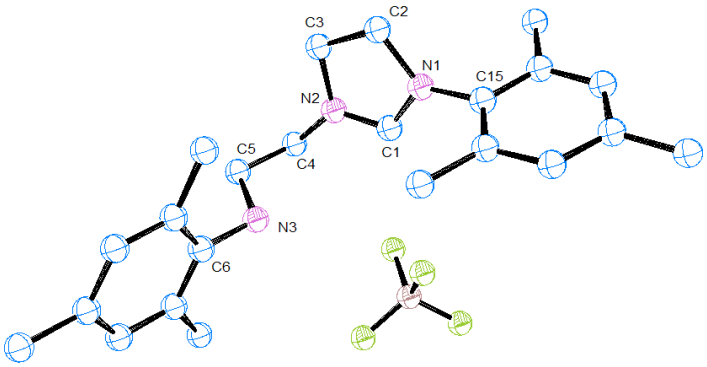

Figure 2.6: Ortep ellipsoid plots at 50% probability of the molecular structure of 3-(2,4,6-trimethylphenyl)-1-{2-[(mesityl)amino]ethyl}-4,5-dihydro-1-imidazol-3-ium tetrafluoroborate salt. Hydrogen atoms are omitted for clarity

Formation of what seems to be thermodynamically favorable, 5-membered saturated imidazolium ring salt has occurred under the forcing conditions of this reaction. The trimethylsilyl protecting group may have been hydrolyzed to form the volatile hexamethyldisiloxane, in the reaction and removed from the mixture during concentration of solvent under reduced pressure at the work-up stage. Consequently, HRMS failed to detect this moiety and gave an unexpected value of the above product.

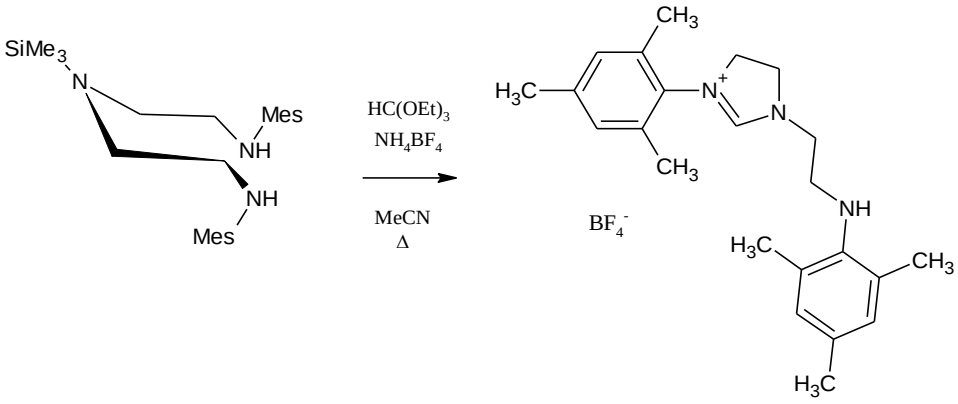

Scheme 2.9. Synthesis of the unexpected 5-membered saturated imidazolium BF_4 salt

The reaction was performed again, but this time using $(MesNHCH_2CH_2)_2NH$ (without the protecting group) with triethylorthoformate and NH_4BF_4 in acetonitrile. The above saturated 5-membered NHC salt was formed after 6 days of reflux with a reasonable yield of 74%. Reported here is the first example of a saturated 3-(2,4,6-trimethylphenyl)-1-{2-[(mesityl)amino]ethyl}-4,5-dihydro-1-imidazol-3-ium tetrafluoroborate salt, carried out from a short three step synthesis through arylamination of diethylenetriamine using Buchwald catalyst. In contrast, the unsaturated version of the 5-membered NHC ring has been reported before.[34] Whilst this is a potentially useful functionalised imidazole based NHC, it was not the precursor to the desired product.

Due to the previous failed attempts of constructing 8-membered NHCs with a nitrogen atom in the rear backbone, efforts were redirected to using bis(2-bromoethyl) ether as the starting precursor instead. This compound is commercially available and should react with the corresponding formamidine under the conventional route used for the synthesis of symmetrical and unsymmetrical 8-NHC salts, thus giving the backbone functionalized 8-membered ring NHC with an oxygen atom. As a result, bis(2,4,6-trimethylphenyl), bis(2,6-dimethylphenyl) and bis(2-methylphenyl) formamidine were all refluxed with bis(2-bromoethyl) ether and K_2CO_3 in acetonitrile (Scheme 2.10) for 16, 15 and 12 days respectively. The yields of these reactions afforded fair amounts between 50-61%.

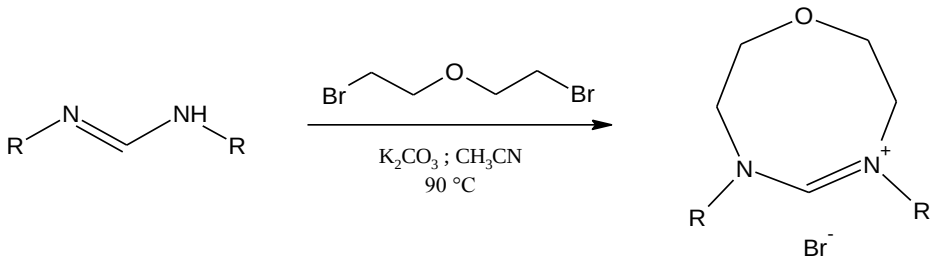

R = Mes, Xyl, *o*-Tol

	Yield
8-O-Mes·HBr	56%
8-O-Xyl·HBr	61%
8-O-*o*-Tol·HBr	50%

Scheme 2.10. Preparation of 8-membered saturated NHC oxadiazocin-4-ium pro-ligands

2.2.3.1. Solution NMR and X-ray analysis of 8-membered NHC salts with functionalised backbone

The C_{NHC}-*H* proton signals are observed between 7.16-7.57 ppm ($CDCl_3$) in the ^1H NMR spectra of the oxadiazocin-4-ium salts. The $^{13}C\{^1H\}$ NMR spectra also show peaks representing the C_{NHC} carbon between 157-158 ppm. This is consistent with those of the symmetrical and unsymmetrical 8-NHC salts. Crystals suitable for X-ray diffraction were grown by diffusion of diethyl ether into a solution of dichloromethane with the product (Figure 2.7). The bond lengths (Å) and bond angles (°) of the oxadiazocin-4-ium salts are presented in Table 2.7 and table 2.8 respectively.

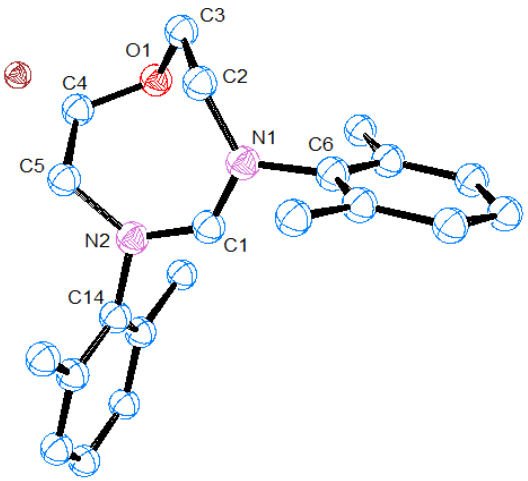

8-O-Xyl·HBr

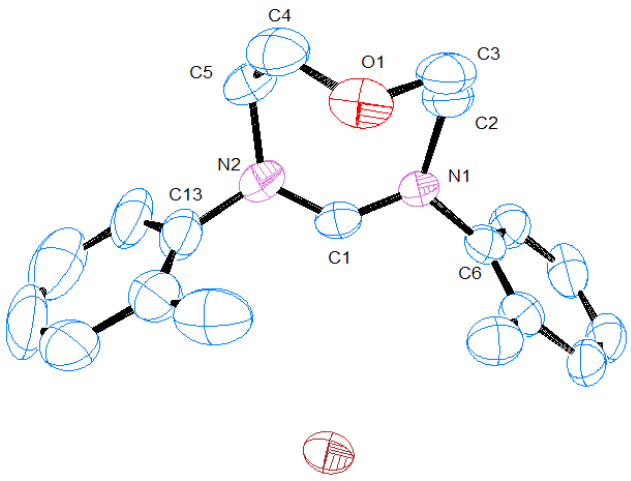

8-O-*o*-Tol·HBr

Figure 2.7: Ortep ellipsoid plots at 50% probability of the 8-membered oxadiazocin-4-ium bromide salts. Hydrogen atoms are omitted for clarity

Table 2.7: Selected bond lengths (Å) for the 8-membered oxadiazocin-4-ium bromide salts

Lengths (Å)	8-O-Xyl·HBr	8-O-*o*-Tol·HBr
C(1)-N(1)	1.321(3)	1.309(8)
C(1)-N(2)	1.326(3)	1.320(8)
C(2)-N(1)	1.482(3)	1.475(7)
C(2)-C(3)	1.530(4)	1.530(10)
C(3)-O(1)	1.426(3)	1.399(8)
O(1)-C(4)	1.420(4)	1.422(8)
C(4)-C(5)	1.531(4)	1.530(9)
C(5)-N(2)	1.478(3)	1.482(8)
C(6)-N(1)	1.456(3)	1.452(8)
C(14)-N(2)	1.458(3)	-
C(13)-N(2)	-	1.452(9)

Table 2.8: Selected bond angles (°) for the 8-membered oxadiazocin-4-ium bromide salts

Angles (°)	8-O-Xyl·HBr	8-O-*o*-Tol·HBr
N(1)-C(1)-N(2)	130.0(2)	130.3(6)
C(1)-N(1)-C(2)	126.2(2)	126.3(6)
C(1)-N(1)-C(6)	114.4(2)	117.6(5)
C(6)-N(1)-C(2)	119.3(19)	116.1(6)
C(1)-N(2)-C(5)	126.7(2)	124.8(6)
C(1)-N(2)-C(14)	115.6(2)	-
C(1)-N(2)-C(13)	-	118.6(6)
C(14)-N(2)-C(5)	117.6(2)	-
C(13)-N(2)-C(5)	-	116.6(6)
N(1)-C(2)-C(3)	111.5(2)	112.2(6)
O(1)-C(3)-C(2)	113.1(2)	114.0(5)
C(4)-O(1)-C(3)	115.2(2)	114.8(5)
C(5)-C(4)-O(1)	114.1(2)	113.0(6)
N(2)-C(5)-C(4)	112.0(2)	111.8(6)

Structural features of the oxadiazocin-4-ium bromide salts show similar characteristics to those previously described for symmetrical and unsymmetrical 8-NHCs. Both 8-O-Xyl·HBr and 8-O-*o*-Tol·HBr salts adopt large $NC_{NHC}N$ angle, 130°, with contracted C_{NHC}-N-$C_{N\text{-substituent}}$ angles of 117.6(2)° and 116.6(6)° respectively. 8-O-*o*-Tol·HBr exhibits a higher ring strain compared to 8-O-Xyl·HBr, with torsion angles (β) of 6.42° and 2.51° respectively. The spatial orientation of the slightly more bulky xylyl groups increases tension around the planar C_{NHC}-N-$C_{N\text{-substituent}}$ atoms, thus reducing twisting of the NHC ring and therefore minimizing (β)° in the latter salt. As the backbone of the NHC ring is neatly folded back towards the C_{NHC} carbon, the distance measured from the oxygen atom to the C_{NHC} centre is 2.91Å for 8-O-*o*-Tol·HBr and 2.93Å for 8-O-Xyl·HBr. Such distances between the oxygen atom and the carbenic carbon atom are within sum of the Van der Waals radii.

2.2.4 Attempted synthesis of 8-membered carbenes with unsaturated backbone

Due to the unsuccessful efforts of allocating a coordinative nitrogen atom at the rear of the 8-membered NHC ring, an alternative plan was to synthesize an unsaturated backbone instead. Such compounds could be used to build chiral NHC systems.[35] Hence it was necessary to prepare 1,5-dihalopent-2-ene to react with formamidine in order to yield the desired asymmetric unsaturated product.

In order to enable ring-closure, the cis(Z)-olefin was required. This required the prior formation of 1,5-dibromopent-2-yne via cuprous salt-catalyzed reaction of 3-butyn-1-ol with aqueous formaldehyde which subsequently converted to the dibromide by treatment with carbon tetrabromide and triphenylphosphine (Scheme 2.11).[36] Characterisations of these compounds can be found in the literature. E-Z isomerism does not exist for alkynes due to the linearity imposed by the carbon-carbon triple bond.

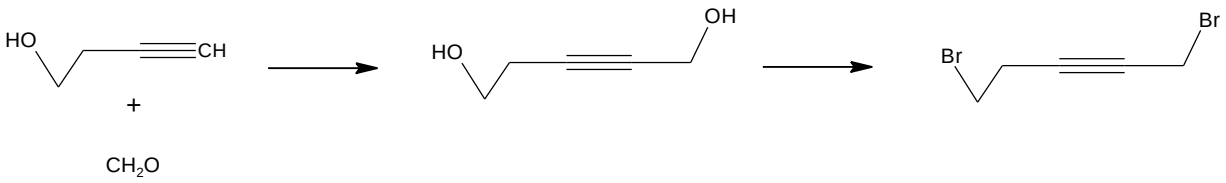

Scheme 2.11. Synthesis of 1,5-dibromopent-2-yne from 3-butyn-1-ol and aq. Formaldehyde via pent-2-yne-1,5-diol

Due to the obvious lack of flexibility in the sp-hybridised carbon atoms of the triple bond, ring closure with formamidine would only be possible if the alkyne was first selectively reduced to the cis-alkene. Hydrogenation of alkynes to Z-alkenes is traditionally performed using Lindlar's catalyst with dihydrogen. This approach requires constant monitoring of hydrogen uptake to prevent over-reduction to alkane. In the past, both Elsevier and Cavell have demonstrated that Pd mono- and/or bis-NHC complexes show good catalytic activity in selective reduction reactions.[37-39] In prior studies it was shown that [Pd(0)(1,3-dimesitylimidazole-2-ylidene)(maleic anhydride)(solvent)][40, 41] was able to stereo- and chemoselectively semihydrogenate aromatic and aliphatic internal alkynes in the presence of an ionic hydrogen donor source, such as formic acid/triethylamine.[42] However using this catalyst in an attempt to reduce 1,5-dibromopent-2-yne to dibromo-2-ene was unsuccessful. Instead, the catalyst was able to reduce 2-pentyn-1,5-diol to the desired *cis*-pent-2-ene-1,5-diol product as a yellow oil in reasonable yields (Scheme 2.12).

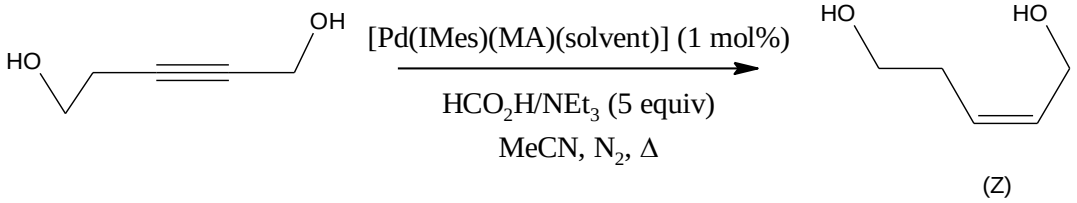

Scheme 2.12. Transfer semihydrogenation of 2-pentyn-1,5-diol to pent-2-ene-1,5-diol with Pd-catalyst and HCO_2H/Net_3 as hydrogen source

The product which was analyzed by ^1H NMR spectroscopy, showed two broad quartet peaks at 5.7 and 5.5 ppm representing hydrogen's attached to sp^2-hydridised carbon atoms in the olefin bond. The coupling constants of the peaks are 6.9 and 7.5 Hz which indicates that the

alkene takes on (Z)-cis orientation. At this point, the focus of this study was on the formation and catalytic testing of complexes of saturated eight-membered NHCs and hence the formation and complexation of unsaturated 8-NHCs was put aside, and unfortunately due to time restraints was not completed. However, if the unsaturated ring could be prepared it offers exciting opportunities for the generation of novel NHC structures.

2.3 Experimental

General remarks

The solvents (acetonitrile, dichloromethane and diethylether) were used as purchased. All reagents (1,5-dibromopentane, bis(2-bromoethyl) ether, triethyl orthoformate, *o*-anisidine, 2,4,6-trimethylaniline, 2,6-dimethylaniline, *o*-toluidine, 2,6-diisopropylaniline, sodium tetrafluoroborate and potassium bis(trimethylsilyl)amide) were used as received. The preparations of free NHCs were performed using standard Schlenk techniques under N_2 atmosphere. Dry tetrahydrofuran was prepared via reflux distillation over Na/K. Air-sensitive compounds were stored and handled in MBraun UNIlab glovebox. Deuterated C_6D_6 for NMR measurements was distilled from Na under N_2 immediately prior to use, following standard literature methods. All reagents were used as received. ^{1}H and ^{13}C spectra were recorded using a Bruker Avance AMX 400 or 500 spectrometer. Chemical shifts δ were expressed in ppm downfield from TMS using the residual protic solvent as an internal standard. Coupling constants *J* are given in Hertz as positive values. The multiplicity of the signals is indicated as "s", "d", "t" or "m" for singlet, doublet, triplet or multiplet, respectively. Mass spectra and high resolution mass spectra were obtained in electrospray (ES) mode unless otherwise reported on a Waters Q-TOF micromass spectrometer. [Pd(ma)(*t*BuDAB)][40] and [Pd(IMes)(ma)(solvent)][42] were synthesized according to the published procedures. Elemental analyses were performed by Medac Ltd., UK.[43]

General procedure for the synthesis of diazocanylidium bromide and tetrafluorophosphate salts

The appropriate formamidine (1 mmol) was dissolved in acetonitrile (50 ml), to which potassium carbonate (0.14 g, 1 mmol) was added. The mixture was stirred for 20 minutes prior to the addition of 1,5-dibromopentane (0.23 g, 1 mmol). The resulting reaction mixture was refluxed for 10-14 days after which the resulting solution was filtered to remove solid impurities, and the solvent was removed in *vacuo*. The residue was dissolved in the minimum

amount of dichloromethane, to which diethyl ether was added, to afford the diazocanylidium bromide salt as a white crystalline solid.

To convert the bromide salts to tetrafluoroborate salts; 1,3-diazocane bromide (0.5 mmol) in acetone (30 ml) and sodium tetrafluoroborate (0.07 g, 0.6 mmol) in water (10 ml) were stirred together at room temperature for 20 minutes. The acetone was evaporated under reduced pressure to afford a suspension of the tetrafluoroborate salt in water. The solid material was collected via filtration, dissolved in dichloromethane (20 ml) and subsequently dried over $MgSO_4$. After filtration, the solvent was concentrated to approximately 2ml and ether was added to the solution until the product precipitated as white crystalline material, which was collected by filtration.

1,3-Bis-(2,4,6-trimethylphenyl)-3,4,5,6,7,8-hexahydro-1,3-diazocin-1-ium bromide, 8-Mes·HBr. White solid, yield; 75%. ^{1}H NMR ($CDCl_3$, 400 MHz, 298K): δ (ppm) 7.33 (s, 1H, NC*H*N), 6.87 (s, 4H, *m*-C*H*), 4.79 (s, 4H, NCH_2), 2.36 (s, 12H, *o*-CH_3), 2.21 (m, 4H, NCH_2CH_2), 2.20 (s, 6H, *p*-CH_3), 1.56 (m, 2H, $NCH_2CH_2CH_2$); ^{13}C {^{1}H} NMR ($CDCl_3$, 100 MHz, 298K): δ (ppm) 158.0 (s, N*C*HN), 141.8 (s, Ar-*C*), 140.1 (s, Ar-*C*), 133.5 (s, Ar-*C*), 130.4 (s, Ar-*m*-*C*H), 53.8 (s, NCH_2), 40.4 (s, NCH_2CH_2), 28.3 (s, $NCH_2CH_2CH_2$), 20.8 (s, Ar-*p*-*C*H_3), 18.7 (s, *o*-*C*H_3). HRMS (ES): m/z 349.2657 ([M – Br]$^+$; $C_{24}H_{33}N_2$ requires 349.2644). Anal. Calcd. for $C_{24}H_{33}N_2Br$: C, 67.13; H, 7.75; N, 6.62. Found C, 66.03; H, 7.78; N, 7.08.

1,3-Bis-(2,4,6-trimethylphenyl)-3,4,5,6,7,8-hexahydro-1,3-diazocin-1-ium tetrafluoroborate, 8-Mes·HBF$_4$. White crystalline solid, yield; 92%. ^{1}H NMR ($CDCl_3$, 400 MHz, 298K): δ (ppm) 7.31 (s, 1H, NC*H*N), 6.90 (s, 4H, *m*-C*H*), 4.46 (s, 4H, NCH_2), 2.33 (s, 12H, *o*-CH_3), 2.22 (s, 6H, *p*-CH_3), 2.10 (m, 4H, NCH_2CH_2), 1.62 (m, 2H, $NCH_2CH_2CH_2$); ^{13}C {^{1}H} NMR ($CDCl_3$, 100 MHz, 298K): δ (ppm) 158.0 (s, N*C*HN), 141.6 (s, Ar-*C*), 140.2 (s, Ar-*C*), 133.5 (s, Ar-*C*), 130.4 (s, Ar-*m*-*C*H), 52.9 (s, NCH_2), 40.5 (s, NCH_2CH_2), 28.3 (s, $NCH_2CH_2CH_2$), 20.8 (s, Ar-*p*-*C*H_3), 18.3 (s, Ar-*o*-*C*H_3). HRMS (ES): *m/z* 349.2651 ([M – BF_4]$^+$; $C_{24}H_{33}N_2$ requires 349.2644).

1,3-Bis-(2,6-dimethylphenyl)- 3,4,5,6,7,8-hexahydro-1,3-diazocin-1-ium bromide, 8-Xyl·HBr. White crystalline solid, yield; 79%. ^{1}H NMR ($CDCl_3$, 400 MHz, 298K): δ (ppm) 7.37 (s, 1H, NC*H*N), 7.16 (t, $^{3}J_{HH}$ = 6.8 Hz, 2H, *p*-C*H*), 7.09 (d, $^{3}J_{HH}$ = 7.6 Hz, 4H, *m*-C*H*), 4.85 (m, 4H, NCH_2), 2.42 (s, 12H, *o*-CH_3), 2.52 (m, 4H, NCH_2CH_2), 2.10 (m, 2H, $NCH_2CH_2CH_2$); ^{13}C {^{1}H} NMR ($CDCl_3$, 100 MHz, 298K): δ (ppm) 157.8 (s, N*C*HN), 144.0 (s, C_{Ar}), 133.9 (s, C_{Ar}), 130.0 (s, *C*H_{Ar}), 129.9 (s, *C*H_{Ar}), 53.8 (s, N*C*H_2), 28.3 (s, NCH_2CH_2), 20.9 (s, $NCH_2CH_2CH_2$), 18.9 (s, *o*-*C*H_3). HRMS (ES): *m/z* 321.2317 ($[M - Br]^+$; $C_{22}H_{29}N_2$ requires 321.2331). Anal. Calcd. for $C_{22}H_{29}N_2Br$: C, 65.83; H, 7.28; N, 6.98. Found C, 64.67; H, 7.31; N, 7.56.

1,3-Bis-(2,6-dimethylphenyl)-3,4,5,6,7,8-hexahydro-1,3-diazocin-1-ium tetrafluoroborate, 8-Xyl·HBF$_4$. White crystalline solid, yield; 91%. ^{1}H NMR ($CDCl_3$, 400 MHz, 298K): δ (ppm) 7.37 (s, 1H, NC*H*N), 7.15 (t, 2H, *p*-C*H*), 7.10 (d, $^{3}J_{HH}$ = 7.6 Hz, 4H, *m*-C*H*), 4.48 (m, 4H, NCH_2), 2.37 (s, 12H, *o*-CH_3), 2.22 (m, 4H, NCH_2CH_2), 2.09 (m, 2H, $NCH_2CH_2CH_2$); ^{13}C {^{1}H} NMR ($CDCl_3$, 100 MHz, 298K): δ (ppm) 158.0 (s, N*C*HN), 143.9 (s, C_{Ar}), 133.9 (s, C_{Ar}), 130.1 (s, *C*H_{Ar}), 129.9 (s, *C*H_{Ar}), 52.9 (s, N*C*H_2), 28.3 (s, NCH_2CH_2), 20.9 (s, $NCH_2CH_2CH_2$), 18.4 (s, *o*-*C*H_3). HRMS (ES): *m/z* 321.2337 ($[M - BF_4]^+$; $C_{22}H_{29}N_2$ requires 321.2331).

1,3-Bis-(2,6-diisopropylphenyl)-3,4,5,6,7,8-hexahydro-1,3-diazocin-1-ium bromide, 8-DIPP·HBr. Crystalline white solid, yield; 44%. ^{1}H NMR ($CDCl_3$, 400 MHz, 298K): δ (ppm) 7.44 (s, 1H, NC*H*N), 7.36 (t, $^{3}J_{HH}$ = 7.7 Hz, 2H, *p*-C*H*), 7.17 (d, 4H, *m*-C*H*), 4.64 (m, 4H, NCH_2), 3.22 (sept, $^{3}J_{HH}$ = 6.7 Hz, 4H, *o*-C*H*$(CH_3)_2$), 2.23 (m, 4H, NCH_2CH_2), 2.04 (m, 2H, $NCH_2CH_2CH_2$), 1.31 (d, $^{3}J_{HH}$ = 6.7 Hz, 12H, *o*-CH(C$H_3)_2$), 1.19 (d, $^{3}J_{HH}$ = 6.8 Hz, 12H, *o*-CH(C$H_3)_2$); ^{13}C {^{1}H} NMR ($CDCl_3$, 100 MHz, 298K): δ ppm 157.0 (s, N*C*HN), 144.8 (s, C_{Ar}), 141.0 (s, C_{Ar}), 130.6 (s, *C*H_{Ar}) 125.5 (s, *C*H_{Ar}), 55.1 (s, N*C*H_2), 28.7 (s, *C*H$(CH_3)_2$), 27.6 (s, CH(*C*$H_3)_2$), 25.1 (s, CH(*C*$H_3)_2$), 24.9 (s, NCH_2CH_2), 21.4 (s, $NCH_2CH_2CH_2$). HRMS (ES): *m/z* 433.3578 ($[M - Br]^+$; $C_{30}H_{45}N_2$ requires 433.3583).

1,3-Bis-(2,6-diisopropylphenyl)-3,4,5,6,7,8-hexahydro-1,3-diazocin-1-ium tetrafluoroborate, 8-DIPP·HBF$_4$. White crystalline solid, yield; 89%. ^{1}H NMR ($CDCl_3$, 400 MHz, 298K): δ (ppm) 7.42 (s, 1H, NC*H*N), 7.30 (t, $^3J_{HH}$ = 7.7 Hz, 2H, *p*-C*H*), 7.14 (s, 4H, *m*-C*H*), 4.75 (m, 4H, NCH_2), 3.21 (sept, $^3J_{HH}$ = 6.7 Hz, 4H, *o*-C*H*(CH_3)$_2$), 2.29 (m, 4H, NCH_2CH_2), 2.08 (m, 2H, $NCH_2CH_2CH_2$), 1.30 (d, $^3J_{HH}$ = 6.4 Hz, 12H, *o*-CH(CH_3)$_2$), 1.18 (d, $^3J_{HH}$ = 6.8 Hz, 12H, *o*-CH(CH_3)$_2$); ^{13}C {^{1}H} NMR ($CDCl_3$, 100 MHz, 298K): δ (ppm) 156.9 (s, N*C*HN), 144.7 (s, C_{Ar}), 140.8 (s, C_{Ar}), 130.8 (s, *C*H$_{Ar}$), 125.5 (s, *C*H$_{Ar}$), 54.3 (s, N*C*H$_2$), 28.7 (s, *C*H(CH_3)$_2$), 27.6 (s, CH(*C*H$_3$)$_2$), 24.9 (s, CH(*C*H$_3$)$_2$), 24.8 (s, NCH_2CH_2), 21.5 (s, $NCH_2CH_2CH_2$). HRMS (ES): *m/z* 433.3581 ([M – BF_4]$^+$; $C_{30}H_{45}N_2$ requires 433.3583).

1,3-Bis-(2-methylphenyl)-3,4,5,6,7,8-hexahydro-1,3-diazocin-1-ium bromide, 8-^{o}Tol·HBr. White semi-crystalline solid, yield; 77%. ^{1}H NMR ($CDCl_3$, 400 MHz, 298K): δ (ppm) 7.55 (s, 1H, NC*H*N), 7.46 (s, 2H, *o*-C*H*), 7.30-7.23 (m, 6H, *m*,*p*-C*H*), 4.04 (s, 4H, NCH_2), 2.47 (s, 6H, CH_3), 2.13 (s, 4H, NCH_2CH_2), 1.89 (m, 2H, $NCH_2CH_2CH_2$); ^{13}C {^{1}H} NMR ($CDCl_3$, 100 MHz, 298K): δ (ppm) 156.8 (s, N*C*HN), 144.1 (s, ipso-*C*), 133.5 (s, C_{Ar}), 132.2 (s, C_{Ar}), 130.0 (s, C_{Ar}), 127.9 (s, C_{Ar}), 53.6 (s, N*C*H$_2$), 27.7 (s, NCH_2CH_2), 20.9 ($NCH_2CH_2CH_2$), 18.3 (s, *C*H$_3$). HRMS (ES): *m/z* 293.2013 ([M – Br]$^+$; $C_{20}H_{25}N_2$ requires 293.2018). Anal. Calcd. for $C_{20}H_{25}N_2Br$: C, 64.34; H, 6.75; N, 7.50. Found C, 63.26; H, 6.82; N, 8.00.

1,3-Bis-(2-methylphenyl)-3,4,5,6,7,8-hexahydro-1,3-diazocin-1-ium tetrafluoroborate, 8-^{o}Tol·HBF$_4$. White crystalline solid, yield; 91%. ^{1}H NMR ($CDCl_3$, 400 MHz, RT): δ (ppm) 7.61 (s, 1H, NC*H*N), 7.44 (s, 1H, *o*-C*H*), 7.31-7.30 (m, 7H, *m*,*p*-C*H*), 4.06 (s, 4H, NCH_2), 2.48 (s, 6H, CH_3), 2.19 (s, 4H, NCH_2CH_2), 2.09 (m, 2H, $NCH_2CH_2CH_2$); ^{13}C {^{1}H} NMR ($CDCl_3$, 100 MHz, 298K): δ (ppm) 157.4 (N*C*HN), 144.2 (s, ipso-*C*), 132.6 (s, C_{Ar}), 130.5 (s, C_{Ar}), 128.4 (s, C_{Ar}), 127.2 (C_{Ar}), 53.0 (s, N*C*H$_2$), 28.1 (s, NCH_2CH_2), 21.5 (s, $NCH_2CH_2CH_2$), 18.1 (s, CH_3). HRMS (ES): *m/z* 293.2005 ([M – BF_4]$^+$; $C_{20}H_{25}N_2$ requires 293.2018).

General procedure for the preparation of free 8-NHCs

To a suspension of 8-NHC·HBr (0.47 mmol) in THF (30 ml) was added 2 equivalents of $KN(SiMe_3)_2$ (0.19 g, 0.95 mmol). The resulting suspension was stirred for 30 min, after which time the residue was filtered into a flame dried Schlenk flask. The solvent was then removed to yield the free NHC as an orange/red solid.

1,3-Dimesityl-1,3-diazocane-2-ylidene, 8-Mes. Yield; 51%. ^{1}H NMR (C_6D_6, 500MHz, 298K): δ (ppm) 6.85 (s, 4H, Ar-CH), 3.25 (br. t, 4H, NCH_2), 2.19 (s, 12H, *o*-CH_3), 2.10 (s, 6H, *p*-CH_3) 1.69 (br. peak 2H, $NCH_2CH_2CH_2$), 1.13 (br. db, 4H, NCH_2CH_2); ^{13}C {^{1}H} NMR (C_6D_6, 125 MHz, 298K): δ (ppm) 245.4 (s, N*C*N), 149.0 (s, C_{Ar}), 135.5 (s, C_{Ar}), 134.0 (s, C_{Ar}), 130.1 (s, C_{Ar}), 128.2 (s, CH_{Ar}), 51.0 (s, NCH_2), 29.5 (s, NCH_2CH_2), 21.0 (s, *p*-Me), 19.2 (s, *o*-Me).

1,3-Bis(2-methylphenyl)-1,3-diazocane-2-ylidene, 8-Xyl. Yield; 51%. ^{1}H NMR (C_6D_6, 500 MHz, 298K): δ (ppm) 6.81-6.92 (m, 6H, CH_{Ar}), 3.19 (m, 4H, NCH_2), 2.18 (s, 12H, *o*-CH_3), 1.24 (m, 4H, NCH_2CH_2), 1.02 (m, 2H, $NCH_2CH_2CH_2$); ^{13}C {^{1}H} NMR ($CDCl_3$, 125 MHz, 298K): δ (ppm) 251.1 (s, N*C*N), 151.8 (s, C_{Ar}), 134.4 (s, C_{Ar}), 129.1 (s, CH_{Ar}), 126.0 (s, CH_{Ar}), 50.6 (s, NCH_2), 29.6 (s, NCH_2CH_2), 20.2 (s, $NCH_2CH_2CH_2$), 19.3 (s, *o*-CH_3). Crystals suitable for X-ray analysis (see **Table 4**) were obtained by precipitation from pentane solution at -34°C in glovebox.

1,3-Diisopropyl-1,3-Diazocane-2-Ylidene, 8-DIPP. Yield; 31%. ^{1}H NMR (C_6D_6, 400 MHz, 298K): δ (ppm) 7.18 (t, $^3J_{HH}$ = 7.6 Hz, 2H, *p*-C*H*), 7.08 (d, 4H, *m*-C*H*), 3.50 (m, 4H, NCH_2), 3.45 (m, 4H, *o*-$CH(CH_3)_2$), 1.80 (m, 2H, $NCH_2CH_2CH_2$), 1.49 (m, 4H, NCH_2CH_2), 1.19 (d, $^3J_{HH}$ = 6.7 Hz, 12H, *o*-$CH(CH_3)_2$), 1.14 (d, $^3J_{HH}$ = 6.3 Hz, 12H, *o*-$CH(CH_3)_2$); ^{13}C {^{1}H} NMR (C_6D_6, 125 MHz, 298K): δ (ppm) 253.2 (s, N*C*N), 147.1 (s, C_{Ar}), 145.5 (s, C_{Ar}), 142.6 (s, CH_{Ar}), 140.6 (s, CH_{Ar}), 65.4 (s, NCH_2), 30.1 (s, $CH(CH_3)_2$), 26.7 (s, $CH(CH_3)_2$), 25.9 (s, $CH(CH_3)_2$), 23.4 (s, $NCH_2CH_2CH_2$), 22.8 (NCH_2CH_2).

Synthesis of 1-(2-methoxyphenyl)-3-(2-methylphenyl)-3,4,5,6,7,8-hexahydro-1,3-diazocin-1-ium bromide, 8-*o*-Tol/*o*-Anis·HBr

N'-(2-methoxyphenyl)-*N*-(2-methylphenyl)imidoformamide (1.08 g, 4.5 mmol) was dissolved in acetonitrile (250 ml), to which potassium carbonate (0.31 g, 2.2 mmol) was added. The mixture was stirred for 20 minutes prior the addition of 1,5-dibromopentane (0.62 ml, 4.5 mmol). The resulting reaction mixture was refluxed for 18 days after which the resulting solution was filtered to remove solid impurities, and the solvent was removed in *vacuo*. The oily residue was thoroughly washed with diethyl ether, to afford a creamy solid, yield; 47%. ^{1}H NMR ($CDCl_3$, 400 MHz, 298K): δ (ppm) 7.77 (dd, $^{3}J_{HH}$ = 7.9 Hz, 1H, *o*-CH_{Ar}), 7.50 (s, 1H, NC*H*N), 7.46 (m, 1H, CH_{Ar}), 7.27 (m, 4H, CH_{Ar}), 6.98 (td, $^{3}J_{HH}$ = 7.7 Hz, 1H, *m*-CH_{Ar}), 6.92 (dd, $^{3}J_{HH}$ = 8.4 Hz, 1H, *m*-CH_{Ar}), 4.55 (m, 4H, NCH_2), 3.86 (s, 3H, CH_3), 2.46 (s, 3H, CH_3), 2.07 (m, 4H, NCH_2CH_2), 2.04 (m, 2H, $NCH_2CH_2CH_2$). ^{13}C {^{1}H} NMR ($CDCl_3$, 125 MHz, 298K): δ (ppm) 157.9 (s, N*C*HN), 133.7 (s, C_{Ar}), 133.5 (s, C_{Ar}), 131.8 (s, C_{Ar}), 130.7 (s, *C*H_{Ar}), 130.1 (s, *C*H_{Ar}), 128.5 (s, *C*H_{Ar}), 128.0 (s, *C*H_{Ar}), 127.5 (s, C_{Ar}), 127.0 (s, *C*H_{Ar}), 121.9 (*s*, *C*H_{Ar}), 121.7 (s, *C*H_{Ar}), 112.0 (s, *C*H_{Ar}), 56.1 (s, *C*H_3), 53.9 (s, N*C*H_2), 53.4 (s, N*C*H_2), 27.8 (s, NCH_2CH_2), 27.7 (s, NCH_2CH_2), 20.4 (s, $NCH_2CH_2CH_2$), 18.0 (s, *C*H_3). HRMS (ES): *m/z* 309.1962 ($[M - Br]^+$; $C_{20}H_{25}N_2O$ requires 309.1967).

General procedure for the synthesis of oxadiazocin-4-ium bromide salts

The appropriate formamidine (1 mmol) was dissolved in acetonitrile (50 ml), to which potassium carbonate (0.14 g, 1 mmol) was added. The mixture was stirred for 20 minutes prior to the addition of bis(2-bromoethyl)ether (0.23 g, 1 mmol). The resulting reaction mixture was refluxed for 12-16 days after which the resulting solution was filtered to remove solid impurities, and the solvent was removed in *vacuo*. The residue was dissolved in the minimum amount of dichloromethane, to which diethyl ether was added, to afford the diazocanylidium bromide salt as a white crystalline solid.

4,6-Bis-(2,4,6-trimethylphenyl)-3,6,7,8-tetrahydro-2*H*-1,4,6-oxadiazocin-4-ium bromide, O-8-Mes·HBr. White crystalline solid, yield; 56%. ^{1}H NMR ($CDCl_3$, 400 MHz, 298K): δ (ppm) 7.36 (s, 1H, NC*H*N), 6.88 (s, 4H, *m*-C*H*Ar), 4.24 (t, 4H, OCH_2), 2.35 (s, 12H, *o*-CH_3), 2.21 (s, 6H, *p*-CH_3). ^{13}C {^{1}H} NMR ($CDCl_3$, 125 MHz, 298K): δ (ppm) 158.4 (s, N*C*HN), 141.0 (s, C_{Ar}), 140.1 (s, C_{Ar}), 133.9 (s, *m*-*C*H$_{Ar}$), 130.2 (s, C_{Ar}), 68.0 (s, O*C*H$_2$), 54.1 (s, N*C*H$_2$), 30.8 (s, N*C*H$_2$), 20.8 (s, *o*-*C*H$_3$), 18.2 (s, *p*-*C*H$_3$). HRMS (ES): *m/z* 351.2436 ([M – Br]$^{+}$;$C_{23}H_{31}N_2O$ requires 351.2436).

4,6-Bis-(2,4-dimethylphenyl)-3,6,7,8-tetrahydro-2*H*-1,4,6-oxadiazocin-4-ium bromide, O-8-Xyl·HBr. White crystalline solid, yield; 61%. ^{1}H NMR ($CDCl_3$, 400 MHz, 298K): δ (ppm) 7.40 (s, 1H, NC*H*N), 7.18 (m, $^{3}J_{HH}$ = 7.5 Hz, 2H, *p*-CH_{Ar}), 7.10 (d, $^{3}J_{HH}$ = 7.6 Hz, 4H, *m*-CH_{Ar}), 4.26 (t, $^{3}J_{HH}$ = 6.0 Hz, 4H, OCH_2), 2.42 (s, 12H, *o*-CH_3), 2.17 (m, 4H, NCH_2). ^{13}C {^{1}H} NMR ($CDCl_3$, 125 MHz, 298K): δ (ppm) 158.3 (s, N*C*HN), 143.2 (s, C_{Ar}), 134.2 (s, C_{Ar}), 130.0 (s, *C*H$_{Ar}$), 129.7 (s, *C*H$_{Ar}$), 68.0 (s, O*C*H$_2$), 54.0 (s, N*C*H$_2$), 18.6 (*o*-CH$_3$). HRMS (ES): *m/z* 323.2124 ([M – Br]$^{+}$; $C_{21}H_{27}N_2O$ requires 323.2123).

4,6- Bis-(2-methylphenyl)-3,6,7,8-tetrahydro-2H-1,4,6-oxadiazocin-4-ium bromide, O-8-*o*-Tol·HBr. White crystalline solid, yield; 50%. ^{1}H NMR ($CDCl_3$, 400 MHz, 298K): δ (ppm) 7.57 (s, NC*H*N), 7.27 (m, CH_{Ar}), 4.09 (m, OCH_2), 2.46 (s, *o*-CH_3). ^{13}C {^{1}H} NMR ($CDCl_3$, 125 MHz, 298K): δ (ppm) 157.7 (s, N*C*HN), 143.7 (s, C_{Ar}), 133.7 (s, C_{Ar}), 132.2 (s, CH_{Ar}), 130.2 (s, CH_{Ar}), 128.0 (s, CH_{Ar}), 127.1 (s, CH_{Ar}), 67.7 (s, OCH_2), 54.2 (s, NCH_2), 17.9 (s, *o*-CH_3). HRMS (ES): *m/z* 295.1818 ([M – Br]$^{+}$; $C_{19}H_{23}N_2O$ requires 295.1810).

Synthesis of Amine-tethered saturated-5-membered-NHC ligand tetrafluoroborate salt (2,4,6-Me$_3$C$_6$H$_2$C$_3$H$_4$NCH$_2$CH$_2$NH-2,4,6-Me$_3$C$_6$H$_2$) ·BF$_4$

(MesNCH$_2$CH$_2$)$_2$NSiMe$_3$ (0.24 g, 0.6 mmol) with triethyl orthoformate (0.12 ml, 0.7 mmol) and ammonium tetrafluoroborate (0.07 g, 0.7 mmol) in acetonitrile (100 ml) was refluxed at 91°C for 20 days. After which the solution was filtered and removed under *vacuo* yielding a thick yellow oil. Solid precipitated upon addition of diethyl ether, yield; 45%. ^{1}H NMR ($CDCl_3$, 400 MHz, 298K): δ (ppm) 8.17 (s, 1H, NC*H*N), 6.82 (s, 2H, CH_{Ar}), 6.72 (s, 2H, CH_{Ar}), 4.26 (m, 2H, NCH_2), 4.08 (m, 2H, NCH_2), 3.86 (t, 2H, CH_2), 3.06 (t, 2H, CH_2), 2.19

(s, 3H, *p*-C*H*$_3$), 2.17 (s, 6H, *o*-C*H*$_3$), 2.16 (s, 6H, *o*-C*H*$_3$), 2.14 (s, 3H, *p*-C*H*$_3$). ^{13}C {^{1}H} NMR ($CDCl_3$, 125 MHz, 298K): δ (ppm) 163.7 (s, N*C*HN), 158.2 (s, C_{Ar}), 157.4 (s, C_{Ar}),137.9 (s, C_{Ar}), 134.5 (s, C_{Ar}), 134.4 (s, C_{Ar}), 129.7 (s, C_{Ar}), 129.6 (s, C_{Ar}), 129.4 (s, C_{Ar}), 128.9 (s, C_{Ar}), 128.9 (s, C_{Ar}), 128.5 (s, C_{Ar}), 128.0 (s, C_{Ar}), 49.9 (s, *C*H$_2$), 48.3 (s, *C*H$_2$), 47.4 (s, *C*H$_2$), 44.1 (s, *C*H$_2$), 29.8 (s, *C*H$_3$), 19.9 (s, *C*H$_3$), 17.2 (s, *C*H$_3$), 17.0 (s, *C*H$_3$), 16.4 (s, *C*H$_3$), 16.3 (s, *C*H$_3$). HRMS (ES): *m/z* 350.2598 ([M – BF_4]$^+$; $C_{23}H_{32}N_3$ requires 350.2596).

Synthesis of 2-pentyn-1,5-diol[36]

Cuprous chloride (4.0 g, 40 mmol) was dissolved in 12% aq. HCl (60 ml), and the solution cooled in ice bath. 40% aq. KOH (60 ml) was added dropwise over 1h. The mixture was filtered with suction and the solid residue was washed with water. The residue was added to 3-butyn-1-ol (13 g, 186 mmol), 37% aq. formaldehyde (21.67 g, 267 mmol), water (4 ml) and $CaCO_3$ (0.2 g). The mixture was refluxed under N_2 for 3 days. The mixture was then cooled to room temperature, diluted with ethyl acetate (250 ml) and dried with anhydrous Na_2SO_4 (10 g). The mixture was filtered with suction and the solids were rinsed with ethyl acetate. The filtrate concentrated and distilled to give brown viscous oil, yield; 79%. ^{1}H NMR (D_2O, 400 MHz, 298K): δ (ppm) 4.08 (s, 2H, C*H*$_2$) 3.69 (t, 2H, C*H*$_2$), 2.33 (t, 2H, C*H*$_2$). ^{13}C {^{1}H} NMR (D_2O, 125 MHz, 298K): δ (ppm) 83.7 (s, ≡*C*), 79.3 (s, ≡*C*), 60.0 (s, *C*H$_2$), 49.7 (s, *C*H$_2$), 21.7 (s, *C*H$_2$).

Synthesis of 2-pentyn-1,5-dibromide

A solution of 2-pentyn-1,5-diol (2.0 g, 20 mmol) and carbon tetrabromide (14.94 g, 45 mmol) in dry CH_2Cl_2 (100 ml) was cooled to 0°C and triphenylphosphine (11.79 g, 45 mmol) was added slowly over 20 min. The mixture was warmed to 20°C over 1 h. The CH_2Cl_2 was removed under reduced pressure and hexane (100 ml) was added to the residue. The mixture was cooled to 0°C and filtered. The solid residue was washed with cold hexane (2 × 25 ml) and the filtrate was concentrated and distilled under vacuum to obtain a pale yellow oil, yield; 83%. ^{1}H NMR ($CDCl_3$, 400 MHz, 298K): δ (ppm) 3.85 (s, 2H, C*H*$_2$) 3.39 (t, 2H, C*H*$_2$), 2.79 (t, 2H, C*H*$_2$). ^{13}C {^{1}H} NMR ($CDCl_3$, 125 MHz, 298K): δ (ppm) 84.3 (s, ≡*C*), 76.7 (s, ≡*C*), 28.9 (s, *C*H$_2$), 23.4 (s, *C*H$_2$), 14.7 (s, *C*H$_2$). HRMS (ES): *m/z* 225.88 ([M]; $C_5Br_2H_6$ requires 225.9091).

Synthesis of pent-2-ene-1,5-diol (general procedure for the hydrogen transfer of alkynes)

Pd(DAB)(MA) (0.019 g, 0.05 mmol) was added into a flamed dried Schlenk containing IMes (0.019 g, 0.06 mmol) with potassium *tert*-butoxide (0.025 g, 0.2 mmol) in anhydrous acetonitrile (15 ml) under N_2 atmosphere. 2-pentyne-1,5-diol (0.5 g, 5 mmol) followed by formic acid (0.94 ml, 0.02 mol) and triethylamine (3.48 ml, 0.02 mol) were added toward the mixture. The reaction was refluxed at 80°C under inert atmosphere for 19 hours. After which cooled to room temperature and filtered through celite. The solution was then concentrated under reduced pressure to yield a pale yellow oil, yield; 84%. ^{1}H NMR ($CDCl_3$, 400 MHz, 298K): δ (ppm) 5.77 (q, 1H, $^3J_{HH}$ = 6.9 Hz, CH_{olefin}), 5.54 (q, 1H, $^3J_{HH}$ = 7.5 Hz, CH_{olefin}), 4.08 (d, 2H, CH_2), 3.55 (t, 2H, CH_2), 2.29 (q, 2H, CH_2). ^{13}C {^{1}H} NMR ($CDCl_3$, 125 MHz, 298K): δ (ppm) 129.3 (s, CH$_{olefin}$), 127.8 (s, CH$_{olefin}$), 59.2 (s, CH$_2$), 55.6 (s, CH$_2$), 28.6 (s, CH$_2$). LRMS (ES): *m/z* 102.13 ([M]; $C_5H_{10}O_2$ requires 102.12).

X-ray crystallography. Suitable crystals were selected and analyzed using a Bruker-Nonius Kappa CCD machine. Data were collected at 150 K using Mo($K\alpha$) (λ = 0.71073 Å) radiation throughout. Details of the data collections, solutions and refinements are shown in the **Appendix**. The structures were solved using SHELX-97 and refined by SHELX-97.[44] Dr Benson Kariuki solved and refined all X-ray crystal data.

2.4 References

1. Saba, S.; Brescia, A. M.; Kaloustian, M. K. *Tet. Let.* **1991**, 32, 5031-5034.
2. Bazinet, P.; Yap, G. P. A.; Richeson, D. S. *J. Am. Chem. Soc.* **2003**, 125, 13314.
3. Mayr, M.; Wurst. K.; Onania, K. H.; Buchmeiser, M. R. *Chem. Eur. J.* **2004**, 10, 1256-1266.
4. Herrmann, W. A.; Schneider, S. K.; Ofele, K.; Sakamoto, M.; Herdtweck, E. *J. Organometallic Chem.* **2004**, 689, 2441-2449.
5. Scarborough, C. C.; Popp, I. A.; Guzei, B. V.; Stahl, S. S. *J. Organomet. Chem.* **2005**, 690, 6143.
6. Scarborough, C. C.; Grady, M. J. W.; Guzei, I. A.; Gandhi, B. A.; Bunel, E. E.; Stahl, S. S. *Angew. Chem. Int. Ed.* **2005**, 44, 5269.
7. Iglesias, M.; Beetstra, D. J.; Stasch, A.; Horton, P. N.; Hursthouse, M. B.; Coles, S. J.; Cavell, K. J.; Dervisi, A.; Fallis I. A. *Organometallics* **2007**, 26, 4800.
8. Iglesias, M.; Beestra, D. J.; Knight, J. C.; Ooi, L.; Stasch, A.; Male, L.; Hursthouse, M. B.; Coles, S. J.; Cavell, K. J.; Dervisi, A.; Fallis, I. A. *Organometallics* **2008**, 27, 3279.
9. Evans, P. A.; Baum, E. W.; Fazal, A. N.; Pink, M. *Chem. Commun.* **2005**, 63.
10. Alcaraza, M.; Roseblade, S. J.; Cowley, A. R.; Fernandez, R.; Brown, J. M.; Lassaletta, J. M. *J. Am. Chem. Soc.* **2005**, 127, 3290.
11. Saravanakumar, S.; Oprea, A. I.; Kindermann, M. K.; Jones, P. G.; Heinicke, J. *Chem. Eur. J.* **2006**, 12, 3143.
12. Vignolle, J.; Cattoen, X.; Bourissou, D. *Chem. Rev.* **2009**, 109, 3333-3384.
13. Arduengo, A. J.; Bock, H.; Chen, H.; Denk, M.; Dixon, D. A.; Green, J. C.; Herrmann, W. A.; Jones, N. L.; Wagner, M.; West, R. *J. Am. Chem. Soc.* **1994**, 116, 6641-6649.
14. Higgins, E. M.; Sherwood, J. A.; Lindsay, A. G.; Armstrong, J.; Massey, R. S.; Alder, R. W.; O'Donoghue, A. C. *Chem. Commun.* **2011**, 1559-1561.
15. Droge, T.; Glorius, F. *Angew. Chem. Int. Ed.* **2010**, 49, 6940-6952.
16. Kirmse, W. *Angew. Chem. Int. Ed.* **2004**, 43, 1767.
17. Iglesias, M.; Beetstra, D. J.; Knight, J. C.; Ooi, L.; Stasch, A.; Male, L.; Hursthouse, M. B.; Coles, S. J.; Cavell, K. J.; Dervisi, A.; Fallis, I. A. *Organometallics* **2008**, 27, 3279.

18. Kolychev, E.L.; Portnyagin, I. A.; Shuntikov, V. V.; Khrustalev, V. N.; Nechaev, M. S. *Organometallics* **2009**, 694, 2454.
19. Jazzar, R. L. H.; Donnadieu, B.; Bertrand, G. *J. Organomet. Chem.* **2006**, 691, 3201.
20. Tapu, D.; Dixon, D. A.; Roe, C. *Chemical Reviews* **2009**, 109, 3385.
21. Alder, R. W.; Blake, M. E. *Chem. Commun.* **1997,** 1513.
22. Alder, R. W.; Butts, C. P.; Orpen, A. G. *J. Am. Chem. Soc.* **1998**, 120, 11526.
23. Alder, R. W.; Allen, P. R.; Murray, M.; Orpen, G. *Angew. Chem., Int. Ed. Engl.* **1996**, 35, 1121.
24. Nonnenmacher, M.; Kunz, D.; Rominger, F.; Oeser, T. *Chem. Commun.* **2006**, 1378.
25. Binobaid, A.; Iglesias, M.; Beestra, D. J.; Kariuki, B.; Dervisi, A.; Fallis, I. A.; Cavell, K. J. *Dalton Trans.* **2009**, 7099.
26. Mayr, M.; Mayr, B.; Buchmeiser, M. R. *Angew. Chem., Int. Ed.* **2001**, 40, 3839.
27. Arduengo, A. J.; Krafczyk, R.; Schmutzler, R.; Craig, H. A.; Goerlich, J. R.; Marshall, W. J.; Unverzagt, M. *Tetrahedron* **1999**, 55, 14523.
28. Antilla, J. C.; Wuff, W. D. Angew. *Chem., Int. Ed. Engl.* **2000**, 39, 4518.
29. Wolfe, J. P.; Wagaw, S.; Buchwald, S. L. *J. Am. Chem. Soc.* **1996**, 118, 7215-7216.
30. Morgan, A. R.; Klosklwski, M.; Kalischewski, F.; Phillips, A. H.; Peterson, J. L. *Organometallics* **2005**, 24, 5383-5392.
31. Clark, H. C. S.; Cloke, F. G. N.; Hitchcock, P. B.; Love, J. B.; Wainwright, A. P. *J. Organometallic Chem.* **1995**, 501, 333-340.
32. Mayr, M.; Wurst, K.; Onania, K. H.; Buchmeiser, M. R. *Chem. Eur. J.* **2004**, 10, 1256-1266.
33. Calder, I. C.; Spotswood, T. M.; Sasse, W. H. F. *Tetrahedron Lett.* **1963**, 2, 95.
34. H. Jong, Pactrick, B. O.; Fryzuk, M. D. *Organometallics* **2011**, 30, 2333-2341.
35. César, V.; Laponnaz, S. B.; Gade, L. H *Chem. Soc. Rev.* **2004**, 33, 619-636.
36. Millar, J. G.; Underhill, E. W. *Can. J. Chem.* **1986**, 64.
37. Sprengers, J. W.; Wassenaar, J.; Clement, N. D.; Cavell, K. J.; Elsevier, C. J. *Angew. Chem. Int. Ed.* **2005**, 44, 2026-2029.
38. Clement, N. D.; Cavell, K. J.; Ooi, L. L. *Organometallics* **2006**, 25, 4155-4165.
39. Kluwer, A. M.; Kloblenz, T. S.; Jonischkeit, T.; Woelk, K.; Elsevier, C. J. *J. Am. Chem. Soc.* **2005**, 127, 15470-15480.
40. Cavell, K. J.; Stufkens, D. J.; Vrieze, K.; *Inorganica Chimica Acta.* **1980**, 47, 67-76.
41. Itoh, K.; Uedo, F.; Hirai, K.; Ishii, Y. *Chem. Lett.* **1977**, 877-880.

42. Hauwert, P.; Maestri, G.; Sprengers, J. W.; Catelli, M.; Elsevier, C. J. *J. Angew. Chem. Int. Ed.* **2008**, 47, 3223-3226.

43. *Medac Ltd*; Alpha 319, Chobham Business Centre, Chertsey Road, Chobham, Surrey, GU24 8JB, UK.

44. Sheldrick, G. M. *Acta. Cryst.* **1990**, A46, 467-473. Sheldrick, G. M. SHELXL-97, *Program for crystal structure refinement*, University of Göttingen, **1997**.

Chapter Three

Synthesis and characterisation of 8-NHC metal complexes

3.1 Introduction

In a comparative study, Glorius and Dröge reviewed a series of NHCs and their electronic and structural properties upon a metal complex.[1] TEP (Tolmam's electronic parameter) is a common method used to measure the CO (A_1) stretching frequency of [Rh/IrCl$(CO)_2$(NHC)] complexes, this leads to a direct probe to quantify the level of electron donation of NHC ligand. Comparison of different size NHC ligands in [IrCl$(CO)_2$(NHC)] complexes reveal that as the ring size increases from 5- to 7-NHCs, the IR stretching frequencies of CO ligands decreases (Table 3.1).[2-4] Hence σ-donor ability of the NHC ligand increases as the ring expands (Figure 3.1).

Table 3.1. Comparison of infrared carbonyl stretching frequencies [cm^{-1}] and TEP values for ligands presented in Figure 3.1

Ligand	ν_{CO} (average)	TEP[a]
1	2026.0	2053.2
2	-	2048.3[b]
3	2018.1	2046.6
4	2015.5	2044.3

[a]TEP values were calculated using the equation obtained by Nolan et. al.[5]; [b]Calculated[6]

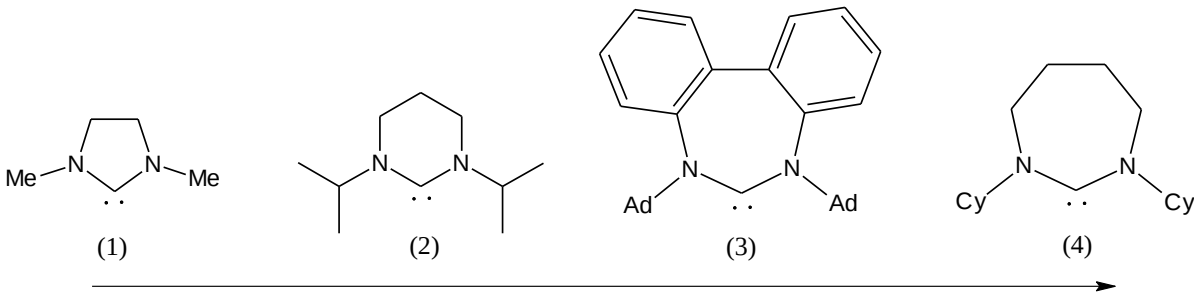

Figure 3.1. Comparison of 5-, 6- and 7-NHCs in [MCl$(CO)_2$(NHC)] (M = Rh/Ir) complexes

Coordination of free carbenes to metal centres leads to an increase in the N-C_{NHC}-N angle of the heterocyclic ring. For instance, 7-Mes angle changes from 116.6(4)° in the free NHC to 118.8(6)° in the silver complex, and the angle also increases for 6-Mes from 114.65(13)° to 118.3(3)°.[7] Unlike the 5- and 6-membered carbenes, the two nitrogen coordination planes in 7-NHC Ag complexes twist to alleviate ring strain.

The buried volume (%V_{bur}) concept was developed to quantify the steric demand of both NHC and phosphine ligands alike.[8] Clavier and Nolan examined a series of buried volumes relating to the NHCs that formed complexes with coinage metals.[9] As the NHC ring size increases from 5- to 7-membered cycles, the %V_{bur} value increases. For example, the buried volume of [AuCl(SIMes)] and [AuCl(6-Mes)] complexes are 36.9 and 42.9 respectively.[10-12] This has a substantial effect on the steric demand of large ring systems.

This chapter examines the structural and electronic features of 8-membered ring carbenes through the synthesis and characterisation of Ag, Rh, Ir (8-NHC) complexes. Their characteristic features are compared to those of the 5-, 6- and 7-NHC metal complex analogues. Air and moisture sensitive [NiX(8-NHC)(PPh_3)] complexes were also prepared, crystal structure data and EPR spectroscopic analysis were used to provide identification and further insight into the molecular structure of these paramagnetic compounds.

3.2 Results and Discussion

3.2.1 Silver(I) diazocanylidene NHC complexes

3.2.1.1 Synthesis and solution NMR studies of silver(I) NHC complexes

Eight-membered silver(I) NHC complexes were prepared by stirring diazocanylidene salts with 0.8 equivalent of Ag_2O and an excess amount of NaBr in dichloromethane under aerobic conditions (Scheme 3.1). The reaction was complete in three days yielding semi-crystalline solids. The formation of silver(I) complexes was monitored by the disappearance of the C_{NHC}-*H* proton in ^{1}H NMR spectra (which ranges between 7.31-7.61 ppm). A more reliable method to identify the existence of a silver complex is to locate the presence of C_{NHC} carbon signals in the $^{13}C\{^1H\}$ NMR spectrum, between the areas of 200-220 ppm which is the expected region for saturated carbenes. Such resonance should appear as two doublets, through coupling of the carbenic carbon with the NMR active isotopes of silver (^{107}Ag and ^{109}Ag) with spin ½. Thus the characteristic C_{NHC} shifts for [AgBr(8-Mes)] and [AgBr(8-Xyl)] were observed at 217.2 ppm ($^1J_C{}^{107}_{Ag}$ = 224 Hz, $^1J_C{}^{109}_{Ag}$ = 256 Hz) and 217.4 ppm ($^1J_{Ag}{}^{107}_{C}$ = 223 Hz, $^1J_C{}^{109}_{Ag}$ = 255 Hz) respectively in the $^{13}C\{^1H\}$ NMR spectrum.

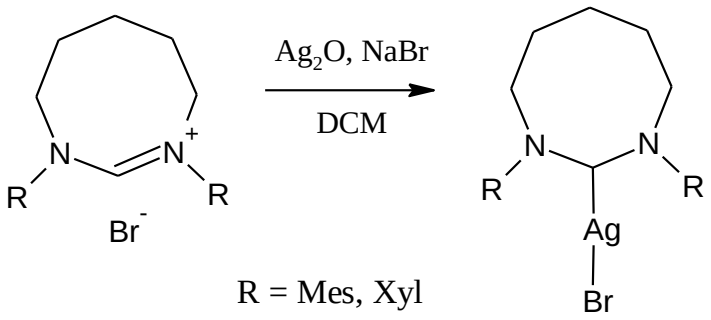

R = Mes, Xyl

	Yield
[AgBr(8-Mes)]	25%
[AgBr(8-Xyl)]	60%

Scheme 3.1. Synthesis of saturated silver (I) eight-membered carbene complexes

3.2.1.2 Solid-state structural analysis of silver (I) complexes

It is also noteworthy that reaction between 8-DIPP·HBr salt and Ag_2O does not proceed at all, despite elongating the reaction period and/or increasing the amount of silver (I) oxide. This is probably due to the size of the ligand which leads to an increase steric hindrance projected by the N-substituents, thus preventing any metal atom from coordinating to the carbene carbon. This is further supported by a crystallographic study of both [AgBr(8-Mes)] and [AgBr(8-Xyl)] complexes and assessment of their buried volumes. Crystals suitable for X-ray analysis were obtained by layering a dichloromethane solution of the corresponding complex with hexane at 0°C. Crystal structures of [AgBr(8-Mes)] and [AgBr(8-Xyl)] complexes are shown in Figure 3.2.

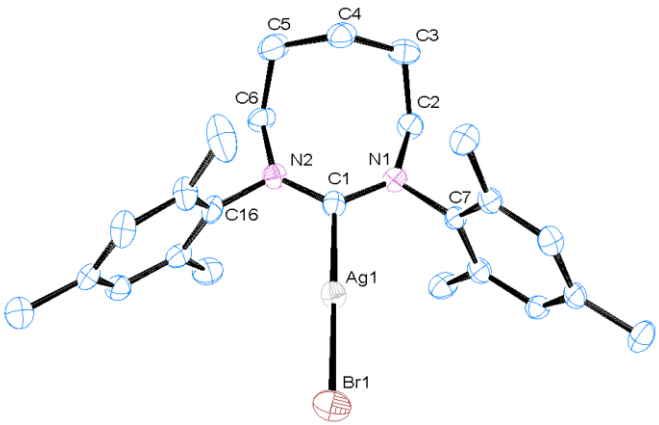

[AgBr(8-Mes)]

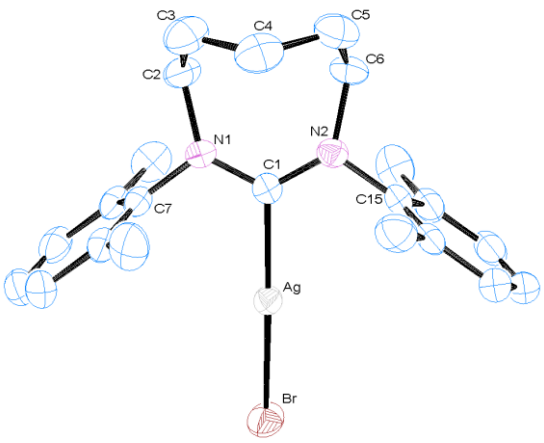

[AgBr(8-Xyl)]

Figure 3.2: Ortep ellipsoid plots at 50% probability of the molecular structure of [AgBr(8-Mes)] and [AgBr(8-Xyl)]. Hydrogen atoms have been omitted for clarity

The structures presented above show that the Ag metal adopts a linear geometry with both carbene and halide. The structure of the coordinating ligands in both complexes shows similar features to that of the corresponding salts and free carbene; the ring adopts a boat conformation with a large N-C_{NHC}-N and small C_{NHC}-N-C_{Ar} angles. A comparison of silver-NHC complexes bearing 5-, 6-, 7-, and 8-membered ring NHCs (Table 3.2) shows the effect of increasing ring size on relevant bond angles and the Ag-C_{NHC} bond lengths. Despite the difference in halide and N-substituents (NHC) between the silver-NHC complexes, a clear structural trend reveals that larger rings cause the aromatic substituents on the ring nitrogens to bend ever closer towards each other and in effect encapsulate the Ag centre. This will lead to increased protection of the metal centre against additional reactions, thus preventing a second bulky NHC (8-DIPP in this case) from coordinating. Such large ligands favour complexes with low coordination numbers.

Table 3.2: Selected bond lengths (Å) and bond angles (°) of structures of 5-, 6-, 7-, and 8-NHC [AgX(NHC)] complexes

	Ag-C_{NHC}	Ag-X	N(1)-C_{NHC}-N(2)	C_{NHC}-N(1)-C_{Ar} C_{NHC}-N(2)-C_{Ar}
[AgCl(5-Mes)] [11, 13]	2.056(7)	2.314(2)	104.4(5)	121.8(3)
[AgCl(5-SDIPP)] [14]	2.059(9)	2.306(2)	107.8(8)	123.1(5)
[AgCl(6-Mes)] [7, 11]	2.095(3)	2.3213(10)	118.3(3)	119.4(2)
				118.5(2)
[AgBr(6-DIPP)] [7]	2.104(6)	2.4254(9)	118.8(5)	118.7(5)
				120.6(5)
[AgBr(7-Mes)] [7]	2.097(6)	2.3792(11)	118.8(6)	117.0(5)
				117.3(5)
[AgI(7-Xyl)] [7]	2.114(6)	2.5659(7)	121.2(5)	116.8(5)
				117.8(5)
[AgBr(8-Mes)]	2.132(4)	2.4553(5)	123.2(3)	115.3(3)
				115.7(3)
[AgBr(8-Xyl)]	2.123(3)	2.4370(5)	123.3(3)	115.1(3)
				115.4(3)

An additional structural characteristic feature is the torsional angles (α), defined by the C_{Ar}–N···N–C_{Ar} atoms. It is a gauge for the spatial twist of the N coordination plane that determines the relative position of the aromatic substituents, thus pointing directly into the coordination sphere of the metal. Torsional angles calculated for silver complexes [AgBr(8-Mes)] and [AgBr(8-Xyl)] were 1.85° and 0.96° respectively. In comparison with [AgBr(7-

Mes)] (α = 30.3°) and [AgI(7-Xyl)] (α = 23.1°),[7] the 8-membered rings exhibit little sign of spatial twisting of the aromatic substituents.

A further illustration of the enhanced steric bulkiness of these expanded ring NHCs (compared mainly between those with the same N-substituents) can be clearly seen by the percentage buried volumes (%V_{bur})[15] calculated for the silver complexes, the results of which are presented in Table 3.3. The buried volume increases considerably as the ring size expands from 5- to 8-membered NHCs; the values represent the high steric demand inflicted by the larger NHC ring sizes. These findings are consistent with the X-ray analysis and other observations such as the change in reactivity. The different halide ions have little influence on the calculated buried volume for these linear complexes, thus the comparison of %V_{bur} shown in Table 3 is legitimate.

Table 3.3: %V_{bur} values for NHCs in [AgX(NHC)] complexes [a]

[AgX(NHC)] complex	%V_{bur}
[AgCl(5-IMes)] [9]	36.1
[AgCl(5-SIMes)] [9]	36.1
[AgCl(6-Mes)] [11]	44.0
[AgBr(7-Mes)] [7]	44.7
[AgBr(8-Mes)]	48.7
[AgBr(8-Xyl)]	49.1

[a] NHC structures extracted from crystal structures cif files. (*r*=3.5 Å, *d*=2.0 Å, Bond radii scaled by 1.17)

3.2.1.3 Attempted synthesis of Ag(8-*o*-Tol/*o*-Anis)Br complex

Several attempts to prepare Ag(I) complexes of expanded, unsymmetrically functionalised NHC using a variety of methods were unsuccessful. Reaction of Ag_2O with 8-*o*-Tol/*o*-Anis bromide salt under normal conditions leads to the hydrolysis of the carbene (Scheme 3.2).

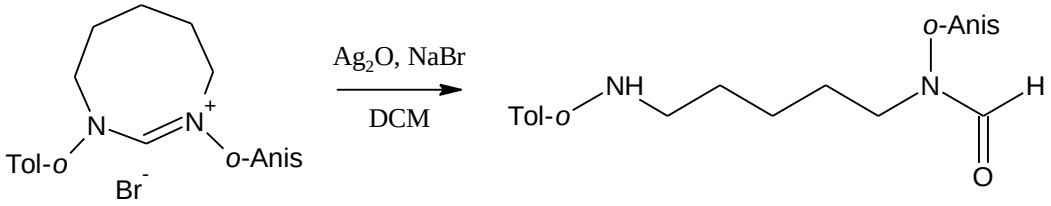

Scheme 3.2. Attempted preparation of an expanded functionalized Ag (I) NHC complex

Examples of Ag(I) complexes with other expanded functionalised 6- and 7-membered NHCs are also absent from literature, this suggests that the same result may have occurred with the corresponding counterparts and formation of such species is not as straightforward as it seems.

3.2.2 Rhodium(I) and Iridium(I) complexes of diazocanylidene NHCs

3.2.2.1 Synthesis of Rhodium(I) and Iridium(I) COD complexes

There is a vast number of [RhCl(NHC)(COD)] and [IrCl(NHC)(COD)] complexes bearing 5-, 6- and 7-membered NHCs.[16-22] What makes these metal-NHC complexes so popular is that they can be easily prepared, handled and also act as an intermediate to form the corresponding Rhodium(I) and Iridium(I) biscarbonyl complexes. The latter species are used in an indirect measure of the σ-donor strength by IR spectroscopy.[23]

Treatment of $[MCl(COD)]_2$ (M = Rh, Ir) with 2 equivalents of *in situ* formed free NHC (application of the corresponding NHC·HBr salt with KHMDS in THF) gives rise to [MCl(8-NHC)(COD)] complexes as yellow air-stable solids (Scheme 3.3). As previously noted, such large ring systems are sterically large and their metal complexes maybe difficult to access. As expected it was found that the 8-Mes ligand was too large to coordinate to the $[MCl(COD)]_2$ dimer and only the less sterically demanding examples of the expanded 8-NHC (e.g. 8-*o*-Tol) were able to yield the corresponding [MCl(8-*o*-Tol)(COD)] metal complexes. However, synthesis of the unsymmetrical 8-NHC-rhodium complex, [RhCl(8-*o*-Tol/*o*-Anis)(COD)] via the free carbene route was unsuccessful. This was a little surprising as the steric size of the unsymmetrical NHC bearing N-substituents of *o*-Tol and *o*-Anis are comparable to that of the symmetrical NHC with *o*-Tol groups. The failure of this reaction is probably due to the slight steric increase at the metal centre imposed by the proximity of the *o*-Anis methoxy group. Hence, this constraint hinders the coordination of the metal and the free carbene. Attempted generation of 8-NHC-rhodium complexes through transmetallation from the corresponding Ag(I) complexes met with no success. Herrmann et al. and Kolychev et al. reported the same outcome when attempting to obtain 6/7-NHC-Pd and Rh complexes via transmetallation of [AgBr(6/7-NHC)] complexes. [11, 24] These results suggest that the expanded ring carbenes possess a higher energy NHC-Ag bond in respect to five membered ring counterparts.[25] In addition, attempts to obtain the correct mass from the mass spectra for the [RhCl(O-8-*o*-Tol)(COD)] complex failed, even after several purifications. This complex was characterized

by ^{1}H and $^{13}C\{^{1}H\}$ NMR spectroscopy, the structure was obtained by single-crystal X-ray diffraction which confirms the nature of the complex (see below).

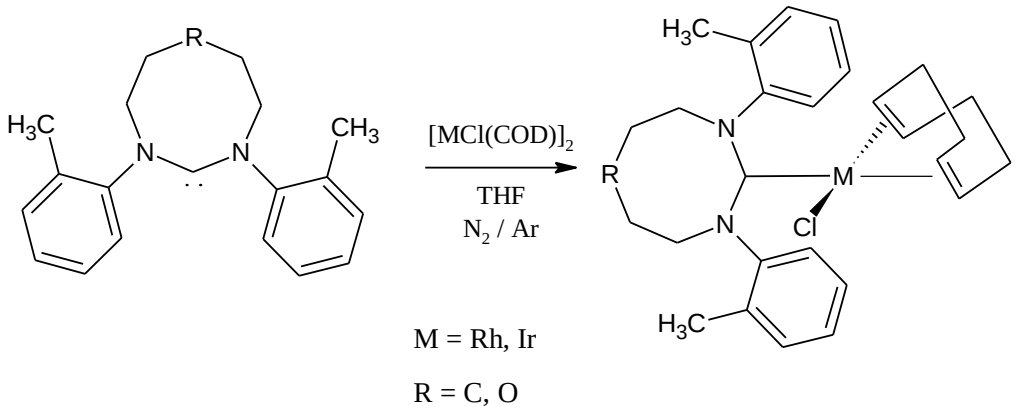

M = Rh, Ir

R = C, O

	Yield
[RhCl(8-*o*-Tol)(COD)]	72%
[IrCl(8-*o*-Tol)(COD)]	52%
[RhCl(O-8-*o*-Tol)(COD)]	73%
[IrCl(O-8-*o*-Tol)(COD)]	61%

Scheme 3.3. Preparation of Rh(I) and Ir(I) COD complexes with expanded 8-NHC ligands (where O represents an oxygen atom at the 8-membered ring backbone '*R*')

3.2.2.2 Solution NMR studies of Rh(I) and Ir(I) COD complexes

The ^{1}H NMR spectrum of 8-NHC Rh(I) and Ir(I) COD complexes reveal a notable downfield shift of the *o*-CH_{Ar} atoms, from the region 7.27 – 7.46 ppm in the pro-ligand salt to 8.53 – 8.60 ppm in the Rh(I) complexes and 8.29 – 8.60 ppm in the Ir(I) complexes (Table 3.4). This change in the ^{1}H NMR spectra is attributed to the close proximity of the *ortho*-H atoms and the electron rich metal centres.[3]

Table 3.4: ^{1}H NMR *o*-C*H*$_{Ar}$ spectral shifts (ppm) for the NHC salt and their Rh(I) and Ir(I) complexes in $CDCl_3$ solution

8-NHC·HBr salt & Rh/Ir complex	δ (*o*-C*H*$_{Ar}$)
8-o-Tol·HBr	7.46
[RhCl(8-*o*-Tol)(COD)]	8.60
[IrCl(8-*o*-Tol)(COD)]	8.29
O-8-o-Tol·HBr	7.26
[RhCl(O-8-*o*-Tol)(COD)]	8.53
[IrCl(O-8-*o*-Tol)(COD)]	8.60

The $^{13}C\{^{1}H\}$ NMR spectral chemical shifts for C_{NHC} carbon atom of the metal complexes are shown in Table 3.5. A slightly upfield shift is observed for the carbon atom in 8-NHC Rh/Ir complexes when compared to [RhCl(7-*o*-Tol)(COD)].[20] Conversely, a significant downfield shift is observed for the carbene atom in [RhCl(7-/8-*o*-Tol)(COD)] when compared to those for [RhCl(5-/6-Mes)(COD)]. For Rh(I) complexes, the carbene carbon atom signal appears as a doublet due to Rh coupling ($^{1}J_{RhC}$). [RhCl(8-*o*-Tol)(COD)] and [RhCl(7-*o*-Tol)(COD)] complexes show identical Rh-C_{NHC} coupling constants, whereas a slightly lower value is seen for [RhCl(O-8-*o*-Tol)(COD)]. Further comparison between the different NHC Rh complexes show that the $^{1}J_{RhC}$ value increases with decreasing ring size: 8-/7- < 6- < 5-NHC.

Table 3.5: $^{13}C\{^{1}H\}$ NMR spectral shifts (ppm) for the C_{NHC} carbon atom of the Ir(I) and Rh(I) complexes with Rh-C_{NHC} coupling constants (Hz) in $CDCl_3$ solution

Complex	δ C_{NHC} ($^{1}J_{RhC}$)
[IrCl(8-*o*-Tol)(COD)]	210.3
[IrCl(O-8-*o*-Tol)(COD)]	214.4
[RhCl(5-Mes)(COD)] [20]	211.6 (48.2)
[RhCl(6-Mes)(COD)] [20]	211.5 (46.9)
[RhCl(7-*o*-Tol)(COD)] [20]	222.8 (45.0)
[RhCl(8-*o*-Tol)(COD)]	215.9 (45.0)
[RhCl(O-8-*o*-Tol)(COD)]	220.7 (44.6)

It has been observed previously that hindered rotation about the N-Ar bond can lead to four possible rotamers (Figure 3.3) which, depending on the rate of the rotation, can be distinguished by NMR spectroscopy.[20] Only one resonance was observed for the two *ortho*-methyl groups in the ^{1}H and $^{13}C\{^{1}H\}$ NMR spectrum, thus suggesting the formation of the *syn* isomer. More specifically, the two methyl groups are positioned on the face of the COD

ligand, away from the chloride atom to avoid steric tension from the encumbered NHC ligand and the metal complex (hence this is further proved by the crystallographic data of the complexes).

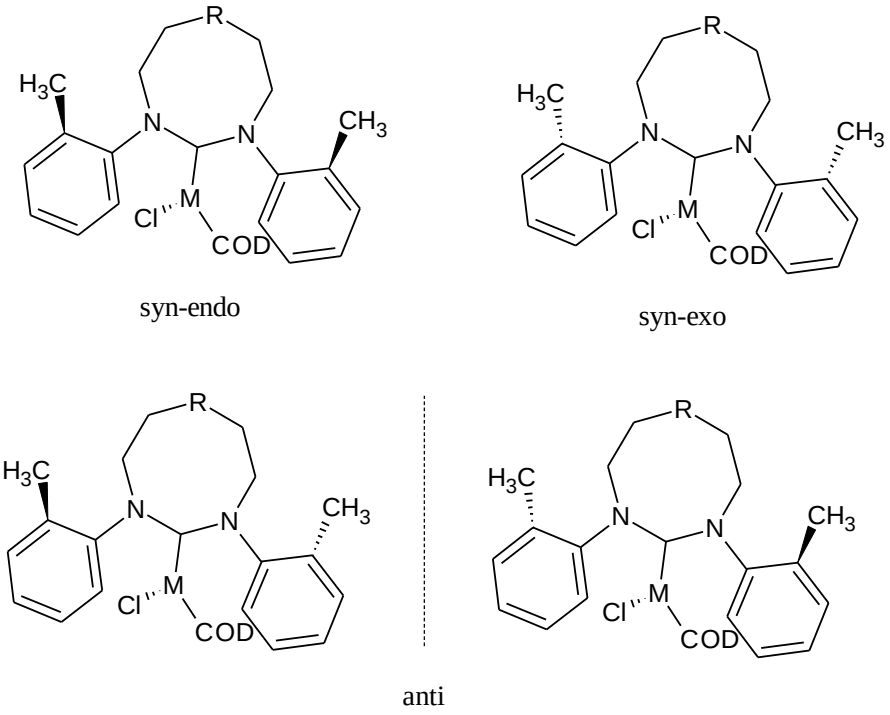

Figure 3.3. Rotamers of [Rh/IrCl(8-NHC)(COD)]

3.2.2.3 Solid state structural analysis of Rh(I) and Ir(I) COD complexes

Crystals of 8-NHC Rh(I) and Ir(I) suitable for X-ray diffraction were obtained by layering a tetrahydrofuran solution of the corresponding complex with hexane at 0°C. Molecular structures of [RhCl(8-*o*-Tol)(COD)], [RhCl(O-8-*o*-Tol)(COD)], [IrCl(8-*o*-Tol)(COD)] and [IrCl(O-8-*o*-Tol)(COD)] are provided in Figure 3.4. A comparison of selected bond lengths and angles with a range of [RhCl(NHC)(COD)] complexes is found in Table 3.6, whereas the [IrCl(NHC)(COD)] complexes are separately listed in Table 3.7.

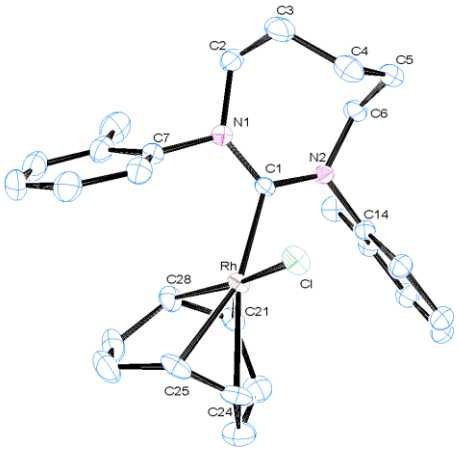

[RhCl(8-*o*-Tol)(COD)]

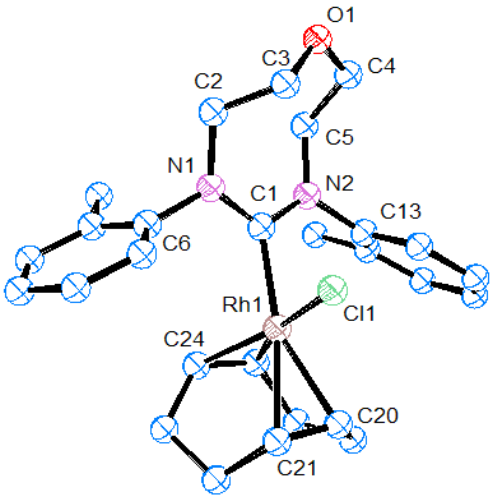

[RhCl(O-8-*o*-Tol)(COD)]

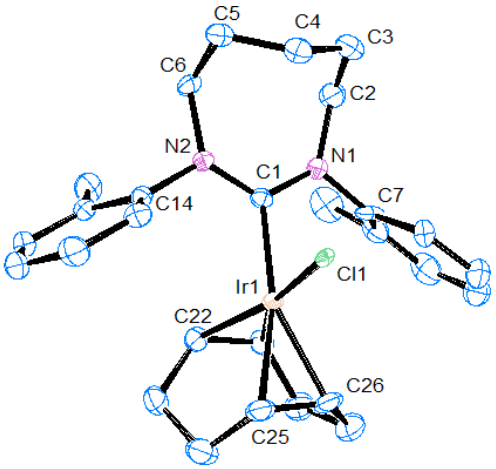

[IrCl(8-*o*-Tol)(COD)]

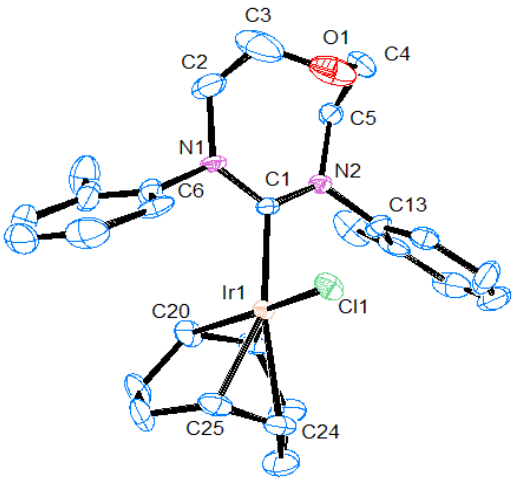

[IrCl(O-8-*o*-Tol)(COD)]

Figure 3.4: Ortep ellipsoid plots at 50% probability of the molecular structures of 8-NHC Rh(I) and Ir(I) COD complexes. Hydrogen atoms have been omitted for clarity

Table 3.6: Selected bond lengths (Å) and bond angles (°) for [RhCl(NHC)(COD)] complexes

	5-Mes[20]	6-Mes[20]	7-Mes[20]	7-*o*-Tol[20]	8-*o*-Tol	O-8-*o*-Tol
Rh–C_{NHC}	2.0513(14)	2.078(4)	2.085(3)	2.030(3)	2.061(3)	2.038(4)
Rh–Cl	2.3665(3)	2.3876(13)	2.3817(8)	2.4470(7)	2.4357(8)	2.4402(11)
C_{Ar}–N–C_{NHC}	127.62(13)	119.5(4)	119.1(2)	117.1(2)	117.3(2)	118.6(4)
	127.06(12)	119.1(4)	117.2(2)	120.5(3)	118.2(2)	117.1(3)
N–C_{NHC}–N	107.29(12)	117.0(4)	118.0(3)	117.2(3)	121.3(2)	118.3(4)
C_{NHC}–Rh–Cl	91.86(4)	86.75(13)	85.27(9)	86.59(8)	88.01(8)	87.42(12)
*Tilt angle θ	59.0	83.5	87.8	81.1	88.4	89.3

*The tilt angle is defined as the angle between the coordination plane and the NHC N-C_{NHC}-N plane

Table 3.7: Selected bond lengths (Å) and bond angles (°) for [IrCl(NHC)(COD)] complexes

	8-*o*-Tol	O-8-*o*-Tol
Ir–C_{NHC}	2.059(5)	2.069(7)
Ir–Cl	2.4651(10)	2.4190(19)
C_{Ar}–N–C_{NHC}	116.0(4)	119.1(7)
	118.7(4)	119.5(6)
N–C_{NHC}–N	121.1(5)	120.9(6)
C_{NHC}–Ir–Cl	88.38(14)	92.3(2)
Tilt angle θ	88.0	87.3

The 8-NHC Rh(I) and Ir(I) complexes adopt a slightly larger N-C_{NHC}-N angle compared to that of the 7-NHC ring with both being significantly larger than the 5-membered ring. This leads to a concomitant compression of the C_{NHC}-N-C_{Ar} angle from an average of 127.34° in 5-Mes to 118.8° in [RhCl(7-*o*-Tol)(COD)] and 117.7° in the [RhCl(8-*o*-Tol)(COD)] equivalent. Consequently, the N-aryl substituents are forced slightly closer towards the metal. Therefore unlike the 7-NHC Rh complex (existing as three isomers with different ratios of *syn* and *anti* rotamers caused by the restricted rotation of the Rh-NHC and N-Ar bonds), the 8-NHC metal counterpart favours only the *syn-endo ortho*-methyl orientation (confirmed in the solid state) due to the rigid steric strain exerted on the metal centre by these large expanded heterocyclic-rings. Such large ring expanded NHC systems exhibit tilt angles θ (defined as the angle between the coordination plane and the N-C_{NHC}-N plane of the NHC) of near 90° for 8-NHCs, whereas 5-membered ring carbenes adopt much smaller tilt angles (59° for [RhCl(5-Mes)(COD)]). Overall, the aromatic substituents on the ring nitrogens of 8-NHCs enclose round the metal centre more than all previous ring sizes, this steric congestion can be a major influence in the reactivity at the metal centre.

3.2.3 Synthesis of Rhodium (I) carbonyl complex cis-[RhCl(8-*o*-Tol)(CO)$_2$]

Exchange of the COD (relatively small capacity for π*-backdonating) with CO (relatively high capacity for π*-backdonating) coupled with the use of IR spectroscopy provides a measure of the relative net donation of electron density to the metal. Hence, [MCl(NHC)(CO)$_2$] (M = Rh, Ir) complexes can be used to compare NHC ligand basicity/donor ability by determination of the carbonyl stretching frequencies.[1, 17, 26]

The [RhCl(8-*o*-Tol)(CO)$_2$] complex was prepared in good yield by passing carbon monoxide through a solution of [RhCl(8-*o*-Tol)(COD)] in dichloromethane at room temperature for 30 minutes (Scheme 3.4).

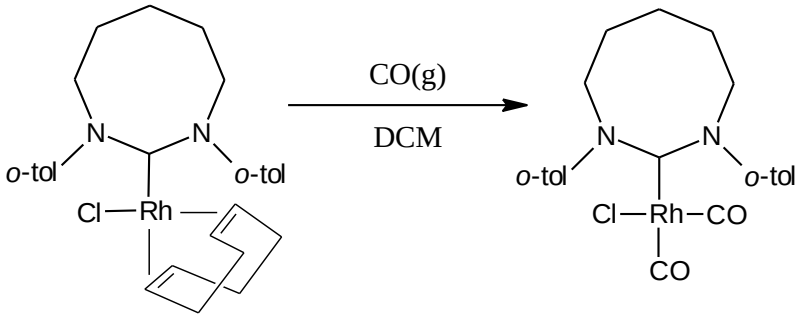

	Yield
[RhCl(8-*o*-Tol)(CO)$_2$]	84%

Scheme 3.4. Synthesis of 8-*o*-Tol Rh carbonyl complex

3.2.3.1 NMR, structural and electronic analysis of [RhCl(8-*o*-Tol)(CO)$_2$] complex

The $^{13}C\{^1H\}$ NMR spectroscopic signal for Rh-C_{NHC} appears as a doublet at 207.1 ppm ($^1J_{RhC}$ = 36 Hz) along with two Rh-*C*O resonances at 185.4 ppm ($^1J_{RhC}$ = 55 Hz) and 182.2 ppm ($^1J_{RhC}$ = 78 Hz). These data are listed in Table 3.8 together with other various carbonyl Rh complexes bearing different ring size NHCs.

Table 3.8: $^{13}C\{^{1}H\}$ NMR spectral shifts (ppm) for the C_{NHC} and $C_{carbonyl}$ carbon atom of the carbonyl Rh complexes with Rh-C_{NHC} and Rh-CO coupling constants (Hz) in $CDCl_3$ solution

Complex	δ C_{NHC} ($^{1}J_{RhC}$)	δ $C_{carbonyl}$ ($^{1}J_{RhC}$)[A]	δ $C_{carbonyl}$ ($^{1}J_{RhC}$)[B]
[RhCl(5-Mes)$(CO)_2$] [20]	205.0 (40.8)	184.2 (57.3)	181.9 (74.4)
[RhCl(6-Mes)$(CO)_2$] [20]	202.9 (40.8)	186.1 (52.5)	183.7 (67.6)
[RhCl(7-Mes)$(CO)_2$] [20]	213.4 (40.8)	187.1 (52.5)	184.5 (77.7)
[RhCl(7-Xyl)$(CO)_2$] [20]	212.2 (40.8)	184.5 (52.5)	182.6 (77.3)
[RhCl(8-*o*-Tol)$(CO)_2$]	207.1 (36)	185.4 (55)	182.2 (78)

[A] CO trans to Cl; [B] CO trans to NHC

A slight upfield shift is observed for the carbon atom in 8-NHC carbonyl Rh complexes when compare to the 7-NHC, but lower than that of the 6- and 5-NHC. However Rh-C_{NHC} spin-spin coupling constant of 8-NHC has the lowest value in the table. The 8-NHC and 7-Xyl Rh complexes show similar shifts for the $C_{carbonyl}$ carbon atoms. The Rh-*C*O coupling constants on the other hand, are higher in value than those of the complexes bearing 6- and 7-NHCs, indicating that the Rh-CO bond in the [RhCl(8-NHC)$(CO)_2$] complex possesses a higher s character than their 6- and 7-NHC counterparts.[27]

Crystals suitable for X-ray analysis were obtained by diffusion of hexane vapour into a dichloromethane solution containing the corresponding compound. The crystal structure of [RhCl(8-*o*-Tol)$(CO)_2$] is shown in Figure 3.5, along with the selected bond lengths and bond angles in Table 3.9.

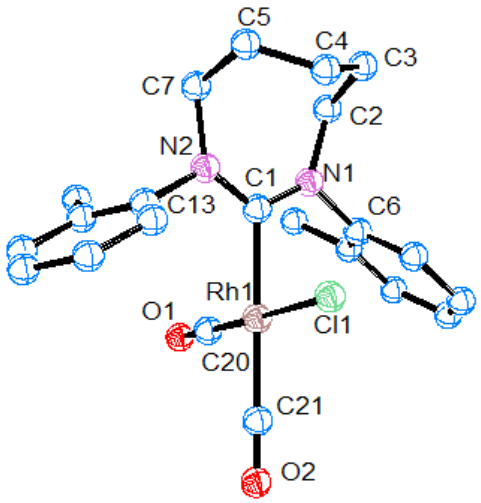

Figure 3.5: Ortep ellipsoid plot at 50% probability of the molecular structure of [RhCl(8-*o*-Tol)$(CO)_2$]. Hydrogen atoms have been omitted for clarity

Table 3.9: Selected bond lengths (Å) and bond angles (°) for [RhCl(8-*o*-Tol)(COD)] complex

Lengths (Å)		Angles (°)	
Rh(1)-C(1)	2.075(8)	N(1)-C(1)-N(2)	122.5(8)
Rh(1)-Cl(1)	2.404(2)	C(1)-N(1)-C(6)	116.8(7)
Rh(1)-C(20)	1.834(12)	C(1)-N(2)-C(13)	118.4(7)
Rh(1)-C(21)	1.902(11)	C(1)-Rh(1)-Cl(1)	88.7(2)
		C(1)-Rh(1)-C(20)	89.5(4)
		C(1)-Rh(1)-C(21)	177.9(4)

This 8-NHC Rh(I) complex adopts a square planar geometry at the metal centre. Also the tilt angle is 87.3°, comparable to those of the Rh(I) 8-NHC COD complexes. Carbonyl stretching frequencies for [RhCl(NHC)(CO_2)] complexes bearing 5-, 6- and 7-membered rings were compared with those of [RhCl(8-*o*-Tol)(COD)] (Table 3.10).

Table 3.10: Infrared carbonyl stretching frequencies [cm^{-1}] for [RhCl(NHC)($CO)_2$] complexes[a]

Complex	$\nu_{s,as}$ [cm^{-1}]	ν_{av} [cm^{-1}]
[RhCl(5-Mes)($CO)_2$] [20, 28]	1995, 2080	2037.5
[RhCl(6-Mes)($CO)_2$] [20]	1987, 2071	2029
[RhCl(7-Mes)($CO)_2$] [20]	1987, 2069	2028
[RhCl(7-Xyl)($CO)_2$] [20]	1986, 2071	2028.5
[RhCl(8-*o*-Tol)($CO)_2$]	1981, 2068	2024.5

[a]Measured in CH_2Cl_2

Carbonyl stretching frequencies for the 6- and 7-membered NHCs show similar donor abilities. Whereas the high frequency values for the 5-membered NHC imply a reduced electron density contribution to the metal from the NHC and thus is consistent with relatively lower ligand basicity. Overall, it would seem that the 8-*o*-Tol NHC, with an average υ(CO) of 2024.5 cm^{-1}, is the better donor of all the NHC ligands in the table. Nevertheless, these figures must be taken with some degree of caution as other methods for determining ligand basicity may well give somewhat different results.[1]

3.2.4 Synthesis of 8-NHCs Rhodium (acac) complexes

With the exception of 8-*o*-Tol NHC, initial attempts to coordinate 8-membered carbenes to $[RhCl(COD)]_2$ failed due to steric constraints. However, when 8-NHC free carbenes reacted with $[Rh(acac)CO_2]$ the expected compounds were obtained by substitution of one of the carbonyl ligands, a full range of [Rh(NHC)(CO)(acac)] complexes were prepared. The reaction was performed in THF under an inert atmosphere at room temperature over 4 hours (Scheme 3.5). Upon addition of the free carbene to $[Rh(acac)CO_2]$ in THF, the colour of the solution changed from light orange to dark green.

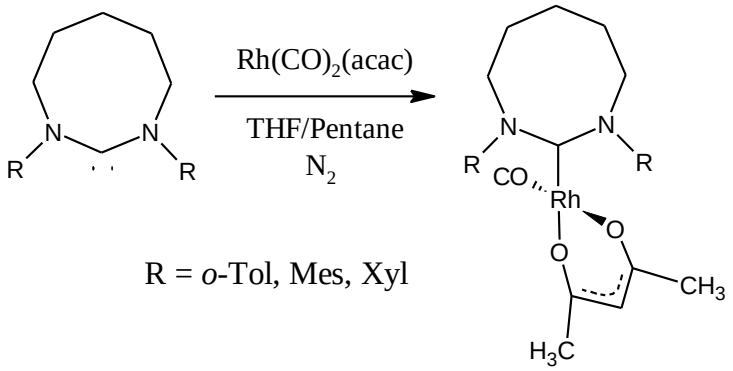

R = *o*-Tol, Mes, Xyl

	Yield
[Rh(8-Mes)(acac)CO]	79%
[Rh(8-Xyl)(acac)CO]	80%
[Rh(8-*o*-Tol)(acac)CO]	87%

Scheme 3.5. Synthesis of [Rh(NHC)(acac)(CO)] complexes

3.2.4.1 Solution NMR and structural analysis of 8-NHC Rhodium (acac) complexes

Characteristic $^{13}C\{^1H\}$ NMR spectral signals for Rh-C_{NHC} and Rh-*C*O (both appear as a doublet) combined with their coupling constants are shown in Table 3.11. These complexes show a slight upfield shift of the C_{NHC} carbon when compared to those of the 8-NHC Rh/Ir COD complexes.

Table 3.11: $^{13}C\{^{1}H\}$ NMR spectral shifts (ppm) for the C_{NHC} and C_{CO} carbon atoms of 8-NHC Rh (acac) complexes with Rh-C_{NHC} and Rh-C_{CO} coupling constants (Hz) in $CDCl_3$ solution

Complex	δ C_{NHC} ($^{1}J_{RhC}$)	δ C_{CO} ($^{1}J_{RhC}$)
[Rh(8-Mes)(acac)CO]	210.8 (52.5)	190.4 (85)
[Rh(8-Xyl)(acac)CO]	210.7 (52.5)	190.3 (85)
[Rh(8-*o*-Tol)(acac)CO]	211.8 (53)	191.7 (84)

Crystals suitable for X-ray diffraction were obtained after standing a pentane solution of the complexes at 0°C. Crystal structures of [Rh(8-NHC)(acac)CO] bearing 8-Mes, 8-Xyl and 8-*o*-Tol are shown in Figure 3.6; selected bond angles and bond lengths are displayed in Table 3.12.

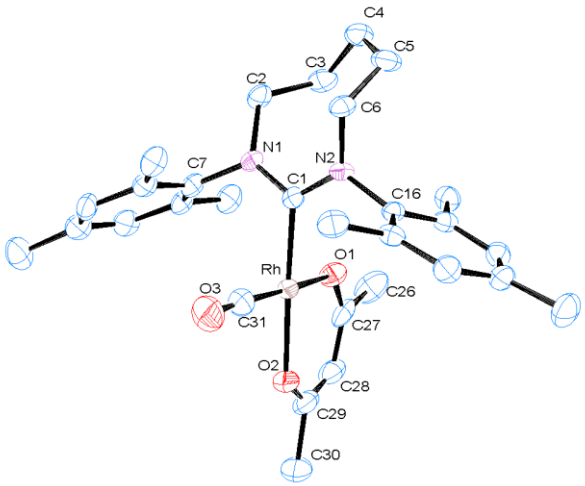

[Rh(8-Mes)(acac)CO]

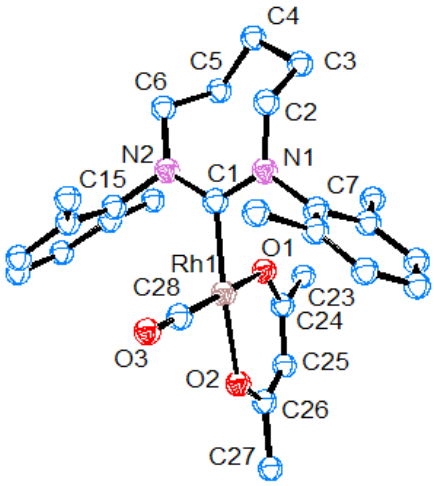

[Rh(8-Xyl)(acac)CO]

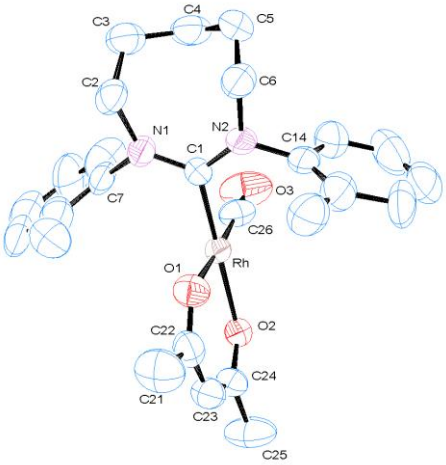

[Rh(8-*o*-Tol)(acac)CO]

Figure 3.6: Ortep ellipsoid plots at 50% probability of the molecular structures of [Rh(8-NHC)(acac)CO] complexes. Hydrogen atoms have been omitted for clarity

Table 3.12: Selected bond lengths (Å) and bond angles (°) for [Rh(8-NHC)(acac)CO] complexes

	8-Mes	8-Xyl	8-*o*-Tol
$Rh–C_{NHC}$	1.997(4)	2.039(4)	1.997(9)
Rh–CO	1.795(6)	1.786(8)	1.807(14)
$C_{Ar}–N–C_{NHC}$	119.5(4)	11.6.9(4)	117.4(7)
	118.6(4)	116.4(4)	118.7(8)
$N–C_{NHC}–N$	118.7(4)	120.9(4)	120.3(8)
$C_{NHC}–Rh–CO$	92.1(2)	92.9(3)	90.2(4)
Tilt angle	85.0	87.5	88.3

Structural analysis reveals that for every Rh (acac) complex, the N-C_{NHC}-N plane of the carbene ligand adopts a perpendicular (90°) arrangement to the planar acac co-ligand, which is the lowest energy conformation for the bulky 8-NHC ligands upon coordination to the metal complex.

3.2.5 Synthesis of 8-NHC Ni(I) complexes

The study of Ni-NHC chemistry has been given far less attention compared to that of Pd, Ru and Rh-NHC complexes. Nevertheless, in recent times there has been an emergence of a number of NHC-Ni(0) and NHC-Ni(II) systems. These species were shown to participate in a range of catalysis such as dehalogenation,[29] dehydrogenation,[30] aryl amination,[31] aryl thiolation,[32] hydrothiolation[33] and cross-coupling reactions.[34]

Several rare but novel 15-electron 6-NHC Ni(I) complexes have been prepared by Whittlesey and Sigman via reacting a Ni(0) complex with carbene in the presence of a Ni(II) species in order to yield the desired Ni(I) product. [35, 36] Hence a solution of 8-NHC free carbene was added to a mixture of $[Ni(COD)_2]$ and $[NiCl_2(PPh_3)_2]$ in toluene. The reaction was stirred overnight at room temperature followed by filtration of the solution; the remaining yellow precipitate was extracted into THF and then filtered into the toluene fraction. The combined solutions were reduced to a minimum via *vacuo* and upon addition of hexane yielded 8-NHC Ni(I) complexes as bright yellow precipitates (Scheme 3.6).

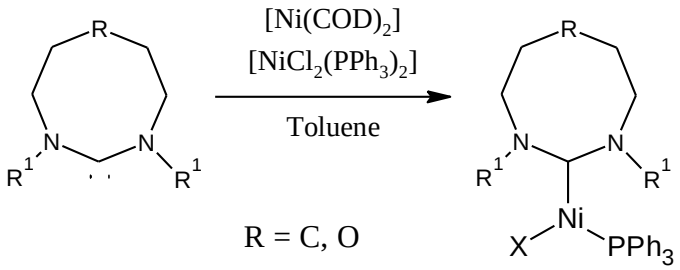

R = C, O

R^1 = *o*-Tol, Mes

X = Br, Cl

	Yield
[NiBr(8-Mes)(PPh_3)]	52%
[NiCl(8-*o*-Tol)(PPh_3)]	60%
[NiCl(8-*o*-Anis/*o*-Tol)(PPh_3)]	41%
[NiBr(O-8-*o*-Tol)(PPh_3)]	36%

Scheme 3.6. Synthesis of [NiX(8-NHC)(PPh_3)] complexes

3.2.5.1 Solid state structural analysis of 8-NHC Ni(I) complexes

Crystals suitable for X-ray crystallography were obtained by the diffusion of hexane into a THF solution of the 8-NHC Ni(I) complex at -35°C in a glovebox. The X-ray crystal structures of these 8-membered NHC complexes showed they exist as a 70:30 mixture of bromide and chloride species as a result of halide exchange with the 8-NHC·HBr counterion; complexes of the dominant halide species are shown in Figure 3.7. Selected bond lengths and bond angles are listed in Table 3.13. Pure [NiCl(8-*o*-Tol)(PPh_3)] and [NiBr(8-*o*-Tol)(PPh_3)] complexes were later prepared using 8-*o*-Tol·BF_4 instead and their elemental analyses were obtained. Unfortunately, crystals appropriate for X-ray diffraction were not obtained for the complex, [NiCl(8-*o*-Anis/*o*-Tol)(PPh_3)]. But high resolution MS-ES gave results consistent with the proposed formulation, giving a pronounced molecular ion peak of *m/z* = 663 that retains the isotope pattern of the complex.

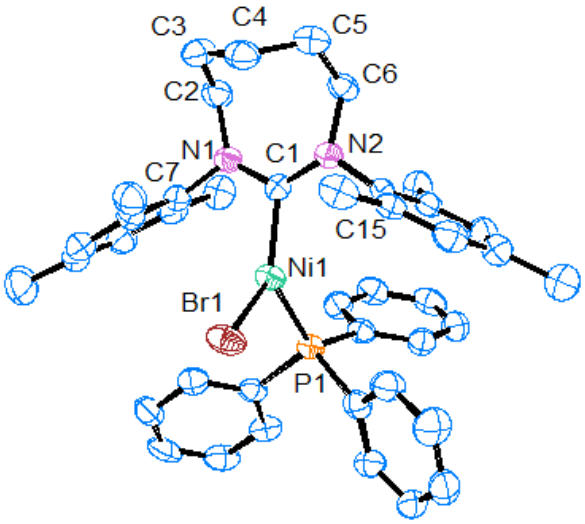

[NiBr(8-Mes)(PPh$_3$)]

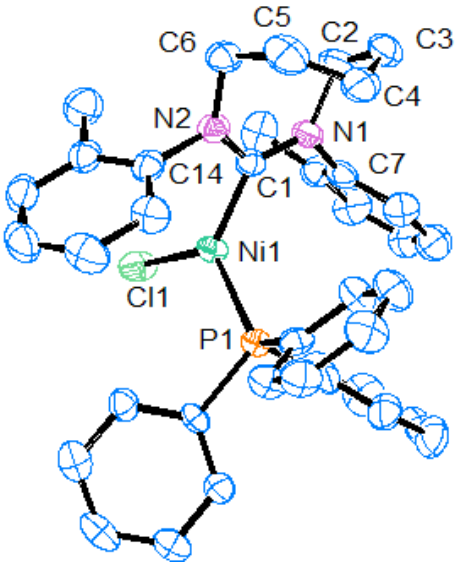

[NiCl(8-*o*-Tol)(PPh$_3$)]

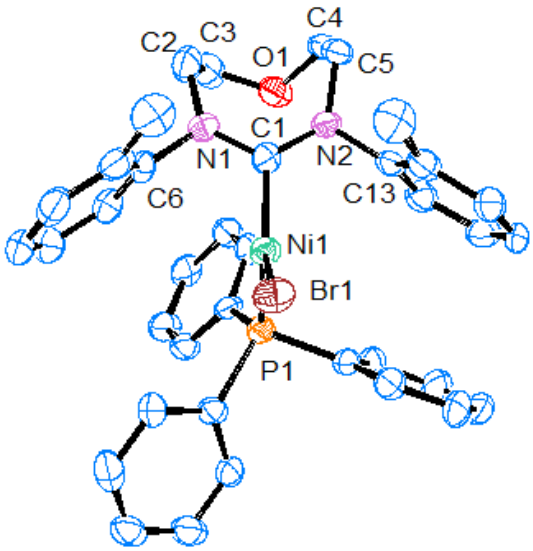

[NiBr(O-8-*o*-Tol)(PPh$_3$)]

Figure 3.7: Ortep ellipsoid plots at 30% probability of the molecular structures of 8-NHC Ni(I) complexes. Hydrogen atoms have been omitted for clarity

Table 3.13: Selected bond lengths (Å) and bond angles (°) for [NiX(NHC)(PPh_3)] complexes

	IPr[37]	6-Mes[35]	8-Mes	8-*o*-Tol	O-8-*o*-Tol
Ni–C_{NHC}	1.930(3)	1.942(2)	1.979(5)	1.951(6)	1.935(7)
Ni–X	2.179(9)	2.3332(3)	2.3310(9)	2.3123(12)	2.3106(12)
Ni-P	2.20(1)	2.2187(6)	2.2211(15)	2.1934(18)	2.1926(19)
C_{Ar}–N–C_{NHC}	121.8(2)	116.04(10)	117.6(4)	117.2(5)	115.7(5)
	122.2(2)	118.55(10)	117.1(4)	114.2(5)	113.4(5)
N–C_{NHC}–N	103.4(2)	117.27(11)	121.8(4)	121.0(6)	120.8(6)
C_{NHC}–Ni–X	134.2(1)	133.45(6)	135.37(14)	130.68(19)	133.80(18)
C_{NHC}–Ni–P	112.1(1)	117.02(6)	121.58(14)	111.95(19)	109.62(19)
P-Ni-X	113.31(4)	109.536(19)	102.97(4)	117.33(6)	116.49(6)
Tilt angle θ	-	-	83.0	88.1	85.3

Similar to the [NiBr(6-Mes)(PPh_3)] and [NiCl(IPr)(PPh_3)] crystal structures, the [NiX(8-NHC)(PPh_3)] complexes reveal a distorted trigonal planar geometry (notably the nickel atom adopts a Y-shape three-coordinate conformation).[37] The large N-C_{NHC}-N angles of the 8-NHC Ni(I) complexes are characteristic of those observed for the other 8-NHC metal complexes already discussed. Again, the 8-NHCs show larger N-C_{NHC}-N angles than their IPr and 6-Mes counterparts. Hence, this leads to the usual compression of the N-C_{NHC}-C_{Ar} angles. The Ni(I) complex bearing 8-Mes results in a slightly elongated Ni-C_{NHC} and Ni-P bond lengths along with a greater C_{NHC}–Ni–P angle to accommodate the sterically bulkier N-mesityl substituents. This is in contrast to that observed for complexes with the 8-*o*-Tol/O-8-*o*-Tol heterocyclic ring and also when compared with IPr and 6-Mes Ni(I) complexes. The tilt angles θ for the 8-NHC complexes adopt a near 90° perpendicular arrangement to the metal coordination plane. For [NiBr(O-8-*o*-Tol)(PPh_3)], the distance between the oxygen atom in the heterocyclic backbone to the Ni(I) atom is 4.7Å. This distance is appreciably longer than that between the oxygen atom and the C_{NHC} carbon (3.0Å). Such distance between the oxygen and the carbenic carbon is within sum of the Van der Waal radii.

3.2.5.2 The use of EPR Spectroscopy for 8-NHC Ni(I) complex studies

The three-coordinate 15-electron d^9 Ni(I) complexes of the type [NiX(8-NHC)(PPh_3)], containing one unpaired electron, are paramagnetic species and are considered to be unsuitable for NMR analysis. Nevertheless, paramagnetic compounds usually show broad peaks at very low shifts in ^{1}H NMR spectra. This effect can be explained by the 'Heisenberg Uncertainty Principle' between the T_1 (spin-lattice longitudinal) and T_2 (spin-spin transverse) relaxation. It states that the relationship between the uncertainty of Energy (ΔE) and the uncertainty of the lifetime of the excited state or relaxation time (Δt) is constant. This is given as:

$$\Delta v = \frac{1}{2\pi\Delta t}$$

(Δv = Peak width of the resonance signal at half height; Δt = Relaxation time)

The equation shows that the resonance frequency peak width is inversely proportional to the relaxation time. Thus a fast relaxation time ($T_2 \leq T_1$) for paramagnetic compounds would directly lead to a broad signal. Non-symmetrical paramagnetic shielding also causes the peaks to be observed at very low fields. Hence paramagnetic shifts are made up of two components: (1) through space dipolar interaction between the magnetic moment of the electron and of the nucleus and (2) contact shift which is the interaction of a nucleus with circulating electrons parallel to the applied field, hence inducing anisotropic magnetic field effects. In light of this, the complex [NiBr(6-Mes)(PPh_3)] reported by Whittlesey et al. gave a series of broad, paramagnetic shifted resonances between the range of +30 to –17 ppm in the ^{1}H NMR spectrum.[35] However, none could be seen for the [NiX(8-NHC)(PPh_3)] (mixed halide species) complexes in that region and beyond. Also, no signals were detected for the PPh_3 ligands in the $^{31}P\{^1H\}$ NMR spectrum. As a consequence, EPR spectroscopy was used to determine the principle oxidation state and provide information on the electronic properties of the metal centre for these complexes.

The X-band FSED EPR spectra and Q-band CW EPR spectra for Ni(I)-NHC (high spin, S = $^3/_2$) complexes are shown below in Figure 3.8 and 3.9 respectively.

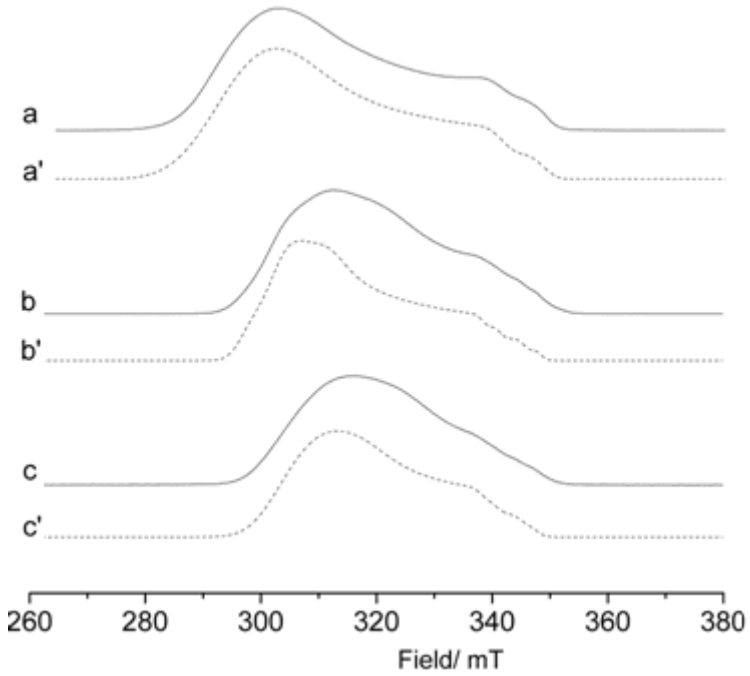

Figure 3.8: X-band FSED EPR spectra (10K) spectra for [NiX(NHC)(PPh_3)] where a) NHC = 8-Mes, X=Cl/Br; b) NHC = 8-*o*-tol, X=Cl/Br; and c) NHC = O-8-*o*-tol, X=Cl/Br. Corresponding simulations are given in a′ - c′

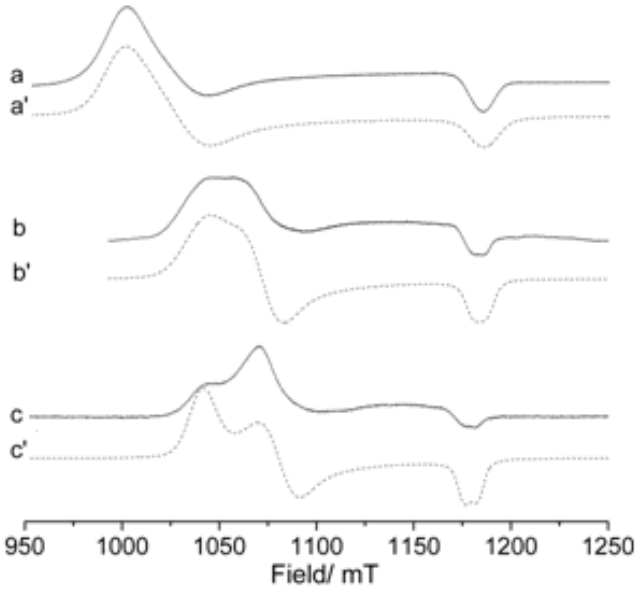

Figure 3.9: Q-Band EPR spectra (10K) spectra of [NiX(NHC)(PPh_3)] where a) NHC = 8-Mes, X=Cl/Br; b) NHC = 8-*o*-tol, X=Cl/Br; and c) O-8-*o*-tol, X=Cl/Br. Corresponding simulations are given in a′ - c′

Signals presented in the EPR spectra and the *g*-values (Landé splitting energy) are dependent on the symmetry of the system. The position of the EPR spectral signals are defined by the effective *g*-values (which is affected by spin-orbit coupling), and it measures the extent to which the magnetic environment of the unpaired electrons differ from that of a free, gas-phase electron (~2 Gauss). Isotropic systems of perfect cubic symmetry such as octahedral or tetrahedral symmetry yield g values (of x, y, z orientation) of equal amounts, $g_{xx} = g_{yy} = g_{zz}$. Molecules of axial symmetry exhibit only two of the principle *g* values with equal values ($g_{xx} = g_{yy} \neq g_{zz}$); g_{zz} is referred to as "*g* parallel" (as it is parallel to the magnetic field direction) while the other *g* values ($g_{xx} = g_{yy}$) are known as "*g* perpendicular". A system of rhombic symmetry presents three distinct *g* values, i.e. $g_{xx} \neq g_{yy} \neq g_{zz}$. Axial and rhombic systems are otherwise known as anisotropic.[38] The *g* anisotropy was determined at Q-band ~35 GHz and the resulting simulation resolved *g* tensor components for [NiX(NHC)(PPh_3)] complexes are presented in Table 3.14.

Table 3.14: Spin Hamiltonian parameters for [NiX(NHC)(PPh_3)] complexes in THF

Complex	g_z	g_y	g_x	$^{P}A_3$ / MHz	$^{P}A_2$ / MHz	$^{P}A_1$ / MHz
[NiBr(8-Mes)(PPh_3)]	2.44	2.37	2.06	*nr*	*nr*	205
[NiCl(8-*o*-Tol)(PPh_3)]	2.34	2.27	2.06	*nr*	*nr*	205
[NiBr(O-8-*o*-Tol)(PPh_3)]	2.34	2.26	2.07	*nr*	*nr*	200

nr = not resolved

All complexes display a rhombic profile with spectra showing broadened linewidths, arising from the superhyperfine coupling to the ^{31}P nuclei with S = ½ at 100% abundance (*vide infra*). The *g* components of d^9 metal centres are sensitive to the coordination environment. Different N-substituents (mesityl or *o*-tolyl) and halide (Cl or Br) affects the spin Hamiltonian parameters as depicted from the changes in Table 13. The $g_{z,y}$ are considerably larger than g_x, which suggests that the unpaired electron is delocalised in an in-plane d_σ orbital. Consequently the $g_{z,y}$ values appear to be very sensitive, even a slight change in the NHC ring affects it (i.e. $g_{z,y}$ = 2.34, 2.26 and 2.44, 2.37 for the O-8-*o*-Tol and 8-Mes complexes respectively, with their corresponding N-C_{NHC}-N angle of 120.8(8)° and 121.8(4)°). The)°). The change in ring size and halide affects the $g_{z,y}$ values while g_x values however remain relatively unchanged; this suggests that the out of plane d_σ orbitals contribute to g_x. Large ^{P}A values with a predominant isotropic contribution are reported for all three Ni(I) complexes bearing coordinated phosphorus, reflecting a high degree of covalency. Unfortunately $A_{2,3}$ components of the phosphorus superhyperfine tensor were unresolved due to the considerably broadened linewidths in the frozen solution spectra.

3.3 Experimental

General remarks

The preparation of free NHCs, Rh , Ir and Ni complexes were performed using standard Schlenk techniques under N_2 or Ar atmosphere, unless otherwise specified. Air-sensitive compounds were stored and handled in an MBraun UNIlab glovebox at <0.1ppm H_2O and O_2. Solvents of analytical grade were obtained using an MBraun SPS-800 solvent purification system. THF was freshly distilled from sodium/benzophenone under nitrogen before use. Deuterated solvents for NMR measurements were distilled from appropriate drying agents under N_2 immediately after use, following standard literature methods. All other reagents were used as received. ^{1}H and $^{13}C\{^{1}H\}$ spectra were recorded using Bruker Avance AMX 400 or 500 spectrometer. Chemical shift values δ were expressed in ppm downfield from TMS using the residual protic solvent as an internal standard. Coupling constants J are given in Hertz as positive values. The multiplicity of the signals is indicated as "s", "d", "t", and "m" for singlet, doublet, triplet, and multiplet, respectively. Mass spectra and high-resolution mass spectra were obtained in electrospray (ES) mode unless otherwise reported on a Waters Q-T micromass spectrometer. Infrared spectra were recorded using a JASCO FT/IR-660 Plus spectrometer. Elemental analyses were performed by Medac Ltd., UK.[39] Samples for EPR Spectroscopic measurements were prepared under an inert N_2 atmosphere in a glove box. All X-band pulsed EPR measurements were recorded on a Bruker E580 spectrometer, microwave frequency 9.8 GHz equipped with a liquid-helium cryostat from Oxford Instruments. All Q-band CW EPR measurements were performed on a Bruker ESP 300E series spectrometer in a Bruker ER5106 QT-E resonator. EPR simulations were performed using the Easyspin toolbox. A solution of each complex was prepared by dissolving 5 mg of [NiX(NHC)(PPh_3)] in 150 μL dry THF to give pale yellow solutions. The solutions were transferred to an EPR tube and sealed in the glove box. The samples were cooled to 77 K before rapid transfer to the pre-cooled EPR cavity. All measurements were performed at 10 K.

Synthesis of Silver complexes

A mixture of 8-NHC·HBr (1.2 mmol), Ag_2O (0.22 g, 0.96 mmol) and NaBr (0.6 g, 5.8 mmol) in dichloromethane (50 ml) was stirred in the dark at room temperature for 3 days. The resulting suspension was filtered and ether was added to the solution until the white microcrystalline material precipitated. The product was isolated by filtration, washed with diethyl ether and dried *in vacuo*. Crystals suitable for X-ray diffraction were obtained by layering a DCM solution of the compound with diethyl ether.

[AgBr(8-Mes)]. White semi-crystalline solid, yield; 25%. ^{1}H NMR ($CDCl_3$, 400MHz, 298K): δ (ppm) 6.85 (s, 4H, *m*-CH), 4.03 (br.t. 4H, NCH_2), 2.27 (s, 12H, *o*-CH_3), 2.17 (s, 6H, *p*-CH_3), 2.08 (s, 2H, $NCH_2CH_2CH_2$), 1.95 (br.m. 4H, NCH_2CH_2). ^{13}C {^{1}H} NMR ($CDCl_3$, 125 MHz, 298K): δ (ppm) 217.2 (d, $^1J_C{}^{107}_{Ag}$ = 224 Hz; d, $^1J_C{}^{109}_{Ag}$ = 256 Hz, N*C*N), 147.9 (s, C_{Ar}), 137.6 (s, C_{Ar}), 133.3 (s, C_{Ar}), 130.4 (s, C_{Ar}), 130.0 (s, CH_{Ar}), 51.7 (s, NCH_2), 29.0 (s, NCH_2CH_2), 21.6 (s, $NCH_2CH_2CH_2$), 20.9 (s, *p*-CH_3), 18.8 (s, *o*-CH_3). HRMS (ES): *m/z* 496.18 ([M – Br + CH_3CN]$^+$; $C_{26}H_{35}N_3Ag$ requires 497.4444). Anal. Calcd. for $C_{24}H_{32}N_2BrAg$: C, 53.75; H, 6.01; N, 5.22. Found C, 53.35; H, 5.98; N, 5.81.

[AgBr(8-Xyl)]. White semi-crystalline solid, yield; 60%. ^{1}H NMR ($CDCl_3$, 400MHz, 298K): δ (ppm) 7.00–7.04 (m, 6H, CH_{Ar}), 4.08 (m, 4H, NCH_2), 2.32 (s, 12H, *o*-CH_3), 2.07 (m, 4H, NCH_2CH_2), 1.99 (m, 2H, $NCH_2CH_2CH_2$). ^{13}C {^{1}H} NMR ($CDCl_3$, 125 MHz, 298K): δ (ppm) 217.4 (d, $^1J_C{}^{107}_{Ag}$ = 223 Hz; d, $^1J_C{}^{109}_{Ag}$ = 255 Hz, N*C*N), 150.4 (s, C_{Ar}), 134.0 (s, C_{Ar}), 130.2 (s, CH_{Ar}), 129.9 (s, CH_{Ar}), 128.4 (s, CH_{Ar}), 51.8 (s, NCH_2), 29.3 (s, NCH_2CH_2), 21.8 (s, $NCH_2CH_2CH_2$), 19.1 (s, *o*-CH_3). HRMS (ES): *m/z* 468.15 ([M – Br + CH_3CN]$^+$; $C_{24}H_{31}N_3Ag$ requires 469.3912). Anal. Calcd. for $C_{22}H_{28}N_2BrAg$: C, 51.99; H, 5.55; N, 5.51. Found C, 51.27; H, 5.57; N, 5.96.

Synthesis of 8-NHC Rhodium and Iridium (COD)Cl complexes

A flame dried Schlenk was charged with 8-NHC (76 mg, 0.20 mmol) and $KN(SiMe_3)_2$ (45 mg, 0.23 mmol) in THF (15 ml) and stirred for *ca.* 30 minutes at room temperature. The solution was subsequently filtered via a cannula into a separate flame dried Schlenk charged with $[RhCl(COD)]_2$ (50 mg, 0.10 mmol) in THF (10 ml) and stirred at room temperature for 2 h. The solvent was removed *in vacuo* yielding a yellow solid which was washed with hexane (2 x 10 ml) and dried *in vacuo*. Crystals suitable for X-ray diffraction were obtained by layering a THF solution of the compound with diethyl ether.

[RhCl(8-*o*-Tol)(COD)]. Yellow solid, yield; 72%. ^{1}H NMR ($CDCl_3$, 500 MHz, 298K): δ (ppm) 8.60 (d, $^3J_{HH}$ = 7.7 Hz, 2H, CH_{Ar}), 7.32 (m, 2H, CH_{Ar}), 7.21 (m, 4H, CH_{Ar}) 4.71 (m, 2H, NCH_2), 4.28 (m, 2H, CH_{COD}), 3.24 (m, 2H, NCH_2), 2.79 (m, 1H, NCH_2CH_2), 2.41 (d, 2H, NCH_{COD}), 2.20 (s, 6H, CH_3), 2.14 (m, 2H, NCH_2CH_2), 1.70 (m, 1H, NCH_2CH_2), 1.60 (m, 2H, $NCH_2CH_2CH_2$), 1.36 (m, 2H, C$H_{2\ COD}$), 1.10 (m, 4H, C$H_{2\ COD}$), 0.95 (m, 2H, C$H_{2\ COD}$). ^{13}C {^{1}H} NMR ($CDCl_3$, 125 MHz, 298K): δ (ppm) 215.9 (d, $^1J_{CRh}$ = 45.0 Hz, C_{NHC}), 147.6 (s, ipso-C_{Ar}), 132.1 (s, C_{Ar}), 131.5 (s, C_{Ar}), 129.2 (s, C_{Ar}), 126.1 (s, C_{Ar}), 125.1 (s, C_{Ar}), 92.7 (d, $^1J_{RhC}$ = 7.5 Hz, CH_{COD}), 64.8 (d, $^1J_{RhC}$ = 15.0 Hz, CH_{COD}), 54.3 (s, NCH_2), 30.4 (s, $CH_{2\ COD}$), 27.3 (s, $CH_{2\ COD}$), 26.2 (s, NCH_2CH_2), 19.4 (s, $NCH_2CH_2CH_2$), 17.4 (s, CH_3). HRMS (ES): *m/z* 503.1942 ($[M - Cl]^+$; $C_{28}H_{36}N_2Rh$ requires 503.5043). Anal. Calcd. for $C_{28}H_{36}N_2ClRh$: C, 62.40; H, 6.73; N, 5.20. Found C, 62.56; H, 6.57; N, 5.04.

[RhCl(O-8-*o*-Tol)(COD)]. Yellow solid, yield; 73%. ^{1}H NMR ($CDCl_3$, 400 MHz, 298K): δ (ppm) 8.53 (d, $^3J_{HH}$ = 7.2 Hz, 2H, CH_{Ar}), 7.34 (td, $^3J_{HH}$ = 10.7 Hz, 3H, CH_{Ar}), 7.24 (td, $^3J_{HH}$ = 7.3 Hz, 3H, CH_{Ar}), 4.37 (td, 2H, CH_{COD}), 4.17 (td, 2H, CH_{COD}), 3.95 (ddd, 4H, OCH_2), 3.60 (ddd, 4H, NCH_2), 2.19 (s, 6H, CH_3), 1.42 (m, 4H, C$H_{2\ COD}$), 1.19 (m, 4H, C$H_{2\ COD}$). ^{13}C {^{1}H} NMR (C_6D_6, 125 MHz, 298K): δ (ppm) 220.7 (d, $^1J_{CRh}$ = 44.6 Hz, C_{NHC}), 147.5 (s, ipso-C_{Ar}), 133.4 (s, C_{Ar}), 132.9 (s, C_{Ar}), 130.3 (s, C_{Ar}), 128.3 (s, C_{Ar}), 127.6 (s, C_{Ar}), 94.5 (s, CH_{COD}), 68.5 (s, OCH_2), 66.4 (s, CH_{COD}), 58.4 (s, NCH_2), 31.6 (s, $CH_{2\ COD}$), 27.3 (s, $CH_{2\ COD}$), 18.3 (s, CH_3).

[IrCl(8-*o*-Tol)(COD)]. Yellow solid, yield; 52%. ^{1}H NMR ($CDCl_3$, 400 MHz, 298K): δ (ppm) 8.29 (d, $^{3}J_{HH}$ = 7.0 Hz, 2H, C*H*$_{Ar}$), 7.16 (m, 4H, C*H*$_{Ar}$), 7.15 (m, 2H, C*H*$_{Ar}$), 4.75 (td, 2H, NC*H*$_2$), 3.85 (m, 2H, C*H*$_{COD}$), 3.31 (ddd, 2H, NC*H*$_2$), 2.80 (m, 1H, C*H*$_{COD}$), 2.22 (s, 6H, C*H*$_3$), 2.18 (m, 1H, C*H*$_{COD}$), 2.16 (m, 2H, NCH$_2$C*H*$_2$), 1.76 (m, 2H, C*H*$_{2\ COD}$), 1.63 (m, 2H, NCH$_2$C*H*$_2$), 1.19 (m, 2H, C*H*$_{2\ COD}$), 0.91 (m, 2H, NCH$_2$CH$_2$C*H*$_2$), 0.74 (m, 4H, C*H*$_{2\ COD}$). ^{13}C {^{1}H} NMR ($CDCl_3$, 125 MHz, 298K): δ (ppm) 210.3 (s, N*C*N), 147.9 (s, ipso-*C*$_{AR}$), 133.4 (s, *C*$_{AR}$), 132.8 (s, *C*$_{AR}$), 130.0 (s, *C*$_{AR}$), 126.9 (s, *C*$_{AR}$), 125.5 (s, *C*$_{AR}$), 78.7 (s, *C*H$_{COD}$), 55.6 (s, NCH$_2$), 55.6 (s, NCH$_2$), 49.3 (s, *C*H$_{COD}$), 32.1 (s, *C*H$_{2\ COD}$), 27.9 (s, NCH$_2$*C*H$_2$), 27.4 (s, NCH$_2$CH$_2$*C*H$_2$), 27.4 (s, *C*H$_{2\ COD}$), 20.0 (s, *C*H$_{2\ COD}$), 19.9 (s, *C*H$_{2\ COD}$), 18.2 (s, *C*H$_3$). HR-MS (ES): *m/z* 591.2491 ([M – Cl]$^+$; $C_{28}H_{36}N_2Ir$ requires 591.2485).

[IrCl(O-8-*o*-Tol)(COD)]. Yellow solid, yield; 61%. ^{1}H NMR (C_6D_6, 400 MHz, 298K): δ (ppm) 8.60 (d, $^{3}J_{HH}$ = 8 Hz, 2H, C*H*$_{Ar}$), 7.56 (m, 6H, C*H*$_{Ar}$), 4.54 (t, 2H, C*H*$_{COD}$), 3.97 (td, 2H, C*H*$_{COD}$), 3.64 (ddd, $^{3}J_{HH}$ = 9.3 Hz, 4H, OC*H*$_2$), 3.30 (ddd, $^{3}J_{HH}$ = 4.7 Hz, 4H, NC*H*$_2$), 1.86 (s, 6H, C*H*$_3$), 1.45 (m, 4H, C*H*$_{2\ COD}$), 1.13 (m, 4H, C*H*$_{2\ COD}$). ^{13}C {^{1}H} NMR (C_6D_6, 125 MHz, 298K): δ (ppm) 214.4 (s, N*C*N), 147.1 (s, ipso-*C*$_{AR}$), 128.8 (s, *C*$_{Ar}$), 128.5 (s, *C*$_{Ar}$), 128.1 (s, *C*$_{Ar}$), 127.7 (s, *C*$_{Ar}$), 126.1 (s, *C*$_{Ar}$), 79.8 (s, *C*H$_{COD}$), 67.9 (s, OCH$_2$), 58.2 (s, NCH$_2$), 49.6 (s, *C*H$_{COD}$), 33.0 (s, *C*H$_{2\ COD}$), 28.2 (s, *C*H$_{2\ COD}$), 18.1 (s, *C*H$_3$). HRMS (ES): *m/z* 593.2280 ([M – Cl]$^+$; $C_{27}H_{34}N_2OIr$ requires 593.2277).

Synthesis of [RhCl(8-*o*-Tol)(CO)$_2$] complex

A solution of [RhCl(8-*o*-Tol)(COD)] (50 mg, 0.93 mmol) in dichloromethane (20 ml) was treated with carbon monoxide for 30 min during which time a colour change from dark to pale yellow was observed. The volatiles were removed under reduced pressure furnishing a pale yellow solid, washed with cold hexane (2 X 30 ml) and dried *in vacuo*, yield; 84%. ^{1}H NMR ($CDCl_3$, 400 MHz, 298K): δ (ppm) 7.67 (m, 2H, C*H*$_{Ar}$), 7.18 (m, 4H, C*H*$_{Ar}$), 7.03 (m, 2H, C*H*$_{Ar}$), 4.85 (m, 2H, NC*H*$_2$), 3.38 (m, 2H, NC*H*$_2$), 2.28 (s, 6H, *o*-C*H*$_3$), 1.84 (m, 2H, NCH$_2$CH$_2$C*H*$_2$), 1.74 (m, 4H, NCH$_2$C*H*$_2$). ^{13}C {^{1}H} NMR ($CDCl_3$, 125 MHz, 298K): δ (ppm) 207.1 (d, $^{1}J_{RhC}$ = 36 Hz, *C*$_{NHC}$), 185.4 (d, $^{1}J_{RhC}$ = 55 Hz, *C*O), 182.2 (d, $^{1}J_{RhC}$ = 78 Hz, *C*O), 146.5 (s, *C*$_{Ar}$), 132.3 (s, *C*$_{Ar}$), 130.8 (s, *C*$_{Ar}$), 129.9 (s, *C*$_{Ar}$), 127.6 (s, *C*$_{Ar}$), 125.5 (s, *C*$_{Ar}$), 53.0 (NCH$_2$), 27.4 (NCH$_2$*C*H$_2$), 20.5 (NCH$_2$CH$_2$*C*H$_2$), 16.5 (s, *o*-CH$_3$). IR: ν = 2068, 1981 cm^{-1} (CH_2Cl_2), ν(CO)$_{av}$ = 2024.5 cm^{-1}. HRMS: m/z 451.0775 ([M – Cl]$^+$; $C_{22}H_{24}N_2O_2Rh$ requires 451.3436).

Synthesis of (8-NHC) Rhodium (acac)CO complexes

A solution of free carbene, prepared by *in situ* deprotonation of 8-NHC·HBr (0.33 mmol) with KHMDS (0.65 mmol) in 10 ml of THF, was added dropwise to a stirred solution of $[Rh(CO)_2(acac)]$ (0.38 mmol) in THF (10 ml). An immediate colour change was observed from yellow to orange to green. After stirring the reaction mixture at room temperature overnight the insoluble impurities were filtered off and the solvent removed *in vacuo*. The yellow solid was washed with pentane (20 ml) and dried.

[Rh(8-Mes)(acac)CO]. Yellow solid, yield; 79%. ^{1}H NMR ($CDCl_3$, 400 MHz, 298K): δ (ppm) 6.84 (s, 2H, *m*-C*H*), 6.72 (s, 2H, *m*-C*H*), 5.03 (s, 1H, CH_{acac}), 4.06 (m, 2H, NCH_2), 3.86 (m, 2H, NCH_2), 2.27 (s, 6H, *o*-CH_3), 2.25 (s, 6H, *o*-CH_3), 2.18 (s, 6H, *p*-CH_3), 2.04 (m, 2H, NCH_2CH_2), 1.95 (m, 4H, NCH_2CH_2), 1.74 (s, 3H, CH_{3acac}), 1.64 (s, 3H, CH_{3acac}). ^{13}C {^{1}H} NMR ($CDCl_3$, 125 MHz, 298K): δ (ppm) 210.8 (d, $^1J_{RhC}$ = 52.5 Hz, N*C*N), 190.4 (d, $^1J_{RhC}$ = 85 Hz, *C*O), 185.7 (s, *C*CH_{3acac}), 181.8 (s, *C*CH_{3acac}), 145.3 (s, C_{Ar}), 135.2 (s, *p*-C_{Ar}), 134.0 (s, *o*-C_{Ar}), 133.2 (s, *o*-C_{Ar}), 128.6 (s, *m*-CH_{Ar}), 128.3 (s, *m*-CH_{Ar}), 98.5 (s, *C*H_{acac}), 53.4 (s, N*C*H_2), 30.5 (s, NCH_2CH_2), 27.4 (s, $NCH_2CH_2CH_2$), 26.7 (s, *C*H_{3acac}), 25.6 (s, *C*H_{3acac}), 22.8 (s, *p*-*C*H_3), 21.6 (s, *p*-*C*H_3), 19.9 (s, *o*-*C*H_3), 18.3 (s, *o*-*C*H_3). HRMS (ES): *m/z* 520.19 (M – acac + $CH_3CN]^+$; 591.24 [M – CO + $CH_3CN]^+$. Anal. Calcd. for $C_{30}H_{39}N_2O_3Rh$: C, 62.28; H, 6.79; N, 4.84. Found C, 62.01; H, 6.71; N, 4.92.

[Rh(8-Xyl)(acac)CO]. Yellow solid, yield; 80%. ^{1}H NMR ($CDCl_3$, 400 MHz, 298K): δ (ppm) 7.03 (m, 4H, *m*-C*H*), 6.92 (m, 2H, *p*-C*H*), 5.00 (s, 1H, CH_{acac}), 4.09 (m, 2H, NCH_2), 3.92 (m, 2H, NCH_2), 2.33 (s, 6H, *o*-CH_3), 2.31 (s, 6H, *o*-CH_3), 2.06 (m, 4H, NCH_2CH_2), 1.99 (m, 2H, $NCH_2CH_2CH_2$), 1.72 (s, 3H, CH_{3acac}), 1.62 (s, 3H, CH_{3acac}). ^{13}C {^{1}H} NMR ($CDCl_3$, 125 MHz, 298K): δ (ppm) 210.7 (d, $^1J_{RhC}$ = 52.5 Hz, N*C*N), 190.3 (d, $^1J_{RhC}$ = 85 Hz, *C*O), 185.7 (s, *C*CH_{3acac}), 181.7 (s, *C*CH_{3acac}), 147.6 (s, C_{Ar}), 134.4 (s, C_{Ar}), 133.6 (s, C_{Ar}), 128.9 (s, *p*-CH_{Ar}), 127.9 (s, *m*-CH_{Ar}), 127.6 (s, *m*-CH_{Ar}), 98.5 (s, *C*H_{acac}), 53.2 (s, N*C*H_2), 26.9 (s, NCH_2CH_2), 26.5 (s, *C*H_{3acac}), 25.5 (s, *C*H_{3acac}), 22.6 (s, $NCH_2CH_2CH_2$), 18.5 (s, *o*-*C*H_3). HRMS (ES): *m/z* 492.15 [M – acac + $CH_3CN]^+$; 521.17 [M – CO]; 562.20 [M – CO + $CH_3CN]^+$.

[Rh(8-*o*-Tol)(acac)CO]. Yellow solid, yield; 87%. ^{1}H NMR ($CDCl_3$, 400 MHz, 298K): δ (ppm) 7.16 (m, 3H, C*H*$_{Ar}$), 7.07 (t, 3H, C*H*$_{Ar}$), 6.99 (m, 2H, C*H*$_{Ar}$), 5.03 (s, 1H, C*H*$_{acac}$), 4.84 (m, 2H, NC*H*$_2$), 3.44 (m, 2H, NC*H*$_2$), 2.25 (s, 6H, *o*-C*H*$_3$), 1.87 (m, 4H, NCH_2CH_2), 1.70 (m, 2H, $NCH_2CH_2CH_2$), 1.62 (s, 3H, C*H*$_{3acac}$), 1.54 (s, 3H, C*H*$_{3acac}$). ^{13}C {^{1}H} NMR ($CDCl_3$, 75 MHz, 298K): δ (ppm) 211.8 (d, $^{1}J_{RhC}$ = 53 Hz, NCN), 191.7 (d, $^{1}J_{RhC}$ = 84 Hz, *C*O), 186.8 (s, *C*CH$_{3acac}$), 182.8 (s, *C*CH$_{3acac}$), 148.7 (s, *C*$_{Ar}$), 135.6 (s, *p*-*C*H$_{Ar}$), 134.7 (s, *p*-*C*H$_{Ar}$), 129.0 (s, *o*-*C*$_{Ar}$), 128.7 (s, *o*-*C*H$_{Ar}$), 127.0 (s, *m*-*C*H$_{Ar}$), 126.9 (s, *m*-*C*H$_{Ar}$), 99.6 (s, *C*H$_{acac}$), 54.3 (s, NC*H*$_2$), 30.4 (s, NCH_2CH_2), 28.3 (s, *C*H$_{3acac}$), 28.0 (s, *C*H$_{3acac}$), 23.7 (s, $NCH_2CH_2CH_2$), 19.6 (s, *o*-*C*H$_3$), 19.5 (s, *o*-*C*H$_3$). HRMS (ES): *m/z* 451.1079 ([M – acac + CO]$^{+}$; 464.1422 ([M – acac + CH3CN]$^{+}$). Anal. Calcd. for $C_{26}H_{31}N_2O_3Rh$: C, 59.77; H, 5.98; N, 5.36. Found C, 59.01; H, 6.02; N, 5.48.

Synthesis of (8-NHC) Nickel (PPh_3)Cl/Br complexes from 8-NHC·HBr

A solution of free carbene 8-NHC (prepared from 8-NHC·HBr (50 mg, 0.12 mmol) and $KN(SiMe_3)_2$ (32 mg, 0.16 mmol)) in toluene (10 ml) was added to a mixture of $[Ni(COD)_2]$ (16 mg, 0.06 mmol) and $[NiCl_2(PPh_3)_2]$ (43 mg, 0.06 mmol) and the mixture stirred at room temperature overnight to yield a dark yellow solution. The solution was filtered and the yellow precipitate extracted into THF (10 ml), filtered, and the THF and toluene fractions combined. The combined solution was reduced to a minimum via *vacuo* and hexane (10 ml) added to form a bright yellow precipitate. The solution was then decanted and the solid dried *in vacuo*.

[NiBr(8-Mes)(PPh_3)]. Bright yellow solid, yield; 52%. HRMS (ES): *m/z* 669.2934 ([M – Br]$^{+}$; $C_{42}H_{48}N_2PNi$ requires 669.2909).

[NiCl(8-*o*-Tol)(PPh_3)]. Bright yellow solid, yield; 60%. HRMS (ES): *m/z* 612.2208 ([M – Cl]$^{+}$; $C_{38}H_{39}N_2PNi$ requires 612.2199).

[NiCl(8-*o*-Tol/*o*-Anis)(PPh_3)]. Bright yellow solid, yield; 41%. HRMS (ES): *m/z* 663.1857 ([M – Cl]$^{+}$; $C_{38}H_{39}N_2OPClNi$ requires 663.1842).

[NiBr(O-8-*o*-Tol)(PPh_3)]. Bright yellow solid, yield; 36%. HRMS (ES): *m/z* 614.2026 ([M – Br]$^{+}$; $C_{37}H_{37}N_2OPNi$ requires 614.1997).

Synthesis of (8-NHC) Nickel (PPh_3)Cl/Br complexes from 8-NHC·HBF_4

Using the same procedure as above, the following [NiCl(8-*o*-Tol)(PPh_3)] and [NiBr(8-*o*-Tol)(PPh_3)] complexes were synthesized from 8-*o*-Tol·BF_4 salts with the corresponding [$NiCl_2(PPh_3)_2$] and [$NiBr_2(PPh_3)$] starting materials.

[NiCl(8-*o*-Tol)(PPh_3)]. Anal. Calcd. for $C_{38}H_{39}ClN_2NiP$: C, 70.34; H, 6.06; N, 4.32. Found C, 70.65; H, 6.07; N, 4.35.

[NiBr(8-*o*-Tol)(PPh_3)]. Anal. Calcd. for $C_{38}H_{39}BrN_2NiP$: C, 65.83; H, 5.67; N, 4.04. Found C, 65.81; H, 5.55; N, 4.14.

X-ray crystallography. Suitable crystals were selected and analyzed using a Bruker-Nonius Kappa CCD machine. Data were collected at 150 K using Mo(*K*α) (λ = 0.71073 Å) radiation throughout. Details of the data collections, solutions and refinements are shown in the **Appendix**. The structures were solved using SHELX-97 and refined by SHELX-97.[40]
Dr Benson Kariuki solved and refined all X-ray crystal data.

3.4 References

1. Droge, T.; Glorius, F. *Angew. Chem. Int. Ed.* **2010**, 49, 6940-6952.
2. Gusev, D. G. 2009, *Organometallics*. p. 6458.
3. Iglesias, M.; Beetstra, D. J.; Stasch, A.; Horton, P. N.; Hursthouse, M. B.; Coles, S. J.; Cavell, K. J.; Dervisi, A.; Fallis I. A. *Organometallics* **2007**, 26, 4800.
4. Scarborough, C. C.; Guzei, I. A.; Stahl, S. S. *Dalton Trans.* **2009**, 2284.
5. Kelly III, R. A.; Clavier, H.; Giudice, S.; Scott, N. M.; Stevens, E. D.; Bordner, J.; Samardjiev, I.; Hoff, C. D.; Cavallo, L.; Nolan, S. P. *Organometallics* **2008**, 27, 202.
6. Gusev, D. G.; *Organometallics* **2009**, 28, 763.
7. Iglesias, M.; Beestra, D. J.; Knight, J. C.; Ooi, L.; Stasch, A.; Male, L.; Hursthouse, M. B.; Coles, S. J.; Cavell, K. J.; Dervisi, A.; Fallis, I. A. *Organometallics* **2008**, 27, 3279.
8. Cavallo, L.; Correa, A.; Costabile, C.; Jacobsen, H. *J. Organomet. Chem.* **2005**, 690, 5407.
9. Clavier, H.; Nolan, S. P. *Chem. Commun.* **2010**, 46, 841.
10. Fremont, P.; Sott, N. M.; Stevens, E. D.; Nolan, S. P. *Organometallics* **2005**, 24, 2411.
11. Herrmann, W. A.; Schneider, K. S.; Ofele, K.; Sakamoto, M.; Herdtweck, E. *J. Organometallic Chem.* **2004**, 689, 2441-2449.
12. Jothibasu, R.; Huynh, H. V.; Koh, L. L. *J. Organomet. Chem.* **2008**, 693, 374.
13. Raminal, T.; Abernethy, C. D.; Spicer, M. D.; McKenzie, I. D.; Gay, I. D.; Clyburne, J. A. C. *Inorg. Chem.* **2003**, 42, 1391.
14. Paas, M.; Wibbeling, B.; Fröhlich, R.; Hahn, F. E. *Eur. J. Inorg. Chem.* **2006**, 158.
15. Cavello, L.; Correa, A.; Costabile, C.; Jacobsen. H. *J. Organomet. Chem.* **2005**, 690, 5407.
16. Lee, H. M.; Jiang, T.; Stevens, E. D.; Nolan, S. P. *Organometallics* **2001**, 20, 1255.
17. Chianese, A. R.; Li, X.; Janzen, M. C.; Faller, J. W.; Crabtree, R. H. *Organometallics* **2003**, 22, 1663.
18. Hanasaka, F.; Fujita, K.; Yamaguchi, R. *Organometallics* **2005**, 24, 3422.
19. Zhang, Y.; Wang, D.; Wurst, K.; Buchmeiser, M. R. *J. Organomet. Chem.* **2005**, 690, 5728.
20. Iglesias, M.; Beetstra, D. J.; Kariuki, B.; Cavell, K. J.; Dervisi, A.; Fallis, I. A. *Eur. J. Inorg. Chem.* **2009**, 1913-1919.

21. Binobaid, A.; Iglesias, M.; Beetstra, D. J.; Kariuki, B.; Dervisi, A.; Fallis, I. A.; Cavell, K. J. *Dalton Trans.* **2009**, 7099-7112.
22. Hudnall, T. W.; Tennyson, A. G.; Bielawski, C. W. *Organometallics* **2010**, 29, 4569.
23. Wolf, S.; Plenio, H. *J. Organomet. Chem.* **2009**, 694, 1487.
24. Kolychev, E. L.; Portnyagin, I. A.; Shuntikov, V. V.; Khrustalev, V. N.; Nechaev, M. S. *J. Organomet. Chem.* **2009**, 694, 2454-2462.
25. Lin, I. J. B.; Vasam, C. S. *Coord. Chem. Rev.* **2007**, 251, 642-670.
26. Mata, J. A.; Poyatos, M.; Peris, E. *Coord. Chem. Rev.* **2007**, 251, 841.
27. J. A. Iggo. *NMR Spectroscopy in Inorganic Chemistry*, Oxford Science Publications. **2000**.
28. Denk, K.; Sirsch, P.; Herrmann, W. A. *J. Organomet. Chem.* **2002**, 649, 219.
29. Massicot, F.; Schneider, R.; Fort, Y.; Illy-Cherrey S.; Tillement, O. *Tetrahedron* **2000**, 56, 4765–4768.
30. Keaton, R. J. K.; Blacquiere, J. M.; Baker, R. T. *J. Am. Chem. Soc.* **2007**, 129, 1844–1845.
31. Desmarets, C.; Schneider, R.; Fort, Y. *J. Org. Chem.* **2002**, 67, 3029–3036.
32. Zhang, Y. G.; Ngeow, K. C.; Ying, J. Y. *Org. Lett.* **2007**, 9, 3495–3498.
33. Malyshev, D. A.; Scott, N. M.; Marion, N.; Stevens, E. D.; Ananikov, V. P.; Beletskaya, I. P.; Nolan, S. P. *Organometallics* **2006**, 25, 4462–4470.
34. Blakey, S. B.; MacMillan, D. W. C. *J. Am. Chem. Soc.* **2003**, 125, 6046–6047.
35. Davies, C. J. E.; Page, M. J.; Ellul, C. E.; Mahon, M. F.; Whittlesey, M. K. *Chem. Commun.* **2010**, 46, 5151-5153.
36. Dible, B. R.; Sigman, M. S.; Arif, A. M. *Inorg. Chem.* **2005**, 44, 3774.
37. Nagao, S.; Matsumoto, T.; Koga, Y.; Matsubara, K. *Chem. Lett.* **2011**, 40, 1036.
38. Weil, J.; Bolton, J.; Wertz. J. *Electron Paramagnetic Resonance: Elemental Theory and Practical Applications*, John Wiley and Sons, New York. **1994**.
39. *Medac Ltd*; Alpha 319, Chobham Business Centre, Chertsey Road, Chobham, Surrey, GU24 8JB, UK.
40. Sheldrick, G. M. *Acta. Cryst.* **1990**, A46, 467-473. Sheldrick, G. M. SHELXL-97, *Program for crystal structure refinement*, University of Göttingen, **1997**.

Chapter Four

Investigation of catalytic transfer hydrogenation and cross-coupling reactions using metal complexes bearing 8-NHC ligands

4.1 Introduction

The most popular use of NHCs to date is as a spectator ligand in homogeneous transition-metal catalyzed reactions. Not long after the first isolation of a free NHC, Herrmann et al. identified the potential of this class of compounds and attempts were carried out on the modification of known transition metal catalysts with NHCs.[1] Early examples of successful catalysis reactions involving NHC ligands include $[PdX_2(NHC)_2]$ complexes in the Heck reaction,[1] [RhCl(NHC)(COD)] complexes in hydrosilylation of alkenes,[2] $[Pd(NHC)_2(MeCN)_2]^{2+}$ complexes in CO/ethylene copolymerization,[3] and $[RuCl_2(NHC)_2(=CHPh)]$ in olefin metathesis.[4] After these initial successes, the development of NHC transition-metal catalysis advanced rapidly until a review appeared shortly after.[5] Examples of NHCs replacing one or more phosphine ligands in known phosphine-based catalysts include Crabtree's catalyst $[Ir(COD)(Py)(PCy_3)]PF_6$,[6] Wilkinson's catalyst $[RhCl(PPh_3)_3]$,[7] and Grubbs catalyst $[RuCl_2(PPh_3)_2(=CHPh)]$.[4] Owing to the stability of the metal-carbene bond, it is thus believed that the carbene ligand generally remains coordinated to the metal throughout the catalytic cycle. In comparison with phosphine catalysts, no excess ligand is required to promote completion of catalytic reactions. Usually a preformed metal NHC catalyst is introduced into the reaction as this has the advantage that the ligand to metal ratio is established, which may not be the case if free carbene or carbene precursor and a metal complex were to be added separately. Several NHC-complex catalyzed reactions will be discussed below, with the emphasis on Rh/Ir and Ni in accord with the complexation studies in Chapter 3.

Transfer hydrogenation of ketones

Preparation of alcohols has become a field of importance for transition metal catalyzed reactions with respect to industrial applications.[8] Rh and Ir have been recognized as effective metals for catalysts in transfer hydrogenation of carbonyl compounds.[9] The reaction is usually conducted in *i*PrOH solvent as this provides the hydrogen source which drives the catalytic reaction (Scheme 4.1).

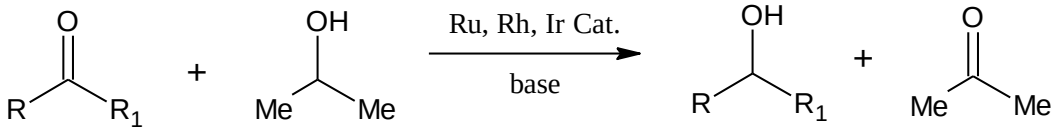

Scheme 4.1. Transfer hydrogenation of carbonyl substrates

The generation of cationic Ir(I)-NHC complex into Crabtree's system, [Ir(COD)(Py)(ICy)]PF_6, for transfer hydrogenation of unsaturated substrates was first reported by Nolan and co-workers.[10] Crabtree and colleagues later demonstrated good catalytic activities in the reduction of acetophenone with Rh(III) and Ir(III)-(chelating bis-carbene) complexes, especially those bearing N-neopentyl and N-isopropyl substituents.[11, 12] They expanded the scope with hydrogen transfer reduction of aldehydes using slightly modified versions of the previously reported N-neopentyl-substituted bis-NHC Ir complexes; this gave good catalytic results (with 0.1 mol% catalyst loading).[13] Shortly afterwards, other chelating bis-carbene complexes were developed and investigated in transfer hydrogenation, but they yielded low catalytic activities.[14, 15] Another example of Rh(III) complex employed in this catalytic reaction involves a tripodal coordinated bis(imidazolylidene) ligand, which displayed good catalytic activity with catalyst loadings of 0.001 mol%.[16] Benzimidazol-2-ylidene derivatives of Rh(I) and Ir(I) complexes bearing symmetrical or unsymmetrical N-substituents also showed high catalytic activity towards reduction of acetophenone and cyclohexanone in 2-propanol.[17] Most of the examples described above are mentioned in a mini-review by Normand and Cavell.[18] Cavell and co-workers later reported their own findings with unsymmetrical N-substituted six- and seven-membered NHCs Rh(I) and Ir(I) complexes.[19] Ir(I) complexes of unsymmetrical *o*-methoxyphenyl-functionalised NHCs (Figure 4.1) were tested in the catalytic transfer hydrogenation of 4-bromoacetophenone, displaying excellent catalytic activity (100% conversion after between 10 to 40 minutes) at loadings as low as 0.01 mol%.

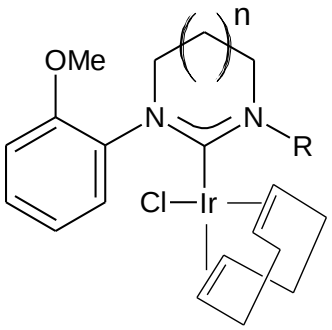

R = Mes, DIPP

n = 1, 2

Figure 4.1: Ir complexes of *o*-methoxyphenyl-functionalised large-ring NHCs employed in transfer hydrogenation of 4-bromoacetophenone

In a subsequent paper, Ir(I) complexes having O- and N-donor functionalized NHC ligands (five-membered NHC version of Figure 4.1) were synthesized and tested with a variety of unsaturated compounds.[20] A proposed catalytic cycle for the transfer hydrogenation of ketones is presented in Figure 4.2. The key to high catalytic activity lies in the weak interaction between the β-H on the alkoxo ligand and the oxygen atom of the methoxy fragment of the NHC ligand. This causes a net destabilization of the alkoxo intermediate which assists the progress of β-H elimination, leading to the formation of key hydrido intermediate species (step i). The hydrogen from the hydride intermediate also exhibits a weak interaction with the methoxy group upon hydride migration to the ketone substrate (step ii).

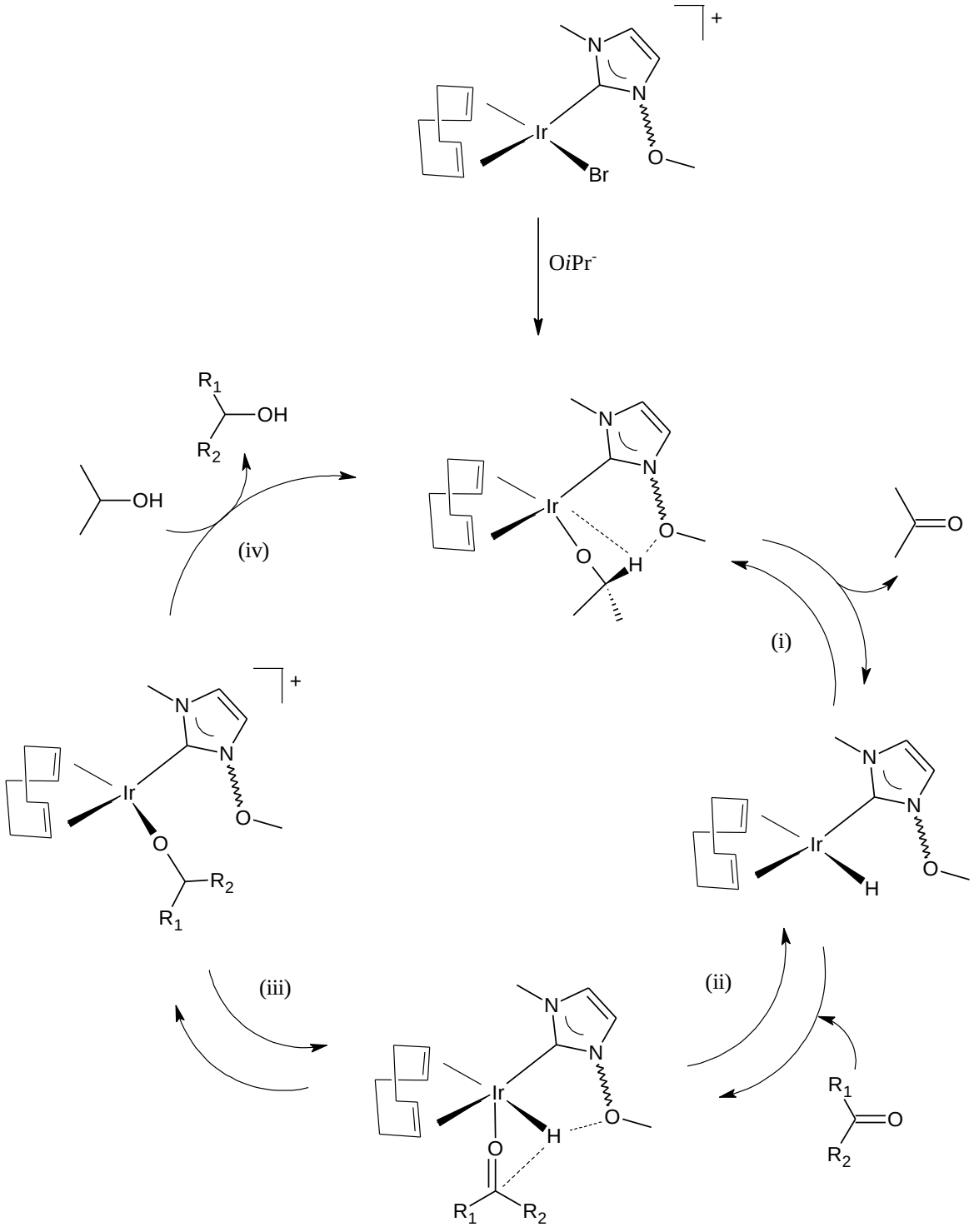

Figure 4.2: Proposed mechanism for transfer hydrogenation of ketones

Cross-coupling reactions

C-C coupling reactions have been the main attraction (largely coupling reactions with aryl halides) when NHC transition-metals are utilized in catalytic experiments. Although palladium is the favoured metal in almost all cases, nickel has been applied on some occasions. The most frequently studied C-C coupling reactions are shown in Scheme 4.2.[21-23] The preference for using NHCs over phosphine complexes are due to the thermal stability of the metal-NHC bond, whereas phosphines have the tendency to degrade under coupling reaction conditions at elevated temperatures. Application of palladium NHC complexes as catalysts in cross-coupling reactions was reviewed in 2008.[24]

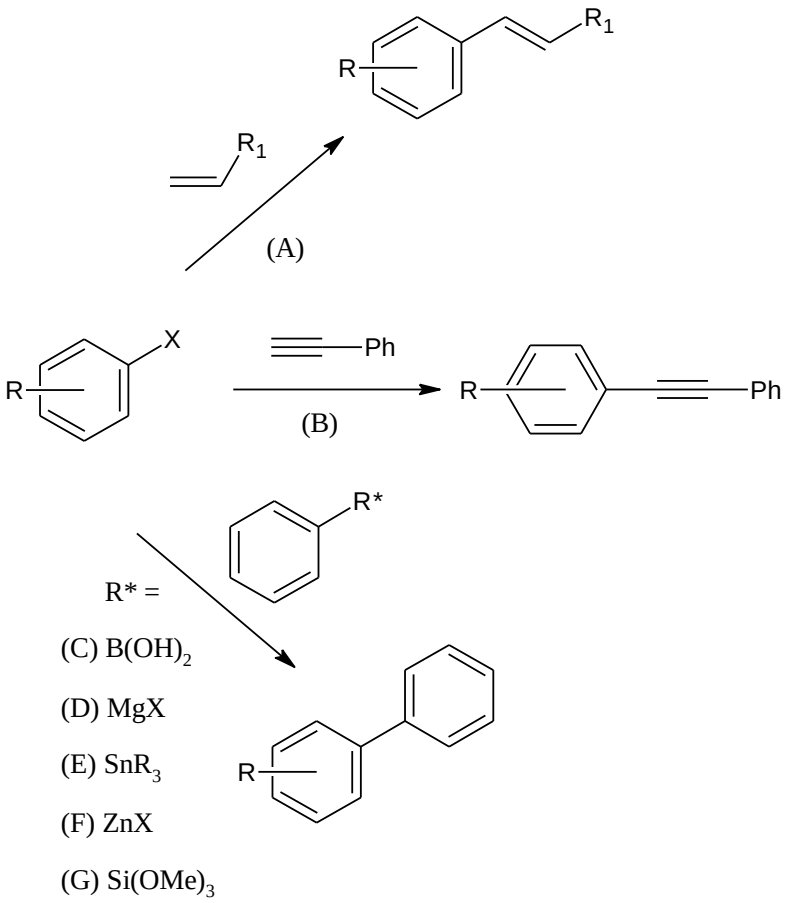

Scheme 4.2: Cross-coupling reactions with aryl halides via (A) Heck reaction; (B) Sonogashira coupling; (C) Suzuki reaction; (D) Kumada cross-coupling; (E) Stille reaction; (F) Negishi coupling; (G) Siloxane cross-coupling

Suzuki coupling of aryl halides with aryl boronic acids with nickel NHC complexes has been reported; Cavell and co-workers reported NHC-Ni complexes in Suzuki coupling reactions in 1999.[25] However, these systems were less efficient than the ones observed with palladium. In some instances, addition of phosphines to the reaction mixture was required to achieve complete conversion.[26, 27] A recent example improves on this by using phosphine-functionalized NHCs.[28] Herrmann was the first to reveal the use of NHC-Ni catalysts in Kumada cross-coupling with aryl chlorides at room temperature.[22, 29] The most effective NHC ligands incorporated into these systems were IMes and IPr. The catalysts were synthesized from reacting equimolar amount (3 mol%) of $[Ni(acac)_2]$ with imidazolium salt in the presence of excess Grignard reagent. This provided the conditions for efficient and selective cross-coupling between various brominated and chlorinated aryl halides and arylmagnesium compounds. A subsequent paper showed that NHC-Ni catalysed Kumada coupling reactions also proceeded efficiently with aryl fluorides as starting materials.[30] An *in situ* generated species functioned equally as well if not better than a preformed $[Ni(NHC)_2]$ complex. Fürstner later demonstrated a different method for the preparation of catalytic cationic mono-diaminocarbene Ni precursors.[31] It involved the combination of $[Ni(COD)_2]$ with PPh_3 to chloroimidazolium salts in THF at ambient temperatures. These complexes were used in the cross-coupling reactions of *p*-methoxyphenylmagnesium bromide with chloro- or bromobenzene and 2-chloropyridine with the presence of 4,4'-dimethoxybiphenyl (15-25%), required to aid the reaction's progress. A preformed $[NiCl_2(PPh_3)(IPr)]$ complex reported by Matsubara et al. showed greater catalytic activity (TON >400) at room temperature than either bis-carbene and bis-phosphine complexes (TON 240 and 40 respectively).[32] However, the efficiency of these complexes was limited to cross-coupling reactions of aryl iodides and bromides. Ni(II) complexes bearing pyridine-functionalized bis(NHC) ligands were later reported by Hiroya and Chen to be highly efficient catalysts for coupling reactions of aryl chlorides, vinyl chlorides and heteroaryl chlorides with aromatic Grignard reagents at room temperature.[33, 34]

This chapter focuses on the catalytic performance of expanded 8-membered ring NHC complexes containing iridium and rhodium in transfer hydrogenation and nickel in Suzuki and Kumada cross-coupling reactions.

4.2 Results and Discussion

4.2.1 Ketone transfer hydrogenation catalysis

The [IrCl(8-*o*-Tol)(COD)] complex was used as the standard catalyst for transfer hydrogenation of various ketone substrates with isopropanol as solvent/hydrogen donor and 10 mol% ^{t}BuOK as cocatalyst (Scheme 4.3). All reactions were heated for 24 h at 80°C using ketone-catalyst-base ratios of 1×10^{4} : 1 : 1000. Each reaction was repeated several times to demonstrate reproducibility and to record a consistent average.

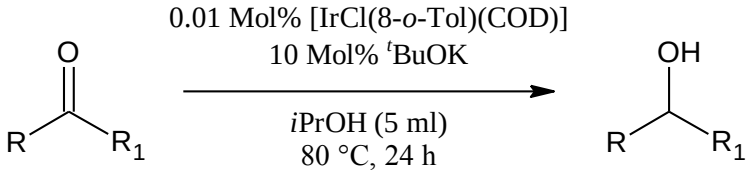

Scheme 4.3. Catalytic transfer hydrogenation of ketones

The results of the catalytic transfer hydrogenations of 4-bromoacetophenone, phenylacetone, cyclohexanone, 2-bromopropiophenone and 4-methylacetophenone are listed in Table 4.1. It seems that iridium (I) complexes of saturated 8-membered carbene show poor conversions and in the case of two substrates, showed no activity. Steric and electronic properties of coordinated NHCs play an important role in controlling the selectivity and reactivity in catalysis. NHCs with less sterically hindered alkyl substituents usually give more active catalysts than those with bulky aryl substituents.[35, 36] Therefore it comes as no surprise that the 8-membered ring NHC complex displays lower catalytic activity (despite different/lower loading used) in contrast to e.g. imidazol-based NHC complexes. The enlarged heterocyclic ring NHCs force the aryl N-substituents closer together, increasing steric hindrance around the metal centre (as described in Chapter 3), making it more difficult for the coordination of substrates onto the metal (hence the formation and reduction of metal-hydride) processes. The influence of the electronic properties of the NHC on catalytic activity and selectivity is more subtle.

Table 4.1: Transfer hydrogenation reactions with [IrCl(8-*o*-Tol)(COD)][a]

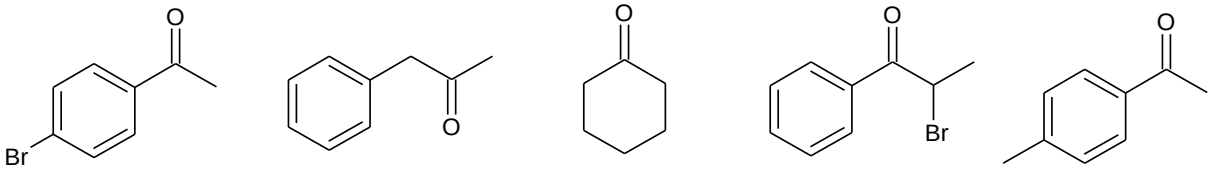

(a) (b) (c) (d) (e)

Entry	Substrate	Conversion (%) [b]
1	a	31
2	b	24
3	c	-
4	d	-
5	e	10

[a] Reaction conditions: 1×10^{-7} mol catalyst (0.01 mol%), 10 mmol ^{t}BuOK (10 mol%), 1 mmol substrate, 5 ml 2-propanol, 80°C, 24 h, each reaction was repeated at least twice. [b] Conversion to product calculated by ^{1}H NMR spectra's.

Such reactions were also tested with 8-NHC rhodium (I) complexes with aromatic N-*o*-tolyl substituents, however it showed no activity at all towards transfer hydrogenation under the previously described conditions.

4.2.2 Cross-coupling catalysis

In recent times, there are increasing numbers of different nickel-based NHC complexes being developed and used as potential cross-coupling catalysts. The use of catalysts based on nickel offers the advantages of favourable cost, higher reactivity toward aryl chlorides and easier removal from the final product.[37] Ni(0), Ni(I) and Ni(II) NHC complexes of the type $[Ni(IMes)_2]$, $[NiX(IMes)_2]$ and $[NiX_2(IMes)_2]$ have been evaluated in Suzuki and Kumada cross-coupling reactions.[32, 38] In fact, certain Ni(0)-based catalysts were shown to be more effective than their Pd counterparts.[39, 40] There are many examples of NHC-based Ni(0) and Ni(II) catalysts,[41] but Ni(I)-based complexes are uncommon and their catalytic reactivity is not well understood.

4.2.2.1 Suzuki cross-coupling catalysis

The Suzuki cross-coupling reaction between aryl bromide and phenylboronic acid in the presence of [NiCl(8-*o*-Tol)(PPh_3)] complex was examined (Scheme 4.4). The reaction was also tested with different catalyst concentrations with catalytic loadings of 1 mol% and 5 mol% being used. The catalytic process was performed under N_2 atmosphere in dry toluene with ^{t}BuOK (as the base promoter) at 80°C for 8 h.

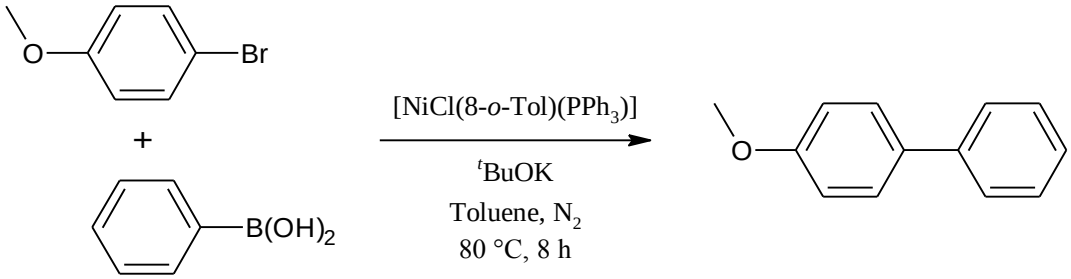

Scheme 4.4. Suzuki-Miyaura reactions between aryl bromide and phenylboronic acid

The reaction at both catalyst loadings showed no sign of catalytic activity towards the synthesis of the desired product. Analysis for both reactions was initially performed using ^{1}H NMR spectroscopy. No clear singlet representing the methyl atom of the product (4-methoxybiphenyl) or starting material in the range 3-5 ppm could be detected. Instead, aromatic peaks were clearly visible in the spectra. Thus further analysis using GC-MS revealed that large amounts of homocoupled boronic acid and toluene side products were formed (this is consistent with ^{1}H NMR spectra). A minute amount of 4-methoxybiphenyl was detected for one of the reactions involving the use of 5 mol% Ni catalyst. It is unclear why the [NiCl(8-*o*-Tol)(PPh_3)] complex yields such poor catalytic performances with odd catalytic behaviour. In contrast, the [Ni(I)X($IMes)_2$] complex was reported to give a good 75% conversion in the same catalytic reaction under the same conditions.[38]

4.2.2.2 Kumada cross-coupling catalysis

Kumada cross-coupling reactions of chlorobenzene and fluorobenzene with Grignard in the presence of [NiCl(8-*o*-Tol)(PPh_3)] and [NiBr(8-Mes)(PPh_3)] complexes were investigated (Scheme 4.5). The process was conducted in dry THF under inert atmosphere with catalyst loading kept at 1 mol% throughout and at variable time and temperature. The results are summarized in Table 4.2.

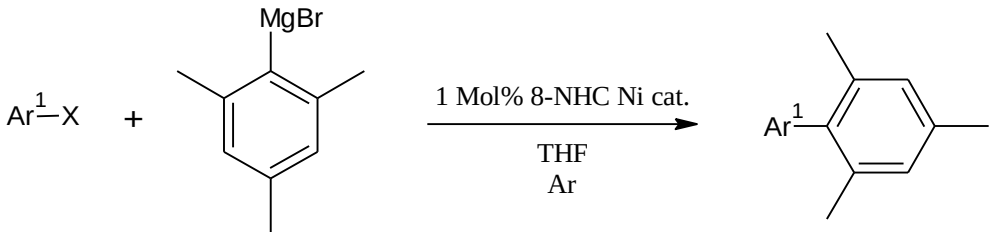

Scheme 4.5. Kumada cross-coupling reactions between aryl halide and Grignard

Table 4.2: 8-NHC Ni(I)-catalyzed Kumada coupling reaction of different aryl halides with excess Grignard reagent at different temperatures and reaction times[a]

Entry	Ni cat. (1 Mol%)	Ar^1	Time (h)	Temp. (°C)	Conversion (%)[b]
1	[NiCl(8-*o*-Tol)(PPh_3)]	fluorobenzene	2.5	r.t.	-
2	[NiBr(8-Mes)(PPh_3)]	fluorobenzene	2.5	r.t.	-
3	[NiCl(8-*o*-Tol)(PPh_3)]	*p*-chlorotoluene	2.5	r.t.	-
4	[NiBr(8-Mes)(PPh_3)]	*p*-chlorotoluene	2.5	r.t.	-
5	[NiCl(8-*o*-Tol)(PPh_3)]	*p*-chlorotoluene	24	r.t.	38
6	[NiBr(8-Mes)(PPh_3)]	*p*-chlorotoluene	24	r.t.	3
7	[NiCl(8-*o*-Tol)(PPh_3)]	*p*-chlorotoluene	24	60	-

[a]Reaction conditions: Ni cat. (1 mol%), Grignard (2 mol%), Aryl halide (mol determined from 1 mol% of Ni cat.) THF (0.5 ml). [b]Isolated yield after flash chromatography (average of two runs), conversion calculated from ^{1}H NMR spectra's.

Reaction of Ni(I) complex bearing 8-*o*-Tol and 8-Mes with fluorobenzene and *p*-chlorotoluene at room temperature for 2.5 h (entries 1-4) showed no catalytic activity whatsoever. It was predicted that conversion of fluorobenzene (especially the insertion of Ni catalyst into the Ar-F bond forming organo-Ni(III) complex) would be particularly difficult due to the strong C-F bond. When Ni catalysts reacted with *p*-chlorotoluene for longer period of time (entries 5 & 6), [NiCl(8-*o*-Tol)(PPh_3)] gave a modest conversion of 38% and

[NiBr(8-Mes)(PPh_3)] 3%. Such percentage differences between these two conversions may be due to the extent of steric hindrance imposed by the different 8-NHCs on the Ni centre, hence the Ni complex bearing the less bulky 8-*o*-Tol carbene presents a wider area of space at the metal centre for catalytic reactions to occur than the more cumbersome 8-Mes NHC (refer to the C_{Ar}–N–C_{NHC}, C_{NHC}–Ni–X and C_{NHC}–Ni–P angles between the two complexes shown in Table 12 - Chapter 3). [NiCl(8-*o*-Tol)(PPh_3)] complex was then reacted with *p*-chlorotoluene at 60°C to promote higher % of conversion (entry 7). However, no desired catalytic activity was detected. Instead, GC-MS analysis revealed that the products formed were mainly of homocoupled products derived from *p*-chlorotoluene and mesitylmagnesium bromide. The same effect is seen in the Suzuki cross-coupling reactions; it is difficult to explain why this happens at the current time. Though it might be that there are one-electron processes occurring here.

In summary, [MCl(8-*o*-Tol)(COD)] (M = Ir, Rh) complexes were found to be poor catalysts for transfer hydrogenation of ketones. The steric hindrance around the metal centre imposed by the N-aryl substituents of the large ring system obstructs the coordination of substrates with the metal, which consequently leads to a low level of catalytic activity. A better [Rh/IrX(8-NHC)(COD)] (X = halide) complex to test in the transfer hydrogenation reactions would have been one with the 8-*o*-Anis/*o*-Tol ligand; this is because the unsymmetrical N-substituted 6- and 7-membered NHCs Rh(I) and Ir(I) complexes were reported to be excellent catalysts for transfer hydrogenation of 4-bromoacetophone.[19]

The Suzuki cross-coupling reaction between aryl bromide and phenylboronic acid in the presence of [NiCl(8-*o*-Tol)($PPh)_3$] complex was examined. The reaction showed no sign of catalytic activity towards the synthesis of the desired product. However, homocoupled products of the starting materials (aryl bromide and phenylboronic acid) were detected using GC-MS. Therefore in future studies, it would be useful to investigate the application of the [NiCl(8-*o*-Tol)($PPh)_3$] complex in the catalytic reductive symmetrical coupling of aryl halides (the Ullmann reaction).[42]

Ni(I) complexes bearing 8-*o*-Tol and 8-Mes were used as catalysts for the Kumada cross-coupling of Grignard reagents with aryl halides. Reaction of *p*-chlorotoluene with PhMgBr in the presence of [NiX(8-NHC)(PPh_3)] complexes gave modest yields of the desired product after 24 h, with the [NiCl(8-*o*-Tol)(PPh_3)] complex showing the highest catalytic activity (the use of the bulkier 8-NHC Ni complex resulted in less effective catalysis). Homocoupled products were also seen when the reaction was carried at elevated temperatures. Ni(I) species

were first introduced in C-C bond forming reactions in 1979,[43] but it is still unclear how the Ni(I) complexes initiate C-C coupling, thus further mechanistic studies are required to solve what oxidation states are present during the actual catalysis.

4.3 Experimental

General remarks

All air sensitive experiments were performed under inert atmosphere by standard Schlenk techniques. Air and moisture sensitive compounds were handled in a MBraun UNIlab glovebox. Solvents of analytical grade were freshly distilled using a MBraun SPS-800 solvent purification system. ^{1}H spectra were recorded using a Bruker Avance AMX 400 spectrometer.

Transfer hydrogenation protocol

Ketone (1 mmol), base (10 mol%) and 8-NHC Ir complex (0.01 mol%) were charged in a flamed dried Schlenk. The solids were degassed and *iso*-propanol (5 ml) subsequently added under a nitrogen atmosphere. The solution was heated to 80°C for 24 hours, volatiles were evaporated and the final conversion calculated by ^{1}H NMR spectroscopy.

Suzuki cross-coupling reaction protocol

p-Bromoanisole (0.1 mmol), phenylboronic acid (0.11 mmol) and ^{t}BuOK (0.315 mmol) were charged in a flame dried Schlenk. The compounds were degassed several times before a solution of the 8-NHC Ni catalyst (0.2 mol%) in toluene (5 ml) was added. The reaction mixture was stirred at 80°C for 8 hours. The solvent was removed under vacuum followed by purification by flash chromatography. Product identities were analyzed using ^{1}H NMR spectroscopy and GC-MS.

Kumada cross-coupling reaction protocol

A solution of the 8-NHC Ni catalyst (1 mol%) in THF (0.5 ml) was added into a flame dried Schlenk. Aryl halide substrate (mol calculated from 1 mol% Ni catalyst) along with 2-mesitylmagnesium bromide solution (2 mol%, 1 M in diethyl ether) were subsequently added under an argon atmosphere. The mixture was stirred at the specified temperature and time. After which, methanol (10 ml) and DCM (10 ml) was added to the solution and then dried

with $MgSO_4$, filtered and concentrated under *vacuo*. The crude substance was purified by flash chromatography (DCM/hexane 2:8 ratio) before determining the % conversion and identities by ^1H NMR spectroscopy (NMR spectroscopic data of the product matched those of the literature report)[44] and GC-MS respectively.

Description of GC-MS analysis

Substrate identities were determined by GC-MS analysis of reaction mixtures using Agilent Technologies 6890N GC system with an Agilent Technologies 5973 inert MS detector with MSD. Column: Agilent 190915-433 capillary, 0.25 mm × 30 m × 0.25 μm. Capillary: 30 m × 250 μm × 0.25 μm nominal. Initial temperature at 50°C, held for 4 minutes; ramp 5°C/minute; next 100°C; ramp 10°C/minute next 240°C and held for 15 minutes. The temperature of the injector and the detector were held at 240°C. The retention times for analyses are given in minutes.

4.4 References

1. Herrmann, W. A.; Elison, M.; Fischer, J.; Kocher, C.; Artus, G. R. *J. Angew. Chem. Int. Ed.* **1995**, 35, 2371.
2. Hill, J. E.; Nile, T. A. *J. Organomet. Chem.* **1977**, 137, 293.
3. Gardiner, M. G.; Herrmann, W. A.; Reisinger, C. P.; Schwarz, J.; Spiegler, M. *J. Organomet. Chem.* **1999**, 572, 239.
4. Weskamp, T.; Schattenmann, W. C.; Spiegler, M.; Herrmann, W. A. *Angew. Chem. Int. Ed.* **1998**, 37, 2490.
5. Herrmann, W. A. *Angew. Chem. Int. Ed.* **2002**, 41, 1291.
6. Lee, H. M.; Jiang, T.; Stevens, E. D.; Nolan, S. P. *Organometallics* **2001**, 20, 1255.
7. Grasa, G. A.; Moore, Z.; Martin, K. L.; Stevens, E. D.; Nolan, S. P.; Paquet, V.; Lebel, H. *J. Organomet. Chem.* **2002**, 658, 126.
8. Enthaler, S.; Jackstell, R.; Hagemann, B.; Junge, K.; Erre, G.; Beller, M. *J. Organomet. Chem.* **2006**, 691, 4652-4659.
9. Zassinovich, G.; Mestroni, G.; Gladiali, S. *Chem. Rev.* **1992**, 92, 1051–1069.
10. Hillier, A. C.; Lee, H. M.; Stevens, E. D.; Nolan, S. P. *Organometallics* **2001**, 20, 4246–4252.
11. Albrecht, M.; Crabtree, R. H.; Mata, J.; Peris, E. *Chem. Commun.* **2002**, 32-33.
12. Albrecht, M.; Miecznikowski, J. R.; Samuel, A.; Faller, J. W.; Crabtree, R. H. *Organometallics* **2002**, 21, 3596–3604.
13. Miecznikowski, J. R.; Crabtree, R. H. *Organometallics* **2004**, 23, 629–631.
14. Miecznikowski, J. R.; Crabtree, R. H. *Polyhedron* **2004**, 23, 2857–2872.
15. Poyatos, M.; McNamara, W.; Incarvito, C.; Peris, E.; Crabtree, R. H. *Chem. Commun.* **2007**, 2267–2269.
16. Mas-Marza, E.; Poyatos, M.; Sanau, M.; Peris, E. *Organometallics* **2004**, 23, 323–325.
17. Türkmen, H.; Pape, T.; Hahn, F. E.; Çetinkaya, B. *Eur. J. Inorg. Chem.* **2008**, 5418–5423.
18. Normand, A. T.; Cavell, K. J. *Eur. J. Inorg. Chem.* **2008**, 2781–2800.
19. Binobaid, A.; Iglesias, M.; Beetstra, D.; Dervisi, A.; Fallis, I.; Cavell, K. J. *Eur. J. Inorg. Chem.* **2010**, 5426–5431.
20. Jimenez, M. V.; Fernandez-Tornos, J.; Perez-Torrente, J. J.; Modrego, F. J.; Winterle, S.; Cunchillos, C.; Lahoz, F. J.; Oro, L. A. *Organometallics* **2011**, 30, 5493–5508.
21. Herrmann, W. A.; Reisinger, C. P.; Spiegler, M. J. *Organomet. Chem.* **1998**, 557, 93.

22. Bohm, V. P. W.; Weskamp, T.; Gstottmayr, C. W. K.; Herrmann, W. A. *Angew. Chem. Int. Ed.* **2000**, 39, 1602.
23. Herrmann, W. A.; Bohm, V. P. W.; Gstottmayr, C. W. K.; Grosche, M.; Reisinger, C. P.; Weskamp, T. *J. Organomet. Chem.* **2001**, 617, 616.
24. Kantchev, E. A. B.; O'Brien, C. J.; Organ, M. G. *Angew. Chem. Int. Ed.* **2007**, 46, 2768.
25. McGuinness, D. S.; Cavell, K. J.; Skelton B. W.; White, A. H. *Organometallics* **1999**, 18, 1596–1605.
26. Liao, C. Y.; Chan, K. T.; Chang, Y. C.; Chen, C. Y.; Tu, C. Y.; Hu, C. H.; Lee, H. M. *Organometallics* **2007**, 26, 5826.
27. Xi, Z. X.; Zhang, X. M.; Chen, W. Z.; Fu, S. Z.; Wang, D. Q. *Organometallics* **2007**, 26, 6636.
28. Lee, C. C.; Ke, W. C.; Chan, K. T.; Lai, C. L.; Hu, C. H.; Lee, H. M. *Chem. Eur. J.* **2007**, 13, 582.
29. Huang, J.; Nolan, S. P. *J. Am. Chem. Soc.* **1999**, 121, 9889–9890.
30. Bohm, V. P. W.; Gstottmayr, C. W. K.; Weskamp, T.; Herrmann, W. A. *Angew. Chem., Int. Ed.* **2001**, 40, 3387–3389.
31. Kremzow, D.; Seidel, G.; Lehmann, C. W.; Furstner, A. *J. Chem. Eur.* **2005**, 11, 1833–1853.
32. Matsubara, K.; Ueno, K.; Shibata, Y. *Organometallics* **2006**, 25, 3422–3427.
33. Inamoto, K.; Kuroda, J. I.; Sakamoto, T.; Hiroya, K. *Synthesis* **2007**, 2853–2861.
34. Xi, Z.; Liu, B.; Chen, W. *J. Org. Chem.* **2008**, 73, 3954–3957.
35. Hahn, F. E.; Holtgrewe, C.; Pape, T.; Martin, M.; Sola, E.; Oro, L. A. *Organometallics* **2005**, 24, 2203-2209.
36. Türkmen, H.; Pape, T.; Hahn, F. E.; Çetinkaya, B. *Organometallics* **2008**, 27, 571–575.
37. Tucker C. E.; De Vries, J. G. *Top. Catal.* **2002**, 19, 111–118.
38. Zhang, K.; Conda-Sheridan, M.; Cooke, S. R.; Louie, J. *Organometallics* **2011**, 30, 2546–2552.
39. Blakey, S. B.; MacMillan, D. W. C. *J. Am. Chem. Soc.* **2003**, 125, 6046–6047.
40. Liu, J.; Robins, M. J. *Org. Lett.* **2004**, 6, 3421–3423.
41. Boeda, F.; Nolan, S. P. *Annu. Rep. Prog. Chem., Sect. B.* **2008**, 104, 184–210.
42. Hassan, J.; Sévignon, M.; Gozzi, C.; Schulz, E.; Lemaire, M. *Chem. Rev.* **2002**, 102, 1359-1469.
43. Tsou, T. T.; Kochi, J. K.; *J. Am. Chem. Soc.* **1979**, 101, 7547-7560.

44. Pal, A.; Ghosh, R.; Adarsh, N. N.; Sarkar, A. *Tetrahedron* **2010**, 66, 5451-5458.

Conclusions and Future Work

Examples of the symmetrical, unsymmetrical and backbone functionalised eight-membered NHC salts have been prepared and subsequent treatment of these precursor salts with KHMDS gave the corresponding free carbenes. The upfield shift of the C_{NHC}-*H* signal in the ^{1}H NMR spectrum for the amidinium HBF_4 salts, coupled with the downfield $^{13}C\{^{1}H\}$ shift of the eight-membered carbenes (the conjugate base) suggests that these NHCs are strong σ donors. The 8-membered NHC ring adopts a boat conformation with the backbone folded over the central C_{NHC} carbon. Their N-C_{NHC}-N angles are found to be around 129° – 130°, larger than their 5-, 6- and 7-NHC counterparts, with the attendant C_{NHC}-N-$C_{N\text{-}Substituent}$ angles being very small. [AgBr(8-NHC)] complexes were synthesized via interaction of the amidinium salts with Ag_2O. Crystallographic studies of these complexes reveal that the large 8-NHC rings encourage the aromatic N-substituents to bend round and essentially enclose the Ag centre. The percentage buried volume (%V_{bur}) of Ag(I) complexes show a dramatic increase as the ring size expands from 5- to 8-membered NHCs, illustrating the enhanced steric bulk inflicted by the larger ring systems. It was discovered that the 8-Mes ligand was too large to coordinate to the $[MCl(COD)]_2$ (M = Rh, Ir) dimer and only the less sterically demanding 8-*o*-Tol ligand was able to successfully yield the corresponding [MCl(8-*o*-Tol)(COD)] complex. The $[RhCl(8\text{-}o\text{-}Tol)(CO)_2]$ complex was prepared by passing carbon monoxide through a solution of [RhCl(8-*o*-Tol)(COD)] in dichloromethane. Comparison of the CO stretching frequencies for $[RhCl(NHC)(CO)_2]$ complexes bearing 5-, 6-, 7- and 8-membered NHC rings reveal that 8-*o*-Tol is the most basic of all the NHC ligands. A series of rare and novel $[NiX(8\text{-}NHC)(PPh_3)]$ (X = halide) complexes were prepared and characterised by EPR spectroscopy. These complexes were also employed as catalysts in cross-coupling reactions. The Suzuki cross-coupling reaction between aryl bromide and phenylboronic acid in the presence of $[NiCl(8\text{-}o\text{-}Tol)(PPh_3)]$ showed no catalytic activity. Kumada cross-coupling of *p*-chlorotoluene with PhMgBr in the presence of $[NiX(8\text{-}NHC)(PPh_3)]$ complexes gave modest yields, with the $[NiCl(8\text{-}o\text{-}Tol)(PPh_3)]$ complex giving the highest catalytic conversion of 38%. Homocoupled products derived from the starting materials were also detected in both catalytic reactions; however it is difficult to explain why this occurs at the current time. Furthermore, [MCl(8-*o*-Tol)(COD)] (M = Ir, Rh) complexes were found to be poor catalysts for transfer hydrogenation of ketones. Their poor catalytic performance is likely due to the steric hinderance imposed by the large 8-membered NHC ring around the metal centre; consequently disrupting it from coordinating with the substrates. Further studies on the potential preparation of 8-membered NHC systems with an unsaturated ring backbone would offer exciting opportunities for the generation of new NHC structures and complexes.

It would also be useful to further examine the catalytic applications of the [NiX(8-NHC)(PPh_3)] complexes in cross-coupling reactions and the extent of homocoupled products that form in the process. Therefore, conducting an investigation into the application of [NiX(8-NHC)(PPh_3)] complexes in the catalytic reductive symmetrical coupling of aryl halides (e.g. Ullmann type reaction) would be a good place to start.

Appendix I

X-Ray Crystallography data

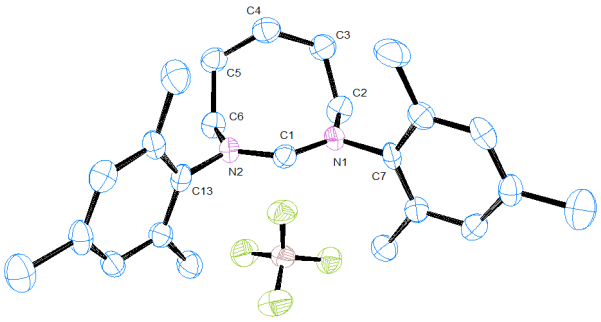

Table 1. Crystal data and structure refinement for **8-Mes·BF_4**

Identification code	kjc0845	
Empirical formula	C24 H33 B F4 N2	
Formula weight	436.33	
Temperature	150(2) K	
Wavelength	0.71073 Å	
Crystal system	Orthorhombic	
Space group	Fdd2	
Unit cell dimensions	a = 28.8300(5) Å	α= 90.000(3)°.
	b = 34.6430(9) Å	β= 90.000(4)°.
	c = 9.3760(12) Å	γ = 90.000(3)°.
Volume	9364.4(12) $Å^3$	
Z	16	
Density (calculated)	1.238 Mg/m^3	
Absorption coefficient	0.094 mm^{-1}	
F(000)	3712	
Crystal size	0.50 x 0.30 x 0.04 mm^3	
Theta range for data collection	2.36 to 21.03°.	
Index ranges	-28<=h<=28, -34<=k<=33, -9<=l<=9	
Reflections collected	8040	
Independent reflections	2409 [R(int) = 0.1099]	
Completeness to theta = 21.03°	98.2 %	
Max. and min. transmission	0.9963 and 0.9546	
Refinement method	Full-matrix least-squares on F^2	
Data / restraints / parameters	2409 / 1 / 286	
Goodness-of-fit on F^2	1.037	
Final R indices [I>2sigma(I)]	R1 = 0.0526, wR2 = 0.1079	
R indices (all data)	R1 = 0.0769, wR2 = 0.1177	
Absolute structure parameter	-0.9(12)	
Largest diff. peak and hole	0.156 and -0.211 $e.Å^{-3}$	

Table 2. Atomic coordinates (x 10^4) and equivalent isotropic displacement parameters ($Å^2$x 10^3) for kjc0845. U(eq) is defined as one third of the trace of the orthogonalized U^{ij} tensor.

	x	y	z	U(eq)
C(1)	3053(2)	11670(1)	18290(5)	29(1)
C(2)	2476(2)	11130(1)	18182(6)	37(1)
C(3)	2390(2)	11005(2)	19732(6)	40(1)
C(4)	2764(2)	11115(1)	20811(6)	40(1)
C(5)	3248(2)	10965(1)	20557(6)	38(1)
C(6)	3474(2)	11082(1)	19142(6)	33(1)
C(7)	2306(2)	11808(1)	17365(6)	29(1)
C(8)	2292(2)	11827(1)	15886(6)	33(1)
C(9)	1969(2)	12072(1)	15265(6)	36(1)
C(10)	1662(2)	12288(1)	16086(6)	35(1)
C(11)	1693(2)	12261(1)	17556(6)	36(1)
C(12)	2018(2)	12028(1)	18237(6)	34(1)
C(13)	2624(2)	11600(1)	14959(6)	43(2)
C(14)	1304(2)	12541(1)	15390(6)	54(2)
C(15)	2043(2)	12018(2)	19843(6)	52(2)
C(16)	3834(2)	11742(1)	18944(6)	31(1)
C(17)	3881(2)	11982(1)	20158(5)	31(1)
C(18)	4271(2)	12218(1)	20216(6)	35(1)
C(19)	4610(2)	12218(1)	19170(6)	36(1)
C(20)	4549(2)	11973(1)	17999(6)	35(1)
C(21)	4167(2)	11735(1)	17866(5)	32(1)
C(22)	3531(2)	11989(1)	21352(6)	43(2)
C(23)	5032(2)	12468(2)	19294(6)	47(2)
C(24)	4107(2)	11487(1)	16547(6)	40(1)
N(1)	2636(1)	11537(1)	18032(4)	29(1)
N(2)	3426(1)	11500(1)	18813(4)	29(1)
B(1)	3425(2)	10741(2)	14596(7)	40(2)
F(1)	3063(1)	10624(1)	13734(3)	49(1)
F(2)	3264(1)	10846(1)	15930(3)	51(1)
F(3)	3744(1)	10444(1)	14742(3)	60(1)
F(4)	3647(1)	11059(1)	13948(3)	59(1)

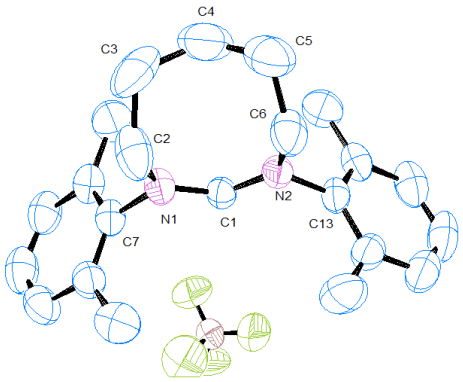

Table 1. Crystal data and structure refinement for **8-Xyl·BF_4**

Identification code	kjc0905b	
Empirical formula	C22 H29 B F4 N2	
Formula weight	408.28	
Temperature	296(2) K	
Wavelength	0.71073 Å	
Crystal system	Orthorhombic	
Space group	P212121	
Unit cell dimensions	a = 8.6050(2) Å	α= 90°.
	b = 14.6890(3) Å	β= 90°.
	c = 16.9750(4) Å	γ = 90°.
Volume	2145.62(8) $Å^3$	
Z	4	
Density (calculated)	1.264 Mg/m^3	
Absorption coefficient	0.097 mm^{-1}	
F(000)	864	
Crystal size	0.40 x 0.20 x 0.10 mm^3	
Theta range for data collection	1.83 to 28.05°.	
Index ranges	-10<=h<=11, -15<=k<=18, -21<=l<=22	
Reflections collected	12713	
Independent reflections	4887 [R(int) = 0.0629]	
Completeness to theta = 28.05°	95.2 %	
Absorption correction	Empirical	
Max. and min. transmission	0.9903 and 0.9620	
Refinement method	Full-matrix least-squares on F^2	
Data / restraints / parameters	4887 / 0 / 267	
Goodness-of-fit on F^2	1.042	
Final R indices [I>2sigma(I)]	R1 = 0.0806, wR2 = 0.2121	
R indices (all data)	R1 = 0.1433, wR2 = 0.2455	

Absolute structure parameter	-0.6(16)
Extinction coefficient	0.057(11)
Largest diff. peak and hole	0.750 and -0.519 e.Å^{-3}

Table 2. Atomic coordinates (x 10^4) and equivalent isotropic displacement parameters (Å^{2}x 10^3) for kjc0905b. U(eq) is defined as one third of the trace of the orthogonalized U^{ij} tensor.

	x	y	z	U(eq)
C(21)	13134(5)	3156(3)	3427(3)	83(1)
C(1)	8928(4)	3036(2)	1197(2)	49(1)
C(2)	7350(4)	3183(3)	1077(2)	60(1)
C(3)	6939(6)	3730(3)	431(2)	74(1)
C(4)	8057(6)	4074(3)	-67(2)	80(1)
C(5)	9597(6)	3916(2)	72(2)	72(1)
C(6)	10087(5)	3385(2)	721(2)	57(1)
C(7)	6091(5)	2813(3)	1608(3)	81(1)
C(8)	11781(5)	3259(3)	894(3)	78(1)
C(9)	9565(3)	2837(2)	2549(2)	42(1)
C(10)	9760(7)	1489(3)	1646(2)	80(1)
C(11)	8582(7)	778(3)	1931(3)	104(2)
C(12)	8086(7)	884(4)	2820(3)	101(2)
C(13)	9279(7)	833(3)	3405(3)	93(2)
C(14)	10549(6)	1529(2)	3358(2)	71(1)
C(15)	10298(4)	3129(2)	3858(2)	47(1)
C(16)	11823(4)	3434(2)	3964(2)	60(1)
C(17)	12094(6)	4013(3)	4583(3)	75(1)
C(18)	10930(8)	4270(3)	5091(3)	87(2)
C(19)	9439(6)	3961(3)	4981(2)	75(1)
C(20)	9067(5)	3382(2)	4345(2)	56(1)
C(22)	7433(5)	3089(3)	4206(2)	72(1)
N(1)	9403(3)	2448(2)	1851(1)	49(1)
N(2)	10021(3)	2490(2)	3218(1)	45(1)
B(1)	3723(6)	10224(3)	2337(3)	68(1)
F(1)	4357(7)	10106(4)	3028(2)	218(3)
F(2)	4737(5)	9944(3)	1772(3)	158(2)
F(3)	2353(4)	9793(2)	2262(2)	113(1)
F(4)	3526(5)	11136(2)	2157(3)	137(1)

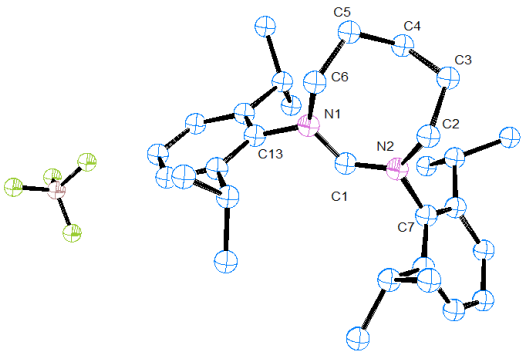

Table 1. Crystal data and structure refinement for **8-DIPP·BF$_4$**

Identification code	kjc0904	
Empirical formula	C30 H46 B F4 N2 O0.50	
Formula weight	529.50	
Temperature	103(2) K	
Wavelength	0.71073 Å	
Crystal system	Monoclinic	
Space group	P21/c	
Unit cell dimensions	a = 15.8730(3) Å	α= 90°.
	b = 9.8610(2) Å	β= 125.4270(10)°.
	c = 22.8750(4) Å	γ = 90°.
Volume	2917.57(10) Å^3	
Z	4	
Density (calculated)	1.205 Mg/m^3	
Absorption coefficient	0.088 mm^{-1}	
F(000)	1140	
Crystal size	0.44 x 0.30 x 0.30 mm^3	
Theta range for data collection	3.01 to 27.50°.	
Index ranges	-20<=h<=20, -12<=k<=12, -29<=l<=29	
Reflections collected	11770	
Independent reflections	6640 [R(int) = 0.0398]	
Completeness to theta = 27.50°	98.9 %	
Absorption correction	Empirical	
Max. and min. transmission	0.9741 and 0.9623	
Refinement method	Full-matrix least-squares on F^2	
Data / restraints / parameters	6640 / 68 / 442	
Goodness-of-fit on F^2	1.027	
Final R indices [I>2sigma(I)]	R1 = 0.0815, wR2 = 0.2147	
R indices (all data)	R1 = 0.1173, wR2 = 0.2418	
Extinction coefficient	0.031(6)	

Largest diff. peak and hole 0.707 and -0.380 e.Å^{-3}

Table 2. Atomic coordinates (x 10^4) and equivalent isotropic displacement parameters (Å^{2}x 10^3) for kjc0904. U(eq) is defined as one third of the trace of the orthogonalized U^{ij} tensor.

	x	y	z	U(eq)
C(1)	5536(2)	390(2)	1406(1)	29(1)
C(2)	4917(2)	-552(2)	1451(1)	32(1)
C(3)	3848(2)	-438(3)	947(1)	39(1)
C(4)	3423(2)	560(3)	429(1)	42(1)
C(5)	4053(2)	1489(3)	405(1)	39(1)
C(6)	5129(2)	1435(2)	896(1)	33(1)
C(7)	5347(2)	-1690(3)	2002(1)	36(1)
C(8)	5394(3)	-3019(3)	1683(2)	51(1)
C(9)	4711(2)	-1890(4)	2307(2)	56(1)
C(10)	5787(2)	2516(3)	880(1)	38(1)
C(11)	5600(3)	2614(4)	148(2)	56(1)
C(12)	5583(3)	3886(3)	1084(2)	60(1)
C(13)	8283(2)	1578(3)	3731(1)	36(1)
C(14)	8212(2)	787(3)	4208(1)	38(1)
C(15)	8407(2)	1411(3)	4824(1)	40(1)
C(16)	8670(2)	2771(3)	4954(1)	41(1)
C(17)	8744(2)	3523(3)	4475(1)	43(1)
C(18)	8547(2)	2949(3)	3847(1)	38(1)
C(19)	7922(2)	-709(3)	4083(1)	40(1)
C(20)	6922(2)	-950(3)	4015(2)	51(1)
C(21)	8789(2)	-1603(3)	4680(2)	50(1)
C(22)	8610(2)	3832(3)	3327(1)	47(1)
C(23)	9714(3)	4290(4)	3649(2)	65(1)
C(24)	7890(3)	5053(4)	3082(2)	83(1)
C(25)	7096(2)	858(2)	2533(1)	29(1)
C(26)	8898(4)	22(7)	3146(3)	38(1)
C(27)	9325(4)	635(6)	2751(3)	51(2)
C(28)	8551(4)	1122(6)	1996(3)	47(1)
C(29)	7780(3)	27(5)	1451(2)	31(1)
C(30)	7145(5)	-723(5)	1679(4)	31(1)
N(1)	8074(1)	932(2)	3083(1)	38(1)

N(2)	6659(1)	270(2)	1902(1)	29(1)
F(1)	8391(7)	8472(12)	5969(4)	107(3)
F(2)	7127(3)	8504(3)	6112(2)	48(1)
F(3)	8734(3)	8218(4)	7068(2)	56(1)
F(4)	8236(5)	10268(5)	6521(5)	119(3)
B(1)	8130(4)	8885(5)	6423(3)	41(1)
C(26A)	9029(4)	720(7)	3098(3)	39(1)
C(27A)	9284(6)	-813(8)	3178(4)	73(2)
C(29A)	7798(7)	-1509(9)	1843(4)	95(3)
C(28A)	8391(7)	-1761(9)	2641(4)	98(3)
C(30A)	7234(6)	-192(9)	1588(4)	57(2)
F(2A)	6947(4)	9270(8)	5732(4)	156(4)
B(1A)	7958(5)	9776(9)	6129(3)	73(3)
F(3A)	8282(5)	9797(8)	6830(2)	107(2)
F(1A)	8543(7)	8917(12)	6039(5)	117(4)
F(4A)	7997(7)	11095(7)	5974(4)	163(3)
N(1A)	8074(1)	932(2)	3083(1)	38(1)
N(2A)	6659(1)	270(2)	1902(1)	29(1)
O(3)	8992(5)	2095(7)	1700(3)	96(2)

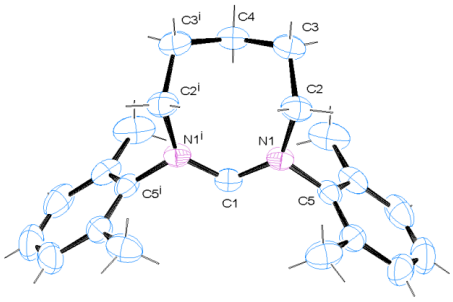

Table 1. Crystal data and structure refinement for **8-Xyl**

Identification code	kjc1032t	
Empirical formula	C22 H28 N2	
Formula weight	320.46	
Temperature	150(2) K	
Wavelength	0.71073 Å	
Crystal system	Orthorhombic	
Space group	Pnma	
Unit cell dimensions	a = 11.2458(3) Å	α= 90°.
	b = 20.1481(7) Å	β= 90°.
	c = 8.1507(3) Å	γ = 90°.
Volume	1846.80(11) $Å^3$	
Z	4	
Density (calculated)	1.153 Mg/m^3	
Absorption coefficient	0.067 mm^{-1}	
F(000)	696	
Crystal size	0.20 x 0.20 x 0.08 mm^3	
Theta range for data collection	3.09 to 27.49°.	
Index ranges	-14<=h<=14, -26<=k<=25, -10<=l<=10	
Reflections collected	3921	
Independent reflections	2163 [R(int) = 0.0517]	
Completeness to theta = 27.49°	99.1 %	
Absorption correction	Empirical	
Max. and min. transmission	0.9947 and 0.9867	
Refinement method	Full-matrix least-squares on F^2	
Data / restraints / parameters	2163 / 0 / 115	
Goodness-of-fit on F^2	1.054	
Final R indices [I>2sigma(I)]	R1 = 0.0573, wR2 = 0.1310	
R indices (all data)	R1 = 0.1007, wR2 = 0.1501	
Extinction coefficient	0.035(5)	
Largest diff. peak and hole	0.179 and -0.171 $e.Å^{-3}$	

Table 2. Atomic coordinates (x 10^4) and equivalent isotropic displacement parameters ($Å^2$x 10^3) for kjc1032t. U(eq) is defined as one third of the trace of the orthogonalized U^{ij} tensor.

	x	y	z	U(eq)
C(1)	-2411(2)	-2500	2004(3)	31(1)
C(2)	-566(1)	-3235(1)	1372(2)	39(1)
C(3)	-248(2)	-3135(1)	-434(2)	45(1)
C(4)	-690(2)	-2500	-1217(3)	42(1)
C(5)	-2537(1)	-3656(1)	2192(2)	34(1)
C(6)	-2463(1)	-3913(1)	3784(2)	38(1)
C(7)	-3122(2)	-4474(1)	4181(3)	53(1)
C(8)	-3834(2)	-4775(1)	3033(4)	65(1)
C(9)	-3899(2)	-4517(1)	1475(3)	61(1)
C(10)	-3262(2)	-3953(1)	1013(2)	44(1)
C(11)	-1710(2)	-3574(1)	5053(2)	49(1)
C(12)	-3372(2)	-3673(1)	-680(2)	64(1)
N(1)	-1834(1)	-3080(1)	1783(2)	32(1)

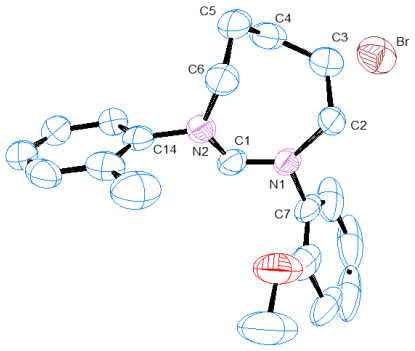

Table 1. Crystal data and structure refinement for **8-*o*-Tol/Anis·HBr**

Identification code	kjc1122	
Empirical formula	C20 H25 Br N2 O	
Formula weight	389.33	
Temperature	200(2) K	
Wavelength	0.71073 Å	
Crystal system	Monoclinic	
Space group	P21/a	
Unit cell dimensions	a = 8.0398(4) Å	α= 90°.
	b = 26.857(2) Å	β= 109.694(4)°.
	c = 9.4168(6) Å	γ = 90°.
Volume	1914.4(2) $Å^3$	
Z	4	
Density (calculated)	1.351 Mg/m^3	
Absorption coefficient	2.156 mm^{-1}	
F(000)	808	
Crystal size	0.15 x 0.15 x 0.15 mm^3	
Theta range for data collection	2.75 to 21.96°.	
Index ranges	-8<=h<=8, -28<=k<=26, -9<=l<=9	
Reflections collected	4308	
Independent reflections	2322 [R(int) = 0.0356]	
Completeness to theta = 21.96°	99.4 %	
Max. and min. transmission	0.7381 and 0.7381	
Refinement method	Full-matrix least-squares on F^2	
Data / restraints / parameters	2322 / 0 / 220	
Goodness-of-fit on F^2	1.058	
Final R indices [I>2sigma(I)]	R1 = 0.0475, wR2 = 0.0991	
R indices (all data)	R1 = 0.0697, wR2 = 0.1081	
Extinction coefficient	0.0152(11)	
Largest diff. peak and hole	0.467 and -0.297 $e.Å^{-3}$	

Table 2. Atomic coordinates (x 10^4) and equivalent isotropic displacement parameters ($Å^2$x 10^3) for kjc1122. U(eq) is defined as one third of the trace of the orthogonalized U^{ij} tensor.

	x	y	z	U(eq)
C(1)	7647(6)	3923(2)	3823(6)	49(1)
C(2)	4932(6)	4083(2)	1580(6)	52(1)
C(3)	4893(7)	3662(2)	507(6)	67(2)
C(4)	5933(7)	3193(2)	1163(7)	67(2)
C(5)	5419(7)	2927(2)	2385(7)	72(2)
C(6)	5577(6)	3236(2)	3771(6)	61(2)
C(7)	7389(6)	4690(2)	2554(8)	61(2)
C(8)	7511(8)	5026(3)	3717(11)	89(2)
C(9)	8052(10)	5509(3)	3636(15)	146(5)
C(10)	8467(13)	5640(4)	2384(18)	178(8)
C(11)	8406(10)	5309(4)	1235(13)	150(5)
C(12)	7834(7)	4818(3)	1321(9)	94(2)
C(13)	7230(10)	5159(3)	6228(11)	162(5)
C(14)	8677(6)	3284(2)	5596(6)	49(1)
C(15)	8574(7)	3297(2)	7051(7)	62(2)
C(16)	9970(9)	3073(2)	8191(6)	66(2)
C(17)	11354(8)	2864(2)	7897(7)	67(2)
C(18)	11455(8)	2866(2)	6479(7)	64(2)
C(19)	10088(7)	3073(2)	5316(6)	54(1)
C(20)	7086(8)	3553(3)	7360(8)	93(2)
N(1)	6713(5)	4199(1)	2680(5)	49(1)
N(2)	7273(5)	3509(2)	4349(5)	52(1)
O(1)	7057(6)	4847(2)	4913(7)	113(2)
Br(1)	808(1)	3677(1)	2043(1)	62(1)

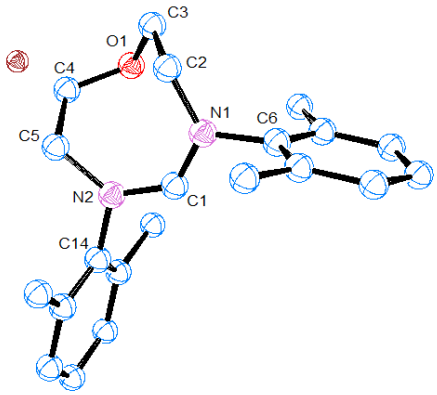

Table 1. Crystal data and structure refinement for **8-O-Xyl·HBr**

Identification code	kjc1123	
Empirical formula	C21.50 H33 Br Cl N2 O3.50	
Formula weight	490.86	
Temperature	150(2) K	
Wavelength	0.71073 Å	
Crystal system	Monoclinic	
Space group	C2/c	
Unit cell dimensions	a = 19.2466(5) Å	α= 90°.
	b = 13.3123(4) Å	β= 115.7970(10)°.
	c = 19.9805(3) Å	γ = 90°.
Volume	4609.1(2) $Å^3$	
Z	8	
Density (calculated)	1.415 Mg/m^3	
Absorption coefficient	1.926 mm^{-1}	
F(000)	2048	
Crystal size	0.35 x 0.35 x 0.35 mm^3	
Theta range for data collection	2.48 to 30.73°.	
Index ranges	-25<=h<=26, -18<=k<=17, -28<=l<=28	
Reflections collected	10141	
Independent reflections	6291 [R(int) = 0.0335]	
Completeness to theta = 30.73°	87.5 %	
Max. and min. transmission	0.5520 and 0.5520	
Refinement method	Full-matrix least-squares on F^2	
Data / restraints / parameters	6291 / 0 / 288	
Goodness-of-fit on F^2	1.026	
Final R indices [I>2sigma(I)]	R1 = 0.0498, wR2 = 0.1123	
R indices (all data)	R1 = 0.0802, wR2 = 0.1284	
Extinction coefficient	0.0045(3)	

Largest diff. peak and hole 0.781 and -1.093 e.Å^{-3}

Table 2. Atomic coordinates (x 10^4) and equivalent isotropic displacement parameters (Å^{2}x 10^3) for kjc1123. U(eq) is defined as one third of the trace of the orthogonalized U^{ij} tensor.

	x	y	z	U(eq)
C(1)	7002(1)	1082(2)	2132(1)	20(1)
C(2)	6552(2)	1882(2)	884(1)	24(1)
C(3)	6153(2)	2838(2)	964(2)	31(1)
C(4)	7099(2)	3470(2)	2131(2)	32(1)
C(5)	7740(2)	2687(2)	2322(1)	26(1)
C(6)	6066(1)	214(2)	1127(1)	20(1)
C(7)	6341(2)	-576(2)	840(1)	23(1)
C(8)	5905(2)	-1460(2)	644(1)	27(1)
C(9)	5233(2)	-1551(2)	729(1)	29(1)
C(10)	4962(2)	-743(2)	983(1)	28(1)
C(11)	5375(2)	157(2)	1192(1)	25(1)
C(12)	7069(2)	-485(2)	745(2)	34(1)
C(13)	5077(2)	1008(2)	1485(2)	33(1)
C(14)	7991(2)	1411(2)	3328(1)	24(1)
C(15)	8735(2)	1042(2)	3516(1)	27(1)
C(16)	9173(2)	743(2)	4248(2)	35(1)
C(17)	8875(2)	787(3)	4765(2)	41(1)
C(18)	8140(2)	1145(2)	4565(2)	36(1)
C(19)	7677(2)	1473(2)	3839(2)	28(1)
C(20)	9054(2)	952(3)	2956(2)	38(1)
C(21)	6873(2)	1868(3)	3622(2)	37(1)
C(22)	5000	3328(4)	2500	55(1)
N(1)	6560(1)	1092(2)	1410(1)	20(1)
N(2)	7535(1)	1723(2)	2560(1)	21(1)
O(1)	6344(1)	3084(2)	1718(1)	29(1)
O(2)	5000	8064(3)	2500	38(1)
O(3)	7161(2)	8815(2)	4342(1)	47(1)
O(4)	3704(2)	-450(2)	2092(1)	35(1)
Br(1)	6263(1)	6675(1)	4059(1)	34(1)
Cl(1)	5633(1)	4063(1)	3241(1)	57(1)

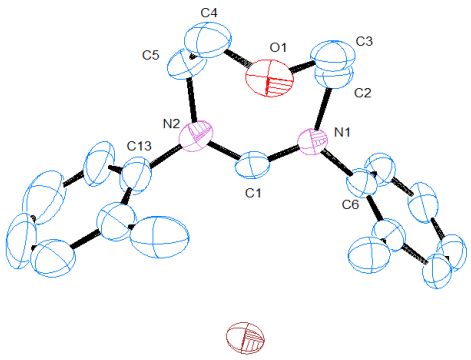

Table 1. Crystal data and structure refinement for **8-O-*o*-Tol·HBr**

Identification code	kjc1125	
Empirical formula	C19 H23 Br N2 O	
Formula weight	375.30	
Temperature	150(2) K	
Wavelength	0.71073 Å	
Crystal system	Orthorhombic	
Space group	P212121	
Unit cell dimensions	a = 9.9538(9) Å	α= 90°.
	b = 12.0381(10) Å	β= 90°.
	c = 14.9627(9) Å	γ = 90°.
Volume	1792.9(2) $Å^3$	
Z	4	
Density (calculated)	1.390 Mg/m^3	
Absorption coefficient	2.299 mm^{-1}	
F(000)	776	
Crystal size	0.30 x 0.20 x 0.20 mm^3	
Theta range for data collection	2.66 to 20.91°.	
Index ranges	-9<=h<=9, -12<=k<=12, -14<=l<=14	
Reflections collected	1872	
Independent reflections	1872 [R(int) = 0.0000]	
Completeness to theta = 20.91°	98.5 %	
Max. and min. transmission	0.6563 and 0.5455	
Refinement method	Full-matrix least-squares on F^2	
Data / restraints / parameters	1872 / 0 / 211	
Goodness-of-fit on F^2	1.156	
Final R indices [I>2sigma(I)]	R1 = 0.0401, wR2 = 0.0859	
R indices (all data)	R1 = 0.0428, wR2 = 0.0870	
Absolute structure parameter	0.018(19)	
Extinction coefficient	0.0154(13)	

Largest diff. peak and hole 0.346 and -0.232 e.Å^{-3}

Table 2. Atomic coordinates (x 10^4) and equivalent isotropic displacement parameters (Å^{2}x 10^3) for kjc1125. U(eq) is defined as one third of the trace of the orthogonalized U^{ij} tensor.

	x	y	z	U(eq)
C(1)	8086(7)	8064(5)	5934(4)	41(2)
C(2)	10230(6)	7082(6)	6249(5)	54(2)
C(3)	10781(7)	7746(7)	7040(4)	60(2)
C(4)	10672(8)	9558(6)	6412(5)	64(2)
C(5)	9948(7)	9341(6)	5527(5)	54(2)
C(6)	7999(6)	6166(5)	6334(5)	45(2)
C(7)	7276(7)	6057(6)	7118(5)	52(2)
C(8)	6597(7)	5039(6)	7251(5)	54(2)
C(9)	6665(8)	4220(6)	6621(6)	60(2)
C(10)	7404(9)	4366(7)	5837(6)	63(2)
C(11)	8053(8)	5327(6)	5696(5)	52(2)
C(12)	7223(7)	6948(6)	7810(4)	56(2)
C(13)	7536(8)	9909(6)	5485(5)	56(2)
C(14)	6893(8)	10458(6)	6160(7)	63(2)
C(15)	5961(9)	11311(7)	5887(9)	90(3)
C(16)	5824(12)	11519(7)	5000(10)	107(4)
C(17)	6444(13)	10945(10)	4331(9)	111(4)
C(18)	7356(9)	10146(8)	4567(7)	88(3)
C(19)	7090(10)	10185(8)	7082(6)	84(3)
N(1)	8758(5)	7175(5)	6170(4)	41(1)
N(2)	8517(6)	9046(5)	5667(4)	44(2)
O(1)	10263(5)	8823(4)	7105(3)	59(1)
Br(1)	4430(1)	7765(1)	6206(1)	51(1)

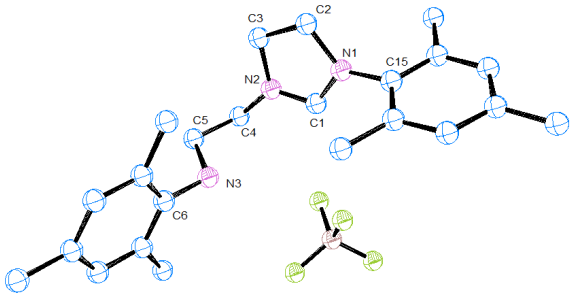

Table 1. Crystal data and structure refinement for **3-(2,4,6-trimethylphenyl)-1-{2-[(2,4,6 trimethylphenyl)amino]ethyl}-4,5-dihydro-1-imidazol-3-ium tetrafluoroborate salt**

Identification code	kjc1119	
Empirical formula	C23 H32 B F4 N3	
Formula weight	437.33	
Temperature	150(2) K	
Wavelength	0.71073 Å	
Crystal system	Monoclinic	
Space group	P21/a	
Unit cell dimensions	a = 9.5442(4) Å	α= 90°.
	b = 16.8164(4) Å	β= 102.129(2)°.
	c = 15.2887(7) Å	γ = 90°.
Volume	2399.05(16) $Å^3$	
Z	4	
Density (calculated)	1.211 Mg/m^3	
Absorption coefficient	0.093 mm^{-1}	
F(000)	928	
Crystal size	0.32 x 0.32 x 0.30 mm^3	
Theta range for data collection	2.50 to 28.30°.	
Index ranges	-12<=h<=12, -22<=k<=21, -20<=l<=20	
Reflections collected	11017	
Independent reflections	5890 [R(int) = 0.0514]	
Completeness to theta = 28.30°	98.7 %	
Max. and min. transmission	0.9727 and 0.9709	
Refinement method	Full-matrix least-squares on F^2	
Data / restraints / parameters	5890 / 218 / 337	
Goodness-of-fit on F^2	1.036	
Final R indices [I>2sigma(I)]	R1 = 0.0700, wR2 = 0.1612	
R indices (all data)	R1 = 0.1458, wR2 = 0.1975	
Extinction coefficient	0.042(4)	
Largest diff. peak and hole	0.241 and -0.208 $e.Å^{-3}$	

Table 2. Atomic coordinates (x 10^4) and equivalent isotropic displacement parameters ($Å^2$x 10^3) for kjc1119. U(eq) is defined as one third of the trace of the orthogonalized U^{ij} tensor.

	x	y	z	U(eq)
C(1)	3353(2)	1200(1)	146(2)	51(1)
C(2)	2472(3)	537(1)	-63(2)	54(1)
C(3)	1587(3)	502(1)	-911(2)	63(1)
C(4)	1574(3)	1092(2)	-1536(2)	68(1)
C(5)	2478(3)	1729(2)	-1312(2)	70(1)
C(6)	3385(3)	1805(1)	-478(2)	63(1)
C(7)	2452(3)	-127(2)	594(2)	74(1)
C(8)	563(4)	1038(2)	-2444(2)	105(1)
C(9)	4346(4)	2520(2)	-251(2)	95(1)
C(10)	3753(2)	1366(1)	1758(1)	46(1)
C(11)	5766(3)	1028(2)	1265(2)	80(1)
C(12)	6101(3)	1094(2)	2287(2)	67(1)
C(13)	4459(3)	1377(1)	3395(1)	54(1)
C(14)	4485(2)	588(1)	3875(2)	55(1)
C(15)	3333(2)	-715(1)	3776(1)	50(1)
C(16)	2486(2)	-899(1)	4384(2)	50(1)
C(17)	2489(2)	-1672(1)	4709(2)	55(1)
C(18)	3334(3)	-2263(1)	4460(2)	55(1)
C(19)	4185(3)	-2060(1)	3870(2)	61(1)
C(20)	4198(3)	-1300(1)	3512(2)	56(1)
C(21)	1574(3)	-277(2)	4704(2)	71(1)
C(22)	3323(3)	-3094(1)	4833(2)	74(1)
C(23)	5109(4)	-1128(2)	2841(2)	87(1)
N(1)	4236(2)	1261(1)	1024(1)	53(1)
N(2)	4703(2)	1276(1)	2492(1)	50(1)
N(3)	3338(2)	68(1)	3401(1)	58(1)
F(1)	509(4)	1067(3)	1746(4)	127(2)
F(2)	-1147(3)	1922(2)	1951(4)	86(1)
F(3)	1106(6)	2021(4)	2748(4)	98(2)
F(4)	-321(5)	1035(3)	3014(3)	133(2)
B(1)	24(5)	1507(3)	2374(3)	56(2)
F(1A)	657(9)	818(4)	2432(10)	135(4)
F(2A)	-1079(8)	1500(8)	1650(5)	98(3)

F(3A)	969(11)	2115(6)	2314(11)	109(4)
F(4A)	-648(8)	1680(10)	3095(5)	134(5)
B(1A)	-19(11)	1538(7)	2397(7)	97(8)

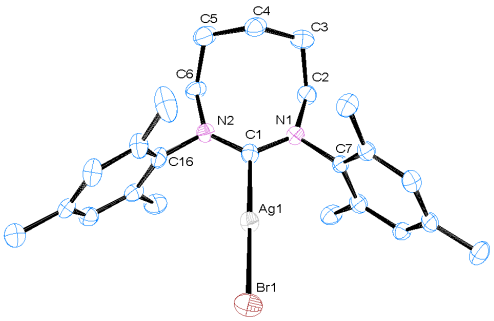

Table 1. Crystal data and structure refinement for **Ag(8-Mes)Br**

Identification code	kjc1012	
Empirical formula	C24 H32 Ag Br N2	
Formula weight	536.30	
Temperature	150(2) K	
Wavelength	0.71073 Å	
Crystal system	Monoclinic	
Space group	P21/n	
Unit cell dimensions	a = 8.4786(2) Å	α= 90°.
	b = 17.6647(5) Å	β= 103.7560(10)°.
	c = 15.7970(3) Å	γ = 90°.
Volume	2298.08(10) $Å^3$	
Z	4	
Density (calculated)	1.550 Mg/m^3	
Absorption coefficient	2.627 mm^{-1}	
F(000)	1088	
Crystal size	0.25 x 0.15 x 0.10 mm^3	
Theta range for data collection	2.89 to 27.48°.	
Index ranges	-10<=h<=11, -22<=k<=20, -20<=l<=20	
Reflections collected	8789	
Independent reflections	5247 [R(int) = 0.0350]	
Completeness to theta = 27.48°	99.7 %	
Max. and min. transmission	0.7791 and 0.5596	
Refinement method	Full-matrix least-squares on F^2	
Data / restraints / parameters	5247 / 0 / 260	
Goodness-of-fit on F^2	1.049	
Final R indices [I>2sigma(I)]	R1 = 0.0411, wR2 = 0.0840	
R indices (all data)	R1 = 0.0573, wR2 = 0.0916	
Extinction coefficient	0.0072(4)	
Largest diff. peak and hole	0.843 and -0.644 $e.Å^{-3}$	

Table 2. Atomic coordinates (x 10^4) and equivalent isotropic displacement parameters ($Å^2$x 10^3) for kjc1012. U(eq) is defined as one third of the trace of the orthogonalized U^{ij} tensor.

	x	y	z	U(eq)
C(1)	5377(4)	1656(2)	2866(2)	23(1)
C(2)	6040(4)	2835(2)	3837(2)	26(1)
C(3)	4430(5)	3162(2)	3962(3)	32(1)
C(4)	2899(5)	2910(2)	3303(2)	31(1)
C(5)	2831(5)	3124(2)	2362(3)	36(1)
C(6)	4213(5)	2827(2)	1981(2)	28(1)
C(7)	6847(4)	1538(2)	4334(2)	20(1)
C(8)	8543(4)	1473(2)	4461(2)	24(1)
C(9)	9372(4)	1020(2)	5140(2)	24(1)
C(10)	8583(4)	632(2)	5689(2)	24(1)
C(11)	6906(5)	719(2)	5546(2)	26(1)
C(12)	6007(4)	1172(2)	4879(2)	23(1)
C(13)	9419(4)	1875(2)	3863(3)	31(1)
C(14)	9500(5)	159(2)	6426(3)	33(1)
C(15)	4203(4)	1246(2)	4762(2)	29(1)
C(16)	4013(4)	1530(2)	1381(2)	25(1)
C(17)	2585(5)	1115(2)	1283(2)	31(1)
C(18)	2108(5)	654(2)	556(2)	33(1)
C(19)	2967(4)	610(2)	-85(2)	27(1)
C(20)	4371(5)	1044(2)	22(2)	30(1)
C(21)	4930(4)	1506(2)	749(2)	26(1)
C(22)	1562(5)	1158(3)	1946(3)	48(1)
C(23)	2382(5)	121(2)	-874(3)	37(1)
C(24)	6498(5)	1944(2)	867(3)	33(1)
N(1)	5975(3)	2016(2)	3623(2)	21(1)
N(2)	4573(4)	2009(2)	2143(2)	23(1)
Br(1)	6112(1)	-913(1)	2773(1)	37(1)
Ag(1)	5727(1)	462(1)	2827(1)	24(1)

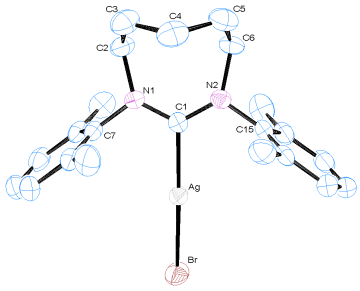

Table 1. Crystal data and structure refinement for **Ag(8-Xyl)Br**

Identification code	kjc1015t	
Empirical formula	C22 H28 Ag Br N2	
Formula weight	508.24	
Temperature	200(2) K	
Wavelength	0.71073 Å	
Crystal system	Orthorhombic	
Space group	Pbca	
Unit cell dimensions	a = 15.7187(3) Å	α= 90°.
	b = 17.1912(3) Å	β= 90°.
	c = 15.7875(4) Å	γ = 90°.
Volume	4266.15(15) $Å^3$	
Z	8	
Density (calculated)	1.583 Mg/m^3	
Absorption coefficient	2.826 mm^{-1}	
F(000)	2048	
Crystal size	0.30 x 0.30 x 0.10 mm^3	
Theta range for data collection	2.99 to 27.52°.	
Index ranges	-17<=h<=20, -21<=k<=22, -20<=l<=20	
Reflections collected	25592	
Independent reflections	4895 [R(int) = 0.0748]	
Completeness to theta = 27.52°	99.7 %	
Absorption correction	Empirical	
Max. and min. transmission	0.7653 and 0.4844	
Refinement method	Full-matrix least-squares on F^2	
Data / restraints / parameters	4895 / 0 / 239	
Goodness-of-fit on F^2	1.029	
Final R indices [I>2sigma(I)]	R1 = 0.0446, wR2 = 0.0978	
R indices (all data)	R1 = 0.0756, wR2 = 0.1105	
Largest diff. peak and hole	0.891 and -1.188 $e.Å^{-3}$	

Table 2. Atomic coordinates (x 10^4) and equivalent isotropic displacement parameters ($Å^2$x 10^3) for kjc1015t. U(eq) is defined as one third of the trace of the orthogonalized U^{ij} tensor.

	x	y	z	U(eq)
C(1)	-1158(2)	-3425(2)	-3340(2)	28(1)
C(2)	-933(3)	-2259(2)	-2346(3)	40(1)
C(3)	-38(3)	-1944(3)	-2514(3)	54(1)
C(4)	341(3)	-2122(3)	-3359(3)	51(1)
C(5)	-145(3)	-1850(2)	-4131(3)	51(1)
C(6)	-1041(3)	-2176(2)	-4224(3)	42(1)
C(7)	-1131(2)	-3614(2)	-1862(2)	31(1)
C(8)	-442(3)	-4066(2)	-1604(2)	38(1)
C(9)	-554(3)	-4549(2)	-906(3)	51(1)
C(10)	-1317(4)	-4577(2)	-482(3)	56(1)
C(11)	-1985(3)	-4129(2)	-737(3)	48(1)
C(12)	-1915(3)	-3642(2)	-1437(2)	36(1)
C(13)	401(3)	-4045(3)	-2058(3)	55(1)
C(14)	-2663(3)	-3173(3)	-1740(3)	52(1)
C(15)	-1261(3)	-3490(2)	-4829(2)	34(1)
C(16)	-573(3)	-3867(2)	-5218(2)	37(1)
C(17)	-744(3)	-4308(2)	-5944(2)	47(1)
C(18)	-1542(4)	-4355(2)	-6273(3)	53(1)
C(20)	-2086(3)	-3534(2)	-5156(2)	40(1)
C(21)	323(3)	-3809(2)	-4877(3)	47(1)
C(22)	-2811(3)	-3133(3)	-4715(3)	59(1)
C(29)	-2206(3)	-3971(2)	-5891(3)	49(1)
N(1)	-1046(2)	-3092(2)	-2579(2)	29(1)
N(2)	-1116(2)	-3031(2)	-4069(2)	31(1)
Br(1)	-2091(1)	-5934(1)	-3330(1)	50(1)
Ag(1)	-1539(1)	-4609(1)	-3359(1)	31(1)

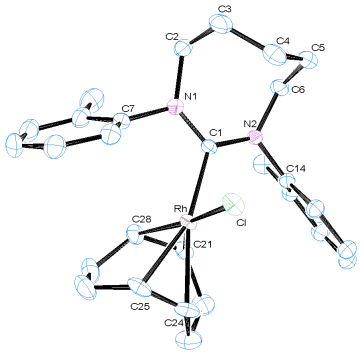

Table 1. Crystal data and structure refinement for **Rh(8-*o*-Tol)(COD)Cl**

Identification code	kjc0915	
Empirical formula	C28 H36 Cl N2 Rh	
Formula weight	538.95	
Temperature	150(2) K	
Wavelength	0.71073 Å	
Crystal system	Monoclinic	
Space group	C2/c	
Unit cell dimensions	a = 35.3100(10) Å	α= 90°.
	b = 9.1520(4) Å	β= 108.3940(10)°.
	c = 16.3260(6) Å	γ = 90°.
Volume	5006.3(3) $Å^3$	
Z	8	
Density (calculated)	1.430 Mg/m^3	
Absorption coefficient	0.807 mm^{-1}	
F(000)	2240	
Crystal size	0.18 x 0.16 x 0.10 mm^3	
Theta range for data collection	2.63 to 29.05°.	
Index ranges	-48<=h<=40, -11<=k<=12, -21<=l<=22	
Reflections collected	13464	
Independent reflections	6227 [R(int) = 0.0588]	
Completeness to theta = 29.05°	92.9 %	
Max. and min. transmission	0.9236 and 0.8683	
Refinement method	Full-matrix least-squares on F^2	
Data / restraints / parameters	6227 / 0 / 292	
Goodness-of-fit on F^2	1.031	
Final R indices [I>2sigma(I)]	R1 = 0.0438, wR2 = 0.0853	
R indices (all data)	R1 = 0.0621, wR2 = 0.0920	
Extinction coefficient	0.00372(19)	

Largest diff. peak and hole 0.628 and -0.598 e.Å^{-3}

Table 2. Atomic coordinates (x 10^4) and equivalent isotropic displacement parameters (Å^{2}x 10^3) for kjc0915. U(eq) is defined as one third of the trace of the orthogonalized U^{ij} tensor.

	x	y	z	U(eq)
Rh	1409(1)	3248(1)	6450(1)	17(1)
Cl	1031(1)	5451(1)	6505(1)	24(1)
C(1)	1065(1)	3018(3)	5177(2)	16(1)
C(21)	1900(1)	2048(4)	6338(2)	22(1)
C(14)	1551(1)	4380(4)	4743(2)	19(1)
C(19)	1848(1)	3727(4)	4463(2)	22(1)
N(2)	1164(1)	3659(3)	4534(1)	17(1)
C(6)	927(1)	3853(4)	3612(2)	23(1)
C(28)	1650(1)	1097(4)	6602(2)	25(1)
C(15)	1617(1)	5690(4)	5186(2)	23(1)
N(1)	712(1)	2313(3)	5026(2)	20(1)
C(12)	685(1)	-13(4)	5745(2)	27(1)
C(4)	375(1)	5077(4)	4091(2)	31(1)
C(24)	1855(1)	3895(4)	7679(2)	28(1)
C(18)	2215(1)	4448(4)	4665(2)	26(1)
C(7)	651(1)	1494(4)	5738(2)	21(1)
C(25)	1565(1)	3093(4)	7852(2)	28(1)
C(2)	353(1)	2276(4)	4245(2)	29(1)
C(23)	2265(1)	3296(5)	7750(2)	38(1)
C(16)	1983(1)	6394(4)	5367(2)	29(1)
C(9)	454(1)	1439(5)	7023(2)	34(1)
C(8)	528(1)	2235(4)	6361(2)	25(1)
C(27)	1741(1)	515(5)	7516(2)	36(1)
C(17)	2284(1)	5740(4)	5115(2)	31(1)
C(10)	505(1)	-55(5)	7060(2)	40(1)
C(5)	624(1)	5092(4)	3481(2)	30(1)
C(26)	1590(1)	1495(5)	8100(2)	39(1)
C(11)	619(1)	-774(4)	6429(2)	36(1)
C(3)	124(1)	3712(5)	4053(2)	38(1)
C(13)	786(1)	-846(5)	5045(3)	41(1)
C(22)	2286(1)	2716(5)	6900(2)	33(1)

C(20)	1778(1)	2332(4)	3954(2)	29(1)

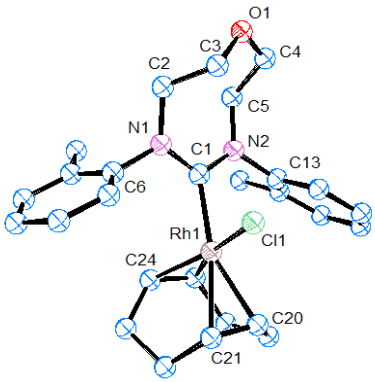

Table 1. Crystal data and structure refinement for **Rh(O-8-*o*-Tol)(COD)Cl**

Identification code	kjc1136	
Empirical formula	C27.50 H35 Cl2 N2 O Rh	
Formula weight	583.39	
Temperature	150(2) K	
Wavelength	0.71073 Å	
Crystal system	Monoclinic	
Space group	P21/n	
Unit cell dimensions	a = 9.9973(5) Å	α= 90°.
	b = 18.9684(5) Å	β= 98.702(2)°.
	c = 13.9425(6) Å	γ = 90°.
Volume	2613.52(19) $Å^3$	
Z	4	
Density (calculated)	1.483 Mg/m^3	
Absorption coefficient	0.881 mm^{-1}	
F(000)	1204	
Crystal size	0.50 x 0.32 x 0.03 mm^3	
Theta range for data collection	2.58 to 27.45°.	
Index ranges	-12<=h<=12, -24<=k<=20, -18<=l<=18	
Reflections collected	10590	
Independent reflections	5900 [R(int) = 0.0517]	
Completeness to theta = 27.45°	98.9 %	
Max. and min. transmission	0.9741 and 0.6671	
Refinement method	Full-matrix least-squares on F^2	
Data / restraints / parameters	5900 / 27 / 318	
Goodness-of-fit on F^2	1.037	
Final R indices [I>2sigma(I)]	R1 = 0.0551, wR2 = 0.1285	
R indices (all data)	R1 = 0.0836, wR2 = 0.1438	
Largest diff. peak and hole	1.362 and -1.399 $e.Å^{-3}$	

Table 2. Atomic coordinates (x 10^4) and equivalent isotropic displacement parameters ($Å^2$x 10^3) for kjc1136. U(eq) is defined as one third of the trace of the orthogonalized U^{ij} tensor.

	x	y	z	U(eq)
C(1)	4274(5)	2186(2)	6950(3)	21(1)
C(2)	6711(5)	2529(2)	6827(4)	33(1)
C(3)	6333(6)	3185(3)	6216(4)	36(1)
C(4)	5277(5)	3933(2)	7248(4)	32(1)
C(5)	4906(5)	3332(2)	7866(3)	27(1)
C(6)	5946(5)	1297(2)	6823(4)	26(1)
C(7)	6433(5)	921(2)	7662(4)	30(1)
C(8)	6811(5)	220(3)	7548(4)	35(1)
C(9)	6735(5)	-84(3)	6638(4)	35(1)
C(10)	6286(5)	309(3)	5818(4)	32(1)
C(11)	5873(5)	1003(2)	5908(3)	27(1)
C(12)	6528(7)	1246(3)	8653(4)	47(2)
C(13)	2558(5)	3026(2)	7213(3)	23(1)
C(14)	1884(5)	3056(2)	8018(3)	25(1)
C(15)	544(5)	3305(2)	7867(4)	31(1)
C(16)	-73(5)	3522(3)	6969(4)	35(1)
C(17)	625(5)	3507(3)	6177(4)	35(1)
C(18)	1928(5)	3258(2)	6301(3)	28(1)
C(19)	2517(6)	2839(3)	9034(4)	36(1)
C(20)	691(5)	1363(3)	5586(4)	30(1)
C(21)	1420(5)	777(2)	5427(4)	30(1)
C(22)	1414(6)	94(3)	6008(4)	36(1)
C(23)	2568(5)	69(3)	6856(4)	35(1)
C(24)	2898(5)	774(2)	7322(3)	28(1)
C(25)	1957(5)	1282(2)	7536(3)	28(1)
C(26)	432(5)	1185(3)	7367(4)	35(1)
C(27)	-215(5)	1444(3)	6365(4)	34(1)
N(1)	5591(4)	2036(2)	6932(3)	24(1)
N(2)	3960(4)	2813(2)	7330(3)	21(1)
O(1)	6395(4)	3811(2)	6762(3)	35(1)
Cl(1)	3230(1)	2079(1)	4739(1)	26(1)
Rh(1)	2751(1)	1572(1)	6259(1)	21(1)
C(28)	-1059(16)	454(9)	9779(19)	164(6)

Cl(2)	-1695(5)	-221(3)	10393(3)	87(1)
Cl(3)	546(9)	269(4)	9611(5)	160(3)

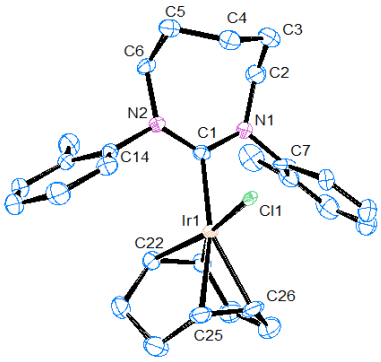

Table 1. Crystal data and structure refinement for **Ir(8-*o*-Tol)(COD)Cl**

Identification code	kjc1127bt	
Empirical formula	C28 H36 Br0.26 Cl0.74 Ir N2	
Formula weight	639.91	
Temperature	150(2) K	
Wavelength	0.71073 Å	
Crystal system	Monoclinic	
Space group	C2/c	
Unit cell dimensions	a = 35.3694(6) Å	α= 90°.
	b = 9.1699(2) Å	β= 108.4990(10)°.
	c = 16.3681(4) Å	γ = 90°.
Volume	5034.42(19) $Å^3$	
Z	8	
Density (calculated)	1.689 Mg/m^3	
Absorption coefficient	5.817 mm^{-1}	
F(000)	2534	
Crystal size	0.25 x 0.25 x 0.22 mm^3	
Theta range for data collection	2.43 to 30.66°.	
Index ranges	-48<=h<=46, -12<=k<=13, -23<=l<=22	
Reflections collected	17639	
Independent reflections	6930 [R(int) = 0.0333]	
Completeness to theta = 30.66°	88.8 %	
Max. and min. transmission	0.3610 and 0.3241	
Refinement method	Full-matrix least-squares on F^2	
Data / restraints / parameters	6930 / 0 / 293	
Goodness-of-fit on F^2	1.054	
Final R indices [I>2sigma(I)]	R1 = 0.0343, wR2 = 0.0805	
R indices (all data)	R1 = 0.0402, wR2 = 0.0843	
Extinction coefficient	0.00169(6)	

Largest diff. peak and hole 3.381 and -2.356 e.Å^{-3}

Table 2. Atomic coordinates (x 10^4) and equivalent isotropic displacement parameters (Å^{2}x 10^3) for kjc1127bt. U(eq) is defined as one third of the trace of the orthogonalized U^{ij} tensor.

	x	y	z	U(eq)
C(1)	1066(1)	1968(4)	189(2)	16(1)
C(2)	354(1)	2709(5)	-753(3)	32(1)
C(3)	126(1)	1280(6)	-948(3)	41(1)
C(4)	377(1)	-89(5)	-920(3)	32(1)
C(5)	627(1)	-83(5)	-1521(3)	32(1)
C(6)	930(1)	1151(5)	-1380(2)	24(1)
C(7)	657(1)	3467(4)	728(3)	21(1)
C(8)	684(1)	4999(4)	744(3)	29(1)
C(9)	616(1)	5748(5)	1432(4)	39(1)
C(10)	496(1)	5032(6)	2048(3)	42(1)
C(11)	446(1)	3539(6)	2008(3)	36(1)
C(12)	523(1)	2760(5)	1349(3)	26(1)
C(13)	789(2)	5822(5)	50(4)	44(1)
C(14)	1553(1)	623(4)	-254(2)	17(1)
C(15)	1849(1)	1279(4)	-531(2)	20(1)
C(16)	2215(1)	567(5)	-334(3)	27(1)
C(17)	2282(1)	-745(5)	103(3)	31(1)
C(18)	1983(1)	-1391(5)	352(3)	30(1)
C(19)	1616(1)	-708(4)	168(3)	23(1)
C(20)	1778(1)	2682(5)	-1028(3)	31(1)
C(21)	1647(1)	3899(4)	1606(3)	21(1)
C(22)	1901(1)	2944(4)	1334(3)	23(1)
C(23)	2294(1)	2335(5)	1901(3)	31(1)
C(24)	2271(1)	1744(5)	2754(3)	33(1)
C(25)	1861(1)	1116(5)	2660(3)	26(1)
C(26)	1567(1)	1930(5)	2839(3)	26(1)
C(27)	1592(2)	3519(6)	3094(3)	37(1)
C(28)	1742(1)	4500(5)	2509(3)	34(1)
Cl(1)	1042(1)	-490(1)	1526(1)	26(1)
Br(1)	1042(1)	-490(1)	1526(1)	26(1)
Ir(1)	1415(1)	1750(1)	1454(1)	16(1)

N(1)	711(1)	2675(4)	29(2)	19(1)
N(2)	1167(1)	1338(4)	-454(2)	18(1)

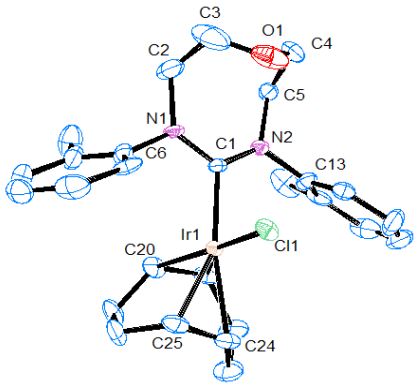

Table 1. Crystal data and structure refinement for **Ir(O-8-*o*-Tol)(COD)Cl**

Identification code	kjc1137	
Empirical formula	C27 H34 Cl Ir N2 O	
Formula weight	630.21	
Temperature	150(2) K	
Wavelength	0.71073 Å	
Crystal system	Monoclinic	
Space group	P21	
Unit cell dimensions	a = 10.0466(3) Å	α= 90°.
	b = 11.9689(4) Å	β= 112.266(2)°.
	c = 10.9963(3) Å	γ = 90°.
Volume	1223.67(6) $Å^3$	
Z	2	
Density (calculated)	1.710 Mg/m^3	
Absorption coefficient	5.587 mm^{-1}	
F(000)	624	
Crystal size	0.15 x 0.15 x 0.15 mm^3	
Theta range for data collection	2.89 to 27.51°.	
Index ranges	-10<=h<=13, -15<=k<=14, -14<=l<=13	
Reflections collected	7335	
Independent reflections	5200 [R(int) = 0.0308]	
Completeness to theta = 27.51°	99.7 %	
Absorption correction	Empirical	
Max. and min. transmission	0.4879 and 0.4879	
Refinement method	Full-matrix least-squares on F^2	
Data / restraints / parameters	5200 / 1 / 293	
Goodness-of-fit on F^2	1.040	
Final R indices [I>2sigma(I)]	R1 = 0.0365, wR2 = 0.0864	
R indices (all data)	R1 = 0.0395, wR2 = 0.0888	

Absolute structure parameter	0.433(13)
Extinction coefficient	0.0144(9)
Largest diff. peak and hole	4.731 and -1.839 e.Å^{-3}

Table 2. Atomic coordinates (x 10^4) and equivalent isotropic displacement parameters (Å^{2}x 10^3) for kjc1137. U(eq) is defined as one third of the trace of the orthogonalized U^{ij} tensor.

	x	y	z	U(eq)
C(1)	1816(7)	5300(6)	6194(7)	18(1)
C(2)	-747(10)	4755(11)	5916(10)	47(3)
C(3)	-1588(11)	5731(15)	5067(12)	71(6)
C(4)	-804(10)	5449(9)	3298(9)	38(2)
C(5)	342(9)	4559(8)	3907(8)	28(2)
C(6)	1051(10)	5256(9)	8035(9)	24(2)
C(7)	1151(10)	4383(8)	8856(9)	33(2)
C(8)	1311(11)	4610(11)	10154(10)	46(3)
C(9)	1336(10)	5684(10)	10594(10)	45(3)
C(10)	1202(11)	6575(10)	9751(11)	45(3)
C(11)	1037(9)	6356(7)	8420(11)	26(2)
C(12)	1060(14)	3170(9)	8408(12)	51(3)
C(13)	2682(14)	5417(10)	4441(12)	24(3)
C(14)	3477(11)	4694(10)	4025(9)	34(2)
C(15)	4459(13)	5143(13)	3488(11)	51(4)
C(16)	4509(13)	6255(14)	3349(12)	53(5)
C(17)	3669(15)	7015(12)	3688(11)	48(4)
C(18)	2734(15)	6567(11)	4243(12)	30(3)
C(19)	3331(13)	3432(9)	4108(10)	47(3)
C(20)	4444(9)	4523(7)	8513(9)	29(2)
C(21)	4951(8)	4643(7)	7493(9)	29(2)
C(22)	6492(9)	4989(10)	7702(10)	38(2)
C(23)	7032(7)	6002(18)	8598(9)	42(2)
C(24)	5814(8)	6788(7)	8502(9)	27(2)
C(25)	5083(9)	6726(7)	9337(8)	28(2)
C(26)	5299(10)	5909(16)	10396(8)	42(3)
C(27)	5324(10)	4686(7)	9957(8)	31(2)
N(1)	781(6)	5058(6)	6658(6)	22(1)
N(2)	1654(6)	5025(6)	4946(6)	19(1)

O(1)	-950(7)	6198(9)	4232(7)	51(2)
Cl(1)	2756(2)	7893(2)	6858(2)	23(1)
Ir(11)	3691(1)	6026(1)	7476(1)	16(1)

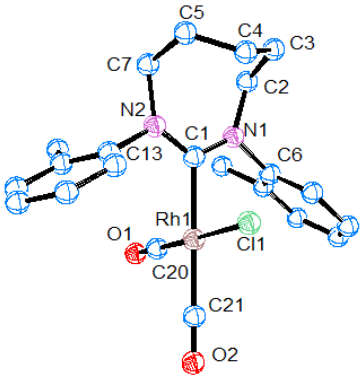

Table 1. Crystal data and structure refinement for **Rh(8-*o*-Tol)(CO)$_2$Cl**

Identification code	kjc1013	
Empirical formula	C22.25 H24.50 Cl1.50 N2 O2 Rh	
Formula weight	508.02	
Temperature	293(2) K	
Wavelength	0.71073 Å	
Crystal system	Tetragonal	
Space group	P42/n	
Unit cell dimensions	a = 25.7090(8) Å	α= 90°.
	b = 25.7090(8) Å	β= 90°.
	c = 7.6612(2) Å	γ = 90°.
Volume	5063.7(3) Å^3	
Z	8	
Density (calculated)	1.333 Mg/m^3	
Absorption coefficient	0.850 mm^{-1}	
F(000)	2068	
Crystal size	0.50 x 0.20 x 0.03 mm^3	
Theta range for data collection	3.10 to 26.71°.	
Index ranges	-32<=h<=32, -22<=k<=22, -9<=l<=9	
Reflections collected	10277	
Independent reflections	5351 [R(int) = 0.1574]	
Completeness to theta = 26.71°	99.7 %	
Absorption correction	Empirical	
Max. and min. transmission	0.9749 and 0.6758	
Refinement method	Full-matrix least-squares on F^2	
Data / restraints / parameters	5351 / 3 / 265	
Goodness-of-fit on F^2	1.020	
Final R indices [I>2sigma(I)]	R1 = 0.0844, wR2 = 0.2048	
R indices (all data)	R1 = 0.2116, wR2 = 0.2577	

Largest diff. peak and hole 1.269 and -2.113 e.Å^{-3}

Table 2. Atomic coordinates (x 10^4) and equivalent isotropic displacement parameters (Å^{2}x 10^3) for kjc1013. U(eq) is defined as one third of the trace of the orthogonalized U^{ij} tensor.

	x	y	z	U(eq)
C(1)	549(3)	8168(3)	3339(10)	29(2)
C(2)	946(4)	7430(3)	1512(12)	41(2)
C(3)	1474(4)	7324(3)	2337(12)	41(2)
C(4)	1709(4)	7772(4)	3340(12)	44(2)
C(5)	1799(4)	8269(4)	2336(12)	45(2)
C(6)	187(4)	7318(3)	3412(13)	42(2)
C(007)	1318(4)	8511(4)	1518(11)	41(2)
C(7)	-249(4)	7195(4)	2366(15)	52(3)
C(8)	-595(5)	6842(4)	3003(18)	71(4)
C(9)	-508(6)	6602(5)	4610(20)	83(5)
C(10)	-82(5)	6716(4)	5637(17)	68(4)
C(11)	278(4)	7084(4)	5011(13)	50(3)
C(12)	-338(4)	7441(5)	607(15)	67(3)
C(13)	806(3)	9065(3)	3495(12)	37(2)
C(14)	533(4)	9431(4)	2551(14)	53(3)
C(15)	508(5)	9933(4)	3299(19)	65(3)
C(16)	736(5)	10054(5)	4840(20)	77(4)
C(17)	996(4)	9694(5)	5751(17)	66(3)
C(18)	1043(4)	9183(4)	5066(12)	49(3)
C(19)	286(5)	9305(4)	826(16)	76(4)
C(20)	-462(4)	8505(4)	3724(15)	52(3)
C(21)	-410(4)	8512(4)	7242(14)	52(3)
O(1)	-763(3)	8606(4)	2734(11)	81(3)
O(2)	-675(3)	8623(4)	8337(10)	87(3)
Cl(1)	707(1)	8117(1)	7398(3)	51(1)
Rh(1)	38(1)	8346(1)	5346(1)	37(1)
N(1)	571(3)	7682(3)	2736(9)	33(2)
N(2)	870(3)	8540(3)	2786(9)	35(2)
Cl(3)	-2380(7)	7285(5)	11198(16)	118(6)
C(22)	-2500	7500	9068(19)	190(30)
Cl(4)	-2318(7)	6969(4)	7775(16)	123(6)

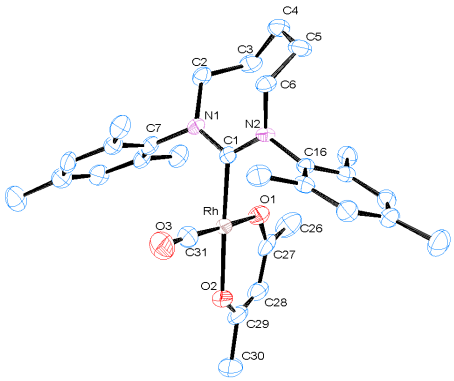

Table 1. Crystal data and structure refinement for **Rh(8-Mes)(acac)CO**

Identification code	kjc1010t	
Empirical formula	C30 H39 N2 O3 Rh	
Formula weight	578.54	
Temperature	150(2) K	
Wavelength	0.71073 Å	
Crystal system	Orthorhombic	
Space group	Pna21	
Unit cell dimensions	a = 25.1127(4) Å	α= 90°.
	b = 23.6294(4) Å	β= 90°.
	c = 9.41910(10) Å	γ = 90°.
Volume	5589.28(14) $Å^3$	
Z	8	
Density (calculated)	1.375 Mg/m^3	
Absorption coefficient	0.644 mm^{-1}	
F(000)	2416	
Crystal size	0.30 x 0.30 x 0.30 mm^3	
Theta range for data collection	1.62 to 27.48°.	
Index ranges	-32<=h<=32, -30<=k<=30, -12<=l<=12	
Reflections collected	12510	
Independent reflections	12510 [R(int) = 0.0000]	
Completeness to theta = 27.48°	99.7 %	
Absorption correction	Empirical	
Max. and min. transmission	0.8304 and 0.8304	
Refinement method	Full-matrix least-squares on F^2	
Data / restraints / parameters	12510 / 1 / 665	
Goodness-of-fit on F^2	1.051	
Final R indices [I>2sigma(I)]	R1 = 0.0489, wR2 = 0.0958	

R indices (all data)	R1 = 0.0688, wR2 = 0.1055
Absolute structure parameter	0.58(3)
Largest diff. peak and hole	0.721 and -0.592 e.Å^{-3}

Table 2. Atomic coordinates (x 10^4) and equivalent isotropic displacement parameters (Å^{2}x 10^3) for kjc1010t. U(eq) is defined as one third of the trace of the orthogonalized U^{ij} tensor.

	x	y	z	U(eq)
C(1)	4945(2)	2322(2)	9697(4)	21(1)
C(2)	4085(2)	2067(2)	11017(5)	29(1)
C(3)	4295(2)	2233(2)	12490(5)	35(1)
C(4)	4506(2)	1738(2)	13371(6)	39(1)
C(5)	5040(2)	1506(2)	12881(5)	37(1)
C(6)	5107(2)	1476(2)	11282(5)	27(1)
C(7)	4085(2)	2429(2)	8580(5)	26(1)
C(8)	3813(2)	2944(2)	8577(6)	30(1)
C(9)	3498(2)	3067(2)	7396(6)	37(1)
C(10)	3433(2)	2695(3)	6275(6)	39(1)
C(11)	3687(2)	2174(2)	6361(5)	35(1)
C(12)	4013(2)	2029(2)	7508(5)	29(1)
C(13)	3862(2)	3364(2)	9774(6)	39(1)
C(14)	3114(2)	2858(3)	4973(6)	50(2)
C(15)	4277(2)	1459(2)	7548(6)	36(1)
C(16)	5826(2)	2125(2)	10629(5)	23(1)
C(17)	6158(2)	1791(2)	9769(5)	27(1)
C(18)	6704(2)	1849(2)	9930(6)	32(1)
C(19)	6928(2)	2210(2)	10911(6)	34(1)
C(20)	6591(2)	2550(2)	11709(6)	31(1)
C(21)	6036(2)	2513(2)	11602(6)	26(1)
C(22)	5949(2)	1358(2)	8729(5)	36(1)
C(23)	7525(2)	2216(3)	11145(7)	47(2)
C(25)	5696(2)	2881(2)	12547(5)	32(1)
C(26)	5048(3)	4365(3)	11114(8)	57(2)
C(27)	5216(2)	4034(2)	9803(6)	38(1)
C(28)	5435(2)	4307(2)	8653(6)	40(1)
C(29)	5604(2)	4050(3)	7420(7)	45(2)
C(30)	5849(3)	4404(3)	6247(7)	58(2)

C(31)	5327(2)	2383(2)	6984(5)	37(1)
C(32)	7547(2)	-164(2)	6369(5)	26(1)
C(33)	7132(3)	-1142(3)	5945(9)	68(2)
C(34)	7237(3)	-1133(4)	4278(9)	86(3)
C(35)	7722(3)	-1406(3)	3828(8)	69(2)
C(36)	8232(3)	-1149(3)	4245(7)	53(2)
C(37)	8260(2)	-871(2)	5685(6)	39(1)
C(38)	6745(2)	-449(2)	7582(6)	32(1)
C(39)	6837(2)	-534(2)	9035(6)	36(1)
C(40)	6413(2)	-421(2)	9968(6)	38(1)
C(41)	5921(2)	-249(2)	9487(7)	41(1)
C(42)	5844(2)	-186(2)	8047(6)	39(1)
C(43)	6247(2)	-292(2)	7066(6)	36(1)
C(44)	7358(2)	-741(3)	9596(6)	46(1)
C(45)	5469(2)	-136(3)	10514(8)	57(2)
C(46)	6127(2)	-226(3)	5514(6)	45(1)
C(47)	8389(2)	156(2)	5480(5)	24(1)
C(48)	8764(2)	297(2)	6522(5)	28(1)
C(49)	9140(2)	715(2)	6207(5)	31(1)
C(50)	9148(2)	989(2)	4901(5)	29(1)
C(51)	8784(2)	828(2)	3881(5)	31(1)
C(52)	8399(2)	407(2)	4147(5)	28(1)
C(53)	8780(2)	20(2)	7964(5)	37(1)
C(54)	9545(2)	1457(2)	4607(7)	43(1)
C(55)	8012(2)	266(2)	2958(5)	36(1)
C(56)	6760(2)	2379(2)	6314(7)	48(2)
C(57)	6856(2)	1767(2)	5931(6)	35(1)
C(58)	6659(2)	1557(2)	4634(6)	38(1)
C(59)	6750(2)	1023(2)	4111(5)	35(1)
C(60)	6520(3)	861(3)	2684(7)	56(2)
C(61)	7590(2)	644(2)	8491(6)	32(1)
N(1)	4408(1)	2269(2)	9793(4)	23(1)
N(2)	5252(2)	2022(2)	10592(4)	23(1)
N(3)	7178(1)	-579(2)	6609(6)	32(1)
N(4)	8017(2)	-302(2)	5777(4)	26(1)
O(1)	5132(1)	3498(1)	9915(4)	34(1)
O(2)	5578(1)	3524(2)	7102(4)	41(1)
O(3)	5365(2)	2076(2)	6047(5)	54(1)

O(4)	7130(1)	1488(1)	6815(4)	30(1)
O(5)	7017(1)	626(1)	4699(4)	32(1)
O(6)	7720(2)	659(2)	9652(4)	57(1)
Rh(1)	5256(1)	2895(1)	8378(1)	25(1)
Rh(2)	7346(1)	645(1)	6687(1)	23(1)

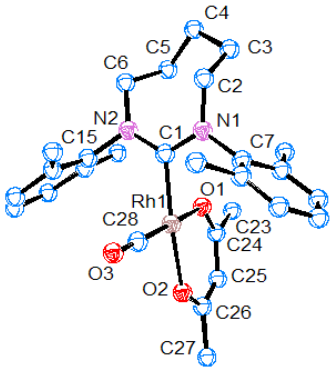

Table 1. Crystal data and structure refinement for **Rh(8-Xyl)(acac)CO**

Identification code	kjc1011	
Empirical formula	C28 H35 N2 O3 Rh	
Formula weight	550.49	
Temperature	150(2) K	
Wavelength	0.71073 Å	
Crystal system	Monoclinic	
Space group	Cc	
Unit cell dimensions	a = 16.2207(5) Å	α= 90°.
	b = 17.4873(4) Å	β= 91.7010(10)°.
	c = 9.0813(3) Å	γ = 90°.
Volume	2574.83(13) $Å^3$	
Z	4	
Density (calculated)	1.420 Mg/m^3	
Absorption coefficient	0.694 mm^{-1}	
F(000)	1144	
Crystal size	0.35 x 0.20 x 0.13 mm^3	
Theta range for data collection	3.71 to 27.49°.	
Index ranges	-21<=h<=21, -22<=k<=21, -11<=l<=11	
Reflections collected	5063	
Independent reflections	5058 [R(int) = 0.0249]	
Completeness to theta = 27.49°	99.2 %	
Absorption correction	Empirical	
Max. and min. transmission	0.9151 and 0.7931	
Refinement method	Full-matrix least-squares on F^2	
Data / restraints / parameters	5058 / 208 / 361	
Goodness-of-fit on F^2	1.046	
Final R indices [I>2sigma(I)]	R1 = 0.0440, wR2 = 0.1001	
R indices (all data)	R1 = 0.0482, wR2 = 0.1033	

Absolute structure parameter	0.55(4)
Extinction coefficient	0.0141(9)
Largest diff. peak and hole	0.623 and -0.628 e.Å^{-3}

Table 2. Atomic coordinates (x 10^4) and equivalent isotropic displacement parameters (Å^{2}x 10^3) for kjc1011. U(eq) is defined as one third of the trace of the orthogonalized U^{ij} tensor.

	x	y	z	U(eq)
C(1)	5929(3)	2426(3)	6741(5)	42(1)
C(2)	5815(8)	3637(5)	5251(9)	73(2)
C(3)	6416(9)	3731(5)	4024(8)	73(3)
C(4)	6231(7)	3139(4)	2795(9)	72(2)
C(5)	6290(7)	2341(4)	3481(11)	75(2)
C(6)	5473(6)	2100(6)	4110(6)	66(2)
C(7)	6546(4)	3575(3)	7707(7)	56(2)
C(8)	6068(5)	3949(4)	8705(8)	69(2)
C(9)	6421(7)	4335(4)	9873(10)	92(3)
C(10)	7260(8)	4393(5)	10003(13)	112(4)
C(11)	7730(6)	4055(6)	8987(14)	89(3)
C(12)	7398(5)	3647(4)	7782(10)	75(2)
C(13)	5117(5)	3928(6)	8592(10)	75(2)
C(14)	7958(5)	3300(5)	6662(11)	98(3)
C(15)	5200(4)	1268(3)	6198(7)	42(1)
C(16)	5655(3)	619(3)	5859(6)	44(1)
C(17)	5354(4)	-85(3)	6296(8)	63(2)
C(18)	4623(4)	-137(4)	7042(9)	76(2)
C(19)	4169(4)	501(4)	7297(8)	68(2)
C(20)	4434(3)	1228(4)	6851(7)	51(1)
C(21)	6446(4)	654(5)	5030(7)	66(2)
C(22)	3902(5)	1922(4)	7025(11)	80(2)
C(23)	8733(4)	1172(6)	6830(8)	83(2)
C(24)	8082(4)	1325(4)	7970(7)	61(2)
C(25)	8232(4)	1081(4)	9415(7)	64(2)
C(26)	7689(4)	1162(4)	10576(7)	55(2)
C(27)	7948(5)	879(5)	12091(7)	80(2)
C(28)	5470(6)	2050(5)	9574(9)	58(2)
N(1)	6141(3)	3154(2)	6481(4)	49(1)

N(2)	5508(3)	2018(3)	5725(4)	50(1)
O(1)	7451(3)	1662(3)	7470(6)	56(1)
O(2)	6965(2)	1441(3)	10457(4)	51(1)
O(3)	4856(4)	2118(4)	10167(7)	105(2)
Rh(1)	6401(1)	1918(1)	8603(1)	41(1)
C(2A)	5737(11)	3687(7)	5418(13)	78(4)
C(3A)	6216(13)	3689(6)	3975(9)	74(3)
C(4A)	6455(8)	2846(8)	3662(19)	76(3)
C(5A)	5665(10)	2422(7)	3149(8)	73(3)
C(6A)	5066(6)	2369(8)	4432(10)	65(3)
N(1A)	6141(3)	3154(2)	6481(4)	49(1)
N(2A)	5508(3)	2018(3)	5725(4)	50(1)

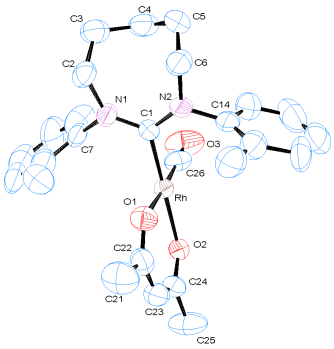

Table 1. Crystal data and structure refinement for **Rh(8-o-Tol)(acac)CO**

Identification code	kjc1004b	
Empirical formula	C26 H32 N2 O3 Rh	
Formula weight	523.45	
Temperature	294(2) K	
Wavelength	0.71073 Å	
Crystal system	Triclinic	
Space group	P-1	
Unit cell dimensions	a = 8.6728(4) Å	• = 79.733(2)°.
	b = 10.6096(5) Å	• = 77.374(2)°.
	c = 14.6223(6) Å	• = 72.399(3)°.
Volume	1242.34(10) $Å^3$	
Z	2	
Density (calculated)	1.399 Mg/m^3	
Absorption coefficient	0.716 mm^{-1}	
F(000)	542	
Crystal size	0.10 x 0.10 x 0.08 mm^3	
Theta range for data collection	2.62 to 27.53°.	
Index ranges	-11<=h<=11, -13<=k<=13, -18<=l<=18	
Reflections collected	8223	
Independent reflections	5549 [R(int) = 0.0547]	
Completeness to theta = 27.53°	97.1 %	
Max. and min. transmission	0.9450 and 0.9319	
Refinement method	Full-matrix least-squares on F^2	
Data / restraints / parameters	5549 / 16 / 289	
Goodness-of-fit on F^2	1.172	
Final R indices [I>2sigma(I)]	R1 = 0.1158, wR2 = 0.3031	
R indices (all data)	R1 = 0.1677, wR2 = 0.3420	
Largest diff. peak and hole	5.042 and -0.933 $e.Å^{-3}$	

Table 2. Atomic coordinates (x 10^4) and equivalent isotropic displacement parameters ($Å^2$x 10^3) for kjc1004b. U(eq) is defined as one third of the trace of the orthogonalized U^{ij} tensor.

	x	y	z	U(eq)
C(1)	2452(12)	-1821(10)	-2171(6)	42(2)
C(2)	4707(13)	-2397(10)	-1149(8)	61(3)
C(3)	4468(16)	-1164(10)	-666(8)	72(3)
C(4)	3503(16)	158(11)	-1134(8)	84(4)
C(5)	4297(18)	523(12)	-2153(8)	92(5)
C(6)	4588(15)	-480(12)	-2852(7)	69(4)
C(7)	2294(14)	-3200(11)	-672(8)	70(4)
C(8)	2731(17)	-4589(12)	-549(9)	86(4)
C(9)	1956(17)	-5281(16)	241(9)	90(5)
C(10)	810(20)	-4519(16)	904(12)	112(7)
C(11)	300(20)	-3123(16)	829(9)	109(6)
C(12)	1129(16)	-2523(16)	33(8)	97(5)
C(13)	3940(20)	-5286(16)	-1255(11)	96(5)
C(14)	2131(13)	-143(11)	-3498(7)	60(3)
C(15)	2544(15)	-376(13)	-4441(7)	76(4)
C(16)	1711(17)	496(16)	-5125(10)	97(6)
C(17)	450(20)	1583(16)	-4808(12)	111(7)
C(18)	-20(20)	1857(14)	-3869(11)	104(5)
C(19)	881(15)	995(12)	-3219(10)	84(4)
C(20)	3830(19)	-1538(15)	-4714(9)	85(4)
C(21)	3479(18)	-5720(15)	-3878(11)	91(4)
C(22)	2018(15)	-4690(12)	-3504(8)	59(3)
C(23)	451(16)	-4762(13)	-3570(9)	64(3)
C(24)	-1040(16)	-3926(12)	-3247(8)	60(3)
C(25)	-2563(18)	-4146(17)	-3421(13)	99(5)
C(26)	-858(15)	-1022(14)	-1770(9)	61(3)
N(1)	3175(10)	-2450(9)	-1427(5)	49(2)
N(2)	3100(10)	-941(8)	-2803(5)	48(2)
O(1)	2287(9)	-3807(8)	-3125(5)	58(2)
O(2)	-1289(8)	-2950(7)	-2781(5)	47(2)
O(3)	-1721(13)	-213(13)	-1316(9)	104(4)
Rh(1)	558(1)	-2326(1)	-2423(1)	42(1)

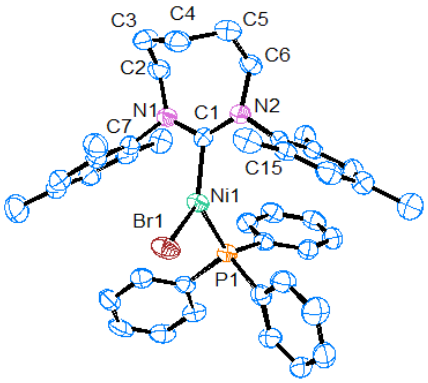

Table 1. Crystal data and structure refinement for **Ni(8-Mes)(PPh_3)Br**

Identification code	kjc1138	
Empirical formula	C42 H47 Br0.71 Cl0.29 N2 Ni P	
Formula weight	736.62	
Temperature	150(2) K	
Wavelength	0.71073 Å	
Crystal system	Monoclinic	
Space group	P21/n	
Unit cell dimensions	a = 11.1633(7) Å	α= 90°.
	b = 17.5068(11) Å	β= 100.254(4)°.
	c = 19.1295(13) Å	γ = 90°.
Volume	3678.8(4) $Å^3$	
Z	4	
Density (calculated)	1.330 Mg/m^3	
Absorption coefficient	1.397 mm^{-1}	
F(000)	1543	
Crystal size	0.50 x 0.50 x 0.50 mm^3	
Theta range for data collection	2.33 to 23.27°.	
Index ranges	-12<=h<=12, -19<=k<=17, -21<=l<=21	
Reflections collected	8658	
Independent reflections	5207 [R(int) = 0.0362]	
Completeness to theta = 23.27°	98.2 %	
Absorption correction	Empirical	
Max. and min. transmission	0.5417 and 0.5417	
Refinement method	Full-matrix least-squares on F^2	
Data / restraints / parameters	5207 / 0 / 431	
Goodness-of-fit on F^2	1.117	
Final R indices [I>2sigma(I)]	R1 = 0.0621, wR2 = 0.1126	
R indices (all data)	R1 = 0.0897, wR2 = 0.1228	

Largest diff. peak and hole 0.557 and -0.407 e.Å^{-3}

Table 2. Atomic coordinates (x 10^4) and equivalent isotropic displacement parameters (Å^{2}x 10^3) for kjc1138. U(eq) is defined as one third of the trace of the orthogonalized U^{ij} tensor.

	x	y	z	U(eq)
C(1)	7811(4)	284(3)	7788(2)	31(1)
C(2)	9552(5)	-643(3)	7634(3)	45(2)
C(3)	10530(5)	-535(3)	8288(3)	52(2)
C(4)	10091(5)	-282(3)	8944(3)	50(2)
C(5)	9134(5)	-786(3)	9172(3)	48(2)
C(6)	7921(5)	-839(3)	8659(3)	39(1)
C(7)	9053(5)	495(3)	6901(3)	36(1)
C(8)	8682(5)	214(3)	6213(3)	43(1)
C(9)	9100(5)	582(3)	5655(3)	49(2)
C(10)	9844(5)	1222(4)	5773(3)	50(2)
C(11)	9803(5)	1134(3)	7035(3)	41(1)
C(12)	7871(5)	-481(3)	6074(3)	55(2)
C(13)	10317(6)	1596(4)	5159(3)	75(2)
C(14)	10295(5)	1428(3)	7769(3)	49(2)
C(15)	6419(4)	191(3)	8586(2)	32(1)
C(16)	5299(5)	-160(3)	8335(3)	37(1)
C(17)	4299(5)	60(3)	8627(3)	47(2)
C(18)	4385(6)	604(3)	9162(3)	49(2)
C(19)	5503(6)	937(3)	9391(3)	46(2)
C(20)	6547(5)	752(3)	9114(3)	37(1)
C(21)	5189(5)	-768(3)	7768(3)	46(1)
C(22)	3278(6)	813(4)	9480(3)	67(2)
C(23)	7737(5)	1141(3)	9396(3)	49(2)
C(24)	4340(5)	2079(3)	7123(3)	38(1)
C(25)	3387(5)	2485(3)	6717(3)	43(1)
C(26)	2591(5)	2911(3)	7038(3)	47(2)
C(27)	2713(6)	2930(3)	7759(3)	53(2)
C(28)	3658(6)	2530(4)	8172(3)	59(2)
C(29)	4467(6)	2113(3)	7855(3)	49(2)
C(030)	10156(5)	1491(3)	6457(3)	49(2)
C(30)	4274(5)	646(3)	6450(3)	35(1)

C(31)	4569(5)	126(3)	5960(3)	43(1)
C(32)	3813(6)	-490(3)	5738(3)	47(2)
C(33)	2762(6)	-590(3)	6008(3)	49(2)
C(34)	2452(5)	-80(3)	6492(3)	50(2)
C(35)	3204(5)	535(3)	6711(3)	40(1)
C(36)	5553(5)	1838(3)	5899(3)	36(1)
C(37)	6704(5)	2081(3)	5834(3)	41(1)
C(38)	6919(6)	2399(3)	5199(3)	48(2)
C(39)	5980(7)	2478(3)	4633(3)	52(2)
C(40)	4838(6)	2232(3)	4689(3)	48(2)
C(41)	4617(5)	1904(3)	5312(3)	45(1)
N(1)	8749(4)	42(2)	7482(2)	35(1)
N(2)	7471(4)	-92(2)	8328(2)	34(1)
P(1)	5351(1)	1417(1)	6754(1)	34(1)
Br(1)	7620(1)	2559(1)	7813(1)	49(1)
Cl(1)	7620(1)	2559(1)	7813(1)	49(1)
Ni(1)	7105(1)	1298(1)	7503(1)	36(1)

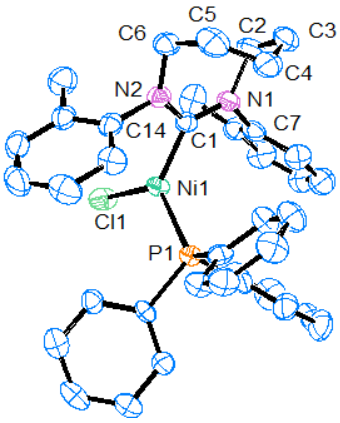

Table 1. Crystal data and structure refinement for **Ni(8-*o*-Tol)(PPh3)Cl**

Identification code	kjc1131	
Empirical formula	C38 H39 Br0.77 Cl0.23 N2 Ni P	
Formula weight	683.08	
Temperature	150(2) K	
Wavelength	0.71073 Å	
Crystal system	Triclinic	
Space group	P-1	
Unit cell dimensions	a = 10.321(2) Å	α= 95.060(9)°.
	b = 10.244(3) Å	β= 89.964(13)°.
	c = 16.104(4) Å	γ = 104.816(14)°.
Volume	1639.3(7) $Å^3$	
Z	2	
Density (calculated)	1.384 Mg/m^3	
Absorption coefficient	1.627 mm^{-1}	
F(000)	710	
Crystal size	0.24 x 0.08 x 0.04 mm^3	
Theta range for data collection	1.27 to 20.83°.	
Index ranges	-10<=h<=10, -10<=k<=10, -16<=l<=15	
Reflections collected	5971	
Independent reflections	3390 [R(int) = 0.1178]	
Completeness to theta = 20.83°	98.3 %	
Absorption correction	Empirical	
Max. and min. transmission	0.9378 and 0.6961	
Refinement method	Full-matrix least-squares on F^2	
Data / restraints / parameters	3390 / 18 / 300	
Goodness-of-fit on F^2	1.145	
Final R indices [I>2sigma(I)]	R1 = 0.1417, wR2 = 0.3335	

R indices (all data)	R1 = 0.2031, wR2 = 0.3692
Extinction coefficient	0.000(3)
Largest diff. peak and hole	1.455 and -0.531 e.Å^{-3}

Table 2. Atomic coordinates (x 10^4) and equivalent isotropic displacement parameters (Å^{2}x 10^3) for kjc1131. U(eq) is defined as one third of the trace of the orthogonalized U^{ij} tensor.

	x	y	z	U(eq)
N(1)	657(14)	4112(17)	3305(8)	60(5)
N(2)	612(13)	4247(17)	1837(8)	56(5)
P(1)	2803(5)	1405(6)	2286(4)	47(2)
Cl(1)	5107(3)	5005(3)	2651(2)	69(2)
Br(1)	5107(3)	5005(3)	2651(2)	69(2)
Ni(1)	2974(3)	3582(3)	2521(2)	51(1)
C(1)	1359(17)	3984(17)	2536(9)	54(6)
C(2)	-573(14)	4480(20)	3570(15)	64(7)
C(3)	-1851(19)	3340(20)	3377(13)	69(7)
C(4)	-2000(20)	2750(20)	2459(12)	74(8)
C(5)	-1927(16)	3740(20)	1791(16)	84(8)
C(6)	-573(8)	4786(9)	1745(6)	77(8)
C(7)	1509(8)	3900(9)	3979(6)	57(6)
C(8)	2508(8)	4923(9)	4393(6)	63(7)
C(9)	3224(8)	4640(9)	5055(6)	73(7)
C(10)	2941(8)	3333(9)	5303(6)	80(8)
C(11)	1941(8)	2309(9)	4889(6)	77(8)
C(12)	1226(8)	2593(9)	4227(6)	61(6)
C(13)	2766(10)	6400(8)	4141(6)	78(8)
C(14)	1273(10)	4021(8)	1058(6)	59(6)
C(15)	2336(10)	5040(8)	816(6)	70(7)
C(16)	2911(10)	4887(8)	45(6)	77(8)
C(17)	2424(10)	3715(8)	-484(6)	73(7)
C(18)	1361(10)	2695(8)	-242(6)	86(9)
C(19)	785(10)	2849(8)	529(6)	72(7)
C(20)	2905(5)	6396(6)	1377(4)	81(8)
C(21)	1254(5)	115(6)	2530(4)	46(6)
C(22)	1231(5)	-789(6)	3128(4)	59(6)
C(23)	32(5)	-1690(6)	3308(4)	58(6)

C(24)	-1146(5)	-1687(6)	2891(4)	57(7)
C(25)	-1123(5)	-783(6)	2293(4)	76(8)
C(26)	77(5)	118(6)	2112(4)	64(7)
C(27)	4064(5)	755(6)	2816(4)	44(5)
C(28)	4431(5)	-403(6)	2501(4)	57(6)
C(29)	5277(5)	-932(6)	2966(4)	66(7)
C(30)	5756(5)	-304(6)	3746(4)	69(7)
C(31)	5388(5)	854(6)	4061(4)	66(7)
C(32)	4542(5)	1384(6)	3596(4)	57(6)
C(33)	3026(5)	915(6)	1186(4)	61(7)
C(34)	3968(5)	1838(6)	768(4)	73(7)
C(35)	4221(5)	1533(6)	-64(4)	89(9)
C(36)	3531(5)	304(6)	-480(4)	101(12)
C(37)	2589(5)	-619(6)	-63(4)	98(10)
C(38)	2336(5)	-313(6)	770(4)	64(7)

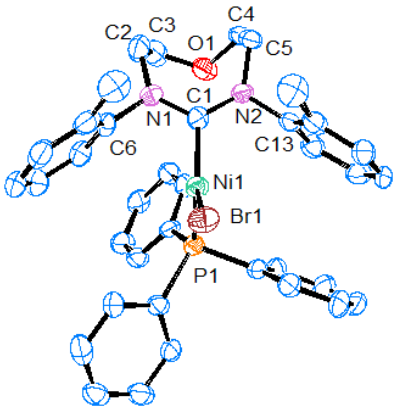

Table 1. Crystal data and structure refinement for **Ni(O-8-*o*-Tol)(PPh3)Br**

Identification code	kjc1133	
Empirical formula	C37 H37 Br0.69 Cl0.31 N2 Ni O P	
Formula weight	681.72	
Temperature	150(2) K	
Wavelength	0.71073 Å	
Crystal system	Triclinic	
Space group	P-1	
Unit cell dimensions	a = 10.2776(7) Å	α= 96.382(4)°.
	b = 10.3430(6) Å	β= 90.831(4)°.
	c = 15.7043(8) Å	γ = 103.338(3)°.
Volume	1612.90(17) $Å^3$	
Z	2	
Density (calculated)	1.404 Mg/m^3	
Absorption coefficient	1.569 mm^{-1}	
F(000)	707	
Crystal size	0.15 x 0.15 x 0.10 mm^3	
Theta range for data collection	2.91 to 24.42°.	
Index ranges	-11<=h<=9, -10<=k<=12, -18<=l<=18	
Reflections collected	8212	
Independent reflections	5259 [R(int) = 0.0560]	
Completeness to theta = 24.42°	99.2 %	
Absorption correction	Empirical	
Max. and min. transmission	0.8588 and 0.7986	
Refinement method	Full-matrix least-squares on F^2	
Data / restraints / parameters	5259 / 0 / 391	
Goodness-of-fit on F^2	1.056	
Final R indices [I>2sigma(I)]	R1 = 0.0717, wR2 = 0.1612	
R indices (all data)	R1 = 0.1204, wR2 = 0.1867	

Largest diff. peak and hole 0.878 and -0.479 e.Å^{-3}

Table 2. Atomic coordinates (x 10^4) and equivalent isotropic displacement parameters (Å^{2}x 10^3) for kjc1133. U(eq) is defined as one third of the trace of the orthogonalized U^{ij} tensor.

	x	y	z	U(eq)
C(1)	1204(6)	4016(6)	2467(4)	32(2)
C(2)	-816(7)	4203(8)	3404(4)	48(2)
C(3)	-1910(8)	3034(8)	2991(5)	54(2)
C(4)	-1852(7)	3706(7)	1584(5)	42(2)
C(5)	-561(7)	4809(7)	1630(5)	41(2)
C(6)	1336(7)	3879(7)	3945(4)	35(2)
C(7)	2313(8)	4931(7)	4351(5)	45(2)
C(8)	3044(8)	4678(9)	5053(5)	52(2)
C(9)	2814(8)	3467(9)	5357(4)	49(2)
C(10)	1782(8)	2423(9)	4966(5)	55(2)
C(11)	1063(8)	2644(8)	4257(4)	46(2)
C(12)	2596(9)	6301(8)	4058(5)	58(2)
C(13)	1424(6)	4157(7)	982(4)	35(2)
C(14)	2445(7)	5190(7)	794(4)	40(2)
C(15)	3126(7)	4993(7)	38(4)	43(2)
C(16)	2755(7)	3828(7)	-505(4)	40(2)
C(17)	1689(8)	2811(8)	-341(5)	49(2)
C(18)	1016(7)	2974(7)	411(4)	42(2)
C(19)	2805(8)	6491(7)	1352(5)	55(2)
C(20)	3015(7)	945(6)	1162(4)	33(2)
C(21)	4116(7)	1693(7)	790(4)	38(2)
C(22)	4379(8)	1370(8)	-62(4)	46(2)
C(23)	3532(7)	341(7)	-560(4)	42(2)
C(24)	2415(7)	-388(8)	-204(4)	44(2)
C(25)	2155(7)	-98(7)	655(4)	37(2)
C(26)	4049(6)	849(6)	2847(4)	33(2)
C(27)	4563(7)	1488(7)	3643(4)	40(2)
C(28)	5414(8)	941(8)	4112(5)	50(2)
C(29)	5767(7)	-219(8)	3785(5)	47(2)
C(30)	5284(7)	-854(8)	2986(5)	47(2)
C(31)	4436(7)	-311(7)	2518(4)	37(2)

C(32)	1228(7)	279(6)	2522(4)	32(2)
C(33)	26(6)	515(6)	2255(4)	34(2)
C(34)	-1177(7)	-349(7)	2400(4)	41(2)
C(35)	-1191(7)	-1431(7)	2844(4)	43(2)
C(36)	3(7)	-1658(7)	3134(5)	46(2)
C(37)	1208(7)	-811(7)	2970(4)	39(2)
Br(1)	5115(1)	4970(1)	2619(1)	44(1)
Cl(1)	5115(1)	4970(1)	2619(1)	44(1)
N(1)	554(5)	4058(5)	3216(3)	36(1)
N(2)	671(5)	4299(5)	1748(3)	33(1)
Ni(1)	2964(1)	3643(1)	2493(1)	32(1)
O(1)	-1774(5)	2692(5)	2100(3)	45(1)
P(1)	2773(2)	1474(2)	2289(1)	31(1)

Appendix II

Publications from this thesis

First Examples of Structurally Imposing Eight-Membered-Ring (Diazocanylidene) N-Heterocyclic Carbenes: Salts, Free Carbenes, and Metal Complexes

Lu, W. Y.; Cavell, K. J.; Wixey, J. S.; Kariuki, B. *Organometallics* **2011**, 30 (21), 5649–5655.

Three-Coordinate Nickel(I) Complexes Stabilised By Six, Seven and Eight Membered Ring N-Hetereocyclic Carbenes: Synthesis, EPR/DFT Studies and Catalytic Activity

Page, M. J.; Lu, W. Y.; Poulten, R.; Carter, E.; Algarra, A. G.; Kariuki, B. M.; Macgregor, S. A.; Mahon, M. F.; Cavell, K. J.; Murphy, D. M.; Whittlesey, M. K. *Chemistry – A European Journal* **0000**, 0-0

(Publication accepted)